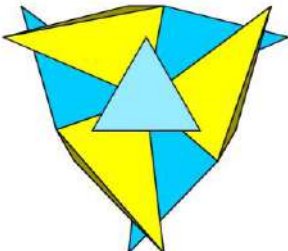




**25 INTERNATIONAL CONFERENCE ON
SOLID COMPOUNDS OF TRANSITION ELEMENTS
&
XVI INTERNATIONAL CONFERENCE ON
CRYSTAL CHEMISTRY OF INTERMETALLIC
COMPOUNDS**

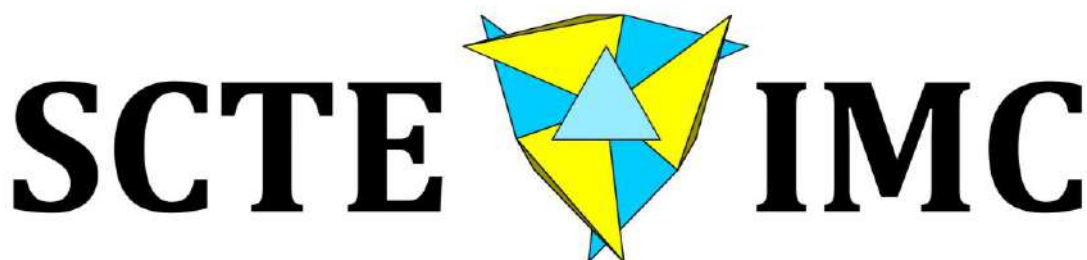
SCTE  **IMC**

**COLLECTED
ABSTRACTS**

**LVIV, UKRAINE – LUBLIN, POLAND
JUNE 15-18, 2026**

**IVAN FRANKO NATIONAL UNIVERSITY OF LVIV
MINISTRY OF EDUCATION AND SCIENCE OF UKRAINE
NATIONAL ACADEMY OF SCIENCES OF UKRAINE
UKRAINIAN CRYSTALLOGRAPHIC COMMITTEE**

**25 INTERNATIONAL CONFERENCE ON
SOLID COMPOUNDS OF TRANSITION ELEMENTS
&
XVI INTERNATIONAL CONFERENCE ON
CRYSTAL CHEMISTRY OF INTERMETALLIC
COMPOUNDS**



**COLLECTED
ABSTRACTS**

**LVIV, UKRAINE – LUBLIN, POLAND
JUNE 15-18, 2026**

Collected Abstracts of the 25th International Conference on Solid Compounds of Transition Elements & the XVI International Conference on Crystal Chemistry of Intermetallic Compounds, Lviv, Ukraine – Lublin, Poland, 15-18 June 2026, Ivan Franko National University of Lviv, 2026, 156 p.

SCTE&IMC ADVISORY COMMITTEE

F. Bartolome	<i>Spain</i>	L. Havela	<i>Czechia</i>
E. Bauer	<i>Austria</i>	D. Kaczorowski	<i>Poland</i>
R. Ben Hassen	<i>Tunisia</i>	M. Kanatzidis	<i>USA</i>
J.-L. Bobet	<i>France</i>	A. Mar	<i>Canada</i>
H. Boller	<i>Austria</i>	T. Mori	<i>Japan</i>
R. Černý	<i>Switzerland</i>	M. Pasturel	<i>France</i>
R. Colman	<i>Czechia</i>	A. Pereira Gonçalves	<i>Portugal</i>
S. De Negri	<i>Italy</i>	R. Pöttgen	<i>Germany</i>
T. Fässler	<i>Germany</i>	K. Richter	<i>Austria</i>
D. Fruchart	<i>France</i>	P. Rogl	<i>Austria</i>
M. Giovannini	<i>Italy</i>	C. Röhr	<i>Germany</i>
R. Gladyshevskii	<i>Ukraine</i>	A. Szytuła	<i>Poland</i>
Yu. Grin	<i>Germany</i>	I. Zavaliy	<i>Ukraine</i>

LOCAL ORGANIZING COMMITTEE

R. Gladyshevskii (<i>chairman</i>)	K. Miliyanchuk
O. Zaremba (<i>secretary</i>)	V. Pavlyuk
K. Cenzual	S. Pukas
G. Dmytriv	Z. Rzączyńska
D. Kołodyńska	Ya. Tokaychuk
I. Melnyk	

Department of Inorganic Chemistry
Ivan Franko National University of Lviv
Kyryla i Mefodiya St. 6, UA-79005 Lviv, Ukraine
telephone: +380 32 2600388; e-mail: scte.imc.2026@gmail.com
website: chem.lnu.edu.ua/about/departments/scte_imc_2026

PLENARY LECTURES

SOLID-STATE CHEMISTRY OF Pnictides

Svilen Bobev

*Department of Chemistry and Biochemistry, University of Delaware,
Newark, DE 19716, USA
bobev@udel.edu*

This talk will deal with the relationships among composition, structure, and electronic structure in Zintl phases. The focus will be on $A-M-Pn$ compounds (A = alkali or alkaline-earth metals, M = Cu, Zn, Cd, Pn = pnictogen, the group 15 elements), *i.e.*, ternary systems of metals/semimetals with very different electronegativities. I will highlight some recent discoveries from the Bobev laboratory and will recount many crystal structures, which, despite the apparent complexity in the bonding arrangements, can be “broken” down to simpler fragments, which are much easier to describe and rationalize. Typical common motifs will be the M -centered tetrahedra of Sb or Bi, MSb_4 and MBi_4 , respectively. Through shared corners and/or edges, MSb_4 and MBi_4 become interconnected to form chains, ribbons, or layers with complex topologies. These structures will represent cases where the strikingly delicate balance between the packing efficiency of ions (size effects) and the overall valence electron count (electronic effects) govern the stability of a particular arrangement over another. Structural connections to some well-known structures with two-dimensional layers or three-dimensional four-connected nets will be discussed as well.

NEW FUNCTIONAL MATERIALS BY CHALLENGING THE REACTIVITY OF INTERMETALLICS WITH HIGHLY ELECTRONEGATIVE ELEMENTS

S. Tencé

CNRS, Univ. Bordeaux, Bordeaux INP, ICMCB, UMR 5026, F-33600 Pessac, France

sophie.tence@icmcb.cnrs.fr

Intermetallics represent an important family of compounds, in which insertion of light elements (hydrogen, boron, carbon, nitrogen) has been widely explored for decades to synthesize novel phases and promote functional materials such as permanent magnets, magnetocalorics, materials for hydrogen storage or negative electrodes for Ni/MH batteries.

In this talk on equiatomic intermetallics RTX (R = rare earth, T = transition metal, X = p -element), I will show that beyond the classical applications, other types of functional properties can be induced by light-element insertion, such as superconductivity or catalytic properties through electronegative character [1,2]. I will focus the presentation on CeScSi-type and CeFeSi-type structures in which we can insert not only hydrogen and carbon elements in different sites, but also, and most surprisingly, oxygen and fluorine elements. Such results were quite unexpected because of the strong reactivity of these highly electronegative elements towards intermetallics. In particular, we have developed a new topochemical method to intercalate fluorine atoms into intermetallics using perfluorocarbon reactants [3]. We have demonstrated that this method is an effective route to provide quantum materials due to the coexistence of both ionic and metallo-covalent blocks within the structure. We also introduce a novel approach in solid-state chemistry for synthesizing transition metal oxy-hydrides and fluoro-hydrides, using intermetallic compounds as precursors where hydrogen, oxygen, and fluorine compete.

- [1] F. Bernardini, G. Garbarino, A. Sulpice, M. Nuñez-Regueiro, E. Gaudin, B. Chevalier, M.-A. Méasson, A. Cano, S. Tencé, *Phys. Rev. B* 97 (2018) 100504(R).
- [2] J. Wu, Y. Gong, T. Inoshita, D.C. Fredrickson, J. Wang, Y. Lu, M. Kitano, H. Hosono, *Adv. Mater.* 29 (2017) 1700924.
- [3] J.-B. Vaney, B. Vignolle, A. Demourgues, E. Gaudin, E. Durand, C. Labrugère, F. Bernardini, A. Cano, S. Tencé, *Nat. Commun.* 13 (2022) 1462.
- [4] K. Alabd, E. Gaudin, A. Villesuzanne, B. Vignolle, E. Durand, N. Daro, E. Suard, C. Ritter, S. Tencé, *J. Am. Chem. Soc.* 147 (2025) 22015-22023.

STUDYING PHASE EQUILIBRIA IN Mg-CONTAINING INTERMETALLIC SYSTEMS: RELEVANCE, DIFFICULTIES, CLASSIC AND NEW APPROACHES

S. De Negri and P. Solokha

*Dipartimento di Chimica e Chimica Industriale, Università degli Studi di Genova,
Via Dodecaneso 31, 16146 Genova, Italy
serena.denegri@unige.it*

Reliable knowledge of phase diagrams is a valuable help for the design of new metallic materials, for example, by guiding exploratory synthesis and identifying compositional regions where new intermetallics may exist. Particularly in multicomponent systems, phase-equilibrium data are essential in revealing relationships among competing phases, interpreting microstructures, and tracing phase transformations. The classic experimental approach to these studies consists of the synthesis and annealing of many alloys and their microstructural (SEM/EDXS) and structural (single-crystal and powder XRD) characterization. This route has some drawbacks (expensive and time-consuming) and encounters difficulties in the case of complex multiphase microstructures out of thermodynamic equilibrium, the existence of phases with similar compositions and structures, and other intrinsic features. Alternative strategies, joining old methods (such as diffusion couple [1]) and new techniques (such as 3D electron nano diffraction [2]) can resolve some of these problems and open new perspectives.

The exemplary Y–Ni–Mg system offers a fertile ground for such explorations: as belonging to the rare earth (*R*) – transition metal (*T*) – magnesium alloy family, it shows applicative interest and its phase diagram has been studied for decades, nevertheless it remains largely unclear and confusing [3]. In this contribution, some of our results on the Y–Ni–Mg phase equilibria are presented, with particular emphasis on families of compounds based on generalized structural concepts, for example:

1) *Mg-rich LPSO phases*. The unprecedented structural elucidation of some of them, achieved mainly thanks to the recently developed 3D ED technique, led to an updated, more general definition of LPSO as phases containing $\text{Mg}@Y_8\text{Ni}_6$ clusters embedded in a magnesium matrix with *fcc* or hybrid *fcc/hcp* layer stacking modes [4].

2) $Y_x\text{Ni}_x\text{Mg}_y$ phases. The crystal structures of several compounds characterized by a 1:1 ratio between Y and Ni were solved and their common architecture was unveiled, depicted by the general formula $(\text{YNi}_2)_{2n}(\text{YMg})_{2n}\text{Mg}_{2(o+e)-2n}$ (where $n = 1$ or 2 ; $o = \text{odd}$ and $e = \text{even integer}$) related to the type and number of characteristic fragments.

These results highlight regularities in structural moieties occurring in different *R–T–Mg* systems, aiding in the broad study of their phase equilibria and supporting the highly desired predictivity in the field of intermetallics.

[1] A.A. Kodentsov *et al.*, *Application of diffusion couples in phase diagram determination*, In: J.C. Zhao (Ed.), *Methods for Phase Diagram Determination*, Elsevier Science Ltd, 2007, pp. 222-245.

[2] M. Gemmi *et al.*, *ACS Cent. Sci.* 5 (2019) 1315.

[3] K. Xu *et al.*, *J. Mater. Sci.* 53 (2018) 9243-9257.

[4] P. Solokha *et al.*, *Acta Mater.* 296 (2025) 121279.

COMPUTATIONAL-DRIVEN OPTIMIZATION OF RENEWABLE ENERGY MATERIALS

Jan-Hendrik Pöhls

*Department of Chemistry, University of New Brunswick,
Fredericton NB, Canada
Jan.Pohls@unb.ca*

Computational methods play a central role in the discovery, design, and optimization of renewable-energy materials, including photovoltaics, lithium-ion batteries, and thermoelectric materials. In particular, those diverse computational approaches are crucial for advancing thermoelectric materials – materials that directly convert heat into electricity – because their electrical and thermal transport properties are strongly intertwined. Improving a single property often reduces the overall energy-conversion efficiency, and hence, the development of novel optimization strategies for thermoelectric materials is very challenging.

In this talk, I will introduce three computational approaches to discover and improve thermo-electric materials: density functional theory, first-principles modelling, and machine learning. First, density functional theory allows us to predict the electrical and thermal properties using high-throughput screening, helping to identify promising high-performance candidates [1,2]. However, the accuracy of these predictions depends on the underlying assumptions and approximations, which can vary across different classes of thermoelectric materials. Second, first-principles calculations can guide the design of new materials by predicting optimal compositions and carrier concentrations. For example, the single parabolic band model can estimate the carrier concentration that maximizes performance, but a deeper understanding of the mechanisms that limit electron transport is essential for reliable predictions of electrical properties [3]. Finally, we combined a Design of Experiments strategy with machine learning to efficiently screen and optimize thermoelectric materials [4]. Using this approach, the thermoelectric properties of AgSbTe₂ were systematically optimized using only a small number of experiments. Together, these approaches do not only accelerate the discovery of new high-efficiency thermoelectric materials but also allow the rapid optimization of established compounds.

- [1] J.-H. Pöhls *et al.*, *J. Mater. Chem. A* 6 (2018) 19502-19519.
- [2] J.-H. Pöhls, M. MacIver, S. Chanakian, A. Zevalkink, Y.-C. Tseng, Y. Mozharivskyj, *Chem. Mater.* 34 (2022) 8719-8728.
- [3] J.-H. Pöhls, Y. Mozharivskyj, *Comput. Mater. Sci.* 206 (2022) 111152.
- [4] J.-H. Pöhls, C.-W.T. Lo, M. MacIver, Y.-C. Tseng, Y. Mozharivskyj, *Chem. Mater.* 37 (2025) 2281-2289.

SYNTHESIS, STRUCTURE, AND PHYSICAL PROPERTIES OF THE RHOMBOHEDRAL $REIr_3$ BINARY COMPOUNDS

K. Górnicka, P. Meena, and T. Klimczuk
*Faculty of Applied Physics and Mathematics and
Advanced Materials Centre, Gdansk University of Technology,
ul. Narutowicza 11/12, 80-233 Gdańsk, Poland
tomasz.klimczuk@pg.edu.pl*

When searching for new chemical compounds, we can select up to approximately 80 elements from the periodic table, consider written and unwritten chemical rules and crystallographic structure. If you are fortunate enough to work with the rare-earth metals, you can expect to discover a series of 13 – or possibly 15 – compounds with successive metals ranging from scandium to lanthanum. You can also work with homologous series, where you modify the blocks of the layered crystal structure.

The family of compounds characterized by the general formula $RE_{2m+n}T_{4m+5n}$, where RE is a rare-earth element and T is a transition metal, is of significance due to its structural complexity and wide range of observed physical properties. The parameters m and n determine the number of $MgCu_2$ -type and $CaCu_5$ -type structural blocks, respectively, thereby providing a systematic framework for understanding structural variations and their influence on the properties. The $REIr_3$ compounds ($m = 1$ and $n = 1$) are known to form in different crystal structure types, depending on the choice of the RE element and the post-synthesis annealing temperature. In this lecture we will present synthesis, structural and physical studies of the rhombohedral (PuNi₃ type) $CeIr_3$, $PrIr_3$, $NdIr_3$, and $ThIr_3$. The key element in this family, which affects the physical properties, is the rare-earth metal. While $LaIr_3$, $CeIr_3$, and $ThIr_3$ are superconductors with $T_c = 3.5$ K [1], 2.5 K [2], and 4.4 K [3], respectively. In contrast, the remaining two are classified as ferromagnets, with the Curie temperature $T_C = 7.5$ K ($PrIr_3$) [4] and 10.6 K ($NdIr_3$) [5]. Interestingly, at around 70 K, both magnetic compounds reveal a structural phase transition. The rhombohedral $R-3m$ crystal structure undergoes a transformation to a monoclinic $C2/m$ structure upon cooling, and further cooling reveals temperature-independent behaviour of the unit cell volume.

Preliminary data on $NpIr_3$ and $PuIr_3$ will also be presented. These binary transuranic compounds have been synthesized and studied at JRC-KA (Germany). While $PuIr_3$ appears to be a paramagnet, $NpIr_3$ is likely to be an itinerant antiferromagnet with $T_N = 17$ K.

The work in Gdansk was supported by the National Science Centre (Poland), Grant No. 2022/45/B/ST5/03916.

- [1] N. Haldolaarachchige *et al.*, *J. Phys.: Condens. Matter* 29 (2017) 475602.
- [2] K. Górnicka *et al.*, *Supercond. Sci. Technol.* 32 (2019) 025008.
- [3] K. Górnicka *et al.*, *Phys. Rev. B* 100 (2019) 214514.
- [4] K. Gornicka *et al.*, *Phys. Rev. B* 110 (2024) 064431.
- [5] K. Górnicka *et al.*, *Phys. Rev. B* 99 (2019) 14430.

FACETS OF CHEMICAL BONDING IN INTERMETALLIC COMPOUNDS FROM POSITION-SPACE ANALYSIS OF 1- AND 2-DENSITIES

F.R. Wagner

*Department of Chemical Metals Science, Max Planck Institute for Chemical Physics of Solids,
Nöthnitzer Str. 40, 01187 Dresden, Germany
frank.wagner@cpfs.mpg.de*

It has long been known that the total energy of a chemical system can be exactly calculated not only from the knowledge of its wave function in Hilbert space but also from its 1- and 2-electron density matrices in position space [1]. This is an important finding, because it allows for an immense condensation of the information contained in the wave function to what is strictly necessary. In contrast to the DFT path to total energies, equations for exactly computing total energies from the 1- and 2-density matrices of the systems are well known [1].

Quantum-chemically “realistic bonding scenarios” are obtained from quantities derived from the electron density (ED) and pair density distributions. A central definition in this framework is the Bader’s QTAIM definition of an atom in position space based on the electron density. This can already be used to calculate effective atomic charges and volumes. Moreover, a definition of topological coordination numbers has recently been developed that is solely based on QTAIM atomic shapes derivable from experimentally measurable electron density distributions [2]. Chemical bonding between QTAIM atoms is then investigated by electron-pair related distributions in position space encoded in the pair density. In this framework the distribution of the ELI-D (and ELF) provides complementary information to the ED one and the combination of both in the ELI-D/QTAIM basin intersection method yields definitions of bonds (bond populations), and bond polarities [3]. Moreover, the overlaps of the distributions of the Fermi hole densities of each QTAIM atom give rise to interatomic delocalization indices (DIs) representing a position-space definition of effective bond orders. From this technique **k**-independent Fermi orbitals for solids [4] can be derived that are intrinsically localized solely by the localization of the Fermi hole density. They are approximately related to exactly computable interatomic interaction energies in the interacting quantum atoms (IQA) method for molecules [5] and solids [6]. In order to bridge the gap between numerical simulations and conceptual frameworks [2-9], the “realistic bonding scenarios” obtained are to be further interpreted relating electronic with chemical behaviour in the spirit of Coulson’s challenge “*Give us Insight, not Numbers*” (1959) [10] or its newer variant “*Give us Insight **and** Numbers*” (Frenking, 2011) [11].

- [1] A.J. Coleman, *Rev. Mod. Phys.* 35 (1963) 668-687.
- [2] F.R. Wagner, R. Freccero, Yu. Grin, *Acta Crystallogr. A* 81 (2015) 221-244.
- [3] F.R. Wagner, Yu. Grin, In: J. Reedijk, K.R. Poeppelmeier (Eds.), *Comprehensive Inorganic Chemistry III*, Vol. 3, Elsevier, Oxford, 2023, pp. 222-237.
- [4] F.R. Wagner, R. Cardoso, B. Boucher *et al.*, *Inorg. Chem.* 57 (2018) 12908-12919.
- [5] M. Blanco, A. M. Pendas, E. Francisco, *J. Chem. Theory Comput.* 1 (2005) 1096-1109.
- [6] D. Menendez-Crespo, F.R. Wagner *et al.*, *J. Phys. Chem. A* 125 (2021) 9011-9025.
- [7] R. Freccero, Yu. Grin, F.R. Wagner, *Dalton Trans.* 52 (2023) 8222-8236.
- [8] F.R. Wagner, *J. Comput. Chem.* 45 (2024) 2862-2877.
- [9] F.R. Wagner, Yu. Grin, *Inorg. Chem.* 63 (2024) 20205-20216.
- [10] C.A. Coulson, *Rev. Mod. Phys.* 32 (1960) 170-177.
- [11] F. Neese, M. Atanasov, G. Bistoniet *et al.*, *J. Am. Chem. Soc.* 141 (2019) 2814-2824.

INVITED LECTURES

TEACHING AND RESEARCH IN WARTIME UKRAINE

R. Gladyshevskii

*Ivan Franko National University of Lviv,
Kyryla i Mefodiya St. 6, 79005 Lviv, Ukraine
roman.gladyshevskii@lnu.edu.ua*

In February 2022, Russia launched a full-scale invasion of Ukraine. In spring 2026, the war goes on and the universities, like the rest of the Society, have had to adapt to this reality. The presentation will focus on the Ivan Franko National University of Lviv (IFNUL), a classic university with 19 faculties and 25'000 students. Lviv is at present not near the frontline, but drone and missile attacks occur periodically.

Except for a short time in 2022, IFNUL has remained open and working. Differently from some other universities in the country, all the university buildings have up to now been preserved. Present and former students and staff members participate in the war, and some have died as soldiers. The war has strengthened the feeling of national unity and solidarity and several volunteer centers operate at IFNUL, providing help to soldiers and civil victims.

Like other universities, our aim is to propose high-quality education. We need to create a safe environment, so that our students and collaborators can stay in Ukraine and continue their activity under reasonably comfortable conditions. The university buildings are equipped with shelters, often where lectures can be given and exams organized. On the whole, the level of knowledge of the students has remained unchanged, however, their motivation has increased.

Focus is on barrier-free education. The integration of a large number of war veterans brings new challenges. To relieve the heavy psychological strains caused by the war, IFNUL has installed counseling psychological services that propose individual consultations and various activities. The student associations play an important role.



The Russian missiles continuously attack the energy infrastructure and electricity has become a critical issue. To remedy for power outages, IFNUL has installed independent power supplies, solar hybrid stations, and batteries.

The main topics of research are the same as abroad, however, research on dual-use materials has been assigned high priority. Initiatives for collaboration have been launched in different countries, particularly in chemistry, physics, and biology. At present one third of the research is financed by Ukrainian state funding, one third by international sources, and one third by industry. With limited means and some universities having been seriously damaged, solidarity is important and technical equipment has been made available to researchers from across the country. An example is the Interdisciplinary Laboratory for Materials Science of Intermetallic Compounds at IFNUL with diffractometers, an electron microscope, DSC, and various devices for property measurements. The creation of startups is strongly encouraged, since the war will be followed by a period of intense reconstruction.

**TRIELIDES – FROM TRIANGLES, TETRAHEDRA AND
TETRAHEDRA PACKINGS:
NEW INTERMETALLIC COMPOUNDS IN THE SYSTEMS Sr/Ba(–Li)–Al/Ga/In**

M. Otteny, Q. Da Cruz, F. Sehmsdorf, M. Wendorff, and C. Röhr
*Institut für Anorganische und Analytische Chemie, Albert-Ludwigs-Universität Freiburg,
Albertstr. 21, 79104 Freiburg/Brsg., Germany
caroline.roehr@ac.uni-freiburg.de*

Structure chemistry and chemical bonding of intermetallic compounds of the heavy alkaline-earth elements (A^{II}) are dominated by the electron transfer to the respective metallic bonding partner (M) leading formally to M polyanions. For the e^- -rich p -block metals like the trieles (M^{III} : Al, Ga, In), formation and stability of distinct polyanions is almost always easily explained using covalent bonding concepts (Zintl phases). For the e^- -poor late d -block metals *e.g.* of the zinc group (metals further to the left in the periodic table do not form A^{II} IMCs at all) such simple rules explaining the polyanions are not applicable and principles of more ‘classic’ IMCs, mainly the concept of dense atom packing, come into play. Accordingly, M tetrahedra packings (t.p.) are common, and complex but frequent structure types of IMCs (like *e.g.* NaZn_{13} , $\text{Th}_6\text{Mn}_{23}$, Laves phases) containing corner-sharing cutouts of t.p. [tetrahedra stars (TS), extended double-TS (eDTS), extended icosahedra (eI) *etc.*] occur.

In our recent studies on the role of Mg in A^{II} zincides [1], we observed several series of related trigonal/hexagonal structures with a striking, but ultimately unsurprising analogy to ternary Li/Al phases with Li:Al ratios of approximately 1:1 [2]. The systematic (re)examination of the ternary systems Sr/Ba–Li–Al revealed a further increased structure diversity, again with many members of the three stacking series from the $\text{Th}_6\text{Mn}_{23}$ - (T) to the $\text{Eu}_3\text{Mg}_{16}$ -type (E) structure [TE: $_{-(n+m)/2}[\text{A}_3]_{n+m}(\text{M}_9^{\text{TS}})_n(\text{M}_{11}^{\text{eDTS}})_m(\text{M}_5^{\text{C}})_{m+n/2}$], from $\text{Ba}_2(\text{Li/Al})_9$ (B, [2]) to $\text{Eu}_3\text{Mg}_{16}$ [BE: $[\text{A}_3]_{m+2}(\text{M}_{21}^{\text{eI}})_n(\text{M}_{11}^{\text{eDTS}})_m(\text{M}_{5-6}^{\text{C}})_{m+n}$] and the new series from $\text{Ba}_2(\text{Li/Al})_9$ to $\text{Sr}_3(\text{Li/Ga})_{10}$ (S, [3b]) [BS: eI/C]. Whereas most of the Mg/Zn and Li/Al compounds exhibit a broad element mixing at the M sites, the element segregation (‘coloring’) in the structurally even more diverse IMCs of the Li/Ga systems is much more pronounced, often even complete. Thus, the members of the fourth series from $_{-1/2}\text{Sr}_3\text{Li}_5\text{Ga}_5$ [3b] to $_{-}\text{Ba}_3\text{Li}_4[\text{Ga}_4]$ [4] contain distinct $[\text{Ga}_4]^{\delta-}$ tetrahedra, $[\text{Ga}_3]$ triangles and isolated gallium atoms within the Li/Ga t.p. This allows for a Zintl-type decomposition into A^{2+} and Li^+ cations and a comparison of the bonding situation within the resulting gallide subunits with *e.g.* those in the new binary gallide BaGa (KGe-type) and in Ba_8Ga_7 ($_{-}\text{Ba}_8[\text{Ga}_4][\text{Ga}_3]$) [4], including a discussion of the compound’s electronegative character [5]. In addition to these related trigonal/hexagonal structure series, the Ba–Li–Ga system yielded several ternary IMCs of already known structure types (*e.g.* $\text{Ca}_6\text{Cu}_6\text{Al}_5$) as well as new and singular compounds like Ba_3LiGa_5 [3a], $\text{Ba}_2\text{Li}_2\text{Ga}_2$, $\text{BaLi}_8[\text{Ga}_4][\text{Ga}_2]$ [6] and $\text{Ba}_2\text{Li}_2\text{Ga}_3$ [7], which are likewise discussed comparing a simple electron count for the gallide anions with the results of band structure as well as molecular DFT calculations.

- [1] K. Köhler, C. Röhr, *Z. Kristallogr. Suppl.* 38 (2018) 86; *ibid.* 42 (2022) 162; *Acta Crystallogr. A* 75 (2019) S424; *Z. Anorg. Allg. Chem.* 645 (2019) 219; K. Köhler, PhD thesis, University Freiburg, 2022.
- [2] U. Häussermann, M. Wörle, R. Nesper, *J. Am. Chem. Soc.* 118 (1996) 11789.
- [3] M. Kotsch *et al.*, *Eur. J. Inorg. Chem.* (2020) 2842; *Z. Anorg. Allg. Chem.* 647 (2021) 1797.
- [4] M.L. Fornasini, *Acta Crystallogr. C* 39 (1983) 943.
- [5] L.A. Burton *et al.*, *Chem. Mater.* 30 (2018) 7521.
- [6] M. Otteny, C. Röhr, *Z. Kristallogr. Suppl.*, 2026, in press.
- [7] M. Otteny, F. Sehmsdorf, *Z. Naturforsch.*, submitted; M. Otteny, PhD, U. Freiburg, 2025.

RARE-EARTH HEXAALUMINATES AS A PLAYGROUND FOR TRIANGULAR LATTICE MAGNETISM

R.H. Colman¹, S. Kumar¹, G. Bastien¹, A. Kancko¹, C.A. Corrêa², P. Gegenwart³,
and T. Treu³

¹ Charles University, Prague, Czechia

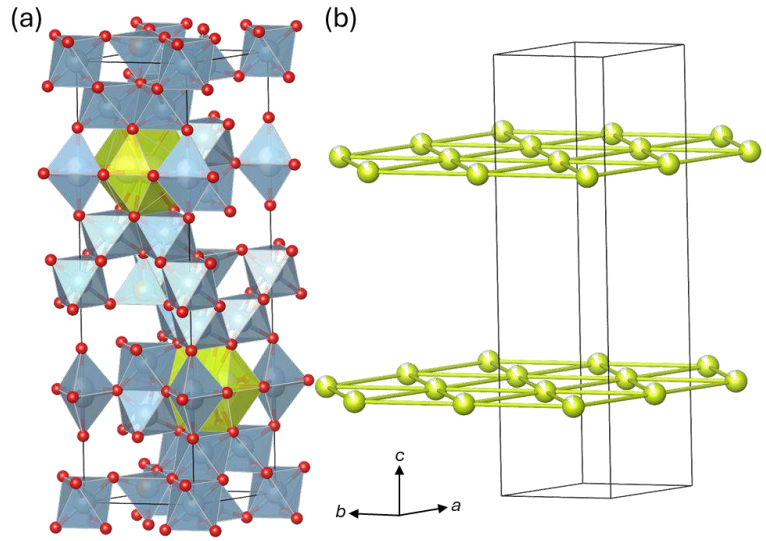
² Institute of Physics of the Czech Academy of Sciences, Na Slovance, Prague, Czechia

³ University of Augsburg, 86159 Augsburg, Germany
ross.colman@matfyz.cuni.cz

Rare-earth hexaaluminates $LnMgAl_{11}O_{19}$ provide an attractive platform for studying frustrated magnetism on well-separated triangular lattices (Figure), where crystal-field effects, strong spin-orbit coupling, and structural disorder combine to generate a wide variety of low-temperature states.

In this talk, I will summarize our recent studies on single crystals of the series with $Ln = Ce, Pr, Nd, Sm,$ and Gd , together with the related compound $EuAl_{12}O_{19}$. Across this family, we find a remarkably broad magnetic landscape despite the common structural motif. $CeMgAl_{11}O_{19}$ forms an effective spin-1/2 triangular magnet with no long-range order down to 30 mK and strong XXZ anisotropy [1], placing it near a field-tuned quantum-disordered regime. $PrMgAl_{11}O_{19}$ instead hosts non-Kramers quantum Ising magnetism [2], while $NdMgAl_{11}O_{19}$ shows pronounced Ising anisotropy, short-range correlations, and strong adiabatic demagnetization cooling [3]. $SmMgAl_{11}O_{19}$ occupies the extreme weak-exchange limit, with a strongly quenched Kramers doublet and predominantly single-ion behaviour. In contrast, $GdMgAl_{11}O_{19}$ behaves as a nearly ideal weakly interacting paramagnet with a large magnetocaloric response, whereas $EuAl_{12}O_{19}$ exhibits quasi-two-dimensional ferromagnetism [4].

These results establish the hexaaluminate family as a versatile playground for investigating triangular lattice magnetism. In all but $Ln = Gd$, strong single-ion anisotropy plays an important role in the low-temperature magnetic properties. I will discuss the interplay of frustration, anisotropy, structural disorder, and magnetocaloric functionality across the investigated systems.



The hexaaluminate structure (a) and the rare-earth triangular lattice (b)

- [1] G. Bastien *et al.*, *ArXiv:2506.16207*, 2025.
- [2] S. Kumar *et al.*, *Phys. Rev. B* 111 (2025) 174444.
- [3] S. Kumar *et al.*, *ArXiv:2505.18898*, 2026.
- [4] G. Bastien *et al.*, *Phys. Rev. B* 110 (2024) 94436; G. Bastien *et al.*, *Adv. Mater.* 36 (2024) 2410282.

CRYSTAL CHEMISTRY OF TERNARY INTERMETALLICS IN SYSTEMS WITH TWO *p*-ELEMENTS OF GROUPS 13-15

Ya. Tokaychuk and R. Gladyshevskii

*Department of Inorganic Chemistry, Ivan Franko National University of Lviv,
Kyryla i Mefodiya St. 6, 79005 Lviv, Ukraine
yaroslav.tokaychuk@lnu.edu.ua*

The crystal-chemical approach constitutes a powerful tool for the analysis of intermetallic compounds, encompassing atomic coordination, interatomic distances, bonding characteristics, structure topology and correlations. It is based on fundamental experimental investigations of the phase equilibria in metallic systems, construction of phase diagrams, precise determination of crystallographic parameters of different phases, and identification of their crystal-chemical features. In this work, several groups of ternary systems with rare-earth metals (*R*), transition *d*-metals (Zr, Hf) and two *p*-elements of groups 13 (Al, Ga), 14 (Si, Ge, Sn), or 15 (Sb, Bi) were investigated.

The ternary systems $R\text{-Ga}\text{-}\{\text{Si,Ge,Sn}\}$, $R\text{-}\{\text{Si,Ge}\}\text{-}\{\text{Sn,Sb,Bi}\}$, and $\{\text{Zr,Hf}\}\text{-}\{\text{Al,Ga}\}\text{-}\{\text{Si,Ge,Sn,Sb}\}$ are characterized by significant solubility of the third component in the binary compounds, which, due to the size effect, is more pronounced for the systems with Si and Ge, compared to the systems with heavy *p*-elements (Sn, Sb, Bi). The formation of ternary compounds with constant and variable compositions was observed in all the studied systems. Their number and compositions differ depending on the *p*-elements. In the systems $R\text{-Ga-Si}$ the formation of 1-4 ternary compounds was established in the concentration range 25-50 at.% *R*, in the systems $R\text{-Ga-Ge}$ 4-10 compounds were found in the range 25-62.5 at.% *R*, and in the systems $R\text{-Ga-Sn}$ 2-5 compounds in the range 25-62.5 at.% *R*. The ternary systems $R\text{-}\{\text{Si,Ge}\}\text{-}\{\text{Sn,Sb,Bi}\}$ are characterized by the formation of 1-5 ternary compounds with 25-60 at.% *R*, and the systems $\{\text{Zr,Hf}\}\text{-}\{\text{Al,Ga}\}\text{-}\{\text{Si,Ge,Sn,Sb}\}$ by 1-5 ternary compounds in the range 25-62.5 at.% *T* (Zr or Hf). Most of the structures of the ternary compounds belong to binary structure types or their ternary ordered variants. The tendency towards ordering of the *p*-elements is more pronounced for the systems with Sn, Sb, and Bi.

The structure types of the ternary compounds that form along the lines with 25 at.% *R* in the systems $R\text{-Ga}\text{-}\{\text{Si,Ge,Sn}\}$ have cubic or hexagonal (rhombohedral) symmetry. They belong to the family of close-packed structures and are characterized by cuboctahedral and anticuboctahedral coordination of the atoms. Substitution of *p*-element atoms of group IV (Si, Ge, Sn) for Ga leads to the formation of structures with lower hexagonality (ratio between hexagonal *h* and cubic *c* stacking). Close-packed structures with tetragonal symmetry form at 25 at.% *T* in the systems $\{\text{Zr,Hf}\}\text{-Al}\text{-}\{\text{Si,Ge,Sn,Sb}\}$. The ternary compounds in the concentration range 33.3-55.5 at.% *R* or *T* adopt structure types with trigonal-prismatic coordination of the *p*-element atoms. Due to strong interactions the *p*-element atoms in these structures often form clusters, chains, or frameworks. At high *R* or *T* contents (60-62.5 at.%) the structures of the ternary compounds are characterized by square-antiprismatic and icosahedral coordination of the *p*-element atoms. The combination of fragments representative of comparatively simple structure types (building blocks) leads to the formation of homologous series of complex intergrowth structures. For example, the structure type $\text{Ce}_2(\text{Ga}_{0.1}\text{Ge}_{0.9})_7$, which is observed in the systems $R\text{-Ga-Ge}$, is formed by intergrowth of BaAl_4 - (square antiprisms), AlB_2 - (trigonal prisms), and $\alpha\text{-Po}$ -type (cubes) slabs in the sequence $(\text{AlB}_2|\text{BaAl}_4|\text{Po}|\text{BaAl}_4)_2$.

Eu–Pd–Sn COMPOUNDS AS A PLAYGROUND FOR COMPLEX MAGNETIC ORDER

M. Giovannini¹, A. Martinelli², I. Trabelsi^{1,5}, J.G. Sereni³, I. Čurlík⁴, and R. Ben Hassen⁵

¹ *Department of Chemistry, University of Genoa, Via Dodecaneso 31, 16146 Genova, Italy*

² *SPIN-CNR, Corso F.M. Perrone 24, 16152 Genoa, Italy*

³ *Department of Physics, CAB-CNEA, CONICET,
8400 San Carlos de Bariloche, Argentina*

⁴ *Faculty of Humanities and Natural Sciences, University of Prešov,
17 novembra 1, Prešov, Slovakia*

⁵ *Laboratory of Materials and Environment for Sustainable Development LR18ES10,
University of Tunis El Manar, Tunisia
mauro.giovannini@unige.it*

The magnetic behaviour of intermetallic compounds based on Eu^{2+} is often unexpected. These compounds form a pure spin system with $J = S = 7/2$ and $L = 0$, which precludes CEF effects. Nevertheless, they frequently exhibit complex anisotropic magnetic ordering.

The goal of this talk is to demonstrate that complex magnetism is a consistent feature in all compounds studied within the ternary Eu–Pd–Sn system. Our group has conducted a systematic study of the crystal structure and magnetic properties of several Eu–Pd–Sn compounds over time, using various laboratory techniques and, for some, synchrotron X-ray and neutron powder diffraction. We will present some of the most intriguing examples. For instance, the study of magnetism in non-centrosymmetric compounds such as $\text{Eu}_2\text{Pd}_2\text{Sn}$ is of great interest due to topologically non-trivial magnetic textures, which offer potential for new magnetic information manipulation and storage technologies [1]. The magnetic phase that develops in $\text{Eu}_2\text{Pd}_2\text{Sn}$ below 14 K is characterized by incommensurate cycloidal ordering in the *ac* plane of the Eu substructure. This magnetic structure shows significant similarities to that observed in EuNiGe_3 , possibly indicating the occurrence of a skyrmion lattice in $\text{Eu}_2\text{Pd}_2\text{Sn}$ as well [2]. In EuPdSn_2 , the magnetic behaviour is unconventional: we will show that antiferromagnetic and ferromagnetic domains compete and coexist in the ground state, which is also confirmed by theoretical calculations [3]. In $\text{Eu}_2\text{Pd}_3\text{Sn}$, the competition between ferromagnetism and antiferromagnetism is triggered by the formation of a canted ferromagnet.

[1] N. Nagaosa *et al.*, *Nat. Nanotechnol.* 8 (2013) 899.

[2] J.G. Sereni *et al.*, *Phys. Rev. B* 108 (2023) 014427.

[3] A. Martinelli *et al.*, *J. Mater. Chem. C* 11 (2023) 7641.

CRYSTAL STRUCTURES AND PHYSICAL PROPERTIES OF Ni–Zn–Sb COMPOUNDS DERIVING FROM THE NiAs-TYPE

P. Rogl¹, G. Rogl¹, H. Michor², R. Podloucky¹, J. Bursik³, O. Kubinec^{1,4}, K. Weiss^{1,4},
P. Broz⁴, V. Bursikova⁴, and G. Giester⁵

¹ *Institute of Materials Chemistry, Universität Wien, Währingerstr. 42, A-1090 Wien, Austria*

² *Institute of Solid State Physics, TU Wien, Wiedner Hauptstr. 8-10, A-1090 Wien, Austria*

³ *Institute of Physics of Materials, Czech Academy of Sciences, Žitkova 22,
61600 Brno, Czechia*

⁴ *Department of Chemistry, Masaryk University, Kotlářská 2, 61137 Brno, Czechia*

⁵ *Department of Mineralogy and Crystallography, Universität Wien, Josef-Holaubek-Platz 2,
A-1090 Wien, Austria*

peter.franz.rogl@univie.ac

Based on X-ray diffraction the crystal structures of τ_2 -Ni₂Zn₂Sb (single-crystal data, fully ordered), τ_3 -Ni_{3-x}Zn_{1-y+z}□_ySb_{2-z} (single-crystal data; $x = 0.62$, $y = 0.58$, $z = 0.50$; □ denotes a vacancy) and τ_4 -Ni_{2+x+y+z}□_{2-x-y}Zn_uSb_{2-z-u} (Rietveld refinement; $x = 0.56$, $y = 0.58$, $z = 0.49$, $u = 0.28$) have been established. Interestingly, all three structures crystallize in space group $P3$ and derive from binary NiSb (NiAs-type, $P6_3/mmc$) with various modes of filling the Wyckoff sites. Whereas the structure of τ_2 is fully ordered, the other two structures (τ_3 , τ_4) reveal a random distribution of at least two atom types in some of the atom sites as well as further defect sites. Selected area electron diffraction (SAED) patterns, collected by TEM from thin lamellae of the samples, were all fully indexed using the parameters of the trigonal structures obtained from the X-ray intensity data refinement – and thus ensure that no ordering exists among the randomly distributed atoms and vacancies.

Physical properties have been studied for all three compounds on single-phase, polycrystalline compacts (high-pressure torsion at 5 GPa, 2 revolutions; relative densities > 95 %), *i.e.* electrical resistivity, Seebeck coefficient, specific heat, magnetism, Vickers hardness, and elastic moduli (RT). The experimental studies were accompanied by DFT calculations providing thermodynamic stabilities and electronic structures of the compounds.

PROBING LIMITS OF 5f MAGNETISM IN U SYSTEMS (XMCD STUDY OF UCu₂P₂ UNDER PRESSURE)

L. Havela¹, O. Kolomiets¹, F. Wilhelm², A. Rogalev,² V. Buturlim,¹ O. Koloskova,¹
S. Černá,¹ K. Miliyanchuk,³ F. Honda,⁴ and D. Kaczorowski⁵

¹ Charles University, Prague, Czechia

² ESRF Grenoble, France

³ Ivan Franko National University of Lviv, Lviv, Ukraine

⁴ Kyushu University, Fukuoka, Japan

⁵ Institute of Low Temperatures and Structural Research, Polish Academy of Sciences,
Wroclaw, Poland

ladislav.havela@matfyz.cuni.cz

5f magnetism of U systems with an intermediate degree of delocalization (between the 3d and 4f types), its easy tunability, and very strong spin-orbit coupling provide new functionalities, connected with orbital magnetism tightly coupled with bonding. The exchange interactions are, in principle, stronger than the indirect exchange RKKY interaction known from rare earths. Nevertheless, the critical temperatures of magnetic ordering do not reach values needed for ambient-temperature applications. The reason can be seen in the relatively weak intra-atomic Coulomb correlations.

We tried to define a situation in which the 5f ferromagnetism would reach ambient temperatures. Instead of intermetallics we turned to polar compounds. The idea is to suppress the 5f-6d hybridization by involving the 6d states in polar bonding. We have been focusing on the compound UCu₂P₂ (trigonal structure of the CaAl₂Si₂ type), isostructural to the Zintl phases RE_2X_2 formed by divalent REs. An example is the narrow-gap antiferromagnetic semiconductor EuZn₂P₂, where external pressure tends to reduce the band gap and increase the Néel temperature [1]. The fact that the Curie temperature T_C of UCu₂P₂ (216 K) tends to be also enhanced by pressure [2] gives credibility to the idea.

Using single crystals, we studied the electrical resistivity of UCu₂P₂, revealing a semi-metallic ground state. A pronounced anomaly related to T_C allows following its pressure dependence up to $p = 8$ GPa, where $T_C \approx 280$ K is reached. Higher pressures could be achieved using XMCD at the U- $M_{4,5}$ edges, revealing that T_C still increases, reaching 295 K at 12.2 GPa. Still higher pressures lead to a collapse of the crystal structure (monoclinic distortions) and T_C drops. XMCD spectra also allow determining the pressure dependence of the U magnetic moments and their spin and orbital components. These can be directly confronted with various *ab initio* calculations so that a realistic description can be found. The calculations suggest that UCu₂P₂ is actually half-metallic, with one spin direction dominating energies around the Fermi level.

This work was supported by the Czech Science Foundation under the project 25-16339 S.

- [1] D. Rybicki, K. Komedera, J. Przewoznik, L. Gondek, C. Kapusta, K. Podgorska, W. Tabis, J. Zukrowski, L.-M. Tran, M. Babij, Z. Bukowski, L. Havela, V. Buturlim, J. Prchal, M. Divis, P. Kral, I. Turek, I. Halevy, J. Kastil, M. Misek, U. Dutta, D. Legut, *Phys. Rev. B* 110 (2024) 014421.
- [2] D. Kaczorowski, R. Duraj, R. Troc, *Solid State Commun.* 70 (1989) 619-621.

TEMPERATURE-DRIVEN ELECTROCHEMICAL OXYGEN SEPARATION

K.T. Wojciechowski, T. Parashchuk, R. Knura, A. Wilmanski, and O. Cherniushok
*Department of Inorganic Chemistry, Faculty of Materials Science and Ceramics,
AGH University of Krakow, Mickiewiczza Ave. 30, 30-059 Krakow, Poland
wojciech@agh.edu.pl*

Electrochemical oxygen separators and oxygen transport membranes are promising technologies for high-purity oxygen production; however, their operation usually requires either external electrical power supply or oxygen partial-pressure gradients. In the present work, we propose a new concept of temperature-driven electrochemical oxygen separation (TD-EOS), in which a temperature gradient directly induces oxygen transport through coupled thermoelectric and ionic transport phenomena.

The proposed concept is based on Onsager-type coupled irreversible transport processes and on the physical separation of ionic and electronic transport channels. The analysis indicates that efficient thermally driven oxygen pumping requires both thermopower asymmetry and balanced ionic/electronic transport. These conditions naturally lead toward composite architectures consisting of an oxygen-conducting ceramic segment and a thermoelectric electronic-conducting segment.

As a proof-of-concept system, p-type $\text{Ce}_{0.8}\text{Gd}_{0.2}\text{O}_{2-\delta}$ oxygen-conducting ceramics and n-type ZnO:CuO thermoelectric materials were synthesized, characterized, and integrated into a TD-EOS uncouple prototype. Transport properties, including the Seebeck coefficient and electrical conductivity, were investigated in the temperature range 600-700 °C. The fabricated devices demonstrated autonomous oxygen transport driven solely by a temperature gradient ($\Delta T \approx 100$ °C), without external electrical power supply.

The measured oxygen flux density reached 0.17-0.25 $\text{ml}\cdot\text{s}^{-1}\cdot\text{m}^{-2}$ for the proof-of-concept demonstrator. The theoretical analysis predicts substantial further enhancement through optimization of membrane thickness, geometry, transport properties, and interfacial engineering. The presented approach extends thermoelectric functionality beyond electrical power generation toward direct heat-driven chemical potential and mass transport engineering.

This work was carried out under the project MAITEG, WEAVE-UNISONO 2022/04/Y/ST5/00139 “Entropy engineering and interface optimization in materials for highly effective thermoelectric energy conversion”, National Science Centre and German Research Foundation, as well as by the AGH Excellence Initiative – Research University (IDUB) program under the Research Teams Support Initiative.

INVESTIGATIONS ON THE INFLUENCE OF TRANSITION METALS ON THE CRYSTAL STRUCTURES AND MAGNETIC PROPERTIES OF CeNiSi₂-TYPE DERIVATIVE COMPOUNDS

Pierric Lemoine¹, Emma Chauvel¹, Samuel Harris¹, Thierry Schweitzer¹, Mathieu Pasturel², Romain Sibille³, Lucas Eichenberger¹, and Yvan Sidis¹

¹ Université de Lorraine, CNRS, IJL, F54000, Nancy, France

² Université de Rennes, CNRS, ISCR, F-35000, Rennes, France

³ Lab. Neutron Scattering and Imaging, Paul Scherrer Institut, Villigen, Switzerland
pierric.lemoine@univ-lorraine.fr

The richness of the periodic table offers quasi-illimited combination possibilities for the design of functional inorganic materials. Among them, intermetallics are highly interesting due to their exceptional diversity of structural and physical properties [1]. This is exemplified by the RGe_2 compounds ($R = Sc, Y, La, Lu, U$) that are known for their superconductor properties at low temperature ($ScGe_2$, $T_c = 1.30$ K; YGe_2 , $T_c = 3.8$ K; $LaGe_2$, $T_c = 1.49$ K; $LuGe_2$, $T_c = 2.6$ K [2]) that can coexist with ferromagnetism in UGe_2 [3], and that, despite their different crystal structures: ThSi₂-type for $R = Y$ and La , ZrSi₂-type for $R = Sc$ and Lu , and ZrGa₂-type for UGe_2 . Interestingly, superconductivity was also observed in several derivative RGe_2 compounds such as (i) $YPd_{0.5}Ge_{1.5}$ ($T_c = 3$ K [4]), $YPt_{0.5}Ge_{1.5}$ ($T_c = 3.3$ K [5]), $YNi_{0.5}Ge_{1.5}$ ($T_c = 0.553$ K [6]), and $LaNi_{0.5}Ge_{1.5}$ ($T_c = 0.394$ K [6]) characterized by a disordered AlB_2 -type structure, (ii) $LuSnGe$ ($T_c = 0.74$ K [7]) crystallizing in a TmSnGe-type structure, an ordered variant of ZrSi₂-type, or (iii) Y_4RuGe_8 ($T_c = 1.3$ K [8]) reported in a transition-metal vacancy-ordered CeNiSi₂-type superstructure of triclinic symmetry. With the aim to discover new materials characterized by superconductivity and/or (ferro)magnetism, we decided to reinvestigate the RT_xGe_2 ($R = Y, Lu$; $T =$ transition metals; $x \leq 1$) compounds, firstly reported in an average crystal structure [9], and determine the influence on the crystal structure and magnetic properties of transition-metal incorporation within the $RSnGe$ ($R =$ rare-earth element) series [10]. In this presentation, I will discuss the influence of transition metals on the synthesis, chemical composition, crystal structures, and magnetic properties of some RT_xGe_2 and RT_xSnGe compounds [11].

- [1] S. Gupta, K.G. Suresh, *J. Alloys Compd.* 618 (2015) 562; M. Shatruk, *J. Solid State Chem.* 272 (2019) 198; M. Nentwich *et al.*, *Acta Crystallogr. B* 76 (2020) 177; B.K. Rai *et al.*, *J. Phys.: Condens. Matter* 34 (2022) 273002; O. Janka, In: *Comprehensive Inorganic Chemistry III*, Elsevier S&T, 2023, Vol. 4, Ch. 6, p. 172; S.M. Kauzlarich, *Chem. Mater.* 35 (2023) 7355.
- [2] B.T. Matthias *et al.*, *Phys. Rev.* 112 (1958) 89; Y.R. Chung *et al.*, *Phys. Rev. B* 70 (2004) 052511.
- [3] S.S. Saxena *et al.*, *Nature* 406 (2000) 587.
- [4] S. Majumdar, E.V. Sampathkumaran, *Phys. Rev. B* 63 (2001) 172407.
- [5] H. Kitô *et al.*, *Physica C* 377 (2002) 185.
- [6] J.W. Chen *et al.*, *Physica C* 477 (2012) 63.
- [7] D. Kaczorowski, A. Szytula, *J. Alloys Compd.* 622 (2015) 640.
- [8] J.K. Bao *et al.*, *Chem. Mater.* 33 (2021) 7839.
- [9] M. François *et al.*, *J. Less-Common Met.* 160 (1990) 197.
- [10] P.H. Tobash *et al.*, *Chem. Mater.* 20 (2008) 2151; A. Gil *et al.*, *J. Solid State Chem.* 184 (2011) 1631.
- [11] E. Chauvel *et al.*, to be published.

PREDICTION AND VALIDATION OF MEDIUM-ENTROPY QUATERNARY ALLOYS AND A15-TYPE SUPERCONDUCTORS

Volodymyr Gvozdetzkyi^{1,2}, Allison Thomé¹, Balaranjan Selvaratnam^{1,3}, and Arthur Mar¹

¹ *Department of Chemistry, University of Alberta, Edmonton T6G 2G2, Canada*

² *Ames National Laboratory, U.S. Department of Energy, Ames, Iowa 50011, USA*

³ *Department of Chemistry, Hunter College, City University of New York, New York, New York 10065, USA*
amar@ualberta.ca

Alloys consisting of four or more elements, called multi-principal element alloys, are stabilized by high configurational entropy. They often exhibit improved mechanical properties, including oxidation resistance, ductility, hardness, and wear resistance. Incorporating disorder into related materials such as A15 (Cr₃Si-type) superconductors, which have relatively simple cubic structures, can also offer greater control over critical temperatures and fields. However, the number of possible combinations of metallic components is enormous, encompassing a vast compositional space of over 10⁵ systems. These compositions can be screened efficiently with the aid of machine learning approaches, through the development of interpretable structure maps to predict new candidates for medium-entropy alloys, and through regression models to predict critical temperatures of medium-entropy A15 superconductors. These predictions are then validated by synthesis and characterization by X-ray diffraction methods.

NOVEL PRINCIPLES TO ENHANCE THERMOELECTRIC POWER GENERATION AND COOLING MATERIALS & DEVICES

T. Mori^{1,2}

¹ *Research Center for Materials Nanoarchitectonics (MANA), NIMS, Tsukuba, Japan*

² *Graduate School of Pure and Applied Sciences, University of Tsukuba, Tsukuba, Japan
takao1195ab@gmail.com*

Thermoelectric (TE) materials can be used for various energy harvesting power generation applications to contribute to energy saving/carbon neutrality and IoT power sources, or Peltier cooling applications, which are expected to significantly expand [1]. We have been developing various novel principles to overcome traditional tradeoffs to enhance TE properties, such as magnon drag, paramagnon drag/magnetic interaction, spin fluctuation, spin entropy, *etc.*, to enhance the Seebeck coefficient, and furthermore, control of disorder and utilization of Anderson localized states, topological insulating states [2], *etc.*

We have recently discovered defect engineering, which enhanced the TE properties of Mg-Sb materials of both n-type and p-type, to be able to surpass the long-time champion Bi₂Te₃ for power generation and rival for cooling. Recently, delocalization of the electrical carriers led to even higher performance of the materials, and a single-leg device of Mg₃Sb₂-type achieved TE conversion efficiency of ~12.6 %. Focusing on the localization of phonons led to a broader range of high performance and achievement of figures of merit $zT > 2$ [3].

The actual performance of the developed materials themselves, compared to the module and device demonstrations, is even higher, requiring urgent further development of the device technology, which also encompasses some interesting material science. Electrode technologies suited for the novel Mg-Sb materials have been developed. A novel concept of “active electrodes” led to high stability and enhancement of the device performance that was previously achieved, also utilized for diffusion barrier materials [4].

Accurate evaluation of the performance of devices is critical for the industrialization of the technology, and we have also laid out the best practices for the evaluation of thermoelectric modules. Radically improved design of TE power generation modules (TEGs) has also been achieved for various novel materials, like these Mg-Sb materials, Heusler alloys, *etc.* [5].

Supported by Mirai Large-scale Program, Japan Science and Technology Agency (JST).

- [1] I. Petsagkourakis *et al.*, *Sci. Technol. Adv. Mater.* 19 (2018) 836; T. Mori, S. Priya, *MRS Bull.* 43 (2018) 176; N. Nandihalli, C.J. Liu, T. Mori, *Nano Energy* 78 (2020) 105186; T. Hendricks, T. Caillat, T. Mori, *Energies (Basel, Switz.)* 15 (2022) 7307.
- [2] T. Mori, *Small* 13 (2017) 1702013; Tarachand *et al.*, *Mater. Today Phys.* 48 (2024) 101568; I. Serhiienko *et al.*, *Adv. Sci.* 11 (2024) 2309291; F. Garmroudi *et al.*, *Nat. Commun.* 13 (2022), 3599; F. Garmroudi *et al.*, *Nat. Commun.* 16 (2025) 2976.
- [3] Z. Liu *et al.*, *Joule*, 5 (2021) 1196; Z. Liu *et al.*, *Nat. Commun.*, 13 (2022) 1120; L. Wang *et al.*, *Adv. Energy Mater.* 13 (2023) 2301667; L. Wang *et al.*, *Nat. Commun.* 15 (2024) 6800; H. Cho *et al.*, *Adv. Funct. Mater.* 44 (2024) 2407017; G. Wu *et al.*, *Nat. Commun.* 16 (2025) 10366.
- [4] R. Chetty, J. Babu, T. Mori, *ACS Appl. Energy Mater.* 7 (2024) 12112; A. Li *et al.*, *Nat. Commun.* 16 (2025) 1502; L. Wang *et al.*, *Adv. Mater.* 37 (2025) 2508270.
- [5] R. Chetty, J. Babu, T. Mori, *Joule* 8 (2024) 556; J. Babu, R. Chetty, T. Mori, *Small* 22 (2026), e08990; Tarachand *et al.*, *Small Methods* 10 (2026) e02360.

**RATIONAL GUIDANCE OF MATERIALS SYNTHESIS AND EXPLORATION
FROM LIMITED DATA:
A BAYESIAN OPTIMIZATION APPROACH IN THE LAB**

Sylvain Le Tonquesse, Swathi Sakthivel, and Frédérine Marie
*Laboratoire CRISMAT, CNRS UMR 6508, ENSICAEN, Normandie Université,
Caen 14050, France
sylvain.letonquesse@cnrs.fr*

The study of complex materials systems often demands the synthesis and characterization of numerous samples to achieve a comprehensive understanding. However, this process is hampered by the inherent challenges of solid-state synthesis, particularly its slow diffusion kinetics, which can require days to weeks to complete. Consequently, experimentalists often rely on experience-based decisions and trial-and-error optimization to determine new sample compositions or synthesis conditions. While effective for simple systems with few variables, such approaches become untenable as the number of parameters or the complexity of the compositional space grows. Bayesian Optimization (BO), an iterative and sample-efficient method, offers a promising solution to this challenge [1]. Despite its potential, BO remains largely underutilized in chemistry to guide experimental decisions, leveraging prior knowledge and past experimental results. This presentation introduces the principles of this Bayesian method and demonstrates its practical applicability in the laboratory through two complementary case studies: (1) the optimization of complex synthesis procedures, and (2) the determination of the stability region of a phase within a large compositional space.

The first case study demonstrates the optimization of synthesis conditions for $(\text{Mn}_x\text{Fe}_{1-x})_5\text{Si}_3$ magnetocaloric materials [2]. Conventional synthesis is challenging due to the narrow stability range of Fe_5Si_3 and the high vapor pressure of Mn. A magnesio-reduction process, which consists in reducing metal oxide precursors with Mg to form intermetallic phases, presents a promising solution. However, this method requires careful optimization of synthesis conditions to achieve phase-pure products. Using BO, seven synthesis parameters were optimized in just five iterations, yielding pure-phase products across the entire composition range.

The second case study addresses the efficient determination of the stability region for highly substituted Fe_3P ferromagnetic compounds [3]. A BO-inspired approach was developed to iteratively predict new compositions, specifically $(\text{Cr}_w\text{Mn}_x\text{Co}_y\text{Ni}_z\text{Fe}_{1-w-x-y-z})_3\text{P}$ ($0 \leq w+x+y+z \leq 0.6$), that maximizes information gain about stability boundaries in this high-dimensional space. In just five iterations and about 30 samples, the method reliably determined the stability region and produced a statistically robust dataset for analysing crystallographic and magnetic properties.

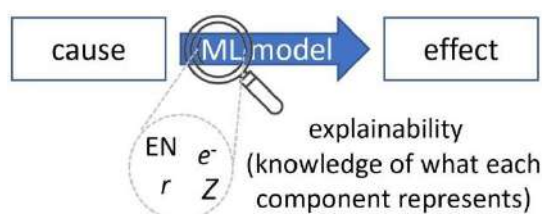
This work was carried out under the project “MagRota” funded by Normandy Region under the program “Normandie Recherche – Labels d'excellence” (n°23E06217) and the project “TexMag” (ANR-24-CE08-6242) funded by the Agence Nationale de la Recherche (ANR).

- [1] K. Wang, A.W. Dowling, *Curr. Opin. Chem. Eng.* 36 (2022) 100728.
- [2] S. Le Tonquesse, L. Agnarelli, S. Sakthivel, *Chem. Mater.* 37(15) (2025) 5740-5752.
- [3] J.V. Leitao, E. Brück, *Results Phys.* 4 (2014) 31-32.

MATERIALS INFORMATICS TOOLS FOR SUPERVISED AND UNSUPERVISED MACHINE LEARNING METHODS TO PREDICT CRYSTAL STRUCTURES

A. Oliynyk

Hunter College of the City University of New York, 695 Park Ave., New York, NY, 10065, USA
anton.oliiynyk@hunter.cuny.edu



Machine learning (ML) successfully predicts crystal structures with supervised methods, where training data has the structure type specified. For the last decade, the datasets of equiatomic compounds, Heusler, perovskites, and spinels have been used to test novel supervised algorithms and approaches. However, unsupervised ML for materials prediction is underexplored. To demonstrate the potential of unsupervised learning methods, a novel PuNi₃-type phase, TbIr₃, was predicted and synthesized, revealing how exploratory chemical decisions could be guided through ML [1]. We developed software to extract useful descriptors from crystallographic information in a high-throughput way to make them ready for unsupervised learning, where the machine needs to find out the differences between the structures on its own and predict the number of structure clusters. Our software focuses on explainable machine learning, with which we gain chemical insights in contrast to common black-box machine-learning methods. To expand the functionality of materials informatics tools, we automated traditional exploratory synthesis strategies with a recommendation engine that visualizes crystal structure trends and proposes the next best element to try when considering exploratory synthesis. Building up on the ML discovery success, we detail the discovery of a novel Gd–Ru–Cd phase, which is an excellent neutron absorber and a material with a negative thermal expansion [2].

- [1] S.S. Sethi, A. Dutta, E.I. Jaffal, N. Yadav, D. Shiryaev, B. Hoang, A. Machathi, S. Lee, K. Das, P.P. Jana, A.O. Oliynyk, *J. Am. Chem. Soc.* 147(17) (2025) 14739-14755.
- [2] B. Xhabrahimi, E.I. Jaffal, D. Shiryaev, N.K. Barua, M. Donohoe, N. Pozdnyakova, M. Ismail, B. Selvaratnam, E. Niknam, H. Kleinke, A.O. Oliynyk, *J. Am. Chem. Soc.* 147(40) (2025) 36589-36603.

NEW ASPECTS OF MERCURIDE STRUCTURAL CHEMISTRY

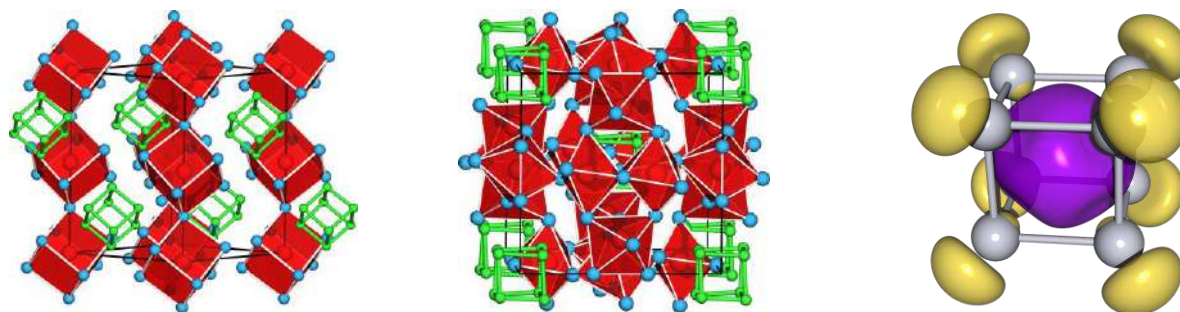
C. Hoch, L. Nusser, S. Feldl, T. Xu, and D. Kraut
Department of Chemistry, Ludwig-Maximilians-Universität München,
Butenandtstrasse 5-13 (D), 81377 München, Germany
c.hoch@lmu.de

The combination of mercury with the most reductive metals (alkaline, alkaline earth, lanthanoid metals) results in the formation of highly polar but still metallic amalgams [1-3], rather than mercuride anions. This is due to the close-shell electron $s^2d^{10}p^0$ configuration of the element.

Mercuride anions can however be stabilized in structures with high enough lattice energy, e.g. in double salts. The most stable anion, cubic $[\text{Hg}_8]^{6-}$, is present in a number of alkali metal mercuride oxides, such as $\text{Cs}_{18}\text{Hg}_8\text{O}_6$ [3], $\text{Cs}_8\text{Hg}_8\text{O}$, or $\text{Cs}_{58}[\text{Hg}_8]_6\text{O}_{12}$, and also in the mercuride iodide $\text{Cs}_7\text{Hg}_8\text{I}$. $[\text{Hg}_{12}]^{6-}$ anions can be found in $\text{Cs}_{14}[\text{Hg}_{12}]\text{O}_4$, and in $\text{Cs}_{14}\text{Hg}_{17}\text{O}_4$ large cluster units $[\text{Hg}_{18}]$ are connected to linear chains by sharing common vertices.

For $[\text{Hg}_8]^{6-}$, quantum mechanical calculations based both on extended solid-state and molecular models suggest that the stability of this unit can be understood in terms of a 3D aromatic system, where the main bonding contributions are based on Hg-6p interactions only. This model also explains the stability of the $[\text{Hg}_{12}]^{6-}$ anion and leads to postulate the existence of a square planar $[\text{Hg}_4]^{6-}$ anion.

All structures were established based on single-crystal and powder X-ray diffraction studies. Phase stability, phase formation, and phase transitions of alkali metal mercurides were studied with thermal analysis and vibrational spectroscopy. EPR spectroscopy shows the closed-shell diamagnetic character of the cluster anions. First experiments have shown that the anions can be solvated in liquid ammonia, and ^{199}Hg NMR and susceptibility measurements on solutions of mercuride anions are ongoing projects.



Unit cells of $\text{Cs}_7\text{Hg}_8\text{I}$ (left) and $\text{Cs}_{18}\text{Hg}_8\text{O}_6$ (centre) with cubic $[\text{Hg}_8]^{6-}$ anions (Cs: blue, Hg: green, O/I: centres of red polyhedra), and a depiction of the HOMO of the 3D aromatic system of $[\text{Hg}_8]^{6-}$ (right)

This work was supported by DFG (Deutsche Forschungsgesellschaft) under the project numbers 545158079 and 513247541.

- [1] H.J. Deiseroth, *Prog. Solid State Chem.* 25 (1997) 73-123.
- [2] M. Wendorff, C. Röhr, *Z. Kristallogr.* 233 (2018) 515-529.
- [3] T. Hohl, R.K. Kremer, S.G. Ebbinghaus, S.A. Khan, J. Minar, C. Hoch, *Inorg. Chem.* 62 (2023) 3965-3975.
- [4] L. Nusser, T. Hohl, F. Tambornino, C. Hoch, *Z. Anorg. Allg. Chem.* 648 (2022) e202100389.

ADVANCED *IN-SITU* TECHNIQUES FOR INVESTIGATION OF PLASTIC DEFORMATION OF HIGH-STRENGTH Mg ALLOYS

D. Drozdenko¹, A. Farkas¹, G. Farkas², P. Dobroň¹, J. Gubicza³, S.-I. Inoue⁴,
G. Garces⁵, K. Máthis¹, and Y. Kawamura⁴

¹ *Department of Physics of Materials, Faculty of Mathematics and Physics,
Charles University, Ke Karlovu 5, 12116 Praha, Czechia*

² *Nuclear Physics Institute, The Czech Academy of Sciences, Hlavní 130, 25068 Řež, Czechia*

³ *Department of Materials Physics, Faculty of Science, ELTE Eötvös Loránd University,
Pázmány P. sétány 1/A, H-1117 Budapest, Hungary*

⁴ *Magnesium Research Center, Kumamoto University, 2-39-1 Kurokami,
Chuo-ku, 860-8555 Kumamoto, Japan*

⁵ *Department of Physical Metallurgy, CENIM-CSIC, Avenida Gregorio del Amo 8,
Madrid, E-28040, Spain*

daria.drozdenko@matfyz.cuni.cz

The current demand for structural materials for engineering applications and the transportation industry requires the development of Mg alloys with enhanced properties. With the aim to improve the mechanical properties of Mg alloys (incl. strength and ductility), various Mg–Zn–RE alloys with long-period stacking ordered (LPSO) phases have recently been developed. These Mg-LPSO alloys have shown enhanced mechanical properties and promising high-temperature properties in comparison to conventional Mg alloys. Recent studies show that in such alloys, besides the dislocation slip, deformation twinning and kinking contribute to the plastic deformation. For the purpose of better biocompatibility and from an economic point of view, a reduction in the amount of RE alloying elements is desirable. To preserve good mechanical properties of Mg–Zn–RE alloys with a reduced RE content, optimization of their processing has to be considered. Among others, the rapidly solidified ribbon-consolidation (RSRC) technique has been found to be beneficial for achieving exceptional mechanical properties of Mg–Zn–RE alloys. Nevertheless, complex microstructures with solute-segregated stacking faults, cluster-arranged layers, and nanoplates, formed in both dynamically recrystallized (DRX) and non-DRX grains, bring a change in active deformation mechanisms compared to those active in Mg-LPSO alloys.

Advanced *in-situ* techniques provide new insights into the dynamics of the dislocation slip, twinning, and kinking processes in Mg-LPSO alloys. Particularly, the combination of *in-situ* techniques (namely acoustic emission (AE), neutron or synchrotron diffraction) with electron microscopy (EM) observations brings essential information about active deformation mechanisms. The AE response particularly provides *in-situ* insight into the temporal evolution and interaction of deformation mechanisms, while EM and diffraction measurements confirm their presence.

THE BEAUTY OF IMPERFECTION: DEFECTS, DISORDER, AND PERFORMANCE IN BATTERY MATERIALS

J. Serrano-Sevillano¹, M. Reynaud¹, A. Saracibar², D. Saurel¹, and M. Casas-Cabanas¹

¹ *CIC energiGUNE, Basque Research and Technology Alliance (BRTA),*

Albert Einstein 48, 01510 Vitoria-Gasteiz, Spain

² *Physical Chemistry Department, Pharmacy Faculty, Basque Country University,*

Vitoria-Gasteiz, Álava, Spain

jserrano@cicenergigune.com

Battery materials are often introduced through ideal crystal structures, but working electrodes are better described as imperfect solids in which departures from periodicity control ion and electron transport, phase transformations, and degradation [1]. This contribution will discuss why defects should be considered not only as unavoidable imperfections, but also as structural descriptors and, in selected cases, design variables for energy-storage materials. This contribution will discuss this idea using representative examples from lithium- and sodium-ion battery electrodes to show how point defects, cation disorder, anti-phase domains, stacking faults, and/or intergrowths can modify electrochemical response.

That the same word, “defect” may refer to very different length scales and physical effects. In olivine phosphates, antisite defects can block fast Li⁺ diffusion pathways; in high-voltage spinels such as LiNi_{0.5}Mn_{1.5}O₄, Ni/Mn ordering and anti-phase domains influence rate capability; in Li- and Na-rich layered oxides such as Li₂MnO₃ and Na₂RuO₃, stacking faults can alter activation and degradation pathways; and in manganese oxides or graphitic carbons, intergrowths and turbostratic disorder define the real structure more accurately than a single average unit cell [2,3]. These examples illustrate that defects are not always detrimental, but they must be identified, quantified, and correlated with electrochemical behaviour.

Particular emphasis will be placed on powder diffraction approaches implemented in FAULTS, where the material is described as a probabilistic stack of layers rather than as a perfect three-dimensional periodic crystal [4]. Combined with complementary techniques such as solid-state NMR, electron microscopy, and *operando* diffraction, this strategy provides access to quantitative descriptors such as stacking-fault probability, domain size, and intergrowth fraction. By connecting these descriptors to electrochemical performance, defect characterization becomes a practical route towards rational microstructural control and defect engineering in battery materials.

- [1] M. Reynaud, J. Serrano-Sevillano, M. Casas-Cabanas, *Chem. Mater.* 35 (2023) 3345-3363.
- [2] B. Mortemard de Boisse, M. Reynaud, J. Ma, J. Kikkawa, S.-i. Nishimura, M. Casas-Cabanas, C. Delmas, M. Okubo, A. Yamada, *Nat. Commun.* 10 (2019) 2185.
- [3] J. Serrano-Sevillano, M. Reynaud, A. Saracibar, T. Altantzis, S. Bals, G. Van Tendeloo, M. Casas-Cabanas, *Phys. Chem. Chem. Phys.* 20 (2018) 23112-23122.
- [4] M. Casas-Cabanas, M. Reynaud, J. Rikarte, P. Horbach, J. Rodríguez-Carvajal, *J. Appl. Crystallogr.* 49 (2016) 2259-2269.

PEROVSKITE-BASED MATERIALS AS INNOVATIVE ELECTRODES FOR INTERMEDIATE-TEMPERATURE SOLID OXIDE CELLS

Marcella Pani^{1,2}, Cristina Artini^{1,4}, Paola Costamagna¹, Sara Massardo³, Sabrina Presto³,
and Massimo Viviani³

¹ DCCI, University of Genoa, Via Dodecaneso 31, 16146 Genoa, Italy

² Institute CNR-SPIN, Corso Perrone 24, 16152 Genoa, Italy

³ Institute CNR-ICMATE, c/o DICCA, University of Genoa, Via all'Opera Pia 15,
16145 Genoa, Italy

⁴ Institute CNR-ICMATE, Via De Marini 6, 16149 Genoa, Italy
marcella.pani@unige.it

Solid oxide cells (SOC), functioning both as energy production means in direct mode and for hydrogen production in reverse mode, represent a class of devices considered essential to the energy transition [1]. The current challenge to develop this technology stands in the stability and compatibility of the different materials, and in the reduction of the working temperature range.

In this work, different perovskite-based MIEC (Mixed Ionic-Electronic Conductor) materials have been studied for their potential application as electrodes in intermediate temperature cells (IT-SOC, $T = 800-1000$ °C), and reversible solid oxide cells (RSOC).

The system $\text{La}_{1-x}\text{Sr}_x\text{Ti}_y\text{Fe}_{1-y}\text{O}_{3-d}$ (LSTF [2]) has been investigated for different La/Sr and Ti/Fe ratios since this material can act both as a fuel-side and air-side electrode in solid oxide fuel cells (SOFC), as well as in solid oxide electrolysis cells (SOEC). Doping LSTF with Ni [3] and the effect on the electrochemical features in both reducing and oxidizing conditions has also been explored.

The system $\text{Ba}_{1-x}\text{Sr}_x\text{Cu}_y\text{Fe}_{1-y}\text{O}_{3-d}$ (BSCuF) has been investigated since it represents a promising Co-free alternative to the widely studied BSCF (Barium Strontium Cobalt Iron Oxide) as air electrode for SOC. Since cobalt substitution is crucial due to its toxicity and supply limitations, Cu has been introduced as an alternative [4]. Although the replacement of Co by Cu typically lowers the electrochemical performance, particularly in terms of oxygen reduction reaction (ORR) activity, structural and electrochemical properties of BSCuF demonstrate its compatibility with ceria-based electrolytes and its potential as an environmentally sustainable air electrode material. Additionally, beneficial effects were observed when doping BSCuF with yttrium, which helps prevent secondary phase formation without compromising catalytic and electrochemical performance [5].

The Italian Ministry of Environment and Energy Sustainability (MASE) is gratefully acknowledged for funding the project "RSH2A_000018 (CUP: F57G25000180006) in the frame of the European Union Next-GenerationEU, Piano Nazionale di Ripresa e Resilienza (PNRR) – Missione 2 "Rivoluzione verde e transizione ecologica", Componente 2 "Energia rinnovabile, idrogeno, rete e mobilità sostenibile", Investimento 3.5 "Ricerca e sviluppo sull'idrogeno" (M2C2I3.5, bando A).

[1] L. Gauckler *et al.*, *Chimia* 58 (2004) 837-850.

[2] L. Liu *et al.*, *ACS Appl. Energy Mater.* 6 (2023) 841-855.

[3] M.B. Hanif *et al.*, *J. Power Sources* 472 (2020) 228498.

[4] K. Song *et al.*, *Ceram. Int.* 38 (2012) 5123-5131.

[5] L. Navarrete *et al.*, *Solid State Ionics* 376 (2022) 115851.

MATERIAL CONTROL AND CONTROLLED MATERIALS IN HETEROGENEOUS CATALYSIS

M. Armbrüster

*Eduard Zintl Institute, Technical University Darmstadt,
Karolinenplatz 5, 64289 Darmstadt, Germany
marc.armbruester@tu-darmstadt.de*

Changing our energy supply towards a renewable and sustainable energy scenario requires the storage and transport of large amounts of renewable energy. Due to their high chemical storage capacity for hydrogen, small molecules like CH₄, NH₃ or methanol are promising candidates. Methanol is liquid at normal conditions and possesses a high volumetric and gravimetric energy density [1]. To release the hydrogen on demand, methanol steam reforming can be applied ($\text{CH}_3\text{OH} + \text{H}_2\text{O} \rightarrow 3 \text{H}_2 + \text{CO}_2$). Since the identification of ZnPd/ZnO as a highly selective catalyst [2], it could be shown that high selectivity is achieved only if ZnPd and ZnO are present [3]. While the necessity could be shown, it is still unclear how the phases contribute to the catalytic cycle.

Recent material development led to the discovery of the very active and selective aerogel-based materials In–Pt/In₂O₃ and In–Pd/In₂O₃ [4,5]. To clarify active phases, the oxide-metal interplay and the role of the oxidic species in the catalysis, numerous *in situ* and *operando* methods as well as isotope-labelling of the reactants, were conducted. This resulted in the detection of a Mars-van-Krevelen mechanism, the involvement of oxygen vacancies in the catalytic cycle as well as a delicate interplay between the oxygen potential of the atmosphere and the phases present in the catalyst. In addition, the underlying reason for the deactivation of the materials could be revealed, opening the possibility for further development of materials – also for methanol synthesis – thus contributing to the energy turnaround.

- [1] F. Asinger, *Methanol – Chemie- und Energierohstoff*, Springer, Berlin and Heidelberg, 1986.
- [2] N. Iwasa *et al.*, *Catal. Lett.* 54 (1998) 119.
- [3] M. Friedrich *et al.*, *J. Catal.* 285 (2012) 41.
- [4] N. Köwitsch *et al.*, *J. Phys. Chem. C* 125 (2021) 9809.
- [5] N. Köwitsch *et al.*, *ACS Catal.* 11 (2021) 304.

***d*-ELEMENT-BASED THERMOELECTRICITY**

F. Garmroudi¹, M. Parzer¹, L. Salamakha¹, J. Kovacevic¹, O. Sologhub¹,
T. Mori², and E. Bauer¹

¹ *Institute of Solid State Physics, Technische Universität Wien, A-1040 Wien, Austria*

² *National Institute for Materials Science (NIMS), Namiki 1-1, Tsukuba 305-0044, Japan*
bauer@ifp.tuwien.ac.at

Thermoelectricity is the ability of materials to convert temperature gradients along a piece of a solid into electricity. It is based on the Seebeck effect, and further, on the electrical resistivity and thermal conductivity of this material. Its thermoelectric performance can be classified by the thermoelectric power factor $PF = S^2/\rho$ and by the thermoelectric figure of merit $ZT = S^2T/(\rho\lambda)$, where S , ρ , λ , are the Seebeck coefficient, the electrical resistivity and the thermal conductivity, respectively. T is the absolute temperature. Materials considered for thermoelectric applications usually exhibit values $ZT \sim 1$ (or above).

Right now, the only commercially available materials are based on Bi_2Te_3 systems and are characterised as strongly degenerate semiconductors. Although this material family forms excellent thermoelectrics, it, however, like other high-performance materials based on SnSe, PbTe, Zn_4Sb_3 (to name just a few), contains – in part – toxic and rare elements with weak mechanical and chemical stability, making scalability and sustainability for mass production of thermoelectric devices rather unlikely.

Referring to the latter and avoiding all kinds of weaknesses in terms of chemical, mechanical, and thermodynamical properties, thermoelectric materials based on *d*-elements offer excellent alternatives to the above-mentioned materials. In this contribution, a survey is given on mostly semimetallic and semiconducting half-Heusler and full-Heusler systems, as well as on more metallic systems (*e.g.*, Ni_3Ge) where large values of the Seebeck coefficient can be found due to the presence of a large logarithmic energy derivative of the electronic density of states (eDOS) near the Fermi energy E_F . While for the former, the gap of the eDOS in the proximity of E_F provides such a condition, narrow *d*-electron-based features near E_F are the reason for unexpectedly large Seebeck values of these materials. Experimental data of these systems will be analysed in terms of DFT-based calculations and phenomenological solid-state physics models, allowing a better understanding of procedures to further enhance the thermoelectric performance.

Work supported by the Japanese JST project MIRAI.

UTe₂ UNDER EXTREME CONDITIONS: INSIGHTS INTO ITS COMPLEX SUPERCONDUCTING PHASE DIAGRAM

M. Vališka¹, T. Haidamak¹, A. Cabala¹, J. Pospíšil¹, V. Sechovský¹, J. Prokleška¹,
A. Hauspurg², and S. Zherlitsyn²

¹ *Department of Condensed Matter Physics, Faculty of Mathematics and Physics,
Charles University, Ke Karlovu 5, 121 16 Prague 2, Czechia*

² *Hochfeld-Magnetlabor Dresden (HLD-EMFL), Helmholtz-Zentrum Dresden-Rossendorf,
01328 Dresden, Germany
michal.valiska@gmail.com*

Uranium ditelluride (UTe₂) has emerged as one of the most intensively studied unconventional superconductors owing to its remarkably rich phase diagram and its possible spin-triplet pairing. Its superconducting state is exceptionally sensitive to external parameters, including magnetic field strength and orientation, pressure, and sample quality, resulting in multiple superconducting regions and additional field-induced phases. These properties make UTe₂ a unique platform for investigating the interplay between superconductivity, magnetism, lattice effects, and electronic structure.

An overview of the current understanding of the UTe₂ phase diagram under extreme conditions is presented, with particular emphasis on studies performed in high magnetic fields and under pressure. It is shown how thermodynamic, transport, magnetic, and elastic probes have revealed the complex evolution of superconductivity, including the relationship between low-field and high-field superconducting phases and the appearance of additional anomalies within the superconducting state. Particular attention is devoted to the strong coupling between the lattice, magnetic fluctuations, and superconductivity, as well as to the crucial role of crystal quality in resolving the intrinsic properties of the material. Altogether, these results establish UTe₂ as an exceptional platform for uncovering new superconducting phenomena and for addressing open questions concerning the nature of its order parameter and the origin of its exotic phases.

MULTI-SCALE INTERFACE DESIGN TO ACHIEVE HIGH-PERFORMANCE CONVERSION EFFICIENCY IN Mg-BASED THERMOELECTRIC DEVICES

Xiaoyuan Li¹, Kaiyu Yang¹, Kai Guo², Yusong Du¹, and Jingtai Zhao¹

¹ *School of Materials Science and Engineering, Guilin University of Electronic Technology, Guilin 541004, China*

² *School of Physics and Materials Science, Guangzhou University, Guangzhou 510006, China*
jtzhao@guet.edu.cn

Mg₃(Sb,Bi)₂ alloys have emerged as a promising alternative to commercial Bi₂Te₃-based thermoelectrics, owing to their excellent thermoelectric performance, cost-effectiveness, and environmentally friendly nature. However, the average zT_{ave} of n-type Mg₃(Sb,Bi)₂ materials is over a wide temperature range significantly constrained by thermally-activated conduction behaviour. In our work, an innovative and simple approach by leveraging the work function principle to design anti-barrier layers for electrons through metal-semiconductor contact engineering is proposed. Specifically, nano-scale tungsten (W) and molybdenum (Mo) particles, which possess a lower work function than the Mg₃(Sb,Bi)₂ matrix, were incorporated as composite materials. The zT_{ave} of the W-doped sample in the 323~773 K range reached 1.34, representing about 36.7 % increase over the undoped sample and ranking among the highest values for Mg₃(Sb,Bi)₂ alloys. Based on the obtained samples, a segmented thermoelectric power-generation device utilizing p-type (BST)₉₇(FeTe₂)₃ and (Ge_{0.91}Sb_{0.09}Te)_{0.99}(InSe)_{0.01} was designed and prepared. When the relative current density (u) and the compatibility factor (s) are well-aligned, the system will operate approaching its maximum efficiency according to the COMSOL simulation results. The typical barrier layer materials, nickel (Ni) and titanium (Ti), were employed in the thermoelectric legs of the thermoelectric device, showing high interface stability and low interface resistivity. At $\Delta T = 440$ K, this device achieved a maximum conversion efficiency of 10.4 % and a peak output power of 0.41 W. These results establish a solid foundation for the development of efficient thermoelectric material combinations.

- [1] X. Li, Y. Du, K.-Y. Yang, S. Li, J. Zhang, L. Li, J. Xing, G.-H. Rao, J.-T. Zhao, K. Guo, *Adv. Funct. Mater.* (2025) e12586.
- [2] K.-Y. Yang, X. Li, Y. Jiang, L. Wang, K. Guo, L. Miao, J. Chen, J. Zhang, L. Li, Y. Du, G.-H. Rao, J. Luo, J.-T. Zhao, *Adv. Sci.* 12 (2025) 2502832.

EARTH-ABUNDANT THERMOELECTRICS: FROM MATERIALS DEVELOPMENT TO DEVICE INTEGRATION

Antonio Pereira Gonçalves

*Centro de Física e Engenharia de Materiais Avançados (CeFEMA), DECN,
Instituto Superior Técnico, Universidade de Lisboa,
Estrada Nacional 10, 2695-066 Bobadela LRS, Portugal
apg@ctn.tecnico.ulisboa.pt*

The increasing demand for sustainable energy has fostered interest in thermoelectric (TE) technologies, which enable the direct conversion of heat into electricity and *vice versa*. Despite their advantages (such as solid-state operation, no noise, reliability, and scalability), the use of TEs remains limited. A main barrier is the dependence on scarce, expensive, or toxic elements (*e.g.*, Te or Pb) in commercial materials. This has motivated extensive research into earth-abundant, low-cost, and environment-friendly alternatives.

In recent years, significant progress was made in the development of sustainable TE materials. Among these, tetrahedrites and magnesium-based compounds have emerged as particularly promising candidates. Tetrahedrites, composed of abundant and relatively non-toxic elements, exhibit intrinsically low thermal conductivity due to a complex crystal structure, making them attractive for TE applications. Similarly, Mg-based materials, including Mg₂Si and its alloys, offer advantages such as low density, abundance, and good performance at intermediate temperatures. Various approaches, like doping, band engineering, nanostructuring, and defect control, were successfully employed to enhance TE efficiency.

Beyond their discovery, the transition from laboratory materials to devices is a critical step toward real-world applications. This involves challenges related to material processing, chemical and mechanical stability, scalability, and long-term performance. Powder metallurgy, thin-film deposition, and additive manufacturing were explored to fabricate high-quality TE elements. In parallel, the development of suitable electrical contacts, diffusion barriers, protective coatings, and stability under thermal cycling is essential.

This presentation gives an overview of the research in earth-abundant TE materials, highlighting the main advances in tetrahedrites and Mg-based systems. It also discusses the key challenges and strategies associated with scaling up from materials to device fabrication. By addressing both fundamental and applied aspects, this work aims to contribute to the advance of sustainable TE technologies able to support the global transition toward cleaner and more efficient energy systems.

This work was partially supported by Horizon Europe through the Marie Skłodowska-Curie Actions programme “MaGnesium Alloys for effiCient solId stAte cooliNg”, grant agreement ID 101227508.

**THERMODYNAMIC AND ELECTRICAL TRANSPORT PROPERTIES
OF NEW REPRESENTATIVES OF THE NODAL-LINE SEMIMETAL
SERIES *LnSbTe***

Grzegorz Chajewski, Tetiana Romanova, Sami Elgalal, and Dariusz Kaczorowski
Institute of Low Temperature and Structure Research, Polish Academy of Sciences,
Okólna 2, 50-422 Wrocław, Poland
d.kaczorowski@intibs.pl

The lanthanide-based *LnSbTe* series represents a family of tetragonal ZrSiS-type semimetals hosting symmetry-protected nodal-line Dirac states, which emerge from the intricate interplay of nonsymmorphic crystal symmetry, spin-orbit coupling, long-range magnetism, and strong *4f*-electron correlations. Building on angle-resolved photoemission spectroscopy (ARPES) studies that established the non-trivial topological character of DySbTe and ErSbTe [1,2], this work explores their thermodynamic and electrical transport behaviour. At zero magnetic field, DySbTe exhibits two successive antiferromagnetic transitions and semimetallic-like transport, characterized by anomalous features within the ordered state. In contrast, while ErSbTe also displays two magnetic transitions, its electrical resistivity lacks the “hump-like” feature typical of other *LnSbTe* analogues, suggesting distinct charge carrier scattering mechanisms. Field-dependent specific heat measurements reveal a complex evolution of the magnetic order in both compounds, indicating rich magnetic phase diagrams. These results provide a macroscopic counterpart to the existing ARPES data, demonstrating how lanthanide magnetism and square-net lattice symmetry govern the unique physical behaviour in these antiferromagnetic nodal-line semimetals.

This work was supported by the National Science Centre (Poland) under research grant No. 2021/41/B/ST3/01141.

- [1] N. Valadez, I.B. Elius, D. James, P. Radanovich, T. Romanova, S. Elgalal, G. Chajewski, F. Masple, E. Thompson, K.T. Chu, M. Yankowitz, A. Ptok, D. Kaczorowski, M. Neupane, *Phys. Rev. B* 112 (2025) 155148.
- [2] I.B. Elius, N. Valadez, D. James, P. Radanovich, S. Elgalal, G. Chajewski, T. Romanova, A. Ptok, D. Kaczorowski, M. Neupane, *Phys. Rev. Mater.* 9 (2025) 114201.

**TOWARDS A BETTER COMPREHENSION OF THE HYDROGEN ABSORPTION
MECHANISM IN HIGH-ENTROPY MULTICOMPONENT ALLOYS OF
HfTiNbVZr COMPOSITION**

Maria Moussa^{1,2}, Jacques Huot², and Jean-Louis Bobet¹

¹ *University Bordeaux, CNRS, Bordeaux INP, ICMCB, UMR 5026, 33600 Pessac, France*

² *Hydrogen Research Institute, Université du Québec à Trois-Rivières, 3351 des Forges,
Trois-Rivières, Quebec, G9A 5H7, Canada
jean-louis.bobet@cnrs.fr*

The structural characterization and hydrogen sorption properties of different high-entropy alloys having the composition $\text{Hf}_{1-x}\text{Ti}_x\text{NbVZr}$ ($x = 0, 0.25, 0.5, 0.75, \text{ and } 1$) have been studied. These alloys were prepared using two different techniques: arc melting and induction melting. Some thermal treatments were also conducted to verify the stability of the materials. Our study showed that the synthesis method (as well as the thermal treatment) and the chemical composition had an effect on the crystal structure and the microstructure of the alloys. The sorption conditions (absorption at room temperature and under 20 bars of hydrogen) were found to be favourable for the activation of the alloys, except for the compositions $\text{Hf}_{0.25}\text{Ti}_{0.75}\text{NbVZr}$ ($x = 0.75$) and TiNbVZr ($x = 1$), synthesized by induction melting. For the entire compositional range studied, the amount of hydrogen absorbed is close to $H/M = 2$. The effect of heat treatment on the phase stability and hydrogen storage capacity within the $\text{Hf}_{0.75}\text{Ti}_{0.25}\text{NbVZr}$ and TiNbVZr alloys were studied. Heat treatment changes the phase composition and reduces the abundance of the body-centred cubic phase (BCC), resulting in (i) a decrease in the hydrogen storage capacity and (ii) an increase in the temperature required for activation.

NONLINEAR TRANSPORT IN THE WEYL-KONDO SEMIMETAL $\text{Ce}_3\text{Bi}_4\text{Pd}_3$

M. Lužnik¹, M. Taupin^{1,4}, X. Yan¹, A. Prokofiev¹, L. Mangeolle^{2,3}, G. Le Roy¹,
and S. Paschen¹

¹ *Institute of Solid State Physics, TU Wien, Wiedner Hauptstr. 8-10, 1040 Vienna, Austria*

² *Physics Department, TUM School of Natural Sciences, Technical University of Munich,
85748 Garching, Germany*

³ *Munich Center for Quantum Science and Technology (MCQST), Schellingstr. 4,
80799 Munich, Germany*

⁴ *present address: Laboratoire National de Métrologie et d'Essais,
29 avenue Roger Hennequin, 78197 Trappes, France
budnowski@ifp.tuwien.ac.at*

In recent years, semimetals with nontrivial topology have attracted considerable interest due to their unconventional transport properties. In particular, nonlinear transverse transport responses can be observed even in time-reversal symmetric systems, which can be related to the Berry curvature of the electronic bands [1].

A notable example is the class of Weyl-Kondo semimetals, with $\text{Ce}_3\text{Bi}_4\text{Pd}_3$ being the first experimentally obtained material [2]. In these systems, the interplay between strong electronic correlations and nontrivial band topology leads to the incorporation of Weyl nodes into the Kondo resonance, thereby strongly enhancing Berry curvature effects [2-5]. Consistent with this picture, $\text{Ce}_3\text{Bi}_4\text{Pd}_3$ exhibits a giant zero-field nonlinear Hall effect [5]. A comparison with noninteracting topological semimetals of similar carrier concentration shows that strong correlations enhance the nonlinear Hall response by several orders of magnitude [6]. This makes $\text{Ce}_3\text{Bi}_4\text{Pd}_3$ an ideal platform for investigating other topological nonlinear transport phenomena [7].

The work was supported by the European Research Council (ERC Advanced Grant 101055088 “CorMeTop”), the Austrian Science Fund (FWF grants SFB F86 “Q-M&S”, I5868-N/FOR5249 “QUAST”, 10.55776/COE1 “quantA”), and the Air Force Office of Scientific Research (AFOSR project No. FA8655-24-1-7018).

- [1] I. Sodemann, L. Fu, *Phys. Rev. Lett.* 115 (2015) 216806.
- [2] S. Dzsaber *et al.*, *Phys. Rev. Lett.* 118 (2017) 246601.
- [3] H.-H. Lai *et al.*, *Proc. Natl Acad. Sci. USA* 115 (2018) 93.
- [4] S.E. Grefe *et al.*, *Phys. Rev. B* 101 (2020) 075138.
- [5] S. Dzsaber *et al.*, *Proc. Natl. Acad. Sci. USA* 118 (2021) e2013386118.
- [6] D.M. Kirschbaum, M. Lužnik *et al.*, *J. Phys. Mater.* 7 (2024) 012003.
- [7] M. Lužnik *et al.*, submitted.

PRESSURE EFFECTS ON A HIGH-ENTROPY ALLOY AND INTERACTIONS IN PROTOTYPIC METALLOCENES

A. Katrusiak¹ and Ł. Rogal²

¹ Department of Materials Chemistry, Faculty of Chemistry, Adam Mickiewicz University, Uniwersytetu Poznańskiego 8, 61-614 Poznań, Poland

² Institute of Metallurgy and Materials Science, Polish Academy of Sciences, Reymonta St. 25, 30-059 Krakow, Poland
katran@amu.edu.pl

The phase stability and decomposition of a high-entropy alloy, Ti₄₀Zr₂₀Nb₂₀Hf₅Ta₁₅ (at.%), under extreme pressure and temperature were investigated using a laser-heated diamond anvil cell (DAC), X-ray diffraction, and selected-area electron diffraction, combined with chemical analysis by high-angle annular dark-field imaging. The initial body-centred cubic (*bcc*) solid solution persists to 34 GPa, whereas on heating it transforms into a multiphase mixture. After pressure release, the recovered microstructure decomposed into sub-microcrystalline Ti-rich *hcp* regions, separated by nanocrystalline Ta- and Nb-containing *bcc/bct* layers and Zr-rich *hcp* phases. This transformation is attributed to pressure-induced shear-assisted diffusional segregation. Simultaneous high-pressure, high-temperature, and reactive-nitrogen conditions were further examined at approximately 2500 K and 32 GPa, causing the precursor *bcc* alloy to decompose and react with nitrogen, yielding several multicomponent high-entropy nitride phases, with grain sizes between 20 and 300 nm. This segregation reflects different chemical affinities of the constituent elements toward nitrogen and demonstrates that extreme pressure-temperature conditions can drive the decomposition of chemically homogeneous high-entropy alloys into complex, nanostructured multiphase systems.

In another study, weak cohesion forces in metal-organic compounds were investigated. They affect the crystal structures of prototypic sandwich compounds. Following the discovery of ferrocene in 1951, its phase I at room temperature, phase II below 164 K and phase III were determined until the early 1980s. For ruthenocene and osmocene, only the structures isostructural with ferrocene phase III were found. We revealed a new ferrocene phase I' above 3.2 GPa [1], and a new modulated phase I'' between 172.9 and 163.5 K [2]. For ruthenocene [3] and osmocene [4], new high-pressure and high-temperature phases were also evidenced above 394.0 K and 421.5 K, respectively [5], which led to consistent phase diagrams of the prototypic metallocenes, strongly dependent on relatively weak CH \cdots π and CH \cdots metal forces.

This research was supported by the National Science Centre, Poland, project OPUS, No. 2021/41/B/ST8/03758 entitled: Development of new high entropy nitrides composites synthesized at high pressure and temperature.

- [1] D. Paliwoda, K. Kowalska, M. Hanfland, A. Katrusiak, *J. Phys. Chem. Lett.* 4 (2013) 4032-4037.
- [2] A. Katrusiak, M. Rusek, M. Dušek, V. Petříček, M. Szafranski, *J. Phys. Chem. Lett.* 14 (2023) 3111-3119.
- [3] I. Moszczyńska, A. Katrusiak, *J. Phys. Chem. C* 126 (2022) 5028-5035.
- [4] I. Moszczyńska, I. Gulaczyk, A. Katrusiak, *J. Phys. Chem. C* 127 (2023) 19250-19257.
- [5] I. Moszczyńska, M. Szafranski, A. Katrusiak, *J. Phys. Chem. Lett.* 16 (2025) 5755-5762.

CRYSTALLOGRAPHIC FRUSTRATION AS A MEANS TO INDUCE COMPLEX SPIN TEXTURES TOWARD NEW QUANTUM MATERIALS

Y.-X. Wang^{1,2}, I. Campbell¹, X. Wang³, and M. Shatruk^{1,4}

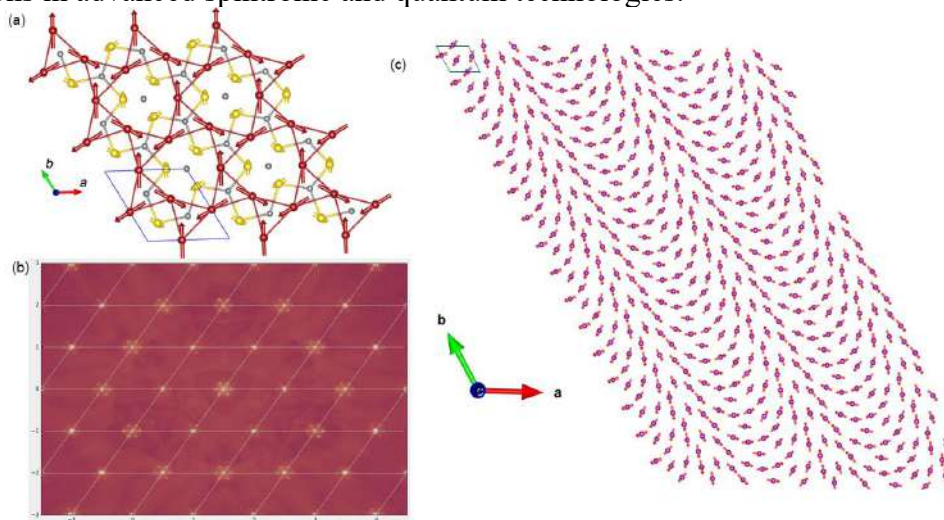
¹ Dept. of Chemistry & Biochemistry, Florida State University, Tallahassee, FL 32306, USA

² Institute of Inorganic Chemistry, RWTH Aachen University, 52056 Aachen, Germany

³ Neutron Scattering Division, Oak Ridge National Laboratory, Oak Ridge, TN 37831, USA

⁴ FSU Quantum Initiative, Florida State University, Tallahassee, FL 32306, USA
shatruk@chem.fsu.edu

Materials with intricate spin textures are attractive from both fundamental and practical perspectives [1,2]. The complex patterns of magnetic moments that develop on crystal lattices could enable reliable information storage and processing, including applications in topological quantum computing. In this work, we report the discovery of a complex, skyrmionic-like spin texture in a non-centrosymmetric material, $\text{MnCoGe}_{1/3}\text{As}_{2/3}$ [3]. This compound arises from structural frustration at the interface between centrosymmetric parent structures of MnCoGe and MnCoAs . Our results demonstrate that this type of structural frustration is a useful indicator for spotting compositional regions where intricate magnetic behavior and associated non-trivial magnetic structures are likely to develop. Specifically, $\text{MnCoGe}_{1/3}\text{As}_{2/3}$ displays a modulated cycloidal antiferromagnetic arrangement of electron spins on a non-centrosymmetric hexagonal lattice of the ZrNiAl -type structure. This work establishes a novel approach for discovering materials with exotic spin textures for potential applications in advanced spintronic and quantum technologies.



The non-collinear magnetic structures of $\text{MnCoGe}_{1/3}\text{As}_{2/3}$. The commensurate structure (a) observed at higher temperatures is converted to an incommensurate cycloidal structure (b,c) observed at lower temperatures.

This work was supported by the U.S. National Science Foundation (grant DMR-2233902).

[1] L. Balents, *Nature* 464 (2010) 199-208.

[2] N. Kanazawa, S. Seki, Y. Tokura, *Adv. Mater.* 29 (2017) 1603227.

[3] Y.-X. Wang, I. Campbell, Z. Tener *et al.*, *J. Am. Chem. Soc.* 147 (2025) 43550-43559.

POLARITY-EXTENDED 8- N_{eff} RULE FOR Cu-CHALCOPYRITE MATERIALS

R. Freccero, G. Palla, F. Tonet, and D. Colombara

Department of Chemistry and Industrial Chemistry, University of Genoa,

via Dodecaneso 31, 16146, Genoa, Italy

riccardo.freccero@unige.it

Semiconductors play a pivotal role in technological innovation, including the development of systems essential for achieving climate neutrality. Over the last decades, research has increasingly focused on chalcopyrite-based materials, particularly for their promising thermoelectric [1] and photovoltaic applications [2]. Despite extensive efforts devoted to understanding and improving their physical properties, comparatively few studies have investigated the nature of chemical bonding in these compounds [3,4]. This work focuses on the $CuECh_2$ ($E = Al, Ga, In, Tl$; $Ch = S, Se, Te$) compounds, all crystallizing with the $tI12-CuFeS_2$ (space group $I\bar{4}2d$; No. 122) structure, related by symmetry reduction to the diamond aristotype. As a consequence, all atomic species exhibit tetrahedral-like environments, both homoleptic ($Cu@Ch_4, E@Ch_4$) and heteroleptic ($Se@Cu_2E_2$). Due to these structural features, the bonding is typically described as polar-covalent, with atomic charges still treated in terms of oxidation states ($Cu^+)(E^{3+})(Ch^{2-})$. Here, we provide a consistent and quantitative bonding picture by means of quantum-chemical techniques in position space based on the Bader's Quantum Theory for Atoms In Molecules (QTAIM) and the Electron Localizability Indicator (ELI-D). The ELI-D distribution shows four maxima along the $Ch-E$ and $Ch-Cu$ contacts, interpreted as polar-covalent interactions based on the ELI-D/QTAIM basin intersections, with the $Ch-E$ bonds being more covalent. Based on these results, the overall bonding scenario is described by applying the polarity-extended 8- N rule in position space, previously employed for semiconducting main-group compounds of the cubic $MgAgAs$ and $TiNiSi$ types [5,6]. Each heteropolar $Ch-E$ and $Ch-Cu$ interaction is decomposed into two-electron covalent bonds (N_{cb}) and (hidden) lone-pair (N_{lp}), which quantify the covalent and polar contributions, respectively. These sum up to 4, thus fulfilling the octet rule. The nature of the chalcogenide species has the main influence on the number of covalent bonds per Ch atom, $N_{cb}(Ch)$, amounting to approximately 1.10, 1.25, and 1.50 for sulfides, selenides, and tellurides, respectively. The studied compounds exhibit a substantial deviation from the limiting scenarios of purely ionic or purely covalent interactions, corresponding to $N_{cb}(Ch)$ values of 0 and 4, respectively. These results enable further investigations into the effects of point defects and extrinsic alkali-ion doping on chemical bonding, essential for the rational design of photovoltaic materials, particularly based on $CuGaSe_2$ and $CuInSe_2$.

This work was carried out under the project of national relevance (PRIN 2022) LEGACY (healing wide-gap chalcopyrite, grant No. 20223ZP4WP).

- [1] H. Xie, S. Hao, S. Cai, T.P. Bailey, C. Uher, C. Wolverton, V.P. Dravid, M.G. Kanatzidis, *Energy Environ. Sci.* 13 (2020) 3693-3705.
- [2] D. Colombara, K. Conley, M. Malitckaya, H.-P. Komsa, M.J. Puska, *J. Mater. Chem. A* 8 (2020) 6471-6479.
- [3] J.E. Jaffe, A. Zunger, *Phys. Rev. B* 28 (1983) 5822.
- [4] T. Maeda, T. Wada, *Jpn. J. Appl. Phys.* 49 (2010) 04DP07.
- [5] D. Bende, F.R. Wanger, Yu. Grin, *Inorg. Chem.* 54(8) (2015) 3970-3978.
- [6] R. Freccero, Yu. Grin, F.R. Wagner, *Dalton Trans.* 52 (2023) 8222-8236.

MATERIALS CHARACTERIZATION USING POWDER DIFFRACTION TECHNIQUES AND THE POWDER DIFFRACTION FILE AND MATERIAL PHASES DATA SYSTEM DATABASES

T. Blanton¹ and R. Caputo²

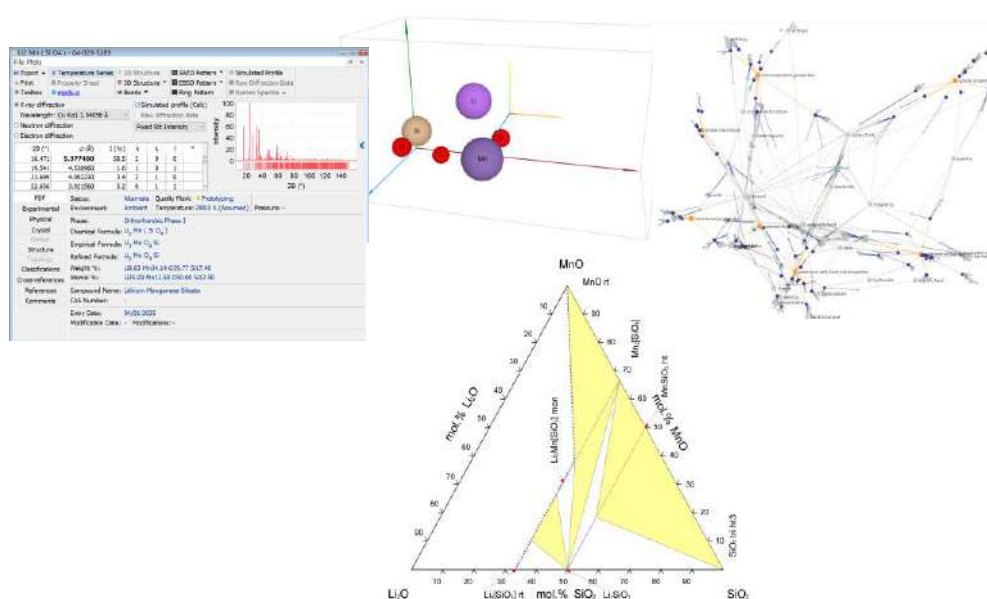
¹ International Centre for Diffraction Data, Newtown Square, PA, USA

² Computational Materials Informatics – CMI S.R.L., Rome, Italy

tblanton@icdd.com

Powder X-ray diffraction (XRD) has historically been the analytical technique of choice for phase identification of crystalline materials. Today advances in radiation sources, optics and detectors, allow scientists to use XRD to probe beyond phase identification and extend studies to investigate material microstructure as well as nanostructure properties. Whether the material of interest being studied is crystalline or amorphous, randomly or preferentially oriented, inorganic or organic, powder or solid, there are many diffraction methods available that can be used to analyze a sample and provide help in understanding how material processing affects material properties. In addition to improvements in diffraction instrumentation, new developments in the ICDD Powder Diffraction File (PDF) and Material Phases Data System (MPDS) databases have produced an array of solid-state analysis tools resulting from a combination of single crystal and powder diffraction structures, physical property, and phase diagram data. Advanced features include atomic coordinates for Rietveld refinement techniques; amorphous and nano material references; digital simulation tools for evaluating X-ray, synchrotron, electron, and neutron diffraction data as well as crystallite size and correlation of crystal structure with material properties.

Diffraction methods and the PDF and MPDS together create a synergy between data collection and data analysis that assist scientists in finding a more complete and correct answer to their materials characterization questions. The origins of the PDF and MPDS will lead to a review of current capabilities of databases and software, resulting in solutions for materials analyses.



STRUCTURE TYPE AND CHEMICAL BONDING IN AN INTERMETALLIC COMPOUND

Yuri Grin

*Max-Planck-Institut für Chemische Physik fester Stoffe,
Nöthnitzer Str. 40, 01187 Dresden, Germany
grin@cpfs.mpg.de*

The structure type is one of the basic terms for the description of crystal structures of inorganic and – in particular – intermetallic compounds. According to the recommendations of IUCR, compounds belonging to the same structure type must be both iso-poinital, *i.e.*, have the same Wyckoff sequence, Pearson symbol, as well as space group, and iso-configurational, *i.e.*, possess a similar atomic arrangement [1,2]. This information allows a fairly unambiguous attribution of a singular structure to a structure type and the systematization of crystal structures based on their crystallographic descriptors. The chemical facets of a compound are involved in the iso-configurational part of the definition of the structure type.

Recent investigations on the chemical bonding in intermetallic compounds, especially applying quantum chemical techniques in position space [3], reveal more complex relations between the crystallographic and bonding descriptors of a crystal structure.

The binary compound Mg_3Pt_2 is isotypic to Eu_3Ga_2 and A_3Bi_2 , $A = K, Rb, Cs$, but differs clearly from the latter compounds from the point of view of chemical bonding. While the minority atoms in Eu_3Ga_2 and A_3Bi_2 form isolated dumbbells arranged along a line with a huge difference between short and long distances within such a “chain”, the platinum atoms in Mg_3Pt_2 form almost linear chains with only moderately alternating Pt–Pt distances in the chains. Analysis of the chemical bonding reveals multi-atomic interactions stabilizing the Pt–Pt chain, while the dumbbells in Eu_3Ga_2 and A_3Bi_2 are separated within the line by “lone pairs”, which are in fact strongly polar multiatomic interactions [4].

Crystallographically, the Ga_3TM compounds in their *ht*-modifications ($TM = Fe, Co, Ru, Rh, Os, Ir$) were reported to belong to the $FeGa_3$ type [5]. A crystal structure of this type was described as a three-dimensional packing of tetra-capped triangular double prisms (*ttdp*) $TM_2@(Ga_{2\frac{8}{2}}Ga_{1\frac{4}{2}})$ embedding a TM – TM dumbbell [6]. From the analysis of the chemical bonding, the construction of the *ttdp* unit is carried out through three- and four-atomic Ga – TM and two-atomic TM – TM interactions. The formation and the number of each of these bonds strongly depends on the TM component, so that there are four (!) bonding patterns forming this atomic arrangement, revealing its flexibility but also sensitivity to electronic concentration, leading also to thermodynamic metastability in the case of Rh [7] and Ir [8].

- [1] J. Lima-de-Faria *et al.*, *Acta Crystallogr. A* 46 (1990) 1-11.
- [2] R. Allmann, R. Hinek, *Acta Crystallogr. A* 63 (2007) 412-417.
- [3] F.R. Wagner, Yu. Grin, In: *Comprehensive Inorganic Chemistry III*, Third Edition, Elsevier, 2023, vol. 3, pp. 222-237.
- [4] L. Agnarelli *et al.*, *Inorg. Chem.* 60 (2021) 13681-13690.
- [5] P. Villars, K. Cenzual (Eds.), *Pearson's Crystal Data – Crystal Structure Database for Inorganic Compounds*, Release 2022/23, ASM International, Materials Park, Ohio, USA.
- [6] F.R. Wagner *et al.*, *Inorg. Chem.* 57 (2018) 12908-12919.
- [7] R. Cardoso-Gil *et al.*, *Inorg. Chem.* 63 (2024) 12156-12166.
- [8] R. Cardoso-Gil *et al.*, *ACS Mater. Au* 2 (2022) 45-54.

MAGNESIUM INTERMETALLICS: FEATURES OF THE CRYSTAL AND ELECTRONIC STRUCTURES, CHEMICAL BONDING, AND HYDROGEN STORAGE PROPERTIES

Volodymyr Pavlyuk

*Department of Inorganic Chemistry, Ivan Franko National University of Lviv,
Kyryla i Mefodiya St. 6, 79005 Lviv, Ukraine
Institute of Chemistry, Jan Długosz University in Częstochowa, al. Armii Krajowej 13/15,
42200 Częstochowa, Poland
volodymyr.pavlyuk@lnu.edu.ua*

Magnesium intermetallic compounds and solid solutions formed between Mg and other elements, which are crucial for improving the mechanical properties, corrosion resistance, and thermal stability of the alloys, are mainly used in lightweight structures (automotive, aerospace) and for hydrogen storage. They increase the creep resistance and strength, although they can sometimes reduce the corrosion resistance [1,2]. Despite the above-mentioned importance of magnesium alloys, their synthesis is complicated by the high vapor pressure and low boiling point of Mg, resulting in significant compositional losses during conventional melting. Other problems include limited solubility in multi-element solids, oxidation, and the need for high-energy non-equilibrium processes to form the desired phases.

The chemical bonding in magnesium intermetallic compounds is complex and involves a combination of metallic, covalent, and ionic properties depending on the alloying elements. Key features include significant charge transfer from Mg to more electronegative partners, strong covalent networks (e.g., in Mg–Al or Mg–Si), and stabilization of complex structures by mixed bonding, which often affects the physicochemical properties. The description of complex magnesium intermetallic compounds relies on integrated concepts from structural chemistry, thermodynamics, and computational materials science. These compounds are defined by their long-range ordering and unique crystal structures, which differ significantly from those of pure Mg. Many complex Mg-based intermetallics are described as intergrowth structures, where slabs of well-known binary structure types (e.g., AlB₂-type, α -Fe, or CsCl-type slabs) stack to form a complex lattice. To describe some ternary and quaternary magnesium intermetallics and understand the nature of the chemical bonding, the Zintl-Klemm concept, or the concept of shell packing of clusters, can be used [3,4]. Structural modification of magnesium intermetallics and their transformation into a high-entropy state can significantly improve their physicochemical properties, particularly hydrogen sorption.

This work was partially carried out under the SFI-PD-Ukraine-00014574 project.

- [1] I.J. Polmear, *Mater. Sci. Technol.* 10(1) (1994) 1-16.
- [2] M. Gupta, S.N.M. Ling, *Magnesium, Magnesium Alloys, and Magnesium Composites*, John Wiley & Sons, 2011.
- [3] P. Solokha, S. De Negri, M. Skrobanska, A. Saccone, V. Pavlyuk, D.M. Proserpio, *Inorg. Chem.* 51(1) (2012) 207-214.
- [4] N. Pavlyuk, G. Dmytriv, V. Pavlyuk, H. Ehrenberg, *Acta Crystallogr. B* 75(2) (2019) 168-174.

TRANSITION METAL INCORPORATION IN BINARY LITHIUM PHOSPHIDES AND ANTIMONIDES: ACCESS TO ROOM-TEMPERATURE Li-ION CONDUCTIVITIES BEYOND 40 mS/cm

Thomas Fässler

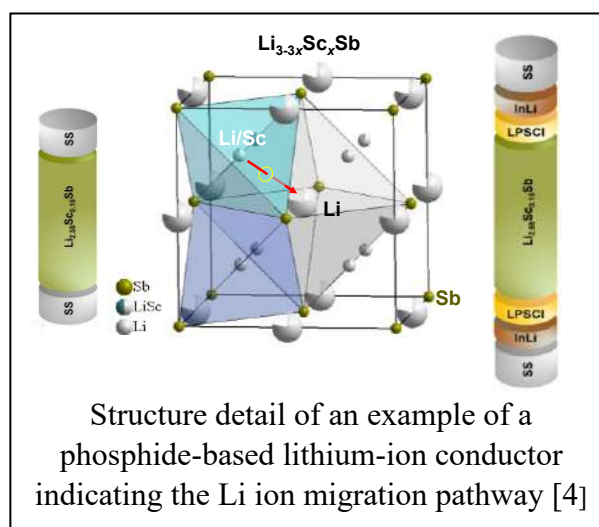
Chair of Inorganic Chemistry with Focus on Novel Materials,
Technical University of Munich, TUM School of Natural Sciences, Germany
Thomas.faessler@lrz.tum.de

Superionic conductors play a critical role as solid-state electrolytes in all-solid-state lithium-ion batteries. Current solid electrolytes include oxides (e.g., garnet- and NASICON-type) and sulfides (e.g., thiophosphates and argyrodites), with optimized sulfide systems reaching the highest room-temperature ionic conductivities of up to 32 mS/cm in rather complex compositions such as $\text{Li}_{9.54}[\text{Si}_{0.6}\text{Ge}_{0.4}]_{1.74}\text{P}_{1.44}\text{S}_{11.1}\text{Br}_{0.3}\text{O}_{0.6}$ [1].

In contrast, starting from structurally simple model systems such as Li_3P or related Li_3Sb , we have recently established a design principle for the development of novel superionic conductors. Aliovalent Li substitution with group-13 ($Tr = \text{Al}, \text{In}, \text{Ga}$) and group-14 elements ($Tt = \text{Si}, \text{Ge}, \text{Sn}$) led to the identification of approximately a dozen new ion-conducting compounds comprising discrete tetrahedral $[\text{TrP}_4]^{9-}$ and $[\text{TtP}_4]^{8-}$ units [2].

We now report on group-3 to group-5 transition metal incorporation in Li_3P and Li_3Sb , which results in a tremendous increase of the ion conductivity [3]. Sc incorporation in Li_3Sb results in a decrease of electronic conductivity and the occurrence of a superionic Li conductivity of 42 mS/cm, thus forming a mixed ionic-electronic conductor [4].

Crystalline materials are obtained by ball mill synthesis from the elements, followed by moderate thermal treatment, and are structurally characterized by X-ray and/or neutron diffraction methods. Li ion mobility is investigated by temperature-dependent NMR and electrochemical impedance spectroscopy. The role of Li occupation in the various tetrahedral and octahedral sites of the cubic close packing of P/Sb atoms is highlighted.



- [1] Y. Li, S. Song, H. Kim, K. Nomoto, H. Kim, X. Sun, S. Hori, K. Suzuki, N. Matsui, M. Hirayama, T. Mizoguchi, T. Saito, T. Kamiyama, R. Kanno, *Science* 381 (2023) 50-53.
- [2] a) S. Strangmüller, H. Eickhoff, D. Müller, W. Klein, G. Raudaschl-Sieber, H. Kirchhain, Ch. Sedlmeier, V. Baran, A. Senyshyn, V.L. Deringer, L. van Wüllen, H.A. Gasteiger, T.F. Fässler, *J. Am. Chem. Soc.* 141 (2019) 14200-14209; b) T.M.F. Restle, C. Sedlmeier, H. Kirchhain, W. Klein, G. Raudaschl-Sieber, V.L. Deringer, L. van Wüllen, H.A. Gasteiger, T.F. Fässler, *Angew. Chem. Int. Ed.* 59 (2020) 5665-5674; c) T.M.F. Restle, S. Strangmüller, V. Baran, A. Senyshyn, H. Kirchhain, W. Klein, S. Merk, D. Müller, T. Kutsch, L. van Wüllen, T.F. Fässler, *Adv. Funct. Mater.* 32 (2022) 2112377.
- [3] S. Merk, S. Kollmannsberger, S. Zeitz, V. Baran, A. Senyshyn, T.F. Fässler, *Inorg. Chem.* 64 (2025) 16902-16911.
- [4] J. Jiang, T. Kutsch, W. Klein, M. Botta, A. Senyshyn, R.J. Spranger, V. Baran, L. van Wüllen, H.A. Gasteiger, T.F. Fässler, *Adv. Energy Mater.* 30 (2025) 2500683.

OXIDATION (AND PROTECTION) OF THERMOELECTRIC SKUTTERUDITES

A. Hodroj¹, R. Bhardwaj², V. Dorcet¹, L. Joanny¹, S. Ollivier¹, C. Prestipino³, E. Alleno², V. Bouquet¹, and M. Pasturel¹

¹ Univ Rennes, CNRS, ISCR UMR6226, ScanMat UAR2025, F-35000 Rennes, France

² Univ Paris Créteil, CNRS, ICMPE, UMR 7182, F-94320 Thiais, France

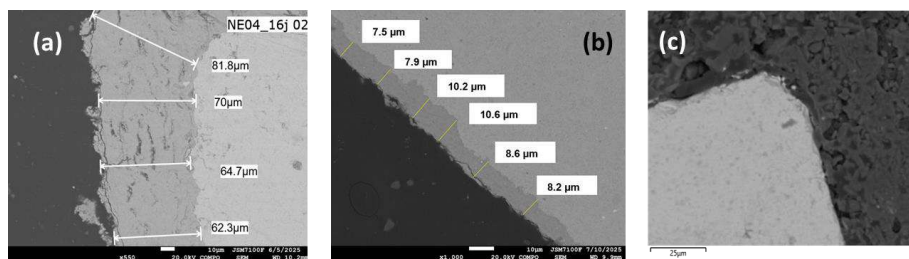
³ Univ Normandie Caen, CNRS, CRISMAT - UMR6508, F-14050 Caen, France
mathieu.pasturel@univ-rennes.fr

With the goal of energy saving, thermoelectric generators are promising to convert waste heat from industrial processes into electricity. They are based on the Seebeck effect, meaning the appearance of an electromotive force between the ends of a material subjected to a temperature gradient, due to the higher concentration of charge carriers on the cold side. To reach a sufficient voltage, tens to thousands of n- and p-type semiconducting legs are connected, electrically in series and thermally in parallel.

Within the realm of thermoelectric materials, skutterudites (SKDs) based on CoSb_3 exhibit several advantages at mid-temperature (600-800 K): (i) n-type and p-type SKDs are available by adapted doping/filling, (ii) both types reach ZT figures-of-merit above 1, meaning reasonable efficiency, and (iii) they are made of non-toxic and poorly critical elements [1]. However, some studies showed that they are prone to oxidation in air at operating temperature, limiting their lifetime [2]. While the chemical composition plays an important role on the resistance to oxidation, no study is available on the behaviour of high-performance n-type $\text{In}_x\text{Co}_4\text{Sb}_{12}$.

This SKD was synthesized *via* two distinct methods: melting / annealing / grinding (MS) and magnesiothermic reduction (MR), leading to different microstructures [3,4]. We will show how these differences affect the oxidation behaviour in air at 650 K.

Then, we employed a dip-coating technique to apply protective oxide and carbide layers for shielding the SKDs from oxidation. We will present how they improve the aging behaviour of n-type $\text{In}_x\text{Co}_4\text{Sb}_{12}$, but remain poorly efficient on the p-type legs with $\text{Ce}_{0.8}\text{Fe}_3\text{CoSb}_{12}$ composition.



SEM images (BSE mode) of $\text{In}_{0.2}\text{Co}_4\text{Sb}_{12}$ samples from different synthesis processes:

(a) MS, (b) MR, and (c) MS coated with Al_2O_3 , and heat-treated at 650 K in air for 16, 31, and 16 days, respectively.

This work was carried out under the “iHephaistos” project (2022-2026) funded by the Agence Nationale de la Recherche (France).

[1] G. Rogl, P. Rogl, *Curr. Opin. Green Sustainable Chem.* 4 (2017) 50-57.

[2] A. Hodroj, PhD thesis, Univ Rennes, 2025, and references therein.

[3] M. Benyahia *et al.*, *J. Alloys Compd.* 735 (2018) 1096-1104.

[4] S. Le Tonquesse *et al.*, *J. Alloys Compd.* 796 (2019) 176-184.

ORAL PRESENTATIONS

CRYSTAL STRUCTURE OF A NOVEL Nd₂Ir₂O₇-TYPE COMPOUND

F. Hájek¹, M. Henriques², D. Staško¹, K. Vlášková¹, J. Kaštil², and M. Klicpera¹

¹*Department of Condensed Matter Physics, Faculty of Mathematics and Physics,
Charles University, Ke Karlovu 5, 121 16 Prague 2, Czechia*

²*Institute of Physics of the Czech Academy of Sciences, Na Slovance 2,
182 21 Prague 8, Czechia
filip.hajek@matfyz.cuni.cz*

The rare-earth $A_2\text{Ir}_2\text{O}_7$ oxides ($A = \text{Y}, \text{Pr-Lu}$) represent an attractive family of materials owing to their exotic properties [1] and significant application potential [2]. Their characteristic geometrically frustrated pyrochlore lattice ($Fd-3m$, No. 227) consists of interpenetrating networks of corner-sharing Ir^{4+} and A^{3+} tetrahedra. Strong spin-orbit coupling, intermediately strong electron correlations, crystal field effects, and $f-d$ coupling between the A and Ir sublattices contribute to the emergence of complex magnetic [2,3] and topological [1,4] phases. By introducing Pb during the synthesis process, we aim to investigate the structural stability of the presumed pyrochlore framework and its influence on magnetic properties.

Single crystals of $\text{Nd}_{1.667}\text{Ir}_{0.885}\text{Pb}_{0.653}\text{O}_{5.792}$ (hereafter NIO) were synthesised using the PbF_2 flux method. The crystal structure was refined by single-crystal X-ray diffraction (SCXRD). The obtained structure is described by the tetragonal space group $I4_1/a$ (No. 88) with lattice parameters $a = 11.3785(5)$ Å and $c = 16.1245(7)$ Å, and $Z = 16$ formula units per unit cell. The chemical composition, spatial homogeneity and reproducibility were verified by complementary spectroscopic techniques, supporting the SCXRD results.

Despite the pronounced tetragonal distortion of the unit cell compared to cubic $\text{Nd}_2\text{Ir}_2\text{O}_7$ [5] and integration of Pb in the structure, the Ir pyrochlore-like tetrahedral network remains preserved. The octahedral oxygen environment responsible for the $j_{\text{eff}} = 1/2$ orbital state of Ir^{4+} is also present in both NIO and $\text{Nd}_2\text{Ir}_2\text{O}_7$. The similarities extend to their magnetic behaviour, with both compounds exhibiting two magnetic transitions below ~ 40 K and ~ 8 K, as observed in magnetisation and specific heat measurements. Analysis of the key structural features of NIO and their influence on magnetism may therefore provide insight into the properties of $\text{Nd}_2\text{Ir}_2\text{O}_7$ and related pyrochlore compounds.

This work was supported by Charles University through project GA UK (No. 111124).

- [1] X. Wan, A.M. Turner, A. Vishwanath, S.Y. Savrasov, *Phys. Rev. B* 83 (2011) 205101.
- [2] M.J. Pearce, K. Götze, A. Szabó, T.S. Sikkenk, M.R. Lees, A.T. Boothroyd, D. Prabhakaran, C. Castelnovo, P.A. Goddard, *Nat. Commun.* 13 (2022) 444.
- [3] M. Kawai, J. Friedman, K. Sherman, M. Gong, I. Giannakis, S. Hajinazar, H. Hu, S.E. Grefe, J. Leshen, Q. Yang, S. Nakatsuji, A.N. Kolmogorov, Q. Si, M. Lawler, P. Aynajian, *Nat. Commun.* 12 (2021) 1377.
- [4] Y. Otsuka, T. Yoshida, K. Kudo, S. Yunoki, Y. Hatsugai, *Sci. Rep.* 11 (2021) 20270.
- [5] H. Takatsu, K. Watanabe, K. Goto, H. Kadowaki, *Phys. Rev. B* 90 (2014) 235110.

UNUSUAL MAGNETIC AND TRANSPORT PROPERTIES IN THE NOVEL Eu-BEARING ZINTL PHASES

Olha Pokhvata¹, Rashed Alam¹, Bhushan Thipe², David Young², Xiaojian Bai²,
and Sviatoslav Baranets¹

¹ *Department of Chemistry, Louisiana State University, Baton Rouge, Louisiana 70803, USA*

² *Department of Physics and Astronomy, Louisiana State University,
Baton Rouge, Louisiana 70803, USA
sbaranets@lsu.edu*

Zintl phases are polar intermetallic compounds characterized by the simultaneous coexistence of covalent and ionic bonding interactions in their structures. Formed from groups 1, 2, or lanthanide metals and the more electronegative elements from groups 13-15, the crystal structures of these materials often exhibit unique (poly)anionic frameworks. The resulting structural complexity can be considered as both the hallmark of Zintl phases and an important element in the design of materials with unique physical properties [1].

Eu-bearing Zintl pnictides [2] and oxypnictides [3] frequently exhibit diverse crystal structures and fascinating physical phenomena, such as complex magnetic properties and unusual transport behaviour. Here, we present the discovery, synthetic challenges, comprehensive structural characterization, detailed characterization of the electronic structure under ambient and high-pressure conditions, transport, and magnetic properties of novel, previously unreported Eu-bearing Zintl arsenides, and provide insight into their applicability to serve as a platform for studying the interplay between magnetism and charge transport. We also present a study of how compression under high pressure affects bonding, transport, magnetic, and CMR/GMR properties in several magnetoresistive ternary Eu–*M*–As (*M* = Zn, In/Sn, Ga/Sn) and binary Eu–As phases.

A specific focus will be placed on the new ternary Zintl phase, Eu₃Zn₂As₄, synthesized via a metal-flux reaction. It crystallizes in the monoclinic crystal system with the space group *C2/m* adopting a Ba₃Cd₂Sb₄-type structure. Magnetic studies indicate a complex magnetic structure, as multiple transitions were observed. Measured transport properties indicate the promise for thermoelectric applications.

[1] S.M. Kauzlarich, *Chem. Mater.* 35 (2023) 7355-7362.

[2] M.M. Islam, S.M. Kauzlarich, *Z. Anorg. Allg. Chem.* 649 (2023) e202300149.

[3] S. Baranets, G. Darone, S. Bobev, *Z. Kristallogr. – Cryst. Mater.* 237(1-3) (2022) 1-26.

STRUCTURAL AND ELECTRONIC PROPERTY MODULATION IN THE MISFIT LAYERED SULFIDE (LaS)_{1.14}(NbS₂) THROUGH CATIONIC SUBSTITUTION AND LANTHANUM DEFICIENCY

Divyesh Parmar¹, Cédric Bourgès², Phillippe Deniard¹, Olivier Hernandez¹, Florent Pawula¹, Jean-Claude Crivello³, Takao Mori², Laurent Cario¹, Stéphane Jobic¹, and David Berthebaud¹

¹ *Nantes Université, CNRS, Institut des Matériaux de Nantes Jean Rouxel, IMN, F-44000 Nantes, France*

² *National Institute for Materials Science (NIMS), WPI-MANA, 1-1-1 Namiki, Tsukuba, 305-0044, Japan*

³ *CNRS-Saint-Gobain-NIMS, IRL 3629, Laboratory for Innovative Key Materials and Structures (LINK), 1-1 Namiki, Tsukuba, 305-0044, Japan*
David.berthebaud@cnrs-imn.fr

Misfit layered sulfides, defined by their composite incommensurate structures, belong to the $(MX)_{1+m}(TX_2)_n$ family ($M = \text{Pb, Bi, Sn, Sb, rare earths}$; $T = \text{Cr, Nb, Ti, V}$; $X = \text{S, Se}$; $m = 0.08-0.28$; $n = 1, 2, 3$). In these systems, the TX_2 host layers facilitate high charge carrier mobility, while the intercalated MX layers act as phonon scattering centres, creating a unique platform for tuning electronic and thermal transport [1,2]. This work investigates the structural and electronic consequences of cationic substitution and lanthanum deficiency in the p-type $(\text{La}_{0.94}\text{S})_{1.14}(\text{NbS}_2)$ system, specifically through the series $(\text{La}_{0.94-x}\text{Ce}_x\text{S})_y(\text{NbS}_2)$ ($x = 0, 0.10, 0.25, 0.50, 0.75, 0.94$).

The solid solution was synthesized *via* sulfurization of binary oxide precursors under H_2S flow at 1000 °C, followed by Spark Plasma Sintering (SPS). The uniaxial pressure applied during SPS induced partial texturing of the inherently anisotropic grains, revealing pronounced anisotropy in electrical and thermal properties. Ce substitution and La deficiency non-linearly modulate both the charge carrier concentration and the effective mass, leading to a decoupling of the electrical conductivity (σ) and Seebeck coefficient (S). This decoupling results in a simultaneous enhancement of σ and S , and an increase in the power factor (PF). Structural point defects introduced by Ce substitution also reduce the lattice thermal conductivity, further demonstrating the potential of structural engineering to tailor transport properties. The partial texturing amplifies in-plane anisotropy, contributing to a 30 % improvement in the figure of merit (ZT). These findings highlight a generalizable strategy for independently tuning σ , S , and κ through controlled cationic substitution and defect engineering in complex layered materials.

[1] P. Jood *et al.*, *Chem. Mater.* 27(22) (2015) 7719-7728.

[2] C. Yin *et al.*, *J. Mater. Chem. A* 6(45) (2018) 22909-22914.

MAGNETISM INVESTIGATION OF FeCoNiZn_x SYSTEMS

A. Nowak¹, K. Berent², M. Marciszko², A. Baczmański¹, and J. Cieślak¹

¹ Faculty of Physics and Applied Computer Science, AGH University, Krakow, Poland

² Academic Centre for Materials and Nanotechnology, AGH University, Krakow, Poland
annaslawek@agh.edu.pl

Medium- and high-entropy alloys (MEA, HEA), based on multicomponent solid solutions, are known to stabilize simple crystal structures due to their high configurational entropy. In particular, FeCoNi-based alloys, both single-phase (*fcc*) and doped with additional elements, often exhibit interesting magnetic properties.

The FeCoNiZn_x alloys ($x < 0.75$) remained single-phase up to approximately $x = 0.5$, indicating relatively high Zn solubility. Because of significant differences in the melting temperatures of the constituent elements, sintering was used as the primary synthesis method. The prepared alloys were subsequently cold-rolled to introduce plastic deformation.

Structural characterization revealed that single-phase *fcc* alloys develop a crystallographic texture with a dominant $\langle 011 \rangle$ orientation. In the two-phase *fcc*+*bcc* alloys, the *fcc* texture was preserved, and an additional *bcc* orientation corresponding to $\langle 223 \rangle$ was observed. The texture intensity of the *fcc* phase was found to depend on the Zn concentration.

Mössbauer spectroscopy indicated that the presence of texture induces ordering of magnetic moments, evidenced by changes in the intensity of the internal lines. In the *bcc* alloys, the easy magnetization direction remained parallel to the sample plane, whereas in the *fcc* alloys it gradually shifted with increasing Zn content, reaching an almost perpendicular orientation.

The influence of the Zn content on the microstructure and magnetic properties, including subtle magnetic parameters, was systematically investigated using XRD, SEM-EDX, VSM, and Mössbauer spectroscopy. The obtained experimental results indicate that both texture development and local magnetic dilution significantly affect the magnetic anisotropy of FeCoNiZn_x alloys.

- [1] J. Cieślak, M. Calvo-Dahlborg, K. Berent, U. Dahlborg, *J. Magn. Magn. Mater.* 518 (2021) 167371.
- [2] Gobinda Chandra Mohanty, Chinmayee Chowde Gowda, Pooja Gakhad, M. Sanjay, Abhishek Singh, Koushik Biswas, Chandra Sekhar Tiwary, *Energy Adv.* 12 (2024) 2972-2985.
- [3] O. Yakovenko, V. Sokolskii, P. Švec, I. Janotová, P. Švec Sr, T. Kulik, G. Cieślak, O. Roik, *J. Alloys Compd.* 1002 (2024) 175312.

A STRUCTURAL BREAK IN THE HOMOLOGOUS $R_3Ni_4Si_2$ SERIES ($R = La-Nd$) OF THE $R-Ni-Si$ SYSTEMS: THE NEW PHASE $Sm_4Ni_5Si_3$

M. Pani¹, A. Provino¹, V. Smetana², P. Solokha¹, S. De Negri¹,
A.-V. Mudring², and P. Manfrinetti¹

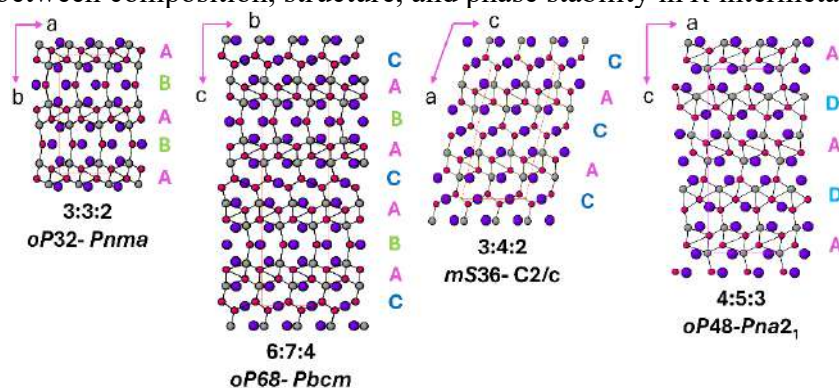
¹ *Department of Chemistry and Industrial Chemistry, University of Genoa, Genoa, Italy*

² *Department of Biological and Chemical Eng. and iNANO,*

Aarhus University, Aarhus, Denmark

pietro.manfrinetti@unige.it

Rare-earth nickel silicides are a rich class of ternary intermetallics with complex crystal chemistry and diverse physical properties, arising from the strong chemical affinity between R elements and the Ni–Si framework, which enables numerous structure types and homologous phases across the lanthanides. Although phase formation and phase diagrams of $R-Ni-Si$ systems have been widely studied, gaps remain and structural relationships are not yet fully understood [1-3]. In this work, we extend the investigation to $R = La-Sm$ to complete the homologous series and identify new phases. We confirm the orthorhombic $R_3Ni_3Si_2$ ($Ce_3Rh_3Si_2$ -type) and $R_6Ni_7Si_4$ ($Pr_6Ni_7Si_4$ -type) phases for all R in this range, and we demonstrate the formation of the monoclinic $R_3Ni_4Si_2$ compound ($Ce_3Ni_4Si_2$ -type) for $R = La-Nd$. Attempts to synthesize the ‘ $Sm_3Ni_4Si_2$ ’ homolog instead yielded a new compound, $Sm_4Ni_5Si_3$, which adopts a new structure type ($Pna2_1$, $oP48$). Its crystal structure consists of a three-dimensional Ni–Si framework built from two distinct layers stacked along the c axis and connected by additional Ni–Si bonds, forming channels occupied by Sm atoms. Although closely related to the structure of the 3:4:2, 3:3:2, and 6:7:4 compounds, $Sm_4Ni_5Si_3$ shows a different stacking sequence, representing a structural “break” in the 3:4:2 homologous series (see figure). Systematic trends in the lattice parameters and unit-cell volumes for $R_3Ni_4Si_2$, $R_3Ni_3Si_2$, and $R_6Ni_7Si_4$ follow the lanthanide contraction, with a deviation for Ce consistent with partial tetravalent character. The results provide new insight into the $R-Ni-Si$ systems and relationships between composition, structure, and phase stability in R intermetallic silicides.



Comparison of the $R_3Ni_3Si_2$, $R_6Ni_7Si_4$, and $R_3Ni_4Si_2$ structures with that of the new $Sm_4Ni_5Si_3$ structure. Large (dark purple), medium (grey), and small (red) spheres represent R , Si, and Ni.

- [1] P. Villars, K. Cenzual (Eds.), *Pearson's Crystal Data: Crystal Structure Database for Inorganic Compounds*. Release 2024/25, ASM International, Materials Park, Ohio, USA.
- [2] M. Pani, A. Provino, V. Smetana, V. Shtender, C. Bernini, A.-V. Mudring, P. Manfrinetti, *CrystEngComm*. 24 (2022) 8219-8228.
- [3] V. Smetana, D. Grilli, V. Shtender, M. Pani, P. Manfrinetti, A.-V. Mudring, *Inorg. Chem.* 63 (2024) 22761-22770.

CLUSTER FORMATION IN INTERMETALLIC COBALT TETRELIDES

T. Braun and V. Hlukhyy

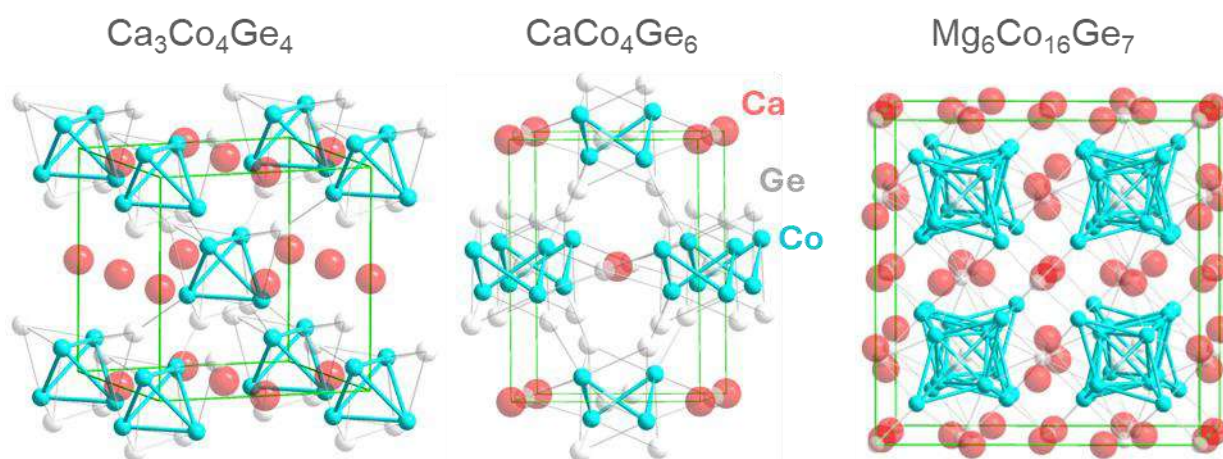
TUM School of Natural Sciences, Technical University of Munich,

Lichtenberstr. 4, 85747 Garching, Germany

viktor.hlukhyy@tum.de

Cobalt-based intermetallic compounds exhibit a remarkable structural diversity, ranging from low-dimensional arrangements to extended frameworks. In this work, new compounds in the Mg/Ca–Co–Si/Ge systems were synthesized by melting in induction or resistance furnaces in sealed niobium ampoules and structurally characterized by single-crystal and powder X-ray diffraction.

The compounds $\text{Ca}_3\text{Co}_4\text{Ge}_4$ and CaCo_4Ge_6 crystallize in $\text{Na}_3\text{Pt}_4\text{Ge}_4$ and YRu_4Sn_6 -type structures, respectively [1,2]. $\text{Ca}_3\text{Co}_4\text{Ge}_4$ contains Co_4 tetrahedra that are enclosed within larger Ge_4 tetrahedra. These motifs are interconnected *via* Co-Ge bonds to form a three-dimensional framework, with calcium cations occupying the resulting voids. In contrast, CaCo_4Ge_6 features open cobalt Co_4 tetrahedra (“butterfly” units), which are likewise embedded in larger, significantly distorted germanium tetrahedra. Co-Ge bonds between these units, together with additional germanium atoms, link the clusters into a three-dimensional polyanionic framework. The $\text{Mg}_6\text{Co}_{16}\text{Ge}_7$ and $\text{Mg}_6\text{Co}_{15.64}\text{Si}_{7.36}$ compounds crystallize in cubic $\text{Mg}_6\text{Cu}_{16}\text{Ge}_7$ -type structures [3] (G-phase family) and are characterized by complex cobalt building units. The Co substructure is based on Co_4 tetrahedra that are further extended into *stella quadrangula* motifs, where each triangular face of the tetrahedron is capped by an additional cobalt atom. These units are embedded in germanium/silicon supertetrahedra and, together with large magnesium octahedra, form a three-dimensional framework. The obtained compounds emphasize the strong propensity of cobalt to form cluster-like coordination environments in intermetallic systems.



Crystal structures of $\text{Ca}_3\text{Co}_4\text{Ge}_4$, CaCo_4Ge_6 , and $\text{Mg}_6\text{Co}_{16}\text{Ge}_7$

[1] W. Thronberens, H.U. Schuster, *Z. Naturforsch. B* 34 (1979) 781-783.

[2] G. Venturini, B. Chafik El Idrissi, J.F. Marêché, B. Malaman, *Mater. Res. Bull.* 25(12) (1990) 1541-1546.

[3] H. Witte, *Z. Angew. Mineral.* 1 (1938) 255-268.

CRYSTAL CHEMISTRY OF $MNi_{2-x}Si_{3+x}$ NICKEL SILICIDES ($M = Sc, Zr, U$) AND THE NEW PHASE $U_2Ni_{5-x}Si_{6+x}$

A. Provino^{1,2}, P. Solokha¹, A. Martinelli², G. Lamura², S. De Negri¹, P. Manfrinetti^{1,2}

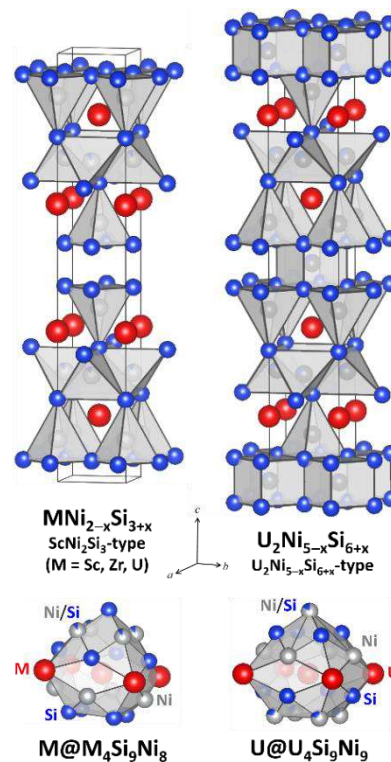
¹ *Department of Chemistry, University of Genoa, Via Dodecaneso 31, 16146 Genova, Italy*

² *Institute SPIN-CNR, Corso Perrone 24, 16152 Genova, Italy*

alessia.provino81@gmail.com

The crystal chemistry of ternary M -Ni-Si intermetallic phases is strongly governed by the chemical nature of the M element, which controls the structural stability and the resulting physical properties [1]. In this context, we investigated the formation of MNi_2Si_3 phases with $M = Sc, Zr,$ and U , in order to compare metals with similar atomic size but different valence states: trivalent Sc^{3+} , tetravalent Zr^{4+} , and multivalent U .

The $ScNi_2Si_3$ compound crystallizes in its own tetragonal structure type ($tI24, I4/mmm, Z = 4$) [2], whereas the structures of the Zr and U homologs were previously only tentatively inferred from X-ray powder diffraction data [3]. Based on single-crystal X-ray diffraction, we confirm that both adopt the structure type $ScNi_2Si_3$ and that all three compounds show Ni/Si solid solubility, leading to the general formula $MNi_{2-x}Si_{3+x}$. In the U -Ni-Si system, we also identified a new phase with composition $U_2Ni_{5-x}Si_{6+x}$, representing a new structural prototype ($tI26, I4/mmm, Z = 2$). Although $MNi_{2-x}Si_{3+x}$ and $U_2Ni_{5-x}Si_{6+x}$ crystallize in the same space group, the structure of the former contains five symmetry-inequivalent atomic sites, while the latter contains six: five correspond to those of the $ScNi_2Si_3$ -type phase, while the $2a$ site is new and introduces two additional atoms per unit cell. Mixed occupation occurs only at the site in Wyckoff position $4d$ in $MNi_{2-x}Si_{3+x}$, and at the $4d$ and $2a$ sites in $U_2Ni_{5-x}Si_{6+x}$. The $U_2Ni_{5-x}Si_{6+x}$ structure can therefore be regarded as a derivative of the $ScNi_2Si_3$ -type with increased structural complexity. The $MNi_{2-x}Si_{3+x}$ compounds and $U_2Ni_{5-x}Si_{6+x}$ show similar lattice parameters, with slightly larger values for $U_2Ni_{5-x}Si_{6+x}$ due to the additional $2a$ atomic site. Magnetic measurements on $U_2Ni_{5-x}Si_{6+x}$ revealed antiferromagnetic ordering below $T_N = 100$ K and a reduced effective magnetic moment compared to that expected for localized U^{3+} or U^{4+} ions, suggesting partially delocalized $5f$ electrons.



- [1] J.H. Westbrook, R.L. Fleischer (Eds.), *Intermetallic Compounds – Crystal Structures of Intermetallic Compounds*, Vol. 1, Wiley, 2000.
- [2] B.Y. Kotur, O.I. Bodak, E.I. Gladyshevskii, *Kristallografiya* 23 (1978) 189-190.
- [3] L.G. Akselrud, L.A. Lysenko, Y.P. Yarmolyuk, E.I. Gladyshevskii, *Dopov. Akad. Nauk Ukr. RSR Ser. A* (1977) 657-660.

FRUSTRATED MAGNETISM IN THE CORRUGATED HONEYCOMB LATTICE SEMICONDUCTORS $\text{CaMn}_2(\text{P}_{1-x}\text{As}_x)_2$

M.B. Gamza¹, E. Faithfull-Evans¹, B. Fernandes¹, P. Manuel², E. Suard³,
and I. Puente-Orench³

¹ *Jeremiah-Horrocks Institute, University of Lancashire, PR1 2HE, Preston, UK*

² *ISIS Neutron and Muon Source, STFC, Rutherford Appleton Laboratory, Harwell Science and Innovation Campus, OX11 0QX, Didcot, UK*

³ *Institut Laue-Langevin, 71 Avenue des Martyrs, CS 20156, 38042 Grenoble, France
monika.gamza@gmail.com*

The AMn_2X_2 ($A = \text{Ca}, \text{Sr}$; $X = \text{P}, \text{As}, \text{Sb}, \text{Bi}$) family of magnetic semiconductors provides a rich platform for studying the effects of competing exchange interactions on a corrugated honeycomb lattice in the presence of single-ion anisotropy [1-9]. Here, we present low-temperature neutron diffraction results on powdered single crystals of CaMn_2P_2 and CaMn_2As_2 .

For CaMn_2As_2 , temperature-dependent measurements reveal a second-order transition $T_N = 62.3(5)$ K to an incommensurate magnetic structure characterized by the propagation vector $\mathbf{k} = (\delta, \delta, 0)$, with $\delta = 0.0570(5)$ at 1.5 K. Critical-exponent analysis of prominent magnetic reflections yields $\beta \approx 0.12(5)$, consistent with the two-dimensional Ising universality class and indicative of strong uniaxial anisotropy. In contrast, CaMn_2P_2 exhibits a first-order transition at $T_N = 69.5(5)$ K to a cycloidal magnetic structure with an in-plane 6×6 magnetic unit cell, consistent with easy-plane anisotropy and in agreement with previous reports [1,2].

To probe the evolution between these two magnetic ground states, ac-calorimetry measurements were performed on single crystals of $\text{CaMn}_2(\text{P}_{1-x}\text{As}_x)_2$ ($0 \leq x \leq 1$) grown from Sn flux. An abrupt drop in the transition temperature, together with pronounced changes in the magnitude and width of the heat capacity anomalies, is observed at $x \approx 0.35$, providing evidence for a first-order phase boundary separating the two distinct magnetic ground states.

[1] N.S. Sangeetha *et al.*, *Proc. Natl. Acad. Sci. USA* 118 (2021) e2108724118.

[2] F. Islam *et al.*, *Phys. Rev. B* 107 (2023) 054425.

[3] D.E. McNally *et al.*, *Phys. Rev. B* 91 (2015) 180407(R).

[4] I.I. Mazin, arXiv:1309.3744, 2013.

[5] B. Mallick *et al.*, *Phys. Rev. B* 112 (2025) 045103.

[6] F. Islam *et al.*, arXiv:2501.02122, 2025.

[7] Q.D. Gibson *et al.*, *Phys. Rev. B* 91 (2015) 085128.

[8] N.S. Sangeetha *et al.*, *Phys. Rev. B* 94 (2016) 094417.

[9] Q.P. Ding *et al.*, *Phys. Rev. B* 104 (2021) 224413.

CRYSTAL STRUCTURE, CHEMICAL BONDING, AND HARDNESS OF Ti_3AlC_2 AND Ti_3SiC_2

A. Patrashko¹, N. Klymentiy¹, S. Pukas¹, R. Cardoso-Gil², U. Burkhardt²,
Yu. Grin², and R. Gladyshevskii¹

¹ *Department of Inorganic Chemistry, Ivan Franko National University of Lviv,
Kyryla i Mefodiya St. 6, 79005 Lviv, Ukraine*

² *Max Planck Institute for Chemical Physics of Solids,
Nöthnitzer St. 40, 01187 Dresden, Germany
anastasiia.broda.hmh@lnu.edu.ua*

Ti_3AlC_2 and Ti_3SiC_2 are remarkable for their unique combination of ceramic and metallic properties, as they are part of the family of MAX phases. The crystal structures of both compounds belong to the hexagonal Ti_3SiC_2 -type (Pearson symbol $hP12$, space group $P6_3/mmc$). $\text{Ti}_{50}\text{Al}_{19}\text{C}_{31}$ and $\text{Ti}_{50}\text{Si}_{27}\text{C}_{23}$ samples were synthesized by spark plasma sintering with the maximum temperatures $T_{\text{max}} = 1350$ and $T_{\text{max}} = 1390^\circ\text{C}$, respectively, to achieve the highest content of Ti_3AlC_2 [1] and Ti_3SiC_2 .

Phase analysis by X-ray diffraction of the sample $\text{Ti}_{50}\text{Al}_{19}\text{C}_{31}$ identified Ti_3AlC_2 as the main phase (95.1(5) mass%) and a small amount of TiC (4.9(2) mass%). The X-ray powder diffraction pattern of the second sample, $\text{Ti}_{50}\text{Si}_{27}\text{C}_{23}$, revealed the presence of three phases: the primary phase was Ti_3SiC_2 (84.2(9) mass%), accompanied by Ti_5Si_3 (11.3(6) mass%), and trace amounts of TiC (4.5(4) mass%). The refined cell parameters of the MAX phases are in good agreement with literature data: $a = 3.07017(8)$, $c = 18.5274(6)$ Å for Ti_3AlC_2 and $a = 3.06526(3)$, $c = 17.6651(2)$ Å for Ti_3SiC_2 . Electronic structure calculations and chemical bonding analysis of Ti_3SiC_2 were performed using the all-electron local-orbital full-potential method (FPLO) within the local-density approximation, applying the Perdew-Wang parametrization. The chemical bonding analysis based on quantum chemical techniques in position space revealed the presence of four-atomic bonds, in which Si or C atoms are bonded with three Ti atoms. These bonds were found to be polar, with carbon and silicon contributing more than 80% of the electronic population within the bond basins.

The microstructure of the samples was investigated by EDXS and WDXS. Consistent with the X-ray powder diffraction data, the $\text{Ti}_{50}\text{Al}_{19}\text{C}_{31}$ sample was found to contain two phases: the primary phase Ti_3AlC_2 , and the secondary phase TiC. The composition of the sample was $\text{Ti}_{43.5}\text{Al}_{25.1}\text{C}_{31.4}$. The presence of two phases was also confirmed for the $\text{Ti}_{50}\text{Si}_{27}\text{C}_{23}$ sample by WDXS: $\text{Ti}_{49.0(2)}\text{Si}_{16.0(1)}\text{C}_{35.0(3)}$ and $\text{Ti}_{52.5(7)}\text{Si}_{34.8(5)}\text{C}_{12.7(12)}$. The composition of the second phase is in agreement with the compound $\text{Ti}_5\text{Si}_3\text{C}$.

Microhardness measurements were carried out using the Vickers method with different loads: 100, 300 and 500 g. From a chemical bonding perspective (alternation of different bonding types along [001]), the compound is expected to exhibit anisotropy, with higher hardness along the [001] direction and lower hardness within the basal plane. The values obtained for the two compounds are comparable, ranging from 3.03 to 5.54 GPa depending on the applied load. An EBSD analysis indicated that this variation is not related to preferred grain orientation, but is instead associated with differences in the number of grains and grain boundaries present within the region of the indentation footprint.

This work was carried out under an EIRENE Grant of the Max Planck Society.

[1] A. Broda, R. Gladyshevskii, *Chem. Met. Alloys* 18 (2025) 36-43.

EXPLORING METAMAGNETIC PROPERTIES OF YCo₁₀Fe₂B₆ SINGLE CRYSTALS

B. Vallet-Simond^{1,2}, J. Pospíšil³, L.V.B. Diop⁴, F. Wilhelm¹, A. Rogalev¹, and O. Isnard²

¹ European Synchrotron Radiation Facility, 71 avenue des Martyrs, 38043 Grenoble, France

² Université Grenoble Alpes, Institut Néel - CNRS, 38042 Grenoble, France

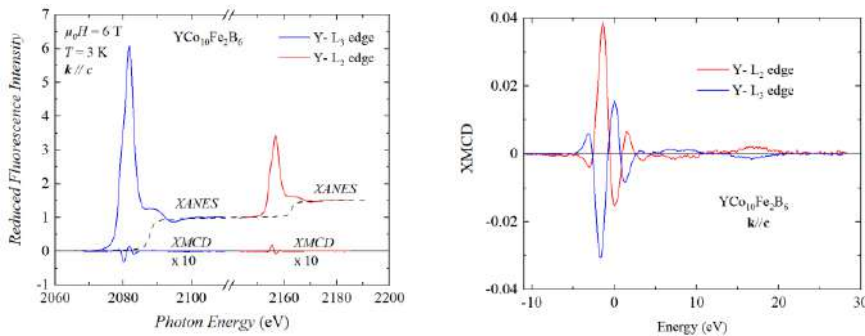
³ Faculty of Physics and Mathematics, Charles University, Prague, Czechia

⁴ Université de Lorraine, CNRS, IJL, F-54000 Nancy, France

baptiste.vallet-simond@esrf.fr

The RM₁₂B₆ family has attracted increasing attention in recent years due to its remarkable diversity of magnetic behaviour, ranging from antiferromagnetic ground states with colossal magnetization jumps (*e.g.*, LaFe₁₂B₆ [1]) to ferromagnetic phases with complex magnetic textures (*e.g.*, YCo₁₂B₆ [2]). It has been shown that a partial substitution of Co with Fe leads to the formation of novel metamagnetic phases [3], but detailed investigations of these phases are still missing. Given the rising interest in field-induced magnetic transitions, element-specific measurements are essential for unravelling the complex magnetic interactions in RM₁₂B₆ intermetallic compounds.

In this context, we report the first growth of YCo₁₀Fe₂B₆ single crystals using a fusion zone furnace at MGML. Magnetization curves along the principal crystallographic directions were obtained on high-quality single crystals. They were recorded using a conventional extraction magnetometer at the Néel Institute. To get insight into element-specific electronic and magnetic properties of YCo_{12-x}Fe_xB₆ we performed detailed hard X-ray spectroscopy studies at the ID12 beamline (ESRF). The figure shows representative X-ray Absorption Near Edge Spectra (XANES) and the corresponding X-ray Magnetic Circular Dichroism (XMCD) signals recorded at the *L*_{3,2} edges of Y along the crystallographic axis *c*. Analysis of these spectra revealed the finite spin and orbital moments of the Y 4*d* states, which are often overlooked in the analysis of magnetic properties. The anisotropy of these induced moments, as well as the magnetic responses of Fe and Co, have also been measured and are discussed. This study links macroscopic magnetic measurements with element-specific spectroscopic data, providing a solid basis for direct comparison with theoretical calculations.



XANES and XMCD measured at the Y *L*_{3,2} edges along the *c*-axis (left).

Zoom on the XMCD spectra measured at the Y *L*_{3,2} edges along the *c*-axis (right).

[1] L.V.B. Diop, O. Isnard, J. Rodriguez, *Phys. Rev. B* 93 (2016) 014440.

[2] B. Vallet-Simond, O. Isnard, L.V.B. Diop, *J. Alloys Compd.* 1037 (2025) 182379.

[3] B. Vallet-Simond, L.V.B. Diop, O. Isnard, *J. Appl. Phys.* 135 (2024) 173901.

COUPLING BETWEEN VACANCY ORDERING AND ELECTRONIC TRANSPORT IN $\text{Ni}_{7-\delta}\text{SnCh}_2$ ($\text{Ch} = \text{S}, \text{Se}$)

Laura Agnarelli¹, Yurii Prots², Marcus Schmidt², Denis Pelloquin¹,
Sylvie Hébert¹, and Antoine Maignan¹

¹ *Laboratoire CRISMAT, UMR 6508, F-14050 Caen Cedex 4, France*

² *Max-Planck-Institut für Chemische Physik fester Stoffe, 01187 Dresden, Germany*
laura.agnarelli@ensicaen.fr

The renewed interest in metallic systems for thermoelectric applications has emphasized the role of complex electronic structures and structural disorder in enhancing transport performance. Intermetallic compounds such as Ni_3Sn [1] and the metal-rich chalcogenides $\text{Ni}_3\text{Sn}_2\text{S}_2$ [2] (and its Co-based analogue [3]) have demonstrated that high carrier concentrations do not preclude significant thermoelectric responses. Within this context, we investigate other Ni-based metal-rich chalcogenides belonging to the $\text{M}_{7-\delta}\text{ECh}_2$ family [4] ($\text{M} = \text{Ni}$ or Pd ; $\text{E} = p$ -element and $\text{Ch} = \text{chalcogen}$), whose intrinsic metal vacancies and structural complexity may influence lattice dynamics and electronic transport.

We present two representative members, $\text{Ni}_{5.7}\text{SnSe}_2$ [5] and $\text{Ni}_{6.34}\text{SnS}_2$, [6] both adopting an intergrowth structure of alternating $[\text{Ni}_3\text{Sn}]$ and $[\text{Ni}_{4-\delta}\text{Ch}_2]$ slabs with intrinsic Ni vacancies in the chalcogenide layers. In $\text{Ni}_{5.7}\text{SnSe}_2$, single-crystal X-ray diffraction, TEM, and variable-temperature synchrotron diffraction reveal a reversible transition near 510 K, associated with long-range vacancy ordering and a symmetry lowering from tetragonal ($I4/mmm$) to monoclinic ($C2/m$). This structural rearrangement correlates with anomalies in resistivity and Seebeck coefficient, evidencing strong coupling between vacancy ordering and electronic transport. In contrast, $\text{Ni}_{6.34}\text{SnS}_2$ retains the average tetragonal $I4/mmm$ symmetry and exhibits weak additional reflections in electron diffraction, whose origin remains unclear and may reflect subtle structural modulations (as reported for $\text{Ni}_{7-\delta}\text{SnTe}_2$ [7]) or a fully developed long-range superstructure. In this case, no electronic transition is observed. Both compounds behave as metallic n-type Pauli paramagnets and display unusually low rt thermal conductivities for metallic systems ($8.4 \text{ W}\cdot\text{m}^{-1}\cdot\text{K}^{-1}$ for $\text{Ni}_{5.7}\text{SnSe}_2$ and $6.7 \text{ W}\cdot\text{m}^{-1}\cdot\text{K}^{-1}$ for $\text{Ni}_{6.34}\text{SnS}_2$), significantly lower than those of binary Ni_3Sn ($\sim 40 \text{ W}\cdot\text{m}^{-1}\cdot\text{K}^{-1}$) [1] and Ni_3S_2 ($\sim 30 \text{ W}\cdot\text{m}^{-1}\cdot\text{K}^{-1}$), [8] a favorable prerequisite for thermoelectric applications.

Ongoing investigations aim to clarify the microscopic origin of the structural transition in $\text{Ni}_{5.7}\text{SnSe}_2$ and understand why a comparable transition is not clearly observed in the sulfide analogue. Additional studies are also underway to explore the link between possible charge-density-wave-like instabilities or order-disorder phenomena, and the atomic-scale mechanisms governing vacancy ordering and associated electronic transitions. Furthermore, systematic substitution on the E and Ch sites is underway to tune electronic and thermal properties.

This work was supported by LabEx EMC3 (ANR-10-LABX-0009, AXMO project) and ANR (ANR-21-CE50-0033).

[1] F. Garmroudi *et al.*, *Phys. Rev. X* 15 (2025) 021054. [2] A. Aziz *et al.*, *Phys. Rev. B* 94 (2016) 165131. [3] C. Fu *et al.*, *APL Mater.* 8 (2020) 040913. [4] A.N. Kuznetsov *et al.*, *J. Inorg. Chem.* 64 (2019) 1625-1640. [5] L. Agnarelli *et al.*, *Chem. Mater.*, in revision. [6] L. Agnarelli *et al.*, *Chem. Commun.* 61 (2025) 12321-12324. [7] A.A. Isaeva, *J. Solid State Chem.* 180 (2007) 221-232. [8] L. Agnarelli *et al.*, in preparation.

HEUSLER COMPOUNDS AND ALLOYS – BURCH RULE AND IMPACT OF CRYSTAL STRUCTURE ON MAGNETIC PROPERTIES STUDIED BY HIGH-THROUGHPUT DFT CALCULATIONS

J. Goraus

*August Chelkowski Institute of Physics, University of Silesia,
75 Pułku Piechoty 1a, 41-500 Chorzów, Poland
jerzy.goraus@us.edu.pl*

Many interesting properties of Heusler compounds, for example, Half-Metallic-Ferromagnet (HMF) or Spin Gapless Semiconductor (SGS) states, are usually possible only in an ordered, inverted structure of a Heusler alloy [1]. There is an empirical rule – the Burch rule [2], which predicts for $3d$ Heusler compounds whether they crystallize in an inverted or a regular structure. Recently, I published a paper [3] that shows that this rule is not always fulfilled, and there are islands of stability of the inverted structure. Here, I would like to discuss the impact of the crystal structure – regular, inverted, or various types of alloying, on the magnetic properties of X_2YAl compounds ($X, Y = 3d$ transition metals). In particular, I would like to present how the disorder affects magnetic moments and magnetic ordering temperatures within this series.

- [1] J. Ma, J. He, D. Mazumdar, K. Munira, S. Keshavarz, T. Lovorn, C. Wolverton, A.W. Ghosh, W.H. Butler, *Phys. Rev. B* 98 (2018) 094410.
- [2] V. Niculescu, T.J. Burch, K. Raj, J.I. Budnick, *J. Magn. Magn. Mater.* 5 (1977) 60-66.
- [3] J. Goraus, *Acta Mater.* 308 (2026) 122015.

THE ROLE OF LATTICE DEFECTS FOR STRUCTURAL, MECHANICAL, AND THERMOELECTRIC PROPERTIES OF HPT-PROCESSED SKUTTERUDITES

G. Rogl, V. Romaka, X. Yan, K. Yubuta, M. Zehetbauer, and P. Rogl
*Institute of Material Chemistry, University of Vienna,
Währingerstrasse 42, 1090 Vienna, Austria
gerda.rogl@univie.ac.at*

Hot-pressed (HP) and high-pressure-torsion-processed (HPT) samples of p-type skutterudite $\text{DD}_{0.7}\text{Fe}_3\text{CoSb}_{12}$ were analysed with respect to the formation and thermal stability of HPT-induced lattice defects to understand the high-temperature maximum of the thermoelectric figure of merit (ZT), which has previously been related to a decrease of electrical resistivity and concomitantly of thermal conductivity. We combined experiments (differential scanning calorimetry, X-ray diffraction, energy-dispersive spectroscopy, scanning electron microscopy) with first-principles calculations and found that the individual thermal stabilities of lattice defects from HPT-processing, with special respect to their densities and arrays, are responsible for the properties observed. Whereas the mechanical properties are mainly governed by dislocations and grain boundaries, the thermoelectric figure of merit ZT is affected by the generation and annihilation of vacancy-type defects, which allow for the formation of low-angle grain boundaries out of the HPT-induced dislocations with increasing misorientation between the grains as a function of deformation and annealing temperature. These low-/high-angle grain boundaries account for a minimum of the product of resistivity and thermal conductivity, and thus of a maximum of $ZT = 1.4$ at 820 K. The same investigations for the n-type half-Heusler alloy $\text{Ti}_{0.5}\text{Zr}_{0.5}\text{NiSn}$ and clathrate $\text{Ba}_8\text{Cu}_{4.6}\text{Ge}_{35}\text{Si}_{6.4}$ revealed similar features.

CHIMNEY-LADDER STRUCTURES IN THE Mo–Ge SYSTEM

B. Korotshyn¹, N. Muts¹, L. Akselrud¹, Ya. Tokaychuk¹, Yu. Grin², and R. Gladyshevskii¹

¹ Department of Inorganic Chemistry, Ivan Franko National University of Lviv,
Kyryla i Mefodiya St. 6, 79005 Lviv, Ukraine

² Max-Planck-Institut für Chemische Physik fester Stoffe,
Nöthnitzer Str. 40, 01187 Dresden, Germany
bohdan.korotshyn@lnu.edu.ua

According to previous investigations, several phases with close compositions and different structures exist in the Mo–Ge system. Brown reported the existence of a phase of approximate composition $\text{MoGe}_{1.7}$ in space group $I4_122$ (cell parameters $a = 5.994$, $c = 43.995$ Å) [1]. The composition was later identified as $\text{Mo}_9\text{Ge}_{16}$ [2] and the structure was theoretically derived during a general study of the chimney-ladder structures [3]. The complete structure of $\text{Mo}_{13}\text{Ge}_{23}$ (space group $P-4n2$, Pearson symbol $tP144$, cell parameters $a = 5.987$, $c = 63.54$ Å), which also belongs to the Nowotny phases with chimney-ladder structures, was determined, whereas for another composition, $\text{Mo}_{23}\text{Ge}_{41}$, only cell parameters were reported ($a = 5.995$, $c = 112.49$ Å) [2]. The aim of this work was to study details of the chimney-ladder structures in the Mo–Ge system.

Two samples of compositions $\text{Mo}_{36}\text{Ge}_{64}$ and $\text{Mo}_{36.5}\text{Ge}_{63.5}$ were synthesized by sintering elementary powders (Mo ≥ 99.8 wt.%, Ge ≥ 99.98 wt.%) in vacuum-sealed quartz ampoules at 1000 °C for 4 days and then at 800 °C for 5 days. X-ray powder diffraction data were collected on a PROTO AXRD Benchtop diffractometer (Cu $K\alpha_1$ radiation).

Two chimney-ladder structures were identified from the X-ray powder diffraction diagrams. The structure of the single-phase sample $\text{Mo}_{36}\text{Ge}_{64}$ was refined considering the ordered model $\text{Mo}_9\text{Ge}_{16}$ (space group $I4_122$, Pearson symbol $tI100$, $a = 5.99324(3)$, $c = 44.0005(3)$ Å). The diffraction pattern of the sample $\text{Mo}_{36.5}\text{Ge}_{63.5}$ could not be indexed with a conventional 3D unit cell. The assumption that the structure belongs to the chimney-ladder family allowed us to determine the parameters of the composite structure. Part of the reflections was used to determine the parameters of the Mo subcell (space group $I4_1/amd$), and the other part those of the Ge subcell (space group $P4/nnc$). Systematic absences $hk\ell m$: $h+k+l \neq 2n$, $hkl0$: $2h-l \neq 4n$, $hk00$: $k \neq 2n$, $00\ell m$: $l \neq 4n$, $m \neq 2n$ pointed to superspace group $I4_1/amd(00\gamma)00ss$. The basic lattice parameters refined to $a = 5.99332(2)$ Å, $c_{\text{Mo}} = 4.88892(2)$ Å, and $c_{\text{Ge}} = 2.75077(1)$ Å, with the z-component of the modulation vector $\gamma = c_{\text{Mo}} : c_{\text{Ge}} = 1.7773(1)$. The commensurate approximant $\text{Mo}_{22}\text{Ge}_{39}$ of the incommensurately modulated phase was refined in space group $P-4c2$ ($tP244$) with $a = 5.98879(3)$, $c = 107.475(1)$ Å.

This work was funded by a grant from the U.S. Office of Naval Research Global (ONRG) and the U.S. National Academy of Sciences (NAS, USA) within the framework of the International Multilateral Partnerships for Resilient Education and Science System in Ukraine (IMPRESS-U) initiative.

[1] A. Brown, *Nature* 206 (1965) 502.

[2] H. Völlenkle, A. Preisinger, H. Nowotny, A. Wittmann, *Z. Kristallogr.* 124 (1967) 9-25.

[3] Yu. Grin, *Monatsh. Chem.* 17 (1986) 921-932.

CHALCOHALIDE PHOSPHORS FOR TUNABLE COLOUR EMISSION AND LUMINESCENCE THERMOMETRY

Trinanjana Dey, Dundappa Mumbaraddi, Pritam Das, and Arthur Mar
Department of Chemistry, University of Alberta, Edmonton, AB, Canada
trinanja@ualberta.ca

The mixed-anion chalcogenides $RE_3Tt_2Ch_8X$ ($RE = \text{La-Er}$; $Tt = \text{Si, Ge}$; $Ch = \text{S, Se}$; $X = \text{Cl, Br, I}$) show substantial compositional flexibility. They are potential candidates for phosphor-converted white light-emitting diodes, display backlighting, and sensing applications. By appropriate substitution of different RE components in $(\text{La}_{1-x}\text{RE}_x)_3\text{Si}_2\text{S}_8\text{I}$ ($RE = \text{Ce, Tb-Er}$), their photoluminescence properties can be controlled. The resulting phosphors can be integrated with near UV LED chips to offer tunable and efficient multicolour emission, while eliminating the blue hazard posed by conventional blue LED-based phosphors currently used in lighting technologies. The Er^{3+} -activated phosphors show luminescence that strongly depends on temperature, offering a way to develop highly sensitive, non-contact temperature sensors that can be used in wearable technologies and small modular reactors.

STRUCTURE AND MAGNETIC PROPERTIES OF $\text{Cu}_x(\text{Cr,Fe,Mn,Ni})_{3-x}\text{O}_4$ SPINEL-STRUCTURED HIGH-ENTROPY OXIDES

M. Szum¹, K. Berent², M. Nowakowska³, J. Dąbrowa³, M. Reissner⁴, M. Sikora⁵,
and J. Cieślak¹

¹ Faculty of Physics and Applied Computer Science, AGH University of Krakow, Poland

² Academic Centre for Materials and Nanotechnology, AGH University of Krakow, Poland

³ Faculty of Materials Science and Ceramics, AGH University of Krakow, Poland

⁴ Institute of Solid State Physics, TU Wien, Wien, Austria

⁵ National Synchrotron Radiation Centre SOLARIS, Jagiellonian University, Poland
szymczak@agh.edu.pl

High-entropy oxides (HEOx) have already attracted increasing interest as functional materials despite their relatively recent introduction in 2015 [1]. Spinel structures provide particularly favourable conditions for exploiting their multicomponent character, thanks to the two non-equivalent cationic sites. The distribution of elements across both sublattices plays a key role in determining the functional characteristics of spinel oxides. However, while providing opportunities for property engineering, it also further increases the complexity of the systems, posing a challenge for structural characterization. So far, there are few studies available concerning the cationic distribution in HEOx spinels. Meanwhile, understanding their structure, and how it affects the observed properties, is required for the design of materials tailored for specific applications [3].

In this work, we study the $\text{Cu}_x(\text{Cr,Fe,Mn,Ni})_{3-x}\text{O}_4$ ($x = 0 \div 2$) series of HEOx. Based on X-ray diffraction we assess the Cu solubility limit and identify the symmetry of the systems, and determine the lattice parameters through Rietveld refinements. We verify the homogeneity of the systems and study the secondary phase precipitates forming beyond the solubility limit through SEM-EDS. Taking advantage of an element-selective probe for a multi-component system, we perform temperature-dependent Mössbauer spectroscopy measurements. The magnetic properties and their temperature dependence were studied by vibrating sample magnetometry. The oxidation state and coordination of the cations were investigated by X-ray absorption spectroscopy (XAS) and X-ray magnetic circular dichroism (XMCD). To further investigate the changes in magnetization at low temperatures, synchrotron studies were also performed at 25 and 80 K.

The single-phased materials crystallize as spinels of $Fd-3m$ symmetry, with CuO forming for higher dopant contents. Introducing copper leads to an increase of the average magnetic moment, with only a small decrease of the ordering temperature. The temperature-dependent magnetization curves show a distinct step at about 50 K, which could correspond to a phase transition, however XAS/XMCD measurements show no temperature-induced structural changes. The extensive analysis provides a detailed description of the cationic distribution in the series, contributing to the knowledge base for designing spinel high-entropy oxides.

Research supported by the Polish National Science Centre (NCN) under project No. UMO-2022/45/B/ST8/.

[1] C.M. Rost *et al.*, *Nat. Commun.* 6 (2015) 8485.

[2] G.H.J. Johnstone *et al.*, *J. Am. Chem. Soc.* 144 (2022) 20590-20600.

[3] A. Sarkar *et al.*, *Dalton Trans.* 50 (2021) 1973-1982.

STRUCTURAL, MAGNETIC, AND TRANSPORT PROPERTIES OF C15 LAVES PHASES SmX_2 ($X = \text{Rh}$ and Ir)

Pavan Kumar Meena, Marcin Łapiński, Michał J. Winiarski, and Tomasz Klimczuk
*Faculty of Applied Physics and Mathematics and Advanced Materials Centre,
Gdansk University of Technology, Narutowicza 11/12, 80-233 Gdansk, Poland
pavan.meena@pg.edu.pl, tomasz.klimczuk@pg.edu.pl*

Rare-earth–transition-metal intermetallics provide a rich platform to explore correlated electron phenomena arising from the interplay of localized $4f$ moments and itinerant d electrons. Among these, AB_2 Laves-phase compounds exhibit diverse ground states, including magnetism, superconductivity, and magnetocaloric effects. Samarium-based systems are particularly intriguing due to the unconventional behaviour of the Sm^{3+} ion, where strong J -mixing and near-cancellation of spin and orbital moments produce unusual magnetic responses. While the $3d$ -based analogues have been extensively studied, the $4d$ and $5d$ counterparts remain comparatively unexplored, in part due to the chemical reactivity of samarium, limiting a unified understanding of how orbital character and spin-orbit coupling shape magnetism across the transition-metal series.

We will discuss the synthesis and bulk characterization of cubic C15 Laves phase ($Fd-3m$) SmX_2 ($X = \text{Rh}, \text{Ir}$) polycrystalline samples prepared *via* solid-state reaction. Magnetic susceptibility, electrical resistivity, and specific heat measurements revealed ferromagnetic ordering with Curie temperatures of 20.4 K for SmRh_2 and 35.5 K for SmIr_2 . The bulk second-order transition was confirmed by λ -type anomalies in the specific heat measurement. Comparison between the $4d$ and $5d$ analogues highlights the role of orbital extension and enhanced spin-orbit coupling in modulating magnetic interactions. These results advance the understanding of samarium magnetism across transition-metal series and emphasize the need for systematic studies of $4d$ and $5d$ intermetallics.

The work conducted at Gdańsk University of Technology was supported by the OPUS-23 NCN project, grant No. 2022/45/B/ST5/03916.

RESISTIVITY AND MICROSTRUCTURE OF Bi–Pb AND Bi–Pb–Sn(Zn) ALLOYS

Yu. Plevachuk, I. Shtablavyi, S. Mudry, Y. Nykyruy, Yu. Kulyk, and N. Popilovskyi
*Department of Metal Physics, Ivan Franko National University of Lviv,
Kyryla i Mefodiya St. 8, 79005 Lviv, Ukraine
yuriy.plevachuk@lnu.edu.ua*

The physical and chemical properties of liquid alloys based on the eutectic Bi–Pb composition are under close scientific attention due to their possible use in safe small nuclear reactors of the new generation [1-3]. The correct choice of liquid metal as a coolant flowing in direct contact with both the reactor core and heat exchangers is of fundamental importance. The main requirements for such coolants are a small neutron absorption cross section in the energy range and a small neutron activation cross section in the energy range from fast to thermal neutrons; low neutron scattering cross section; high heat capacity and thermal conductivity; high boiling point and low melting point; low vapor pressure; inexpensive, easily accessible; chemical compatibility with all structural materials that make up the first coolant circuit; high temperature stability of these characteristics over a long period to prevent the formation of “blood clots” on the reactor walls and overheated local areas, non-toxic, environmentally safe. The emergence of these potential sources of danger is associated with the temperature dependence of the microstructure and properties of these alloys.

In this work, the resistivity of the eutectic and near-eutectic Bi–Pb and Bi–Pb–Sn(Zn) alloys was investigated in a wide temperature range from room temperature to the liquid state. The influence of phase transformations on the behaviour of the resistivity in the melting-solidification temperature range was analysed.

This work was supported by the Ministry of Education and Science of Ukraine, project No 0126U002266 “New nanocomposite metal melt-based coolants for small modular reactors”.

- [1] D.A. Arostegui, *CRS Report: Advanced Nuclear Reactors: Technology Overview and Current Issues*, 2019.
- [2] S. Chen, Z. Deng, J. Liu, *Nanotechnology* 32 (2021) 092001.
- [3] X. Wang, *Appl. Therm. Eng.* 192 (2021) 116937.

EFFECT OF YTTRIUM SUBSTITUTION ON THE HYDROGEN UPTAKE OF Mg₁₇Al₁₂

O. Zelinska¹, V. Kordan¹, N. Pavlyuk¹, G. Dmytriv¹, V. Pavlyuk^{1,2},
B.H. Silva³, A. Kumar⁴, S. Sartori³, B.C. Hauback⁵, A.O. Sjøstad⁴

¹ *Department of Inorganic Chemistry, Ivan Franko National University of Lviv,
Kyryla i Mefodiya St. 6, 79005 Lviv, Ukraine,*

² *Institute of Chemistry, Jan Długosz University,*

al. Armii Krajowej 13/15, 42-200 Częstochowa, Poland,

³ *Department of Technology Systems, University of Oslo,
Gunnar Randers vei 19, Kjeller 2027, Norway,*

⁴ *Centre for Materials Science and Nanotechnology, Department of Chemistry,
University of Oslo, Sem Sælandsvei 26, Oslo 0371, Norway,*

⁵ *Department of Hydrogen Technology, Institute of Energy Technology,
P.O. Box 40, Kjeller, Norway
oksana.zelinska@lnu.edu.ua*

The binary intermetallic compound Mg₁₇Al₁₂ demonstrates favourable hydrogenation behaviour, making it a potential candidate for hydrogen storage applications. Despite extensive studies on its hydrogenation properties, the enhancement of these properties through alloying with other metals remains insufficiently explored. This study aims to elucidate the effects of yttrium substitution on the hydrogenation behaviour of Mg₁₇Al₁₂, focusing on kinetic performance and associated phase changes.

The synthesis of binary Mg₅₉Al₄₁ and ternary Mg_{56.5}Al₄₁Y_{2.5} alloys was carried out by melting pure metals in an arc furnace. Structural analysis based on XRPD data from (Bruker D8 Advance and PROTO AXRD diffractometers, FullProf program package) confirmed that the binary alloy with nominal composition Mg₁₇Al₁₂ crystallises with its own cubic type structure, while the addition of yttrium results in the formation of a substitutional Mg_{17-x}Y_xAl₁₂ variant, and YAl₂ with some dissolved Mg, in addition to Mg₁₇Al₁₂. SEM/EDS analyses, performed using a Tescan Vega3 LMU system equipped with an Oxford Instruments X-MaxN20 detector or a high-resolution Hitachi SU-8230 FE-SEM coupled with a Bruker XFlash6I10 EDS analyser, revealed that yttrium is not uniformly distributed, but segregates into the grains of the above-mentioned Y-containing phases.

The hydrogen absorption experiments were performed using a Sieverts-type apparatus (SETARAM® PCT-Pro) at 350 °C without activation treatment, under a pressure of ~55 bar of high-purity H₂ (≥ 99.999 %). The results show a clear improvement in the storage properties of the Y-containing sample (2.5 and 4.4 wt.% H₂ after 15 and 65 h), compared with the binary Mg₁₇Al₁₂ (1.8 and 3.4 wt.% H₂ after 15 and 65 h), which can be attributed to the presence of multiphase structures and interphase boundaries that provide more favourable sites for hydrogen uptake and diffusion. Yttrium substitution significantly affects the hydrogenation kinetics, with Mg₁₇Al₁₂-Y forming 41.2 wt.% MgH₂ after 15 h, compared to 12.7 wt.% for Mg₁₇Al₁₂, and 54.7 wt.% MgH₂ after 65 h, compared to over 20 wt.% for the binary phase. To verify whether hydrogen is also partially incorporated into the structural voids of the initial intermetallic compound simultaneously with the formation of MgH₂, the structures of the intermetallic phase and possible hydride will be investigated using neutron diffraction of a deuterated sample.

CRYSTALLOGRAPHIC AND MAGNETIC STUDY OF NOVEL INTERMETALLIC COMPOUNDS $R_2\text{MoSi}_2\text{C}$ ($R = \text{Y, Gd-Tm, Lu}$)

I. Sarr, B. Malaman, L.V.B. Diop, and A. Vernière

Institut Jean Lamour, Université de Lorraine, CNRS, F-54000 Nancy, France

ibrahima.sarr@univ-lorraine.fr

Intermetallic compounds occupy a special place among solid materials, owing to the great diversity in both their crystal chemistry and physical properties. Rare-earth (R) based intermetallics have attracted significant interest from the viewpoint of modern technological applications as well as from the fundamental research side, offering a plethora of tunable structural, electronic, and magnetic properties. There is a broad range of successful uses of intermetallics in functional applications comprising permanent magnets, magneto-mechanical sensors and actuators, magnetocalorics, superconductors, hydrogen storage, or magneto-optical recording, to name but a few [1-6]. Intermetallic materials with the most outstanding magnetic properties are enabling many functionalities in motors, generators, sensors, actuators, robotics, advanced prosthetics, and energy conversion devices in general.

Here, we report the discovery of novel quaternary intermetallic compounds $R_2\text{MoSi}_2\text{C}$ ($R = \text{Y, Gd-Tm, Lu}$) during a survey of the $R\text{-Mo-Si-C}$ phase diagram. The alloys were synthesized by high-frequency induction melting and subsequent appropriate annealing treatment. The crystal structures were solved by means of single-crystal and powder X-ray diffraction. The analysis of the X-ray diffraction data revealed that the $R_2\text{MoSi}_2\text{C}$ compounds crystallize in a tetragonal lattice (space group $P4/mbm$, Pearson symbol $tP12$) [7] with unit-cell parameters that follow the conventional lanthanide contraction. Magnetization and specific-heat measurements indicate that the $\text{Y}_2\text{MoSi}_2\text{C}$ and $\text{Lu}_2\text{MoSi}_2\text{C}$ systems are paramagnetic (PM) over the investigated temperature range (2-300 K), whereas the compounds with $R = \text{Gd-Tm}$ exhibit an antiferromagnetic (AFM) ground state below the Néel temperature ($T_N = 2.4\text{-}25$ K). Interestingly, the Gd-based compound undergoes a spin reorientation transition at $T_{SR} = 15$ K. It is noteworthy that the magnetic ordering temperature T_N does not obey the de Gennes scaling. Such a breakdown can be attributed to crystal field effects on the R ions. It is further shown that the AFM state gets transformed into a ferromagnetic (FM) state via a magnetic-field-induced metamagnetic phase transition. Another salient feature is: the deduced saturation magnetic moment for the field-driven FM state is much smaller than the free-ion saturation magnetic moment. This reduced saturation moment is most likely due to crystal field effects. The observed effective magnetic moment is higher than the theoretical μ_{eff} expected for the R^{3+} ions; this difference may reflect a contribution from the d -electrons. In other words, this difference may be ascribed to the positive spin polarization of $5d$ states.

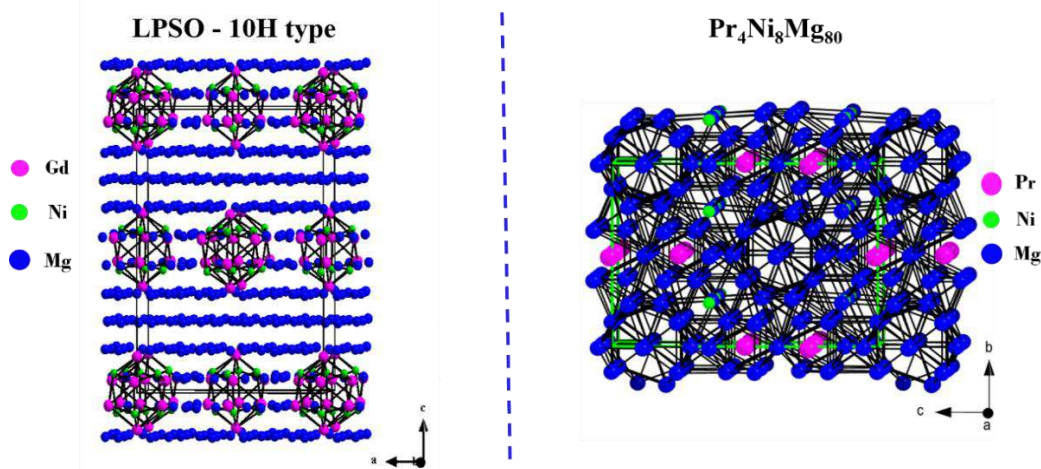
- [1] M. Sagawa, S. Fujimura, N. Togawa *et al.*, *J. Appl. Phys.* 55 (1984) 2083.
- [2] N.H. Duc, D.T. Kim Anh, P.E. Brommer, *Physica B* 319 (2002) 1-8.
- [3] S. Engel, E.C.J. Giebelmann, M.K. Reimann *et al.*, *ACS Org. Inorg. Au* 4 (2024) 188.
- [4] A.E. Clark, H.S. Belson, *Phys. Rev. B* 5 (1972) 3642.
- [5] U.B. Paramanik, Anupam, U. Burkhardt *et al.*, *J. Alloys Compd.* 580 (2013) 435.
- [6] Z. Liu, B. Li, Y. Xiao *et al.*, *Sci. China-Phys. Mech. Astron.* 64 (2021) 277411.
- [7] A. Vernière, L.V.B. Diop, I. Sarr *et al.*, *Acta Crystallogr. B* 80 (2024) 504.

MAGNESIUM-RICH PHASES (LPSO AND TERNARIES) FOR HYDROGEN STORAGE

Mohamed Najib El Rhazfouri, Etienne Gaudin, and Jean-Louis Bobet
*Université de Bordeaux, CNRS, Bordeaux INP, ICMCB, UMR 5026,
Avenue du Dr Albert Schweitzer 87, 33600 Pessac, France
mohamed-najib.el-rhazfouri@u-bordeaux.fr*

In order to discover new Mg-rich phases with interesting hydrogen storage properties, the Mg-rich region of the Gd–Ni–Mg ternary diagram was explored. Along the Gd/Ni = 4/3 composition line, which corresponds to the formation of Gd₈Ni₆ clusters and therefore to the potential formation of long-period stacking ordered (LPSO) phases, the sample with the nominal composition Gd_{11.4}Ni_{8.6}Mg₈₀ showed a single and unreported 10H-type LPSO phase. X-ray diffraction and transmission electron microscopy confirmed the 10H-type structure with the lattice parameters $a = 11.20 \text{ \AA}$ and $c = 26.10 \text{ \AA}$ by considering the space group $P6_3/mcm$. Its structure can be described as a periodic stacking of one pure-Mg layer sandwiched by four layers of Mg containing Gd₈Ni₆ clusters (see figure). The hydrogen sorption properties of this phase were investigated and a two-step hydrogen absorption mechanism was observed. The first step leads to the irreversible decomposition of Gd_{11.4}Ni_{8.6}Mg₈₀ into three distinct hydrides: GdH₂, Mg₂NiH₄, and MgH₂, while the second step consists in the reversible hydrogen absorption of these hydrides, which mainly relies on the sorption reversibility of MgH₂ and, to a lesser extent, of Mg₂NiH₄. An activation energy for H₂ absorption of *ca.* $E_a = 36 \text{ kJ}\cdot\text{mol}^{-1}$ (three to four times lower than that of pure Mg) was determined.

Moreover, to investigate the influence of the nature of the rare earth on the formation of LPSO phases, gadolinium was replaced by praseodymium, a light rare-earth element. The compositions investigated along the Pr/Ni = 4/3 line did not lead to the formation of LPSO phases. However, a new compound with the composition Pr₄Ni₈Mg₈₀ that crystallizes in a tetragonal structure with lattice parameters $a = 11.291 \text{ \AA}$ and $c = 15.952 \text{ \AA}$ in the space group $I4_1/amd$ was discovered. The structure consists of a three-dimensional Mg framework in which isolated Pr and Ni atoms are embedded (see figure). Hydrogenation of this compound leads to its decomposition into three hydrides: PrH₃, Mg₂NiH₄, and MgH₂. The cycling performance at 300°C and 20 bar of H₂ shows a significant improvement in the hydrogenation kinetics reaching an optimal regime after the third cycle.



This work was supported by a French government grant managed by the Agence Nationale de la Recherche under the France 2030 program, with the reference “ANR-22-PEHY-0007”.

AXIS-DEPENDENT CONDUCTION POLARITY AND LARGE NERNST EFFECT IN SEMIMETAL MoSi₂

O. Pavlosiuk and M.J. Winiarski

*Institute of Low Temperature and Structure Research, Polish Academy of Sciences,
50-422 Wrocław, Poland
o.pavlosiuk@intibs.pl*

Transverse thermoelectric effects have recently attracted considerable interest as an alternative route for enhancing thermoelectric energy conversion, particularly in topological semimetals demonstrating high carrier mobilities and nearly perfect charge carrier compensation [1]. However, topologically trivial semimetals with similar carrier characteristics may also offer promising opportunities. In this work, we report a comprehensive study of the electronic transport, thermoelectric properties, and electronic structure of semimetal MoSi₂. Our results show that MoSi₂ simultaneously exhibits axis-dependent conduction polarity (ADCP), consistent with recent reports [2], and, additionally, a large ordinary Nernst effect (ONE). We find that both the Seebeck coefficient and Hall resistivity are positive along [100] direction, while they are negative along [001] direction, confirming the presence of ADCP. A two-band Drude analysis revealed that the charge transport along different axes is dominated by different carrier types and that ADCP originates from strong anisotropy in carrier mobilities. This conclusion is supported by electronic structure calculations showing mixed dimensionality of the Fermi surface. Hall effect and magnetoresistance data demonstrate nearly perfect electron-hole compensation and high carrier mobilities, which, together with a phonon-drag contribution, give rise to the large Nernst response observed in this material. At $T = 31$ K and $B = 9$ T, MoSi₂ exhibits large Nernst thermopower, reaching $S_{yx} = 199$ $\mu\text{V}/\text{K}$, which corresponds to a Nernst power factor of 520 $\mu\text{W}/(\text{cm}^1 \text{K}^2)$. These findings identify MoSi₂ as a rare system in which ADCP and large ONE coexist, underscoring its potential for transverse thermoelectric applications.

This work was supported by the National Science Centre (Poland) under the project No. 2023/51/D/ST3/01564.

[1] G. Yang *et al.*, *Adv. Mater.* 37 (2025) 2506417.

[2] H. Manako, S. Ohsumi, S. Yoshida, R. Okazaki, Y.J. Sato, *Commun. Mater.* 7 (2025) 41.

INVESTIGATION OF TRANSPORT AND MAGNETIC PROPERTIES OF INTERCALATED 2H-NbS₂ AND 2H-TaS₂

Gaurav Pransu¹, Naveen Dhama^{1,2}, Wojciech Sas^{1,3}, Bruno Gudac¹, Yuki Utsumi Boucher¹, Mario Novak⁴, Mirta Herak¹, Neven Barišić^{4,5}, and Petar Popčević¹

¹ *Institut za Fiziku, Bijenička Cesta 46, 10000 Zagreb, Croatia*

² *Université Paris-Saclay, CNRS, Laboratoire de Physique des Solides, Orsay, France*

³ *Institute of Nuclear Physics, Polish Academy of Sciences, Kraków, Poland*

⁴ *Physics Department, Faculty of Science, University of Zagreb, Zagreb, Croatia*

⁵ *Institute of Solid State Physics, TU Wien, 1040 Vienna, Austria*

gpransu@ifs.hr

Transition metal dichalcogenides (TMDs) are a layered class of materials known for their rich physical properties, including charge density waves (CDWs) and superconductivity. Their layered crystal structure allows the intercalation of first-row transition metals into the van der Waals gaps, which significantly modifies the physical properties of the host material, suppressing CDW and superconducting ground states while inducing magnetic order and enabling potential applications in spintronics and novel electronics [1].

In this study, we synthesized high-quality single crystals of Ni_xNbS₂ across a broad intercalation range ($0.01 < x < 0.6$), as well as stoichiometric Co_{1/3}TaS₂. Both systems exhibit antiferromagnetic ordering; however, a measurable ferromagnetic component was also observed in each, indicating the presence of Dzyaloshinskii-Moriya interactions.

We investigated the influence of intercalation on the electronic structure, magnetic and transport properties using angle-resolved photoemission spectroscopy (ARPES) and magnetotransport measurements [2]. Ongoing work involves applying both uniaxial and hydrostatic pressure to further understand the coupling between the metallic and magnetic subsystems [3].

[1] R.H. Friend, A.D. Yoffe, *Adv. Phys.* 36 (1987) 1-94.

[2] Y.U. Boucher *et al.*, *Phys. Rev. B* 109 (2024) 085135.

[3] P. Popčević *et al.*, *Phys. Rev. B* 107 (2023) 235149.

PHASE FORMATION IN ALUMINUM-BASED GRADIENT ALLOYS OBTAINED BY SELECTIVE LASER MELTING

I. Shtablavyi, Yu. Kulyk, N. Popilovskyi, R. Serkiz, O. Kovalskyi, Yu. Plevachuk,
and S. Mudry

*Department of Metal Physics, Ivan Franko National University of Lviv,
Kyryla i Mefodiya St. 8, 79005 Lviv, Ukraine
ihor.shtablavyi@lnu.edu.ua*

Selective laser melting is widely used for the production of metal parts with complex geometries and for rapid prototyping [1]. This method also enables the fabrication of metallic alloys with unique properties using additive manufacturing technology. In particular, it allows the synthesis of gradient materials with a continuous distribution of phase composition, grain size, and shape in the direction perpendicular to the printing plane during laser 3D printing.

Aluminum-based alloys are of particular interest for additive manufacturing due to their favorable properties, post-processing capability, and relatively low cost [1-3]. However, due to the rapid melting and solidification processes that occur during selective laser melting, controlling phase formation in alloys in order to achieve the required physical properties remains a challenge. This is especially important when alloys are produced from mixtures of elemental powders.

In view of this, the present work investigates phase formation during selective laser melting of elemental powders in the Al–Cu–Ni and Al–Cu–Zn systems with different compositions, depending on the laser processing parameters. A low-power fiber laser was used for alloy synthesis. To control the absorbed laser energy, the laser beam power, scanning speed, and hatch distance were varied. The obtained alloys were studied using scanning electron microscopy and X-ray diffraction, and their mechanical properties were also investigated. The possibility of controlling the gradient of the phase composition in aluminum-based alloys was demonstrated, which in turn leads to improved mechanical properties.

This work was supported by the National Research Foundation of Ukraine, project No. 2025.06/0016.

- [1] N.T. Aboulkhair, M. Simonelli, L. Parry, I. Ashcroft, C. Tuck, R. Hague, *Progr. Mater. Sci.* 106 (2019) 100578.
- [2] H. Wu, Y. Ren, J. Ren, L. Liang, R. Li, Q. Fang, A. Cai, Q. Shan, Y. Tian, I. Baker, *J. Alloys Compd.* 873 (2021) 159823.
- [3] H. Wu, Y. Ren, J. Ren, A. Cai, M. Song, Y. Liu, X. Wu, Q. Li, W. Huang, X. Wang, I. Baker, *Virtual Phys. Prototyping* 15 (2020) 570-582.

A COMPARATIVE STUDY OF RARE-EARTH-BASED HALF-HEUSLER BISMUTHIDES $RTBi$ AND ANTIMONIDES $RTSb$ ($T = Pd, Pt$)

A. Agarwal, O. Pavlosiuk, P. Wisniewski, and D. Kaczorowski
Institute of Low Temperature and Structure Research, Polish Academy of Sciences
Okolna 2, 50-422, Wroclaw, Poland
a.agarwal@intibs.pl

Rare-earth-based half-Heusler (HH) compounds have attracted significant interest over the past decade, driven by theoretical predictions of their non-trivial electronic band structures. These compounds crystallize in a non-centrosymmetric face-centered cubic structure (space group $F-43m$) and exhibit strong spin-orbit coupling, which facilitates band inversion. Notably, several non-magnetic $RPtBi$ and magnetic $RPdBi$ bismuthides have been identified as unconventional superconductors, providing an ideal platform to study the interplay between superconductivity, magnetism, and non-trivial topology.

To date, the corresponding antimonides, $RPtSb$ and $RPdSb$, have received comparatively little attention. In this work, we report the successful flux growth of single-crystalline $RPtSb$ ($R = Gd, Tb, Dy, \text{ and } Ho$) and $RPdSb$ ($R = Er \text{ and } Ho$) and present a detailed investigation of their thermodynamic and electrical transport properties. We identified several features common to the bismuthide analogues, including low-temperature antiferromagnetic ordering, semimetallic-like resistivity, a multiband Hall effect, and weak antilocalization in magnetotransport. Conversely, unlike their Bi-based counterparts, the $RPdSb$ compounds do not exhibit large negative longitudinal magnetoresistance or an enhanced anomalous Hall conductivity, *i.e.*, features often associated with the chiral magnetic anomaly. Interestingly, however, such signatures appear in $GdPtSb$ and $HoPtSb$, likely due to stronger spin-orbit coupling than in the Pd-containing phases. Furthermore, both compounds exhibit a systematic evolution of the angular magnetoresistance in external magnetic fields, probably indicating a field-induced reconstruction of their electronic band structures.

In this talk, we compare the physical properties of the HH bismuthides and antimonides, demonstrating that the latter phases are as intriguing as their Bi-based counterparts and offer a viable route for tuning the electronic properties of this family of materials.

This work was supported by the National Science Centre (Poland) under project No. 2021/40/Q/ST5/00066.

PHASE TRANSFORMATIONS IN THE Co–Cr–Cu–Fe–Ni SYSTEM: CALPHAD DESCRIPTION AND EXPERIMENTAL STUDY

M. Bulanova¹, I. Fartushna¹, P. Agraval², and M. Turchanin²

¹ *Frantsevich Institute for Problems of Materials Science, NAS Ukraine*

² *Donbas State Engineering Academy*

mvbulanova2@gmail.com

The Co–Cr–Cu–Fe–Ni system is of considerable practical interest due to the possibility of obtaining high-entropy structural alloys (HEAs). The rational choice of their compositions and optimization of technological parameters for their production requires understanding the nature of phase transformations. For multicomponent systems, this is possible through thermodynamic modeling. This work is devoted to CALPHAD calculations of the Co–Cr–Cu–Fe–Ni quinary phase diagram and its experimental verification.

The simulation results are presented as polythermal sections at temperatures from the liquidus to 1000 K. Equiatomic and near-equiatomic alloys turned out to be either single-phase FCC1 or two-phase FCC1+FCC2 (FCC1 and FCC2 are Cu-depleted and Cu-enriched solid solutions, respectively).

The experimental study was performed on six near-equiatomic alloys of the calculated sections (Table). The samples were arc-melted from pure components and annealed at 1273 K / 8.5 h. The samples were tested by SEM, EPMA, XRD, and DTA. Microhardness measurements were performed.

Chemical and phase composition of the studied alloys

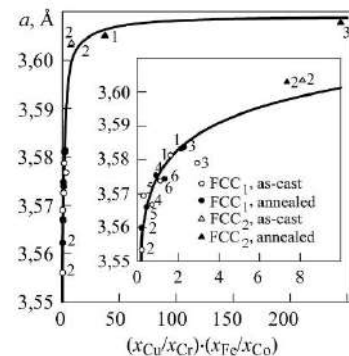
#	Nominal chemical composition, x_{Me}	Phase composition	
		As-cast	Annealed at 1273 K / 8.5 h
1	$Cu_{0.200}Cr_{0.080}Fe_{0.200}Co_{0.200}Ni_{0.320}$	FCC1 + FCC2	FCC1 + FCC2
2	$Cu_{0.125}Cr_{0.125}Fe_{0.125}Co_{0.5}Ni_{0.125}$	FCC1 + FCC2	FCC1 + FCC2
3	$Cu_{0.125}Cr_{0.125}Fe_{0.5}Co_{0.125}Ni_{0.125}$	FCC1 + FCC2	FCC1 + FCC2
4	$Cu_{0.125}Cr_{0.125}Fe_{0.125}Co_{0.125}Ni_{0.500}$	FCC1 + (Cu,Ni) ¹	FCC1
5	$Cu_{0.100}Cr_{0.135}Fe_{0.135}Co_{0.270}Ni_{0.360}$	FCC1 + (Cu,Ni) ¹	FCC1
6	$Cu_{0.100}Cr_{0.135}Fe_{0.270}Co_{0.135}Ni_{0.360}$	FCC1 + (Cu,Ni) ¹	FCC1

¹ Nonequilibrium phase

The XRD and DTA results show excellent agreement with the calculated sections. Alloys # 2, 3, both cast and annealed, have a typical two-phase structure; alloys # 4-6 have a typical cellular structure. Alloy # 1 combines both types of structure. The nature of the microstructures agrees well with the calculated vertical sections. The microhardness of the FCC1 phase (matrix) in the cast alloys lies within $220 \pm 20 \dots 295 \pm 8$, and $238 \pm 7 \dots 300 \pm 10$ in the annealed alloys.

Two contributions have been established that affect the lattice parameters of the phases. One reflects the influence of Cu and Cr, the second is due to Fe, Co, Ni. The parameter $P = (x_{Cu}/x_{Cr}) \cdot (x_{Fe}/x_{Co})$ is proposed, which combines these two influences and defines the values of the lattice parameters (the concentration of the components is taken from the microprobe data). The dependence is shown in the Figure.

The results of the CALPHAD modeling show the potential of the system for producing dispersion-strengthened HEAs, both by low-temperature aging and by forming frozen emulsion-type structures by melt quenching.



Lattice periods of FCC1 and FCC2 phases versus the P parameter

MULTIBAND SUPERCONDUCTIVITY IN THE KAGOME-LATTICE COMPOUND Re_2Zr

Gabriel Kuderowicz and Bartłomiej Wiendlocha
Faculty of Physics and Applied Computer Science,
AGH University of Krakow, Aleja Mickiewicza 30, 30-059 Krakow, Poland
wiendlocha@agh.edu.pl

Kagome-lattice materials have recently attracted considerable interest due to their potential to host unusual electronic states such as flat bands, Dirac dispersions, strong electronic correlations, and unconventional superconductivity. The hexagonal Laves phase compound Re_2Zr contains a kagome lattice of Re atoms and becomes superconducting below $T_c = 6.65$ K. Recent experiments [1] suggested possible time-reversal symmetry breaking in the superconducting state and suggested spin-fluctuations as the pairing mechanism, motivating a theoretical investigation of the origin of superconductivity in this material.

In this work, we present a comprehensive first-principles study of the electronic structure, lattice dynamics, electron–phonon interaction, and superconducting properties of Re_2Zr . Electronic structure calculations reveal a complex multiband character with the Fermi surface consisting of a mixture of quasi-two-dimensional cylindrical sheets associated with the kagome Re planes and three-dimensional pockets originating from hybridization with Zr states. Spin-orbit coupling strongly modifies the band structure and produces flat bands near the Fermi level, leading to a van Hove singularity located near E_F . Phonon spectra and electron-phonon interaction were calculated using density functional perturbation theory. The phonon spectrum extends up to about 7 THz and exhibits several flat optical modes. The Eliashberg spectral function shows that the electron-phonon coupling is distributed relatively uniformly across the phonon spectrum, resulting in a moderate coupling strength $l \approx 0.88$.

The superconducting state was investigated using anisotropic density functional theory for superconductors [2], including electron-phonon interaction, dynamically screened Coulomb repulsion, and longitudinal spin fluctuations. The calculations predict a strongly anisotropic multiband superconducting state with superconducting gaps distributed across different Fermi surface sheets. The electron-phonon coupling varies significantly across the Fermi surface, while Coulomb repulsion is enhanced on sheets associated with the kagome lattice. The resulting superconducting gap distribution corresponds to $2\Delta/k_B T_c = 3$ to 4.5. The calculated critical temperature is $T_c = 7.7$ K without spin fluctuations and decreases to $T_c = 6.4$ K when spin fluctuations are included, in excellent agreement with the experimental value. These results demonstrate that superconductivity in Re_2Zr can be quantitatively described within a conventional phonon-mediated mechanism, while exhibiting pronounced multiband character and strong gap anisotropy arising from the complex electronic structure of the kagome lattice system.

- [1] Manasi Mandal, A. Kataria, P.K. Meena, R.K. Kushwaha, D. Singh, P.K. Biswas, R. Stewart, A.D. Hillier, R.P. Singh, *Phys. Rev. B* 111 (2025) 054511.
- [2] M. Kawamura, Y. Hizume, T. Ozaki, *Phys. Rev. B* 101 (2020) 134511.

**THE EFFECT OF SILICON SUBSTITUTION BY BORON IN α -Nb₅Si₃:
STRUCTURAL AND PHYSICAL PROPERTIES OF THE II-TYPE
SUPERCONDUCTOR Nb₅Si₂B**

M. Falkowski¹, J. Kaczkowski¹, Z. Śniadecki¹, T.J. Bednarchuk², G. Chełkowska³,
and A. Kowalczyk¹

¹ *Institute of Molecular Physics, Polish Academy of Sciences,
Smoluchowskiego 17, 60-179 Poznań, Poland*

² *Institute of Low Temperature and Structure Research, Polish Academy of Sciences,
Okólna 2, 50-422 Wrocław, Poland*

³ *University of Silesia, August Chelkowski Institute of Physics,
75 Pułku Piechoty 1a, 41-500 Chorzów, Poland
michal.falkowski@ifmpan.poznan.pl*

The binary boron-free compound, Nb₅Si₃, is characterized by phase duality manifested by different crystal structures depending on the temperature. In general, two main phases can be distinguished: (i) the low-temperature α -Nb₅Si₃ phase, which crystallizes in a tetragonal Cr₅B₃-type structure (prototype), and (ii) the high-temperature β -Nb₅Si₃ phase, which crystallizes in a tetragonal variant of the W₅Si₃-type structure. However, the two cases differ not only in terms of structural type, but also in that the α -Nb₅Si₃ phase was found to be a normal metal down to 0.01 K, while the β -phase of Nb₅Si₃ exhibits the properties of a II-type superconductor with a superconducting transition temperature of 0.7 K [1].

Based on the phase diagram for the Nb–Si–B ternary system, the α -phase can exist within the solubility range represented by Nb₅Si_{3-x}B_x with $0 \leq x \leq 2$, where the boron doping effect additionally promotes the formation of superconductivity [2]. Consequently, substituting B for one Si atom leads to the formation of the Nb₅Si₂B compound, which also crystallizes in a tetragonal Cr₅B₃-type structure with space group *I4/mcm*. There are 32 atoms in the unit cell (20 Nb, 8 Si, 4 B atoms), situated in a layered arrangement along the *c*-axis, where the Nb atoms occupy two crystallographic sites, 4*c* and 16*l* – the same as for the prototype compound Nb₅Si₃.

Nb₅Si₂B is a II-type superconductor with $T_c = 8.2$ K. The compound is characterized by a moderately increased electron-phonon coupling $\lambda_{\text{el-ph}} = 0.62$ and possible unconventional character of the superconducting state. A feature that may indicate this is the small jump in specific heat $\Delta C_{\text{el}}/\gamma_n T_c = 0.3$, the magnitude of which is considerably smaller than the classical BCS value (= 1.43), as well as the incompatibility of the C_p data with the spherical single-gap model below T_c , thus suggesting the presence of anisotropic or multi-gap superconductivity in this material [3]. The combination of DFT calculations with experimental investigations allowed the interpretation of the measured XPS valence band spectrum of Nb₅Si₂B and the conclusion that it is formed mainly by the Nb 4*d* states, which hybridize weakly with Si 3*p*, 3*s*, and to a negligible extent with B 2*p*, 2*s* [4].

- [1] J.O. Willis, R.M. Waterstrat, *J. Appl. Phys.* 50 (1979) 2863.
- [2] A. Brauner, C.A. Nunes, A.D. Bortolozzo, G. Rodrigues, A.J.S. Machado, *Solid State Commun.* 149 (2009) 467.
- [3] M. Falkowski, Z. Śniadecki, T.J. Bednarchuk, A. Kowalczyk, *J. Appl. Phys.* 133 (2023) 243901.
- [4] M. Falkowski, J. Kaczkowski, G. Chełkowska, A. Kowalczyk, *Metall. Mater. Trans. A* 55 (2024) 4639.

ENHANCED THERMOELECTRIC POWER IN SEMICONDUCTOR-WEYL NANOCOMPOSITE MATERIALS

S. Samanta¹, N. Tsujii¹, and T. Mori^{1,2}

¹ *International Centre for Materials Nanoarchitectonics (MANA),*

National Institute for Materials Science, Tsukuba, Ibaraki 305-0047, Japan

² *Graduate School of Pure and Applied Sciences, University of Tsukuba, Tsukuba, Japan*
MORI.Takao@nims.go.jp

How to overcome thermoelectric performance deterioration of a material in the intrinsic excitation regime remains a central challenge. Addressing this challenge, we show magneto-thermoelectric correlation as a promising approach to govern concurrently large thermopower and Seebeck coefficient in a wide temperature regime, including room temperature [1-3]. Here, we synthesised magnetic nanocomposite thermoelectric materials by integrating a topological Weyl magnet (x) as an inclusion in a semiconductor $\text{Fe}_2\text{V}_{0.95}\text{Ta}_{0.05}\text{Al}$ matrix ($x = 1$, and 2 %). The promising properties of magnetic topological nanoparticles, such as robustness of the topological effect to grain boundary scattering, linear band dispersion, and large magneto-Seebeck effect, yield an unveiled strategy to explore high thermopower in composite materials [3,4].

We present the synthesis of composites from micro- to nanoscale *via* powder processing and spark plasma sintering techniques. We demonstrate, based on magneto-transport, thermal, and thermoelectric measurements, how spin-fluctuation and phonon-scattering can simultaneously act as an efficient strategy for boosting high thermoelectric performance by finetuning nanostructure thermoelectric materials. This result may lead to a new guiding tool for overcoming a gap of high performance below and above room temperature in the familiar Fe_2VAl p-type thermoelectric materials [4].

This work was carried out under the project “Mirai project funding” JST Mirai Program, Grant JPMJMI19A1.

- [1] N. Tsujii, A. Nishide, J. Hayakawa, T. Mori, *Sci. Adv.* 5 (2019) eaat5935.
- [2] M.V. Costache, G. Bridoux, I. Neumann, S.O. Valenzuela, *Nat. Mater.* 11(3), (2012) 199-202.
- [3] C. Fu, Y. Sun, C. Felser, *APL Mater.* 8 (2020) 4.
- [4] F. Garmroudi, I. Serhienko, M. Parzer, S. Ghosh, P. Ziolkowski, G. Oppitz, H.D. Nguyen, C. Bourgès, Y. Hattori, A. Riss, S. Steyrer, G. Rogl, P. Rogl, E. Schafner, N. Kawamoto, E. Müller, E. Bauer, J. de Boor, T. Mori, *Nat. Commun.* 16 (2025) 2976.

***f*-ELEMENT HIGH-ENTROPY ALLOYS: NEW MATERIALS FOR HYDROGEN APPLICATIONS**

Michal Šálka, Shanmukh Veera Venkata U. K. Devanaboina, and Silvie Černá
*Department of Condensed Matter Physics, Faculty of Mathematics and Physics,
Charles University, 12116 Prague, Czechia
silvie.cerna@matfyz.cuni.cz*

Hydrogen is considered to be a fuel of the future. The biggest challenges in hydrogen storage are its volume and reactivity. Therefore, the interaction of hydrogen with solid materials has come to the forefront. Certain types of metallic materials can absorb large amounts of hydrogen and release it again upon heating. Recently, a new class of alloys, namely, high-entropy alloys (HEAs), started to be investigated for hydrogen storage as they can form metal hydrides.

One of the first studies on hydrogen absorption by *f*-based HEAs/MEAs (MEA = medium-entropy alloy) was performed by M. Balcerzak *et al.* [1]. Stabilization of a single-phase *fcc* structure induced by the hydrogen absorption process was observed. Moreover, a measured high storage capacity of 2.5 H/M was observed after hydrogenation conducted under mild conditions.

We have been studying the hydrogen sorption properties of selected *f*-element (*RE* and *U*) HEAs. From the group of *RE*-HEAs, results on Ho–Dy–Y–Gd–Tb [2,3] will be presented. It contains yttrium, which belongs to the rare-earth group being similar to the lanthanides. At the same time, it represents the first element in the group of transition metals (*d*-metals). This makes it possible to gradually include *d*-elements as one of the components, thus further increasing the mixing entropy. We have been testing the concentration limits for the stability of a single-phase material by gradually adding transition metals (Ti and Zr) – due to decreasing atomic radii. The Ti- and Zr-substitutions have different impact on the crystal structure of the parent HEA. While Ti-substitution leads to multiple phases (hexagonal *P6₃/mmc* and trigonal *R-3m*), the Zr-substituted alloys crystallize in a single phase (hexagonal *P6₃/mmc*).

Hydrogen absorption (hydride with 3 H at./f.u) leads to the stabilization of a single phase with a trigonal structure (*P-3c1*). Thanks to partial desorption it was possible to obtain a hydride with 2 H at./f.u (cubic, *Fm-3m*). Full desorption was not possible due to the limited temperature range of the hydrogenation apparatus. Preliminary data on a similar high-entropy alloy, Gd_{0.2}Dy_{0.2}Er_{0.2}Ho_{0.2}Tb_{0.2} (unpublished data), show that temperatures around 1350 K are necessary to desorb all hydrogen.

Several members of the *U–T* (*T* = transition metal) HEA family were synthesized, as well. We will present results of a H-absorption study on Nb–Ta–Mo–W–U alloys. These alloys show very promising H-sorption properties.

This work was supported by the Faculty of Mathematics and Physics through a Student faculty grant (SFG) and by the Czech Science Foundation under the project 25-16339 S.

- [1] M. Balcerzak *et al.*, *J. Am. Chem. Soc.* 146 (2024) 5283-5294.
- [2] M. Feuerbacher *et al.*, *Mater. Res. Lett.* 3(1) (2015) 1-6.
- [3] J. Luznik *et al.*, *Phys. Rev. B* 92 (2015) 224201.

MAGNON EXCITATIONS AND FIELD EVOLUTION IN THE NON-COPLANAR ANTIFERROMAGNET MnTe₂

David Sviták¹, Nikolaos Biniskos^{1,2}, Manuel dos Santos Dias³, Stéphane Raymond²,
Frédéric Bourdarot², and Petr Čermák¹

¹ *Department of Condensed Matter Physics, Faculty of Mathematics and Physics,
Charles University, Ke Karlovu 5, 121 16 Prague 2, Czech Republic*

² *Université Grenoble Alpes, CEA, IRIG, MEM, MDN, F-38000 Grenoble, France*

³ *Scientific Computing Department, STFC Daresbury Laboratory, Warrington, UK
david.svitak@matfyz.cuni.cz*

Topological band structures are well known in electronic systems and can also emerge for bosonic quasiparticles such as magnons, the collective spin excitations of magnetically ordered materials [1,2]. Weyl magnons correspond to linear band crossings that act as monopoles of Berry curvature in momentum space and may lead to phenomena such as anomalous thermal Hall responses [3]. Their formation depends strongly on the symmetry of the magnetic structure. In systems with both inversion symmetry and an effective time-reversal symmetry, such as the cubic antiferromagnet MnTe₂, the Berry curvature vanishes and Weyl points are not allowed in the magnon spectrum of the symmetric phase.

Recent time-of-flight neutron measurements reported nodal-line magnons and field-induced Weyl magnons in MnTe₂ [4]. Here we study the magnetic excitation spectrum using higher-resolution triple-axis neutron spectroscopy. Single crystals were grown by chemical vapor transport [5] and coaligned using the Automatic Laue Sample Aligner (ALSA) [6]. Measurements were performed on the IN22 and IN12 triple-axis spectrometers in zero field and in a field of 10 T. The spectra were analyzed using linear spin-wave theory to determine a microscopic model of the magnon dispersion and its field dependence. We quantify the dual role of the Dzyaloshinskii-Moriya interaction in stabilizing the magnetic ground state and in the magnon spectrum.

- [1] L. Zhang *et al.*, *Phys. Rev. B* 87 (2013) 144101.
- [2] M. dos Santos Dias *et al.*, *Nat. Commun.* 14 (2023) 8437.
- [3] A. Mook *et al.*, *Phys. Rev. B* 99 (2019) 014427.
- [4] A.E. Fahmy *et al.*, *arXiv:2512.18534*, 2025.
- [5] P. Burlet *et al.*, *Phys. Rev. B* 56 (1997) 14013.
- [6] Charles Automata, <https://charlesautomata.cz/alsa>.

INFLUENCE OF SYNTHESIS METHOD AND HYDROGEN INCORPORATION ON THE SUPERCONDUCTING PROPERTIES OF A TiVZrNb MEDIUM-ENTROPY ALLOY

G. Pristáš¹, S. Gabáni¹, O. Onufriienko¹, K. Flachbart¹, M. Moussa², J.-L. Bobet², J. Zorych³, and J. Huot⁴

¹ *Centre of Low Temperature Physics, Institute of Experimental Physics, Slovak Academy of Sciences, Watsonova 47, SK-04001 Košice, Slovakia*

² *Hydrogène et Intermétalliques, ICMCB - CNRS - Université de Bordeaux, 87 Av. du Dr. Schweitzer, F-33600 Pessac, France*

³ *Faculty of Electrical Engineering and Informatics, Technical University, SK-04200 Košice, Slovakia*

⁴ *Hydrogen Research Institute, Université du Québec à Trois-Rivières, 3351 des Forges, Trois-Rivières, QC G9A 5H7, Canada
gabriel.pristas@saske.sk*

We report on the influence of the synthesis method on the superconducting properties of a TiVZrNb medium-entropy alloy. We prepared an equimolar medium-entropy TiVZrNb alloy by three different preparation methods. The main aim of our study was to elucidate the relationship between the crystallographic quality and the superconducting performance. We observed a transition temperature T_C in the range from 6.144 K up to 6.455 K and an upper critical magnetic field B_{C2} from 9.070 T up to 9.804 T. These parameters were determined by magnetic susceptibility, resistivity, and specific heat measurements. Our results show that the superconductivity in TiVZrNb is of conventional strong coupling s-wave type with a high energy gap $2\Delta_0$ to T_C ratio $2\Delta_0/k_B T_C = 4.3$ and an intermediate electron-phonon coupling parameter $\lambda_{ep} = 0.69$. Our results demonstrate that different preparation methods for a medium-entropy alloy of the same composition can influence the superconducting parameters, e.g., T_C by around 4.8 % and B_{C2} by around 7.4 %. Moreover, we examined the influence of hydrogen incorporation on the superconductivity. The hydrogenation of this alloy, which appears to be promising for hydrogen storage, led to suppression of superconductivity in the derived (TiVZrNb)H_x hydrides, where $x = 0.5, 1.75, \text{ and } 2$. A possible reason for this may be related to the high concentration of disorder (defects) in the hydrides, which originates from the preparation method during which the initial alloy disintegrates into powder.

The work was supported by the Slovak Research and Development Agency under the contract no. APVV-23-0624, and by the Slovak Scientific Grant Agency under Contract No. VEGA 2/0091/24. Liquid nitrogen for the experiments was sponsored by U. S. Steel Košice, s.r.o. The synthesis of the samples was supported by ANR-22-PEHY0007.

SURFACE CHEMISTRY OF LaNi₅ INTERMETALLIC CATALYST: CRYSTAL GROWTH, SURFACE STABILITY, AND MOLECULES BINDING

G. Palla¹, E. Spennati², G. Garbarino², P. Riani¹, and R. Freccero¹

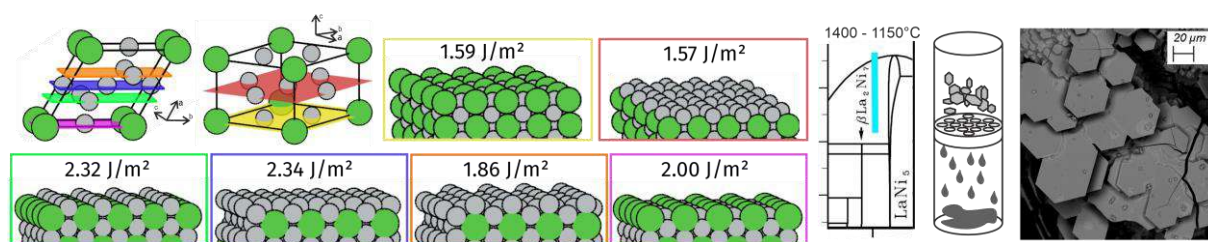
¹ Department of Chemistry and Industrial Chemistry, University of Genoa, Genoa, Italy

² Department of Civil, Chemical and Environmental Engineering,
University of Genoa, Genoa, Italy
giorgio.palla@edu.unige.it

Among the key technological routes for reducing the carbon footprint, CO₂-related reactions play a relevant role [1]. Recently, LaNi₅ and CeNi₅ were found to decompose through a complex mechanism when tested as Sabatier catalysts [2]. Clarifying this mechanism is essential for the rational improvement of reaction conversion and selectivity, especially for intermetallic-based catalysts [3].

To achieve this goal, the first step was to investigate surface stability through combining *ab initio* and experimental studies. Several terminations of the crystal structure were modelled in a supercell with Density Functional Theory (DFT) at the PBEsol level of theory. Micrometric, hexagonally shaped crystals of the target phase were obtained employing the self-flux growth technique in a Canfield-type crucible. Indexing of the exposed crystal facets, performed by SC-XRD, revealed a predominance of the (001) surface, compared to (100), in good agreement with the calculated surface energies. The surface chemistry of the materials was investigated by adsorbing H₂ molecules on different sites and in various geometries, in order to explore the complex potential energy surface of the system. This analysis revealed highly active sites in all possible terminations of the (001) and (100) surfaces and confirmed that H₂ dissociation into hydrides is favored at surface sites featuring dangling bonds, as located through Electron Localizability Indicator (ELI-D) mapping of the model.

These insights provide the basis for the fine-tuning of machine-learned interatomic potentials for molecular dynamics and the study of interactions with other relevant molecules, including CO₂, N₂, and CH₄.



Surface terminations and corresponding energies of the LaNi₅ (001) and (100) planes (left), and SEM micrographs with preparation details of the self-flux-grown LaNi₅ single crystals

[1] Wang Wei, Gong Jinlong, *Front. Chem. Sci. Eng.* 5 (2011) 2-10.

[2] R. Freccero, E. Spennati, G. Garbarino, P. Riani, *Appl. Catal. B* 343 (2024) 123532.

[3] S. Furukawa, T. Komatsu, *ACS Catal.* 7(1) (2017) 735-765.

NOWOTNY CHIMNEY-LADDER PHASE(S) (Mo,Ru)₈Ge₁₃: CRYSTAL AND ELECTRONIC STRUCTURES

K. Pryga¹, B. Korotoshyn², N. Muts², Ya. Tokaychuk², L. Akselrud², O. Cherniushok³,
T. Parashchuk³, K.T. Wojciechowski³, B. Wiendlocha¹, Yu. Grin⁴, and R. Gladyshevskii²

¹ Faculty of Physics and Applied Computer Science, AGH University of Krakow,
Mickiewicza Ave. 30, 30-059 Krakow, Poland

² Department of Inorganic Chemistry, Ivan Franko National University of Lviv,
Kyryla i Mefodiya St. 6, 79005 Lviv, Ukraine

³ Thermoelectric Research Laboratory, Faculty of Materials Science and Ceramics,
AGH University of Krakow, Mickiewicza Ave. 30, 30-059 Krakow, Poland

⁴ MPI Chemische Physik fester Stoffe, Nöthnitzer Str. 40, 01187 Dresden, Germany
pryga@agh.edu.pl

Nowotny chimney-ladder (NCL) phases constitute a promising class of compounds for the development of advanced thermoelectric materials, due to their modulated composite crystal structures, the presence of relatively heavy elements, and their semiconducting behaviour [1]. Moreover, their complex structure can potentially be utilized to achieve the highly sought-after Slack's phonon-glass electron-crystal concept.

A sample of composition Mo_{11.9}Ru_{26.2}Ge_{61.9} was prepared by sintering metal powders in a vacuum-sealed quartz ampoule at 1000 °C for 4 days and at 800 °C for the next 5 days. X-ray powder diffraction data from a polycrystalline sample were obtained using a PROTO AXRD Benchtop diffractometer (Cu K α ₁ radiation).

According to the powder X-ray diffraction pattern, the sample contained two ternary chimney-ladder phases of compositions Mo_{11.7(4)}Ru_{27.3(4)}Ge_{61.0(1)} and Mo_{9.9(6)}Ru_{29.3(6)}Ge_{60.8(1)}. A chimney-ladder type structure model was developed in the superspace group $P: I4_1/amd(00ss): P4/nnc(q0q0)$, using the concept of modulated composite crystal structures in (3+1)-dimensional superspace [2]. Two isopointal commensurate approximants (Mo,Ru)₈Ge₁₃ were refined in space group $P-4c2$ (Pearson symbol $tP84$) with the following cell parameters: $a = 5.8570(8)$, $c = 37.889(6)$ Å for the Mo-rich phase and $a = 5.812(2)$, $c = 37.34(2)$ Å for the Mo-poor phase.

A theoretical study of the electronic structure of the ternary NCL phase Mo_{2.5}Ru_{5.5}Ge₁₃ showed that it is a p-type semiconductor with a relatively narrow band gap and multi-valley valence band structure. Fully-relativistic DFT calculations were performed using the all-electron full-potential linearized augmented plane wave (FP-LAPW) method, as implemented in the WIEN2k package. Analysis of the transport properties performed using the BoltzTraP code predicts high anisotropy for both the electrical conductivity and the Seebeck coefficient. The positions of the atoms within the Ge "ladders" play a crucial role and both the electronic structure and the thermopower are heavily affected by structural relaxation.

The work was supported by a grant (BPN/NSF/2023/1/00010) from the Polish National Agency for Academic Exchange (NAWA) under the International Multilateral Partnerships for Resilient Education and Science System in Ukraine IMPRESS-U initiative.

[1] N. Chauhan, S. Sara, A. Bhattacharya, T. Mori, Y. Miyazaki, *Adv. Funct. Mater.* 34 (2024) 2313948.

[2] L. Akselrud, R. Cardoso Gil, M. Wagner-Reetz, Yu. Grin, *Acta Crystallogr. B* 71 (2015) 707-712.

FROM SPIN GLASS TO RANDOM SINGLETS: DISORDER-DRIVEN QUANTUM MAGNETISM IN NaCdCu₂F₇

A. Kancko¹, H. Sakai², C.A. Corrêa³, P. Proschek¹, J. Prokleška¹, T. Haidamak¹,
M. Uhlarz⁴, A. Berlie⁵, Y. Tokunaga², and R.H. Colman¹

¹ *Department of Condensed Matter Physics, Faculty of Mathematics and Physics, Charles University, Ke Karlovu 5, 121 16 Prague, Czechia*

² *Advanced Science Research Centre, Japan Atomic Energy Agency, Tokai, Ibaraki 319-1195, Japan*

³ *Institute of Physics, Czech Academy of Sciences, Na Slovance 2, 182 00 Prague, Czechia*

⁴ *Hochfeld-Magnetlabor Dresden (HLD-EMFL), Helmholtz-Zentrum Dresden-Rossendorf (HZDR), 01328 Dresden, Germany*

⁵ *ISIS Neutron and Muon Source, Rutherford Appleton Laboratory, Science and Technology Facilities Council, Chilton, Oxfordshire OX11 0QX, United Kingdom*
andrej.kancko@matfyz.cuni.cz

The interplay of geometric frustration and quenched disorder can stabilize unconventional magnetic ground states such as the random-singlet (RS) state. It is characterized by a broad distribution of exchange couplings $P[J] \sim J^{-\alpha}$, leading to the formation of localized singlets over multiple length scales and weakly-coupled “orphan spins”. This is noted by a power-law scaling of bulk and local-probe thermodynamic quantities, with data collapse as a function of temperature and field T/H [1].

We report evidence for an RS ground state in the very rare instance of a $S = \frac{1}{2}$ Heisenberg pyrochlore antiferromagnet – NaCdCu₂F₇ [2], where intrinsic cationic Na⁺/Cd²⁺ disorder induces random Cu²⁺–F⁻–Cu²⁺ superexchange interactions on the frustrated lattice of corner-sharing tetrahedra. No long-range magnetic order or canonical spin freezing is observed down to 58 mK *via* muon spin relaxation (μ SR) and ²³Na nuclear magnetic resonance (NMR) measurements. Magnetic susceptibility, isothermal magnetization, and specific heat indicate a disorder-driven network of random singlets and orphan spins. Convincingly, evidence of power-law scaling and data collapse can be found in each of these experimental probes.

Importantly, this behaviour contrasts with previously studied higher-spin NaAM₂F₇ [3-8] ($A = \text{Ca, Sr, Cd}$; $M = \text{Co, Ni, Mn, Fe}$) pyrochlore fluorides, where comparable magnetic bond disorder leads to conventional spin-glass freezing. The absence of spin freezing in NaCdCu₂F₇ indicates that strong $S = \frac{1}{2}$ quantum fluctuations suppress the glassy state and instead stabilize a quantum-disordered RS phase.

These results establish NaCdCu₂F₇ as the first realization of a random-singlet state in a three-dimensional frustrated pyrochlore magnet, highlighting the key role of disorder and quantum fluctuations in stabilizing novel quantum phases.

- [1] I. Kimchi *et al.*, *Nat. Commun.* 9 (2018) 4367.
- [2] A. Kancko *et al.*, *Phys. Rev. Res.* 8 (2026) 013344.
- [3] A. Kancko, G. Giester, R.H. Colman, *Phys. Scr.* 98 (2023) 075947.
- [4] A. Kancko, C.A. Corrêa, R.H. Colman, *J. Alloys Compd.* 1024 (2025) 180142.
- [5] J.W. Krizan, R.J. Cava, *Phys. Rev. B* 89 (2014) 214401.
- [6] J.W. Krizan, R.J. Cava, *J. Phys. Condens. Matter* 27 (2015) 296002.
- [7] J.W. Krizan, R.J. Cava, *Phys. Rev. B* 92 (2015) 014406.
- [8] M.B. Sanders *et al.*, *J. Phys. Condens. Matter* 29 (2017) 045801.

CHEMICAL BONDING AND ELECTRONIC STRUCTURE OF THE CUBIC LAVES PHASE NaAg₂

Z. Borchert, T. Klimczuk, and M.J. Winiarski

*Faculty of Applied Physics and Mathematics and Advanced Materials Centre,
Gdansk University of Technology, Narutowicza 11/12, Gdansk 80-233, Poland
michal.winiarski@pg.edu.pl*

We prepared a sample of the cubic Laves phase (*Strukturbericht* C15) NaAg₂ by prolonged low-temperature annealing (300 °C, 3 months) of elemental sodium and silver. The compound was found to exhibit metallic properties and no superconducting transition was observed down to $T = 2$ K in heat capacity measurements [1].

The crystal structure of NaAg₂ contains an Ag pyrochlore network. Based on density functional theory calculations, chemical bonding analysis, and tight binding models, we studied the contribution of [Ag₄]²⁻ fragment orbitals, the relation of the electronic band structure with the simple four-orbital pyrochlore tight binding model, and the importance of higher-order neighbour interactions.

[1] Z. Borchert, T. Klimczuk, M.J. Winiarski, *Inorg. Chem.* 65(7) (2026) 4184-4190.

QUANTUM OSCILLATIONS AND TRANSPORT PROPERTIES OF LAYERED SINGLE-CRYSTAL SrCu₄As₂

Sudip Malick¹, Michał J. Winiarski¹, Joanna Bławat², Hanna Świątek¹, John Singleton²,
and Tomasz Klimczuk¹

¹ *Faculty of Applied Physics and Mathematics, Gdansk University of Technology,
Narutowicza 11/12, 80-233 Gdańsk, Poland*

² *National High Magnetic Field Laboratory, Los Alamos National Laboratory,
Los Alamos, New Mexico 87545, USA
sudip.malick@pg.edu.pl*

We will present a comprehensive study of the physical properties and Fermi-surface topology of a high-quality SrCu₄As₂ single crystal using electrical resistivity, magnetotransport, and quantum-oscillation measurements at high magnetic fields, along with band-structure calculations. The single crystals were grown using a Bi-flux method. Temperature-dependent electrical resistivity revealed a hysteretic phase transition at $T_P = 59$ K, most likely associated with a structural change. Hall resistivity data suggest a marked change in the average hole density resulting from the structural change near T_P . A large, linear, nonsaturating magnetoresistance is observed at low temperatures, likely due to a multipocket Fermi surface. We measured quantum oscillations using the proximity-detector oscillator (PDO) technique in a 60 T pulsed magnet and ³He cryostat. The quantum oscillation data reveal five fundamental oscillation frequencies with low effective masses, indicating Dirac-like band dispersion in this compound, as suggested by band-structure calculations. Angle-dependent PDO measurements indicate a quasi-2D nature of the Fermi surface, with two of the Fermi pockets being highly anisotropic. Overall, our findings suggest that SrCu₄As₂ has a complex Fermi surface with a Dirac-like state [1].

The work at Gdansk University of Technology was supported by the National Science Centre (Poland), Grant No. DEC-2024/08/X/ST3/00338 and DEC-2/2/2023/IDBU/I.1B/Pt. The work at NHML, Los Alamos, was supported by the National Science Foundation Cooperative Agreement No. DMR-2128556, the US Department of Energy (DoE), and the State of Florida.

[1] S. Malick, M.J. Winiarski, J. Bławat, H. Świątek, J. Singleton, T. Klimczuk, *Phys. Rev. B* 112 (2025) 155138.

FROM ELECTRON-PRECISE TO MULTICENTER BONDING IN $RE-\{Ni,Cu\}-Sb$ SYSTEMS

V.V. Romaka

*Technische Universität Dresden (TUD), Bergstrasse 66, 01069 Dresden, Germany
vitaliy.romaka@tu-dresden.de*

Variations in the number of electrons available to the more electronegative components in heteropolar intermetallics give rise to fascinating quantum effects and unconventional chemical bonds. In this light, the $RE-\{Ni,Cu\}-Sb$ systems (RE = rare-earth) are of great interest due to the formation of phases over diverse component concentrations and structural complexity.

The electron-precise intermetallic compounds, half-Heusler $RENiSb$ and $RE_3Cu_4Sb_4$ ($Y_3Au_3Sb_4$ -type structure), have already attracted attention due to their promising thermoelectric properties. While the bonding in these stoichiometric compounds can be explained within the Zintl-Klemm concept, the formation of the homogeneity region in the $RENi_{1-x}Sb$ phases requires a qualitatively different chemical bonding analysis. The application of an orbital-based approach enabled the identification and quantification of the roles of different local defects in the overall structural stability and explained the differences in defect formation of other half-Heusler $MNi_{1+x}Sn$ ($M = Ti, Zr, Hf$) phases. The partial destabilizing role of Ni–Sb and Cu–Sb interactions is reflected in the $RENiSb_2$ and $RECuSb_2$ ($HfCuSi_2$ -type), as well as $RE_3Ni_6Sb_5$ ($Y_3Ni_{5.8}Sb_5$ -type), compounds, where the necessity to lower the electron count leads to the formation of vacancies in the transition metal sublattice. The significantly reduced Sb content in RE_5Ni_2Sb (Mo_5SiB_2 -type) and $RE_3Cu_{22}Sb_9$ ($Dy_3Cu_{20+x}Sb_{11-x}$ -type) causes the formation of multicenter bonding between rare-earth atoms in the first case and between Cu atoms in the second case, leading to high ductility and metallic conductivity. This bonding evolution is further reflected in the average effective charge on the Sb atoms in various binary and ternary compounds of the $RE-\{Ni,Cu\}-Sb$ systems, which depends almost linearly on the number of rare-earth cations in the compound and reveals changes in the chemical bonding topology.

The work was supported by the SFB1143 project of the German Research Foundation (DFG). High-performance computing resources were provided by the NHR Center of TU Dresden (p_quantummat project).

**INFLUENCE OF THE *p*-ELEMENT ON THE HYDROGENATION OF
Tb₂CoM₂ (M = Si, Ge)**

N. Saidov¹, K. Miliyanchuk¹, S. Mašková-Černa², L. Havela², and R. Gladyshevskii¹

¹*Department of Inorganic Chemistry, Ivan Franko National University of Lviv,
Kyryla i Mefodiya St. 6, 79005 Lviv, Ukraine*

²*Department of Condensed Matter Physics, Charles University,
Ke Karlovu 5, 121 16 Prague 2, Czechia
nazar.saidov@lmu.edu.ua*

The representatives of the Hf₃Ni₂Si₃-type (space group *Cmcm*) and Sc₂CoSi₂-type (space group *C2/m*), belonging to the CrB-TiNiSi structural intergrowth series [1] were found to form hydrides at H₂ pressures below 1 bar. Our previous studies have shown that the compounds Tb₃Co₂Ge₃ (structure type Hf₃Ni₂Si₃) and Tb₂CoGe₂ (structure type Sc₂CoSi₂) exhibit extremely slow hydrogenation rates (several days reaction time) and require high temperatures (250 °C) to complete the reaction. The hydrogen absorption is moderate (1.6 H at./f.u. and 0.9 H at./f.u., respectively), the crystal structure type of the metallic matrix is preserved after hydrogenation, and the strongly anisotropic lattice deformation upon hydrogenation results in a relative increase in the cell volume not exceeding 1 %. In this work, we report on the hydrogenation properties of the Si-containing compound Tb₂CoSi₂, focusing on the role of the *p*-element in composition-structure-properties relationships.

Tb₂CoSi₂ was synthesized by arc-melting and used in the as-cast state for hydrogenation. Hydrogenation was carried out under a H₂ pressure of 790 mbar (770 mbar for Tb₂CoGe₂). Increasing the temperature to 150 °C (250 °C for Tb₂CoGe₂) was sufficient to complete the reaction. The pressure drop in the system corresponded to a hydrogen content of 1.3 H at./f.u. for the Tb₂CoSi₂ hydride (0.9 for Tb₂CoGe₂). Phase identification and crystal structure determination were performed by X-ray powder diffraction.

Substitution of Si for Ge showed differences in the hydrogenation properties of the Sc₂CoSi₂-type compounds. Tb₂CoSi₂ forms hydrides more easily than Tb₂CoGe₂: a lower temperature is needed and the amount of absorbed hydrogen is ~44 % higher. Similarly to Tb₂CoGe₂, hydrogenation results in strongly anisotropic lattice deformation, the lattice expansion along the *a*-axis being partially compensated by lattice contraction in the two other directions. The relative increase in the cell volume is higher than for Tb₂CoGe₂: $\Delta a/a = 3.7\%$, $\Delta b/b = -1.7\%$, $\Delta c/c = -0.2\%$, $\Delta V/V = 1.4\%$ (see table). Chemical substitution at the positions of the *p*-element atoms opens up new opportunities to design hydrogen-sorption materials combining composition and structure design.

Cell parameters (*a*, *b*, *c*, β , *V*) for Sc₂CoSi₂-type intermetallics before and after hydrogenation

Compound	<i>a</i> , Å	<i>b</i> , Å	<i>c</i> , Å	β , °	<i>V</i> , Å ³
Tb ₂ CoGe ₂	10.5276(5)	4.2062(4)	10.1888(5)	118.083(2)	398.05(5)
Tb ₂ CoGe ₂ H _{0.9}	10.9455(5)	4.1356(2)	10.1555(5)	119.189(2)	401.33(4)
Tb ₂ CoSi ₂	10.4594(5)	4.1472(3)	10.0140(5)	118.967(2)	380.04(4)
Tb ₂ CoSi ₂ H _{1.3}	10.8457(6)	4.0764(3)	9.9982(5)	119.372(2)	385.21(4)

This work was supported by the Ministry of Education and Science of Ukraine under the grants No. 0124U000989 and No. 0125U000767.

[1] J.T. Zhao and E. Parthé, *Acta Crystallogr. C* 45 (1989) 1853-1856.

CATION DISORDER AND ULTRALOW THERMAL CONDUCTIVITY IN CuCd₂Ga_{1-x}In_xSe₄ DIAMOND-LIKE SEMICONDUCTORS

H. Donyk¹, O. Cherniushok¹, O. Smitiukh², K.T. Wojciechowski¹, and T. Parashchuk¹

¹ *Thermoelectric Research Laboratory, Department of Inorganic Chemistry,
Faculty of Materials Science and Ceramics, AGH University of Krakow,
Mickiewicza Ave. 30, 30-059 Krakow, Poland*

² *Department of Inorganic and Physical Chemistry, Lesya Ukrainka Volyn National
University, Voli Ave. 13, 43025 Lutsk, Ukraine
hannadonyk@agh.edu.pl*

Diamond-like semiconductors (DLS) are promising thermoelectric materials due to their intrinsically low lattice thermal conductivity and tunable phonon transport. Here, we investigate the quaternary CuCd₂Ga_{1-x}In_xSe₄ ($0 \leq x \leq 1$) system, which has so far received very limited attention and has only been briefly discussed in terms of crystal structure.

Powder X-ray diffraction confirmed the formation of a continuous single-phase cubic $F\bar{4}3m$ phase across the entire compositional range. SEM analysis revealed homogeneous microstructures without detectable secondary phases. Partial substitution of In for Ga leads to systematic lattice expansion due to the larger ionic radius of In³⁺ and introduces local distortions within the tetrahedral cation framework characteristic of diamond-like semiconductors. Thermal analysis indicated the absence of structural phase transitions within the investigated temperature range, confirming the good thermal stability of the materials.

All the compositions exhibit semiconducting behaviour with a temperature-dependent Seebeck coefficient, indicating a transition from p-type to n-type conduction. The Seebeck coefficient reaches values of up to $\sim 600 \mu\text{V K}^{-1}$, while the estimated band gap decreases systematically from 0.75 eV ($x = 0$) to 0.31 eV ($x = 1$), indicating progressive band-gap narrowing upon In substitution.

The investigated samples exhibit exceptionally low thermal conductivity: κ remains below $0.6 \text{ W m}^{-1} \text{ K}^{-1}$ at 773 K for all compositions, with the minimum value of $\sim 0.39 \text{ W m}^{-1} \text{ K}^{-1}$ observed for $x = 0.25$ at 773 K. Ultrasonic measurements revealed relatively low longitudinal and transverse sound velocities, reflecting softened elastic properties and favourable conditions for strong phonon scattering. To clarify the origin of the suppressed lattice thermal conductivity, phonon scattering was analysed using ultrasonic data together with the Klemens formalism for point-defect scattering. The strain-field contribution (Γ_S), estimated within the Abeles approach, exceeds the mass-fluctuation term (Γ_M) by more than an order of magnitude, demonstrating that local strain fluctuations associated with the Ga/In ionic-size mismatch dominate the phonon scattering.

Overall, the results demonstrate that phonon transport in CuCd₂Ga_{1-x}In_xSe₄ is strongly governed by local structural disorder and strain-field fluctuations within the cation sublattice. These findings provide new insight into the mechanisms responsible for ultralow thermal conductivity in quaternary diamond-like semiconductors.

This work was funded by the National Science Centre (Poland) under the research project "OPUS-26" UMO-2023/51/B/ST11/00329.

[1] T. Luo, Y. Hu, S. Liu, F. Xia, J. Qiu, H. Peng, K. Liu, Q. Guo, X. Li, D. Yang, X. Su, J. Wu, X. Tang, *Mater. Today Phys.* 37 (2023) 101211.

LINKING INCOMMENSURATE STRUCTURE AND TRANSPORT PROPERTIES IN Fe₂Ge₃ NOWOTNY CHIMNEY-LADDER PHASE

Oleksandr Cherniushok¹, Illia Lukashchuk¹, Kacper Pryga², Raisa Tahiyah³,
Taras Parashchuk¹, Yaroslav Tokaychuk⁴, Lev Akselrud⁴, Bartłomiej Wiendlocha²,
Roman Gladyshevskii⁴, Yuri Grin⁵, Alexandra Zevalkink³, and Krzysztof T. Wojciechowski¹
¹ *Thermoelectric Research Laboratory, Department of Inorganic Chemistry,
Faculty of Materials Science and Ceramics, AGH University of Krakow,
Mickiewicza Ave. 30, 30-059 Krakow, Poland*
² *Faculty of Physics and Applied Computer Science, AGH University of Krakow,
ul. Władysława Reymonta 19, 30-059 Krakow, Poland*
³ *Department of Chemical Engineering and Materials Science, Michigan State University,
East Lansing, MI, USA*
⁴ *Department of Inorganic Chemistry, Ivan Franko National University of Lviv,
Kyryla i Mefodiya St. 6, 79005 Lviv, Ukraine*
⁵ *Max-Planck-Institut für Chemische Physik fester Stoffe,
Nöthnitzer Str. 40, 01187 Dresden, Germany*
sashach@agh.edu.pl

The Nowotny chimney-ladder (NCL) phase in the Fe–Ge system near the Fe₂Ge₃ composition exhibits a characteristic coexistence of degenerate electronic transport and strongly suppressed lattice thermal conductivity, yet the structural and compositional origins of this behaviour remain incompletely understood. Synchrotron diffraction showed that samples prepared with nominal Fe₂Ge₃ composition crystallize as an incommensurately modulated NCL phase close to FeGe_{1.52}. From the superspace description, we derived and refined for the first time a three-dimensional commensurate approximant, Fe₂₇Ge₄₁ (*tP272*). Chemical-bonding analysis based on the model of Fe₂Ge₃ revealed a three-dimensional framework of heteroatomic multiatomic Fe–Ge interactions without homoatomic Fe–Fe or Ge–Ge bonds. DFT calculations for the Fe₂₇Ge₄₁ approximant showed that slight Ge excess in comparison with Fe₂Ge₃ shifts the Fermi level into the conduction band, yielding a nominal carrier concentration of $\sim 10^{21}$ cm⁻³, consistent with Hall measurements, and explaining the degenerate n-type behaviour without extrinsic donors. The electronic structure is characterized by a high density-of-states effective mass ($\sim 11 m_e$), arising from convergence of flat conduction bands near the Fermi level. Despite high elastic moduli and a moderate Grüneisen parameter, the lattice thermal conductivity is low (~ 1.8 W m⁻¹ K⁻¹ at 300 K), reflecting ultrashort phonon mean free paths imposed by the incommensurate bonding inhomogeneity. These results link the incommensurate structure of the Fe–Ge Nowotny chimney-ladder phase to the coexistence of degenerate electronic transport and phonon-glass thermal behaviour.

This work was funded by grants from the Polish National Agency for Academic Exchange (NAWA) (BPN/NSF/2023/1/00010), from the U.S. Office of Naval Research Global (ONRG) and the U.S. National Academy of Sciences (NAS, USA) within the framework of the International Multilateral Partnerships for Resilient Education and Science System in Ukraine (IMPRESS-U) initiative. TP and OC also acknowledge support from the National Science Centre (NCN) under the research project “OPUS-26” (UMO-2023/51/B/ST11/00329).

ENTROPY-STABILIZED γ -Cu₈Si_xSe_{6-x} ARGYRODITES: CRYSTAL CHEMISTRY, ELECTRONIC STRUCTURE AND THERMOELECTRIC PROPERTIES

Taras Parashchuk¹, Oleksandr Cherniushok¹, Bartłomiej Wiendlocha², Janusz Tobola², Raúl Cardoso-Gil³, Jeffrey G. Snyder⁴, Yuri Grin³, and Krzysztof T. Wojciechowski¹

¹ *Thermoelectric Research Laboratory, Department of Inorganic Chemistry, Faculty of Materials Science and Ceramics, AGH University of Krakow, Mickiewicza Ave. 30, 30-059 Krakow, Poland*

² *Faculty of Physics and Applied Computer Science, AGH University of Krakow, ul. Władysława Reymonta 19, 30-059 Krakow, Poland*

³ *Max-Planck-Institut für Chemische Physik fester Stoffe, Nöthnitzer Str. 40, 01187 Dresden, Germany*

⁴ *Department of Materials Science and Engineering, Northwestern University, Evanston, IL 60208, USA
parashchuk@agh.edu.pl*

Cu-based argyrodites have recently emerged as promising thermoelectric materials due to their intrinsically low lattice thermal conductivity and environmentally friendly, Te-free composition. In this work, we investigate the influence of entropy engineering on the structural stability, electronic structure, and thermoelectric performance of Cu₈Si_xSe_{6-x} argyrodites ($0 \leq x \leq 6$). Partial substitution of Se by S increases the configurational entropy of the system and effectively suppresses the $\alpha \rightarrow \gamma$ polymorphic transition below room temperature. As a result, compositions with $x = 1-3$ crystallize directly in the high-symmetry cubic γ -phase over the entire operating temperature range.

Structural investigations confirmed stabilization of the cubic γ -phase and systematic lattice contraction with increasing sulphur content. The entropy-stabilized γ -phase promotes improved microstructural homogeneity and cleaner grain-boundary contacts, resulting in enhanced weighted carrier mobility compared to compositions undergoing structural transitions. Electronic structure calculations revealed multivalley valence bands with strong Cu-3d/chalcogen-*p* hybridization and high density-of-states effective masses up to 2.4-3.0 m_e , favourable for efficient p-type thermoelectric transport. The investigated argyrodites exhibit ultralow lattice thermal conductivity of 0.18-0.35 W m⁻¹ K⁻¹ over 298-773 K due to bonding inhomogeneity, complex Cu-Cu, Cu-Se(S), and Si-Se(S) interactions, and enhanced point-defect phonon scattering. Optimized compositions achieve a power factor of 4.2 μ W cm⁻¹ K⁻² and a maximum thermoelectric figure of merit $zT = 1.24$ at 773 K for Cu₈Si₃Se₃. These results demonstrate that entropy stabilization of the γ -phase is an effective strategy to simultaneously improve electronic transport and maintain ultralow thermal conductivity in low-cost thermoelectric materials for medium-temperature waste heat recovery applications.

The research was funded by the Foundation for Polish Science (FNP) under the First-Team programme, project no. FENG.02.02-IP.05-0012/25, “EcoCool: Eco-Friendly Semiconductor Cooling Solution with Dual-Use Applications”, co-financed by the European Union under the European Funds for a Modern Economy Programme (FENG 2021-2027).

[1] T. Parashchuk, O. Cherniushok, B. Wiendlocha, J. Tobola, R. Cardoso-Gil, J.G. Snyder, Yu. Grin, K.T. Wojciechowski, *Adv. Funct. Mater.* 35(34) (2025) 2502163.

POSTER PRESENTATIONS

CRYSTAL GROWTH AND LOW-TEMPERATURE PROPERTIES OF $\text{Li}_3\text{Zn}_2\text{Sn}_4$

A. Bullmann and T. Klimczuk

*Faculty of Applied Physics and Mathematics and Advanced Material Centre,
Gdańsk University of Technology, ul. Narutowicza 11/12, Gdańsk 80-233, Poland
s198817@student.pg.edu.pl, tomasz.klimczuk@pg.edu.pl*

$\text{Li}_3\text{Zn}_2\text{Sn}_4$ crystals were grown using a self-flux method with an excess of Sn relative to the stoichiometric mass required for the amounts of Li and Zn used. The dimensions of the crystals were approximately $5 \times 5 \times 3$ mm, and characterisation was performed on $2 \times 1 \times 1$ mm samples, as the compound disintegrated into Sn and Zn when pulverised. The X-ray diffraction pattern confirmed the expected crystallographic structure in space group $P6_3/mmc$ (194), with lattice parameters approaching those previously reported by S. Stegmaier and T.F. Fässler [1]. EDS analysis of a single crystal provided additional verification that the material maintains a zinc-to-tin ratio of 1:2.

Preliminary measurements revealed the metallic nature of the electrical resistivity of $\text{Li}_3\text{Zn}_2\text{Sn}_4$. Low-temperature heat capacity data were used to obtain the Sommerfeld coefficient $\gamma = 4.40(3) \text{ mJ mol}^{-1} \text{ K}^{-2}$ and Debye temperature $\Theta_D = 273(1) \text{ K}$. Furthermore, no phase transition was observed within the 0.4-300 K range.

The work at Gdańsk University of Technology was supported by the National Science Centre (Poland), Grant No. 2022/45/B/ST5/03916.

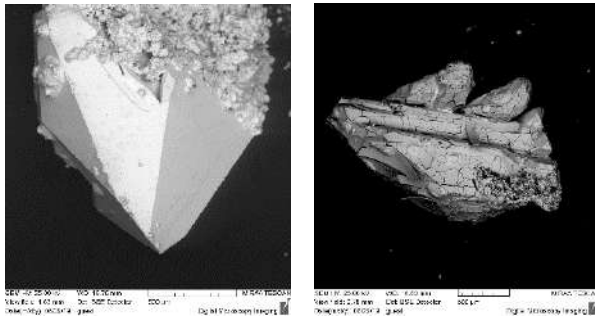
[1] S. Stegmaier, T.F. Fässler, *Inorg. Chem.* 52(6) (2013) 2809-2816.

SYNTHESIS OF $U_3X_4T_3$ ($X = \text{Bi, Sb}$ and $T = \text{Ni, Pd, Pt}$) SINGLE CRYSTALS

Volodymyr Buturlim, Anežka Bendová, Jiří Pospíšil, and Jeroen Custers
*Department of Condensed Matter Physics, Faculty of Mathematics and Physics,
Charles University, Ke Karlovu 5, 121 16 Prague 2, Czechia
jeroen.custers@matfyz.cuni.cz*

Strong spin-orbit coupling (SOC) is an essential ingredient in the formation of topological materials. Topological Kondo insulators (TKIs) differ in nature from the vastly studied topological insulators based on simple semiconductors. The typically narrow band gap in TKIs is formed by a strong interaction between f and conduction electrons, known as Kondo interaction. It is this Kondo interaction in combination with strong SOC that results in gapless, spin-polarized topological surface states, which are of great fundamental interest as new states of quantum matter.

SmB_6 has attracted significant attention as a potential TKI [1]; however, despite numerous studies, the issue remains controversial. This unresolved question has recently redirected attention toward Ce-based Kondo systems, where topology may be more controllable. Notably, the canonical Ce-based Kondo insulator $\text{Ce}_3\text{Bi}_4\text{Pt}_3$ (cubic, space group $I\bar{4}3d$) provides a striking example: reducing the strength of the spin-orbit coupling drives the system from an insulating state into a Weyl-Kondo semimetal. Such tuning has been achieved experimentally through $\text{Pt} \rightarrow \text{Pd}$ substitution [2,3], replacing a heavier element with a lighter one and thereby weakening the SOC. In this line we speculate that, by enhancing SOC to the extreme, $U_3\text{Bi}_4\text{Pt}_3$ may be transformed into a topological Kondo insulator, and propose to do this by a U-for-Ce substitution (U is the heaviest sufficiently stable element prone to Kondo interaction). Moreover, several U-based compounds exist in the same 343-type cubic structure allowing for a similar type of investigation as previously performed. Here we present our first attempts to synthesize single crystals of $U_3X_4T_3$ with X (Sb, Bi) and T (transition element) from Sb, In, and Bi flux.



SEM images (BSE detector) of $U_3\text{Pt}_4\text{Bi}_3$ (left) and $U_3\text{Ni}_4\text{Bi}_3$ (right) single crystals

Work supported by the Czech Ministry for Education, Youth and Sports program INTERCOST (Grant No. LUC24139).

- [1] V. Alexandrov, P. Coleman, O. Erten, *Phys. Rev. Lett.* 114 (2015) 177202.
- [2] S. Dzsaber *et al.*, *Phys. Rev. Lett.* 118 (2017) 246601.
- [3] H.-H. Lai *et al.*, *Proc. Natl. Acad. Sci. USA* 115 (2018) 93.
- [4] T. Takabate *et al.*, *J. Phys. Soc. Jpn.* 59 (1990) 4412.
- [5] T. Klimczuk *et al.*, *Phys. Rev. B* 7 (2008) 245111.

SUBTLE BUT SIGNIFICANT: STRUCTURAL VERSATILITY IN $\text{Eu}M_2\text{Te}_4$

P. Das, C. McLeod, and A. Mar
Department of Chemistry, University of Alberta,
Edmonton, Alberta, Canada T6G 2G2
pritam1@ualberta.ca

The growing global demand for clean energy underscores the limited efficiencies of current renewable technologies, positioning thermoelectric materials as promising candidates for recovering waste heat by converting it into electricity [1]. Rare-earth tellurides offer strong potential for high thermoelectric performance due to their complex crystal structures and the presence of heavy atoms [2]. Motivated by the scarcity of reported compounds in the $\text{Eu}-M-\text{Te}$ ($M = \text{Al}, \text{Ga}$) systems, we discovered and characterized a new structure type for EuAl_2Te_4 and EuGa_2Te_4 , both adopting the *Ibam* space group. Furthermore, EuGa_2Te_4 exhibits a temperature-dependent structural transition from the previously reported *Cccm* structure [3] to *Ibam*, as confirmed by variable-temperature powder X-ray diffraction and differential scanning calorimetry. Optical diffuse reflectance measurements reveal narrow band gaps of 0.6-0.9 eV for these compounds, suggesting favourable electrical transport properties and highlighting these compounds as promising candidates for thermoelectric energy conversion.

- [1] Q. Sun, C. Du, G. Chen, *Adv. Nanocomposites* 2 (2025) 15-31.
- [2] R.C. Vickery, H.M. Muir, *Adv. Energy Convers.* 1 (1961) 179-186.
- [3] O.M. Aliev, *Izv. Akad. Nauk SSSR, Neorg. Mater.* 16 (1980) 1514-1518.

SYNTHESIS AND CRYSTAL STRUCTURE OF COPPER(I) II-COMPLEXES WITH 3-THIOALLYL-4-ALLYL-5-(2-PYRIDYL)-4H-1,2,4-TRIAZOLE

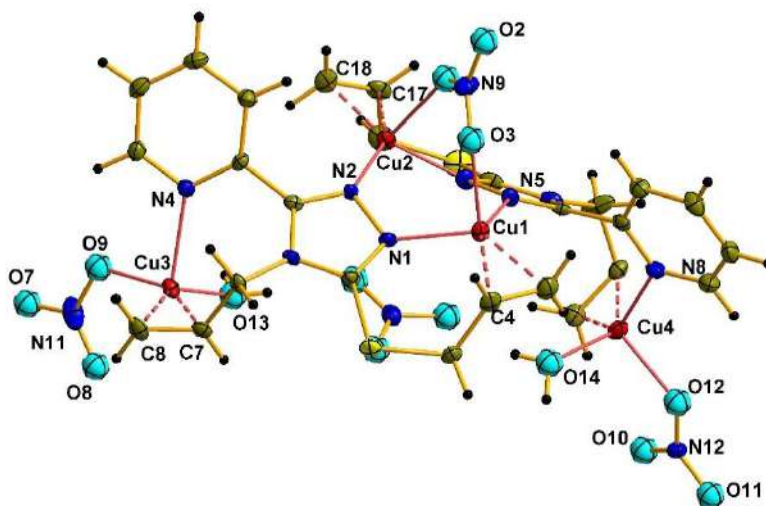
D. Dmytriv¹, Yu. Slyvka¹, and E. Goreshnik²

¹ Ivan Franko National University of Lviv, Kyryla i Mefodiya St. 6, 79005 Lviv, Ukraine

² Jožef Stefan Institute, Jamova cesta 39, 1000 Ljubljana, Slovenia
dm.dmytriv@gmail.com

1,2,4-Triazoles have a wide range of applications in pharmaceutical chemistry and were found to be excellent instruments for the crystal engineering of versatile transition-metal organometallic compounds possessing catalytic, luminescent, nonlinear, biochemical and spin-crossover activities. By means of the alternating-current electrochemical method two novel π,σ -coordination compounds, $[\text{Cu}_2(\text{L}1)\text{Cl}_2]$ (**1**) and $[\text{Cu}_4(\text{L}1)_2(\text{NO}_3)_4]$ (**2**) ($\text{L}1 = 4\text{-allyl-3-allylsulfanyl-5-(2-pyridyl)-4H-1,2,4-triazole}$) were obtained in single-crystalline form.

In the crystal structure of **1** there are two crystallographically independent Cu(I) atoms with different coordination environments: Cu1 adopts a trigonal pyramidal coordination environment composed of an allylic C=C bond, two triazole N and Cl atoms, while Cu2 has a distorted tetrahedral environment formed by a pyridyl N atom and three μ_2 -Cl atoms. The angle between the pyridyl and triazole planes is 77.20° .



Fragment of the crystal structure of **1** (displacement ellipsoids at the 50% probability level)

The π,σ -complex **2** $[\text{Cu}_4(\text{L}1)_2(\text{NO}_3)_4]$ crystallizes in the centrosymmetric space group $P2_1/n$ with two $\text{L}1$ units and four Cu(I) atoms in the asymmetric unit. Both organic ligands use all available coordination centres when coordinating to the central atoms. The Cu1 and Cu2 atoms are coordinated by thioallyl groups and nitrogen atoms of two triazole nuclei, forming two seven-membered rings $\{\text{CuNSC}_4\}$ and a six-membered ring $\{\text{Cu}_2\text{N}_4\}$ (Figure). This type of fragment has previously been encountered in most structures with thioallyl-1,2,4-triazole ligands. The coordination of the pyridyl substituents to the Cu(I) atoms also contributes to the π coordination of the allylic groups at position 4 of the triazole nucleus. All four independent cuprous atoms have a deformed trigonal pyramidal environment: Cu1 and Cu2 are coordinated by the C=C bond of the allylic group, nitrogen atoms of the triazole rings, and oxygen atoms of the bridging nitrate anion. Cu3 and Cu4 are in an environment formed by the C=C bond of the N-allylic group, the N atom of the pyridyl substituent, an O atom of the nitrate anion, and a water molecule.

ELECTRONIC PROPERTIES OF TELLURIUM-RICH $\text{TaTe}_x\text{Se}_{2-x}$

E. Doucet and J.-H. Pöhls

*Department of Chemistry, University of New Brunswick,
Fredericton, NB, E3B 5A3, Canada*

edoucet@unb.ca

Tantalum-based transition metal dichalcogenides (TMDCs) exhibit electronic properties that are strongly influenced by crystal structure, composition, and lattice symmetry. While selenium-rich compositions in the $\text{TaTe}_x\text{Se}_{2-x}$ system have been widely investigated, the tellurium-rich regime remains mostly unexplored. In this work, we examine the structural evolution and electronic characteristics of tellurium-rich $\text{TaTe}_x\text{Se}_{2-x}$ ($1.4 \leq x \leq 2.0$) using both polycrystalline and single-crystal samples.

Polycrystalline compounds were synthesized using a solid-state method, and single crystals were grown using chemical vapor transport. Structural and compositional characterization were performed using powder X-ray diffraction, scanning electron microscopy and energy-dispersive X-ray spectroscopy. The electronic properties were measured as a function of temperature and magnetic field. Experimental results will be compared to density functional theory calculations to delineate the underlying mechanisms of the electrical properties. This project aims to establish composition-structure-property relationships in tellurium-rich $\text{TaTe}_x\text{Se}_{2-x}$, providing a foundation for the design of next-generation electronic and quantum materials.

DEVELOPMENT OF A SYNTHESIS METHOD AND INVESTIGATION OF MIXED Ge(IV) – 3d METAL COMPLEXES WITH ETHYLENEDIAMINETETRAACETIC ACID AND 1,10-PHENANTHROLINE

D. Pechinka¹, O. Finik², and O. Martsynko¹

¹ *Department of Inorganic Chemistry and Chemical Education, Odesa I.I. Mechnikov National University, Vsevoloda Zmiiienka 2, 65082 Odesa, Ukraine*

² *LLC “Bureau Veritas Commodities Ukraine”, Udilny Lane 1, 65044 Odesa, Ukraine
elenacheb159@gmail.com*

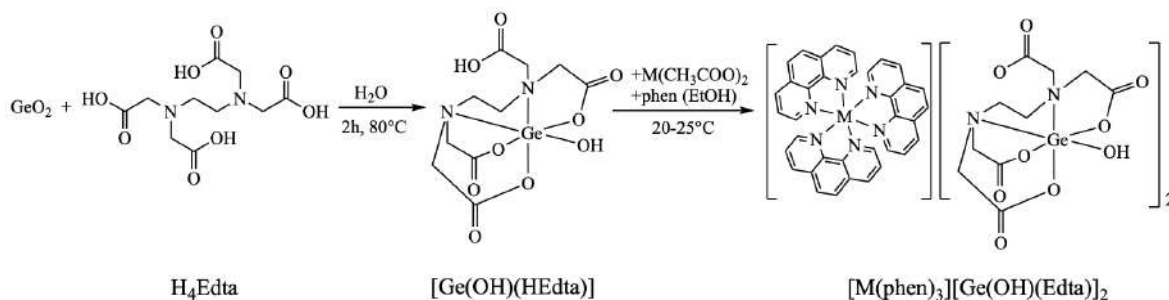
Metal complexes of ethylenediaminetetraacetic acid have attracted considerable scientific interest for many decades due to their diverse structural features and wide range of physicochemical and biological properties. It has been demonstrated that soil treatment or foliar application of solutions containing ethylenediaminetetraacetates of 3d transition metals can significantly enhance the productivity of cereal crops such as buckwheat, oats, barley, rye, and flax, while also promoting seed germination and stimulating early vegetative growth [1].

A general synthesis method was developed and coordination compounds with various metals $[M(\text{phen})_3][\text{Ge}(\text{OH})(\text{Edta})]_2 \cdot n\text{H}_2\text{O}$ (H_4Edta – ethylenediaminetetraacetic acid, phen – 1,10-phenanthroline, $M = \text{Mn}(\text{II}), \text{Co}(\text{II}), \text{Ni}(\text{II}), \text{Cu}(\text{II}), \text{Zn}$) were obtained in the solid state. The complexes were comprehensively characterized using modern physicochemical methods, including ICP-AES, IR spectroscopy, mass spectrometry, and thermogravimetry.

The IR spectra of the obtained complexes in the region associated with the germanium coordination environment are very similar to those reported for previously synthesized ethylenediaminetetraacetatogermanic acid. This indicates that the octahedral polyhedron of germanium is formed through the binding of one hydroxyl group, three oxygen atoms from carboxylate groups, and two nitrogen atoms of the Edta-ligand. A series of characteristic absorption bands attributed to $\nu(\text{C}-\text{H}_{\text{bipy}})$, $\nu(\text{C}-\text{N}_{\text{bipy}})$ vibrations confirms the presence of 1,10-phenanthroline in the complexes and its coordination to the 3d metal ions.

Analysis of the mass spectra of the compounds revealed that the ESI(+) spectra recorded in the positive ion mode contain low-intensity signals corresponding to protonated phenanthroline Hphen^+ and the $[\text{M}(\text{phen})_2]^{2+}$ ion, together with more intense signals attributed to the doubly charged cations $[\text{M}(\text{phen})_3]^{2+}$. In the negative ion mode, the mass spectra display a prominent signal at $m/z \sim 379$ assigned to the $[\text{Ge}(\text{OH})(\text{Edta})]^-$ anion. Several additional unassigned signals are also observed, which are most likely associated with fragmentation processes of this anionic species.

The synthesis scheme of the mixed Ge(IV) – 3d metal complexes can be represented as follows:



[1] O. Trunova, *Ukr. Chem. J.* 12 (2022) 91-138.

STRUCTURAL CHARACTERIZATION OF SOLID SOLUTIONS WITH FIXED 5 % INDIUM CONTENT IN THE Ga₂O₃–Al₂O₃–In₂O₃ PSEUDOTERNARY SYSTEM

Yu. Hirskyi¹, V. Hreb¹, V. Stadnik¹, Ya. Zhydachevskyy², and L. Vasylechko¹

¹ *Department of Semiconductor Electronics, Lviv Polytechnic National University,
S. Bandery St. 12, 79013 Lviv, Ukraine*

² *Institute of Physics, Polish Academy of Sciences,
Aleja Lotników 32/46, 02-668 Warsaw, Poland
yurii.v.hirskyi@lpnu.ua*

Exploring multi-component alloying is a highly effective strategy for engineering the crystal structure and bandgap of ultra-wide bandgap β -Ga₂O₃ semiconductors. While simultaneous substitution with Al³⁺ and In³⁺ provides an independent pathway to modulate electronic and lattice properties, the structural stability limits within the Ga₂O₃–Al₂O₃–In₂O₃ pseudoternary system require comprehensive evaluation [1].

In this study, we report on the synthesis and detailed structural characterization of a specific cross-section of (Ga_{0.95-x}Al_xIn_{0.05})₂O₃ solid solutions. To maintain compositional homogeneity, polycrystalline samples with a fixed indium concentration of 5 % and variable aluminum substitution level ($0.35 \leq x \leq 0.75$) were synthesized utilizing a facile sol-gel citrate route. The precursor powders underwent a final high-temperature calcination at 1500 °C in air to reach the thermodynamically stable materials. The crystal structure was subsequently investigated using XRD, coupled with full-profile Rietveld refinements.

The XRD phase analysis demonstrated the formation of a single-phase solid solution, isostructural to monoclinic β -Ga₂O₃ (space group *C2/m*) for (Ga_{0.95-x}Al_xIn_{0.05})₂O₃ compositions up to $x < 0.55$. At higher aluminum contents, the stability limit of the solid solution is exceeded, as evidenced by the precipitation of secondary phases. Rietveld refinements of the compositions (Ga_{0.95-x}Al_xIn_{0.05})₂O₃ in the single-phase region revealed a linear contraction of the unit-cell parameters: as x increases from 0.35 to 0.75, the a , b , and c lattice constants decrease, leading to an overall unit-cell volume reduction from 204.54 Å³ to 192.98 Å³. Concurrently, a slight increase of the monoclinic angle β from 103.87° to 104.05° was observed. Site occupancy analysis confirmed a partly ordered cationic distribution: the tetrahedral Ga1 site is exclusively shared by Ga³⁺ and Al³⁺, whereas the larger In³⁺ ions, along with Ga³⁺ and Al³⁺, reside in the octahedral Ga2 positions.

The synthesis and structural characterization of (Ga_{0.95-x}Al_xIn_{0.05})₂O₃ solid solutions demonstrate highly controlled crystal lattice tuning by complex cation substitution. Stability limits and atomic distribution models guide the development of lattice-matched substrates and bandgap-engineered architectures for next-generation power and optoelectronic devices.

The work was supported by the Ministry of Education and Science of Ukraine under the project N0125U001768 (DB/GALIO) “Development of principles of formation of properties of ultra-wide bandgap semiconductors based on Ga₂O₃ for power electronics and UV optoelectronics” and by the Polish National Science Centre (project No. 2024/53/B/ST11/01108).

[1] L. Vasylechko *et al.*, *Sci. Rep.* 15 (2025) 37128.

ELECTROCHEMICAL SYNTHESIS OF LI-CONTAINING MULTICOMPONENT SOLID SOLUTIONS BASED ON TbSn₂

V. Kordan¹, N. Pavlyuk¹, I. Tarasiuk¹, O. Kretkovskiy¹, V. Milashius¹, G. Dmytriv¹,
and V. Pavlyuk^{1,2}

¹ *Department of Inorganic Chemistry, Ivan Franko National University of Lviv,
Kyryla i Mefodiya St. 6, 79005 Lviv, Ukraine*

² *Institute of Chemistry, Jan Długosz University,
al. Armii Krajowej 13/15, 42-200 Częstochowa, Poland
vasyl.kordan@lnu.edu.ua*

Real experiments and quantum-chemical calculations show that disordered and high-entropy systems can be used as materials for batteries, fuel, and solar cells. The main requirements for these materials are high energy efficiency, high thermal and chemical stability, cost-effectiveness, high electrical and thermal conductivity, and environmental friendliness. This work aimed to investigate the mechanism of electrochemical Li insertion into the structures of the Tb₃₃Sn₅₇Al₁₀ (TbSn_{2-y}Al_y), La₅Tb₂₈Sn₅₇Al₁₀ (La_xTb_{1-x}Sn_{2-y}Al_y), La₅Tb₂₈Sn₄₇Al₁₀Sb₁₀ (La_xTb_{1-x}Sn_{2-y-z}Al_ySb_z), and Y₅Tb₂₈Sn₄₇Al₁₀Sb₁₀ (Y_xTb_{1-x}Sn_{2-y-z}Al_ySb_z) phases and analyse the products of electrochemical interactions.

Alloys with compositions Tb₃₃Sn₅₇Al₁₀, La₅Tb₂₈Sn₅₇Al₁₀, La₅Tb₂₈Sn₄₇Al₁₀Sb₁₀, and Y₅Tb₂₈Sn₄₇Al₁₀Sb₁₀ were synthesized by arc-melting and annealing at 400 °C. A two-electrode prototype “Swagelok-cell” was used for the lithiation. Electrochemical Li insertion was carried out in the galvanostatic mode at 0.5 mA/cm². Powder samples were tested as negative electrode materials during discharge process. We used rhombohedral LiCoO₂ as positive electrode and an 1M Li[PF₆] solution in 1:1 ethylenecarbonate/dimethylcarbonate as electrolyte. The chemical composition and surface morphology before and after the electrochemical lithiation were studied by scanning electron microscopy (Tescan Vega3 LMU) and energy-dispersive X-ray spectroscopy (Oxford Instruments AZtec ONE System). Powder diffraction data were collected using a Proto AXRD Benchtop automatic diffractometer (Cu K α radiation, Ni filter). The lattice parameters were determined using least-squares refinements. The electronic structure of TbSn₂ and the “TbSn₂Li_x, x = 1” model was calculated using the tight-binding linear muffin-tin orbital method in the atomic spheres approximation (TB-LMTO-ASA).

All the studied alloys contained a main phase with ZrSi₂-type structure (space group *Cmcm*, Pearson symbol *oS12*) and trace amounts of α -Tb₃Sn₇ or Tb₁₁Sn₁₀. During the first stage of the electrochemical lithiation Li-atoms occupy Wyckoff position (4c) with formation of a CeNiSi₂-superstructure (space group *Cmcm*, Pearson symbol *oS16*). The second stage of the lithiation includes partial substitution of Sn, Al and Sb atoms by Li with formation of by-products such as Li₁₇Sn₄, LiAl₃, and Li₃Sb. The amounts of electrochemically active lithium during discharge were: 0.125 Li/f.u. (4.2 at.% Li) for Tb₃₃Sn₅₇Al₁₀, 0.175 Li/f.u. (5.8 at.% Li) for La₅Tb₂₈Sn₅₇Al₁₀, 0.241 Li/f.u. (8.0 at.% Li) for Y₅Tb₂₈Sn₄₇Al₁₀Sb₁₀, and 0.249 Li/f.u. (8.3 at.% Li) for La₅Tb₂₈Sn₄₇Al₁₀Sb₁₀ alloys as electrodes in the battery prototype. We observed block-like grains with a size of 2-10 μ m before lithiation, which decreased in size to form irregular shape aggregates (0.6-5 μ m) after lithiation. Quantum-chemical calculations confirm the results of the experimental studies; calculated interaction energies between atoms are $-i\text{COHP}(\text{Sn1}-\text{Sn1}) = 1.48$ eV, $-i\text{COHP}(\text{Sn2}-\text{Sn2}) = 1.18$ eV, $-i\text{COHP}(\text{Tb}-\text{Sn}) = 0.97$ eV.

This work was carried out under the project of the Ministry of Science and Education of Ukraine “High-capacity power elements and ultra-hard ceramic coatings for civilian and military purposes” (No. 0124U001013).

BONDING-CONTROLLED CHEMICAL PRESSURE TUNING OF f -ELECTRON HYBRIDIZATION IN $Ce_3T_4P_4O_2$ ($T = Cu, Ni$)

Szymon Królak¹, Michał J. Winiarski¹, Tomasz Klimczuk¹, and Duygu Yazici^{1,2}

¹ Faculty of Applied Physics and Mathematics and Advanced Materials Center, Gdansk University of Technology, Narutowicza 11/12, 80-233 Gdansk, Poland

² The Scientific and Technological Research Council of Turkey, Atatürk Bulvarı No: 221, Kavaklıdere 06100, Ankara, Turkey
szymon.krolak@pg.edu.pl

Chemical pressure is widely used to tune electronic ground states in f -electron materials and is most often associated with atomic size effects. Here, we report the synthesis, crystal structure, and physical property characterization of the layered oxypnictides $Ce_3Cu_4P_4O_2$ and $Ce_3Ni_4P_4O_2$ in polycrystalline form. Magnetization, electrical transport, and heat capacity measurements show that $Ce_3Cu_4P_4O_2$ is a local-moment system, showing the onset of a magnetic transition at $T = 1.9$ K, whereas $Ce_3Ni_4P_4O_2$ exhibits intermediate-valence character, indicative of strong hybridization. By correlating the experimentally determined structures with previously established bonding trends in the La-analogues, we attribute this behaviour to differences in the (Cu/Ni)–P bonding that generate internal chemical pressure at the Ce sites, which is larger for $Ce_3Ni_4P_4O_2$. These results highlight chemical bonding as a promising route for chemically tailoring f -electron hybridization beyond atomic size effects.

This work was supported by the Polish state budget funds awarded by the Minister of Science under the program „Perły Nauki II” No. PN/02/0002/2023 (S.K.). D.Y. acknowledges Nobelium Joining Gdańsk Tech Research Community project (38/2022/IDUB/I.1) and Platinum Establishing Top-Class Research Teams (2/2/2023/IDUB/I.1B/Pt).

SYNTHESIS AND CRYSTAL STRUCTURE OF TERNARY COMPOUNDS IN THE SYSTEMS $AF-LuF_3$ ($A = NH_4, Li-Cs$)

O. Matselko¹, F. Šimko¹, Z. Netriová¹, A. Rakhmatullin², I. Dovgaliuk³, and M. Boča¹

¹ *Institute of Inorganic Chemistry, Slovak Academy of Sciences,
Dúbravská cesta 9, 84536 Bratislava, Slovakia*

² *CEMHTI UPR3079 CNRS, Université d'Orléans, F-45071 Orléans, France*

³ *Institut des Matériaux Poreux de Paris, UMR 8004 CNRS, 75005 Paris, France
oksana.matselko@savba.sk*

Fluorides are well known for their diverse industrial applications, and significant research efforts have focused on their optical properties, particularly in rare-earth-doped systems [1,2]. A systematic investigation of ternary fluoride formation in the $AF-LuF_3$ systems ($A = NH_4$ or $Li-Cs$) was carried out using mild hydrothermal synthesis combined with solid-state reactions. Compounds with stoichiometries of 1:1:4, 1:2:7, and 1:3:10 were obtained. The hydrothermal synthesis was performed in solutions sealed in Teflon-lined stainless-steel autoclaves under autogenous pressure at 200 °C. Under these conditions, the outcome of the synthesis is strongly influenced by several parameters, including the ratio of the starting components (which often deviates from the stoichiometry of the targeted compounds), reaction time, temperature, solvent, and pH. Solid-state reactions were conducted by heating stoichiometric mixtures of binary fluorides at temperatures below the decomposition temperatures of the compounds in an Ar atmosphere, followed by slow cooling.

The obtained products were characterised by X-ray powder diffraction (XRPD), solid-state NMR spectroscopy, differential scanning calorimetry (DSC), and scanning electron microscopy with energy-dispersive X-ray spectroscopy (SEM-EDXS). The ¹⁹F solid-state NMR results indicate a different number of fluorine environments in the compounds with 1:2:7 stoichiometry and in $CsLu_3F_{10}$ than in the possible structure types reported in the literature, *i.e.* KEr_2F_7 (*oP80, Pnma*), KEr_2F_7 (*oP80, Pna2_1*), $RbSm_2F_7$ (*oP100, Pnna*), or $RbLu_3F_{10}$ (*oS112, Cmce*) [3]. These results confirm the complexity of the crystal chemistry of the synthesised compounds and highlight the need for further detailed structural investigation. Moreover, $RbLu_2F_7$ and $CsLu_3F_{10}$ have not yet been structurally characterised in detail and have only been mentioned previously as potential host matrices for optical applications [4,5].

This work was supported by the Slovak Grant Agency VEGA grant No. 2/0043/26.

- [1] F. Wang, Y. Han, C.S. Lim, Y. Lu, J. Wang, J. Xu, H. Chen, C. Zhang, M. Hong, X. Liu, *Nature* 463 (2010) 1061-1065.
- [2] F. Wang, X. Liu, *Chem. Soc. Rev.* 38 (2009) 976-989.
- [3] P. Villars, K. Cenzual (Eds.), *Pearson's Crystal Data – Crystal Structure Database for Inorganic Compounds*, Release 2024/25, ASM International, Materials Park, Ohio, USA.
- [4] Y. Gao, T. Wang, Q. Lyu, *Opt. Instrum.* 47 (2025) 58-67.
- [5] D. Avignant, J. Metin, D. Chatonier, J.C. Cousseins, *J. Fluorine Chem.* 23 (1983) 438.

SYNTHESIS AND CRYSTAL STRUCTURE OF A Cu(I) π,σ -COMPLEX WITH N,S-DIALLYL-2-MERCAPTOBENZIMIDAZOLE

O. Pavlyuk

Department of Inorganic Chemistry, Ivan Franko National University of Lviv,
Kyryla i Mefodiya St. 6, 79005 Lviv, Ukraine
oleksiy.pavlyuk@lnu.edu.ua

Olefinic π -complexes of copper(I) are widely used in various fields of science and technology, including biochemical research, as catalysts in fine organic syntheses, and as effective tools in crystal engineering of coordination compounds. In recent years, particular attention has been given to the synthesis and structural investigation of Cu(I) π -complexes with allyl derivatives of heterocyclic compounds, since the simultaneous coordination of the metal atom by the heterocyclic core and the associated allyl group plays an important role in stabilizing unique or previously unknown inorganic fragments [1].

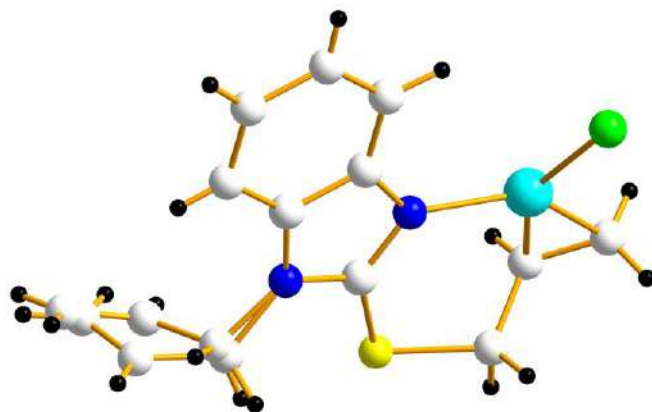
Continuing our research on the coordination behaviour of heterocycle allyl derivatives towards Cu(I), the crystalline compound $[\text{C}_8\text{H}_4\text{N}_2\text{S}(\text{C}_3\text{H}_5)_2\text{CuCl}]$ (**1**) was obtained under *ac* electrochemical technique conditions [2] from an ethanol solution of copper chloride and 2-mercaptobenzimidazole with a copper wire after 3 days. The diffraction data were collected on an automatic diffractometer equipped with a CCD detector, using graphite-monochromated Mo $K\alpha$ radiation.

In the structure of **1**, the copper atoms possess a distorted trigonal-planar coordination environment formed by the C=C bond of an allyl group of the ligand (Cu–*m* = 1.914 Å), a nitrogen atom of the imidazole core (Cu–N = 1.975 Å) and a chlorine atom (Cu–Cl = 2.216 Å).

Only one allylic group of the N,S-diallyl-2-mercaptobenzimidazole ligand is coordinated to the metal. The second allylic substituent is distorted between two conformation variants in the ratio 0.875/0.125.

Due to the chelate function of the N,S-diallyl-2-mercaptobenzimidazole molecule, isolated topological units $\{\text{C}_8\text{H}_4\text{N}_2\text{S}(\text{C}_3\text{H}_5)_2\text{CuCl}\}$ are formed in the crystal structure (see figure).

C–H \cdots Cl hydrogen bonds play an important role in the formation of the structure, additionally linking the topological units into a three-dimensional framework.



Organic-inorganic topological units $\{\text{C}_8\text{H}_4\text{N}_2\text{S}(\text{C}_3\text{H}_5)_2\text{CuCl}\}$ in **1**

[1] Yu. Slyvka, E. Goreshnik, O. Pavlyuk, M. Mys'kiv, *Open Chem.* 11 (2013) 43-61.

[2] B. Mychalichko, M. Mys'kiv, Ukraine Patent UA 25450, *Bull.* No. 6, 1998.

SYNTHESIS, FLUX GROWTH, AND CHARACTERIZATION OF THE $R_2Pd_3Si_5$ SERIES (R = RARE EARTH ELEMENTS)

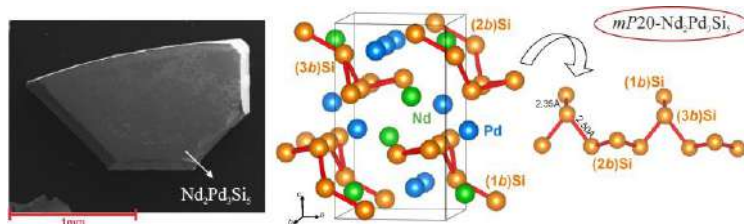
G. Repetto¹, S. De Negri¹, P. Solokha¹, T. Guizouarn², V. Porée², M. Pasturel²,
and R. Freccero¹

¹ *Department of Chemistry and Industrial Chemistry, University of Genoa,
Via Dodecaneso 31, 16146 Genoa, Italy*

² *Univ Rennes, CNRS, UMR 6226 ISCR, 35042 Rennes, France
giulia.repetto@edu.unige.it*

The $R_2M_3X_5$ family of polar intermetallic compounds (R : rare-earth and actinide elements; M : transition metal; X : p -block element) exhibits a remarkable compositional and structural variety, with more than 200 known compounds crystallizing in eight different structure types, with several representatives featuring distinct physical properties [1]. Despite this, some element combinations which might lead to $R_2M_3X_5$ intermetallics, still need to be investigated. This was the case for the $R_2Pd_3Si_5$ series, only reported for $R = La, Ce, Sm, Eu$ with $oI40$ - $U_2Co_3Si_5$ structure. Therefore, this study focuses on investigating the stability, formation, structural behaviour and physical properties of $R_2Pd_3Si_5$ compounds as a function of R . Samples were synthesized using conventional methods, such as arc- and induction-melting, as well as non-reactive metal flux technique [2]. The use of Sn-flux proved crucial for obtaining large and high-quality single crystals of the target phase, overcoming the formation of the RPd_2Si_2 secondary phase. This approach enabled a simplified and reliable characterization by scanning electron microscopy, energy-dispersive X-ray spectroscopy, powder and single-crystal X-ray diffraction. The $oI40$ crystal structure of $R_2Pd_3Si_5$ was confirmed with $R = La$ and Ce . In contrast, the phases containing $R = Nd, Sm, Gd$, crystallize as $mP20$ - $Nd_2Pd_3Si_5$ ($a = 5.8014(3)$ Å, $b = 5.9398(2)$ Å, $c = 10.0561(7)$ Å, and $\beta = 89.996(6)^\circ$), representing a new prototype (figure). Interestingly, $Pr_2Pd_3Si_5$ can adopt both structure types, depending on the synthesis method employed.

$Nd_2Pd_3Si_5$ has a ferromagnetic-like behaviour with $T_C = 4.5(1)$ K while $Sm_2Pd_3Si_5$ exhibits a more complex magnetic phase diagram with 3 transitions occurring below 12 K in weak magnetic fields.



SEM micrograph (left) and crystal structure representation (right) of monoclinic $Nd_2Pd_3Si_5$. Si-Si contacts at distances compatible with covalent interactions are indicated by red sticks.

- [1] W.K. Brown, M.A. Plata, M.E. Raines, J.Y. Chan, *Structural and Physical Properties of $R_2M_3X_5$ Compounds*, In: *Handbook on the Physics and Chemistry of Rare Earths*, J.-C.G. Bunzli, S.M. Kauzlarich (Eds.), Elsevier, 2023, Vol. 64, pp 1-92.
- [2] M.G. Kanatzidis, R. Pöttgen, W. Jeitschko, *Angew. Chem. Int. Ed.* 44(43) (2005) 6996-7023.

GROWTH AND CHARACTERIZATION OF REAsSe SINGLE CRYSTALS

Tetiana Romanova and Dariusz Kaczorowski

*Institute of Low Temperature and Structure Research, Polish Academy of Sciences,
Wrocław, Poland
t.romanova@intibs.pl*

The discovery of topological materials has led to intensive theoretical and experimental studies of new quantum states of matter. Systems where topological electronic states coexist with magnetic order are especially interesting, as they may enable advances in spintronics and quantum technologies. In rare-earth (*RE*) materials, the presence of *4f* electrons leads to magnetic moments and correlation effects, making these systems an interesting platform for studying the interplay between magnetism and electronic topology. In this context, *REAsSe* compounds appear to be promising candidates, but their structural and physical characteristics are still largely unknown. One of the main difficulties in studying these materials is the lack of single crystals of sufficient quality and size. High-quality crystals are required to facilitate accurate structural, magnetic, and transport measurements, especially under extreme conditions, such as low temperatures, strong magnetic fields, and/or high pressures.

Motivated by this challenge, we conducted a series of syntheses of *REAsSe* single crystals aimed at optimizing growth conditions to obtain samples with good crystal-chemical quality and suitable dimensions. Crystal growth was performed using the chemical vapor transport method with iodine as the transport agent. The chemical composition and homogeneity of the products were examined by means of energy-dispersive X-ray spectroscopy (EDS), while the phase composition and the lattice parameters were determined from powder X-ray diffraction (XRD) data.

Here, we present an overview of the performed crystal growth attempts and preliminary results of the crystal-chemical characterization of the obtained single-crystalline samples.

This work was supported by the National Science Centre, Poland, under grants No. 2025/09/X/ST5/00398 (MINIATURA 9) and 2021/41/B/ST3/01141 (OPUS 21), which is gratefully acknowledged.

SYNTHESIS AND ELECTROCHEMICAL PROPERTIES OF THE $\text{Ho}_{1-x}\text{Lu}_x\text{Ge}_2$ PHASES

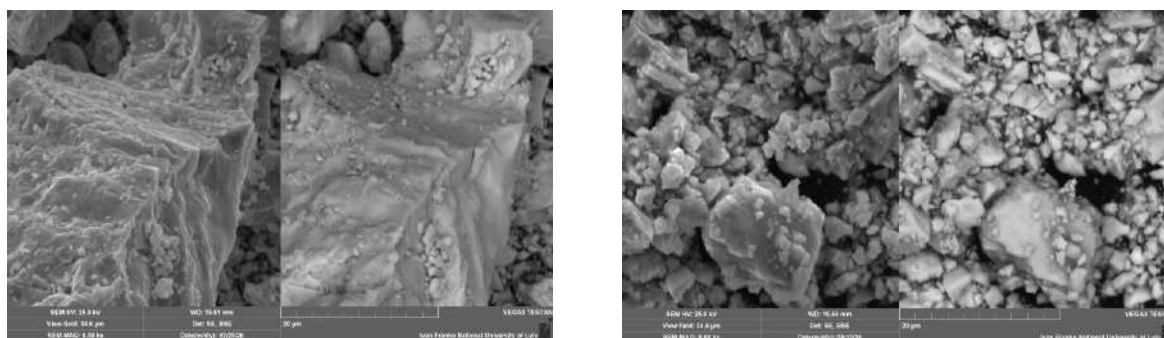
Z. Shpyrka, O. Darmonuk, V. Kordan, and V. Pavlyuk

Department of Inorganic Chemistry, Ivan Franko National University of Lviv,
Kyryla i Mefodiya St. 6, 79005 Lviv, Ukraine
zinoviya.shpyrka@lnu.edu.ua

Modern lithium-ion energy storage systems require advanced electrode materials combining high specific capacity, structural stability, and fast lithium diffusion. Intermetallic germanides are promising candidates due to their structural flexibility and ability to accommodate lithium without complete structural degradation. The present work investigates the mechanism of electrochemical Li-intercalation into $\text{Ho}_{1-x}\text{Lu}_x\text{Ge}_2$ phases and evaluates the amount of inserted lithium.

Alloys with nominal compositions $\text{Ho}_{20}\text{Lu}_{14}\text{Ge}_{66}$ and $\text{Ho}_{10}\text{Lu}_{24}\text{Ge}_{66}$ were synthesized by arc-melting high-purity metals (> 99.9 wt.%) under an argon atmosphere. The samples were annealed at 600 °C for 720 h in evacuated quartz ampoules followed by quenching in ice water. Structural characterization was performed by powder X-ray diffraction using a DRON-2.0M diffractometer (Fe $K\alpha$ radiation) and PowderCell [1] software. Scanning electron microscopy (Tescan Vega3 LMU scanning electron microscope) was applied for surface morphology studies. The qualitative and quantitative compositions of the electrodes before and after the electrochemical processes were determined by energy-dispersive X-ray spectroscopy (Oxford Instruments AZtec ONE System). Electrochemical lithiation/delithiation experiments were carried out in a two-electrode Swagelok-type cell using LiCoO_2 powder as the cathode material, a 1M LiPF_6 solution as the electrolyte, and a galvanostat MTech G410-2.

The $\text{Ho}_{1-x}\text{Lu}_x\text{Ge}_2$ phases, crystallizing in the ZrSi_2 structure type (Pearson symbol $oS12$), exhibit lithium intercalation governed by a combined insertion-substitution mechanism. The initial stage involves lithium insertion with formation of a $\text{Li}_y\text{Ho}_{1-x}\text{Lu}_x\text{Ge}_2$ phase. Further lithiation leads to partial replacement of Ge atoms by lithium atoms and formation of $\text{Li}_{y+k}\text{Ho}_{1-x}\text{Lu}_x\text{Ge}_{2-k}\text{Li}_{m-k}\text{Ge}_k$ compositions. As a result, the ZrSi_2 type transforms into the CeNiSi_2 type (Pearson symbol $oS16$) without a change of symmetry (space group $Cmcm$). SEM-images of the polycrystalline $\text{Ho}_{10}\text{Lu}_{24}\text{Ge}_{66}$ alloy before and after lithiation are presented in the figure. The obtained results (0.155 Li/f.u. and 0.137 Li/f.u. for electrodes based on the $\text{Ho}_{20}\text{Lu}_{14}\text{Ge}_{66}$ and $\text{Ho}_{10}\text{Lu}_{24}\text{Ge}_{66}$, respectively) demonstrate that the $\text{Ho}_{1-x}\text{Lu}_x\text{Ge}_2$ solid solution is capable of reversible lithium accommodation through a structurally adaptive intercalation mechanism, indicating their potential as alternative electrode materials.



SEM-images of $\text{Ho}_{10}\text{Lu}_{24}\text{Ge}_{66}$ alloy before (left) and after lithiation (right)

[1] W. Kraus, G. Nolze, PowderCell for Windows, Berlin, 1999.

STRUCTURAL EVOLUTION AND PROPERTIES OF Zr-BASED MELT-SPUN ALLOYS: THE IMPACT OF “BIG CUBE” Zr₂Ni PHASE FORMATION

O. Shved^{1,5}, V. Girzhon², I. Shtablavyi¹, O. Smolyakov², P. Dörflinger^{3,4}, H. Riedl^{3,4},
A. Prokofiev⁵, and S. Mudry¹

¹ *Department of Physics of Metals, Ivan Franko National University of Lviv,
Kyryla i Mefodiya St. 8, 79005 Lviv, Ukraine*

² *Department of Physical Materials Science, National University “Zaporizhzhia Polytechnic”,
Zhukovsky St. 66, 69063, Ukraine*

³ *Christian Doppler Laboratory for Surface Engineering of High-Performance Components,
TU Wien, A-1060 Wien, Austria*

⁴ *Institute of Materials Science and Technology, TU Wien, A-1060 Wien, Austria*

⁵ *Institute of Solid State Physics, TU Wien, A-1040 Wien, Austria
olenkawved01@gmail.com*

Multicomponent Zr–Ni-based systems occupy a distinct position in modern materials science due to their exceptional glass-forming ability and potential for developing bulk metallic glasses (BMGs). This study focuses on structural modification by replacing the widely used but toxic Cu by Cr and incorporating Ag. While Cr improves strength characteristics, Ag plays a key role in controlling the phase transformation kinetics. We have investigated the structural evolution of quinary Zr₆₅Al_{7.5}Ni₁₀Cr_{17.5-x}Ag_x alloys ($0 \leq x < 17.5$), Zr₆₇₍₆₈₎Al₃₍₂₎Ni₁₀Cr_{7.5}Ag_{12.5} and quaternary Zr₇₀Ni₁₀Cr_{12.5(7.5)}Ag_{7.5(12.5)} alloys.

Ribbons (~0.03 mm thick), produced by melt-spinning at ~10⁵-10⁶ K/s, were characterized using XRD and SEM. The analysis revealed a complex phase hierarchy, including the formation of a metastable “big-cube” phase (Ti₂Ni-type, $Fd\bar{3}m$) and *fcc* Zr₂Ni. From a structural point of view, the icosahedral atomic clusters of these phases act as structural “bridges” mediating the transition from the disordered amorphous state to the long-range crystalline order.

Experimental results for the Zr₇₀Ni₁₀Cr_{12.5}Ag_{7.5} alloy show the coexistence of nanocrystalline “big-cube” and *fcc* Zr₂Ni phases, resulting in significant mechanical reinforcement. The calculated fracture strength σ_f , derived from nanoindentation measurements ($H \approx 3 \cdot \sigma_f$), reaches up to 3.12 GPa. This value is notably higher than previously reported data for melt-spun Zr-based alloys, underscoring the crucial role of the dual-phase nanocrystalline structure in the overall mechanical performance.

The temperature dependence of the resistivity in the range of 4-295 K reveals a Mooji correlation: as the absolute resistivity increases, the temperature coefficient of resistance systematically decreases, eventually changing its sign. The presence of the crystalline Zr₂Ni (“big-cube”) phase increases the resistivity of the alloys compared to completely amorphous samples.

STRUCTURE, SURFACE PROPERTIES, AND SORPTION CAPACITY OF A XYLARATE Sn(IV)-Co(II) POROUS COORDINATION POLYMER

K. Tsymbaliuk^{1,2}, O. Martsynko¹, V. Kordan³, R. Gladyshevskii³, O. Finik²,
and O. Snurnikova²

¹ Department of Inorganic Chemistry and Chemical Education, Odesa I.I. Mechnikov National University, Vsevoloda Zmiiienka St. 2, 65082 Odesa, Ukraine

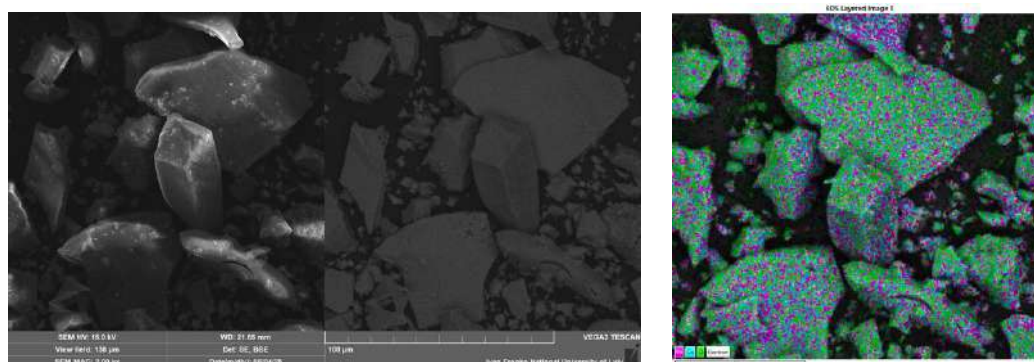
² LLC “Bureau Veritas Commodities Ukraine”, Udilny Lane 1, 65044 Odesa, Ukraine

³ Department of Inorganic Chemistry, Ivan Franko National University of Lviv, Kyryla i Mefodiya St. 6, 79005 Lviv, Ukraine
martsinkoelena@gmail.com

Metal-organic frameworks, as a class of hybrid organo-inorganic materials with a porous structure formed by coordination metal-ligand bonds, are increasingly attracting the attention of scientists for their application in various industries due to their large surface area, uniform nanoscale cavities, and chemical stability.

A stepwise synthesis method in aqueous solution was developed, and a solid-state Sn(IV)-Co(II) complex with xylaric acid was isolated. The compound was studied using a combination of physicochemical methods. It was shown to be a porous coordination polymer with a framework structure using the bridging function of xylarate and oxo ligands. The complex is characterized by high thermal stability, hierarchical porous morphology, and uniform metal distribution in the structure.

SEM analysis (Figure) showed that this substance has a polydisperse distribution of particles with a dominant lamellar morphology. The surfaces of the particles exhibit a hard texture with microroughness, local defects and cracks, which may indicate fragility. The size of the large lamellar particles ranges between 50 and 200 μm , while the medium fragments measure 5 to 50 μm . The finely dispersed fraction contains particles in the submicron-micron range (0.5-5 μm) that form a dense, powdery layer between the larger particles.



SEM images and elemental mapping of the surface of the sample by EDX

Elemental mapping by energy-dispersive X-ray spectroscopy (EDX) showed a uniform distribution of Sn, Co, and O on the surface of the sample, with no signs of phase segregation, indicating high chemical homogeneity.

The analytical efficiency of the Sn(IV)-Co(II) coordination polymer with xylaric acid as a sorbent for the preparation of aqueous samples by solid-phase extraction for the chromatographic-mass spectrometric determination of polychlorinated dibenzo-*p*-dioxins, dibenzofurans, and biphenyls was demonstrated.

UNRAVELING THE PHYSICAL PROPERTIES OF DISTORTED KAGOME CANDIDATES RE_3ScBi_5 ($RE = Pr, Nd, \text{ and } Sm$)

Bernard Walenczak, Tomasz Klimczuk, and Sudip Malick
*Faculty of Applied Physics and Mathematics, Gdansk University of Technology,
Narutowicza 11/12, 80-233, Gdansk, Poland
s194295@student.pg.edu.pl, sudip.malick@pg.edu.pl*

The physical properties of the distorted kagome system RE_3ScBi_5 ($RE = Pr, Nd, \text{ and } Sm$) have been investigated by means of magnetic, thermodynamic, and transport properties on high-quality single crystals grown using Bi-flux. The X-ray diffraction (XRD) data show that the crystals form in a hexagonal structure with space group $P6_3/mcm$ (No. 193). Temperature-dependent magnetic susceptibility, heat capacity, and electrical resistivity data indicate that all the compounds exhibit antiferromagnetic ordering at low temperatures. Pr_3ScBi_5 shows an antiferromagnetic (AFM) phase transition at 5.4 K, whereas Nd_3ScBi_5 exhibits two AFM transitions at $T_{N1} = 5.6$ K and $T_{N2} = 4.7$ K, which is consistent with a previous report [1]. Three consecutive AFM transitions are seen at $T_{N1} = 11.5$ K, $T_{N2} = 8.7$ K, and $T_{N3} = 7.1$ K in Sm_3ScBi_5 . Interestingly, all three phase transition temperatures in Sm_3ScBi_5 are robust against an external magnetic field up to 5 T. Magnetic susceptibility data further reveal strong magnetocrystalline anisotropy and a crystalline electric-field (CEF) effect in all compounds. The presence of CEF is also evident in the magnetic component of the heat capacity data, which shows a Schottky anomaly. Field-dependent magnetization data show several metamagnetic phase transitions in Pr_3ScBi_5 and Nd_3ScBi_5 . Intriguingly, heat capacity data obtained using the heat-pulse single-slope analysis method reveal a first-order phase transition in Nd_3ScBi_5 and Sm_3ScBi_5 . Electrical resistivity data show unusual behaviour under an external magnetic field. Our overall finding on these compounds suggests complex magnetism and unusual transport behaviour.

This research was supported by the PLATINUM Grant Programme of Gdańsk University of Technology, grant No. DEC-2/2/2023/IDUB/I.1B/Pt.

[1] K. Gornicka, B.R. Ortiz, H. Zhang, A.D. Christianson, A.F. May, *Phys. Rev. Mater.* 9 (2025) 064414.

**QUATERNARY RARE-EARTH SULFIDES $RE_2Ag_2SnS_6$ ($RE = Nd, Sm, Gd, Tb$)
WITH TWO- AND THREE-COORDINATE SILVER**

Qichao Wu and Arthur Mar

Department of Chemistry, University of Alberta, Edmonton T6G 2G2, Canada

qichao2@ualberta.ca

Binary and ternary silver-containing chalcogenides have applications in non-linear optics (*e.g.*, $AgGaS_2$), thermoelectrics (*e.g.*, Ag_2Se , $AgInSe_2$), and ionic conductors (*e.g.*, Ag_2S). Quaternary phases are relatively few (*e.g.*, RE_3AgMS_7 , $Ba_2REAg_5S_6$, $BaREAgS_3$, $Eu_7Ag_2Ge_4S_{16}$, $La_4Ag_2In_4S_{13}$, $TlREAg_2S_3$). Here, we report the synthesis and characterization of $RE_2Ag_2SnS_6$ ($RE = Nd, Sm, Gd, Tb$), which adopt an orthorhombic structure that showcases the versatility of silver coordination geometries.

PHASE EQUILIBRIA IN THE $\text{La}_2\text{O}_3\text{--Fe}_2\text{O}_3\text{--Sm}_2\text{O}_3$ SYSTEM AT 1400 °C

O. Chudinovych, S. Korichev, and M. Zamula
Frantsevich Institute for Problems of Materials Science of NAS of Ukraine
Omeliana Pritsaka St. 3, 03142 Kyiv, Ukraine
chudinovych_olia@ukr.net

Systems based on rare-earth oxides and transition metals have attracted considerable attention due to the formation of perovskite-like and garnet-like phases, which exhibit promising magnetic, electrical, and catalytic properties [1-2]. Knowledge about the $\text{La}_2\text{O}_3\text{--Fe}_2\text{O}_3\text{--Sm}_2\text{O}_3$ phase diagram is a prerequisite for the targeted synthesis of new functional materials with tailored properties. Analysis of phase diagrams makes it possible to determine the stability regions of ordered phases and solid solutions, and evaluate the influence of temperature and composition on the stability of the compounds.

The phase equilibria in the $\text{La}_2\text{O}_3\text{--Fe}_2\text{O}_3\text{--Sm}_2\text{O}_3$ ternary system at 1400 °C were studied by X-ray diffraction (XRD) and scanning electron microscopy (SEM) in the whole concentration range. La_2O_3 , Sm_2O_3 (99.99 %), and $\text{Fe}(\text{NO}_3)_3 \cdot 9\text{H}_2\text{O}$ were used as starting materials. The samples were prepared with a concentration step of 1-5 mol.%. The oxides were dissolved in HNO_3 (1:1), followed by evaporation of the solutions and decomposition of the nitrates at 800 °C for 2 h. The samples were then heat-treated at 1400 °C (for 100 h) in air. The phase composition of the samples was studied by X-ray diffraction (DRON diffractometer), microstructural phase and electron microprobe X-ray analyses. Elemental analysis of the samples was performed by X-ray spectral microanalysis (XMR) using an energy-dispersive spectrometer (EDX) INCA 450 (OXFORD Instruments).

Solid-state interactions among the three oxides result in the formation of the following phases: A– La_2O_3 , B– $(\text{La,Sm})_2\text{O}_3$, R, $\text{Sm}_3\text{Fe}_5\text{O}_{12}$, Fe_2O_3 . The largest homogeneity region corresponds to the continuous solid solutions based on the R phase. The R phase represents an ordered ternary (quasibinary) compound exhibiting a wider compositional stability range than those observed in the corresponding boundary binary systems. The isothermal section of the $\text{La}_2\text{O}_3\text{--Fe}_2\text{O}_3\text{--Sm}_2\text{O}_3$ system at 1400 °C is characterized by two three-phase regions (A + B + R, R + $\text{Sm}_3\text{Fe}_5\text{O}_{12}$ + Fe_2O_3), four single-phase fields (A– La_2O_3 , B– $(\text{La,Sm})_2\text{O}_3$, R, $\text{Sm}_3\text{Fe}_5\text{O}_{12}$), corresponding to solid solutions based on the initial components, and several two-phase regions (A + B, B + R, A + R, $\text{Sm}_3\text{Fe}_5\text{O}_{12}$ + R, R + Fe_2O_3) separating them. The homogeneity range of the solid solutions based on the R-phase extends from 43 to 47 mol.% Fe_2O_3 . The solubility of La_2O_3 and Sm_2O_3 in Fe_2O_3 is negligible.

[1] R.L. White, *J. Appl. Phys.* 40 (1969) 1061-1069.

[2] Z. Zhou, L. Guo, H. Yang, Q. Liu, F. Ye, *J. Alloys Compd.* 583 (2014) 21-31.

PECULIARITIES OF THE INTERACTION OF THE COMPONENTS IN THE R -Cr-Ge ($R = Y, Gd, Dy, Er, Tm$) SYSTEMS

M. Konyk¹, L. Romaka¹, V.V. Romaka², and Yu. Stadnyk¹

¹ Department of Inorganic Chemistry, Ivan Franko National University of Lviv,
Kyryla i Mefodiya St. 6, 79005 Lviv, Ukraine

² Technische Universität Dresden (TUD), Bergstrasse 66, 01069 Dresden, Germany
mariya.konyk@lnu.edu.ua

Experimental studies of the interaction of the components in metallic systems provide important information on the formation, temperature, concentration stability, and crystal structures of intermediate phases, to search for new materials with valuable properties.

Phase equilibrium diagrams of the R -Cr-Ge ($R = Y, Gd, Dy, Er, Tm$) systems were constructed at 1070 K based on X-ray diffraction, metallographic analysis and energy-dispersive X-ray spectroscopy [1-5]. The crystal structures were refined from X-ray powder diffraction data (diffractometer STOE Stadi P, Cu $K\alpha_1$ radiation; FullProf Suite program package).

The R -Cr-Ge systems are characterized by the formation of two or three ternary compounds, among which the most studied are series of RCr_6Ge_6 and RCr_xGe_2 germanides. The YCr_6Ge_6 compound crystallizes in the $MgFe_6Ge_6$ (or $HfFe_6Ge_6$) structure type, RCr_6Ge_6 germanides with $R = Gd, Dy, Er, Tm$ crystallize in the $SmMn_6Sn_6$ structure type, a disordered variant of the $MgFe_6Ge_6$ structure type. RCr_xGe_2 compounds with a structure of the $CeNiSi_2$ type are formed with the rare earths Y, Gd, Dy, and Er, and are characterized by defects in the crystallographic position of the transition metal. According to the X-ray diffraction and EPM analyses the existence of a small homogeneity range with variable Cr content, $x = 0.27-0.31$, $x = 0.28-0.30$, $x = 0.28-0.38$, was established for the $GdCr_xGe_2$, $DyCr_xGe_2$, and $ErCr_xGe_2$ germanides, respectively. No homogeneity range was observed for $YCr_{0.23}Ge_2$. In the Tm-Cr-Ge system the formation of an insertion-type solid solution $TmCr_xGe_2$ based on the binary germanide $TmGe_2$ ($ZrSi_2$ -type) was observed up to the limiting composition $TmCr_{0.33}Ge_2$.

$R_{117}Cr_{52}Ge_{112}$ compounds with a giant unit cell ($Tb_{117}Fe_{52}Ge_{112}$ -type) are formed in the R -Cr-Ge ($R = Gd, Dy$) systems. In the system with Tm the compound $Tm_4Cr_4Ge_7$ with $Zr_4Co_4Ge_7$ -type structure was found.

The work was carried out within the framework of the Ministry of Education of Ukraine (grant No. 0124U000989).

- [1] M. Konyk, L. Romaka, L. Orovčik, V.V. Romaka, Yu. Stadnyk, *Visn. Lviv. Univ. Ser. Chem.* 60(1) (2019) 38-47.
- [2] M. Konyk, L. Romaka, Yu. Stadnyk, V.V. Romaka, V. Pashkevych, *Phys. Chem. Solid State* 22(2) (2021) 248-254.
- [3] L. Romaka, Yu. Stadnyk, V.V. Romaka, Yu. Yatskiv, M. Konyk, *Phys. Chem. Solid State* 26(3) (2025) 592-597.
- [4] M. Konyk, L. Romaka, Yu. Stadnyk, V.V. Romaka, R. Serkiz, A. Horyn, *Phys. Chem. Solid State* 20(4) (2019) 376-383.
- [5] L. Romaka, Yu. Stadnyk, V.V. Romaka, M. Konyk, *Phys. Chem. Solid State* 23(4) (2022) 633-639.

THE TERNARY SYSTEM Zr–Al–Sb AT 600 °C

D. Maryshevych, Ya. Tokaychuk, and R. Gladyshevskii

Department of Inorganic Chemistry, Ivan Franko National University of Lviv,

Kyryla i Mefodiya St. 6, 79005 Lviv, Ukraine

danylo.maryshevych@lnu.edu.ua

The isothermal section of the phase diagram of the ternary system Zr–Al–Sb at 600 °C was constructed in the whole concentration range by means of X-ray diffraction and spectroscopy of 61 binary and ternary alloys. Ingots were synthesized from high-purity metals (Zr ≥ 99.95 mass%; Al ≥ 99.99 mass%; Sb ≥ 99.97 mass%) by arc melting under argon using a water-cooled copper hearth, a tungsten electrode, and Ti sponges as a getter. The alloys were annealed at 600 °C for 1 month under vacuum and quenched into cold water. Phase analysis and structure refinements were performed using X-ray powder diffraction data collected at room temperature on diffractometers DRON-2.0M (Fe $K\alpha$ -radiation), PROTO AXRD Benchtop (Cu $K\alpha$ -radiation), and STOE Stadi P (Cu $K\alpha_1$ -radiation). The profile and structural parameters were refined by the Rietveld method using the FullProf Suite program package. The compositions of the phases were determined by energy-dispersive X-ray spectroscopy, performed on a scanning electron microscope TESCAN Vega3 LMU, equipped with an energy-dispersive X-ray analyzer Oxford Instruments Aztec ONE with a detector X-Max^N20.

The existence of 14 compounds at 600 °C was confirmed in the boundary binary systems Zr–Al and Zr–Sb: Zr₃Al (structure type Cu₃Au), Zr₂Al (Co_{1.75}Ge), Zr₃Al₂ (Zr₃Al₂), Zr₄Al₃ (Zr₄Al₃), ZrAl (TiI), Zr₂Al₃ (Zr₂Al₃), ZrAl₂ (MgZn₂), ZrAl₃ (ZrAl₃), Zr₃Sb (Ni₃P), Zr₂Sb (La₂Sb), Zr₅Sb₃ (Mn₅Si₃), Zr₅Sb₄ (Ti₅Ga₄), ZrSb (ZrSb), and ZrSb₂ (PbCl₂). The binary antimonides Zr₅Sb₄ and Zr₅Sb₃ dissolve 11.1 and 2.5 at.% Al, respectively, forming limited solid solutions of the substitution type. The other binary compounds do not dissolve significant amounts of the third component. The isothermal section of the phase diagram of the ternary system Zr–Al–Sb at 600 °C contains 22 single-phase, 45 two-phase and 24 three-phase fields. The highest numbers of equilibria (9) are formed with the solid solution based on the binary compound Zr₅Sb₄ and the ternary compound Zr₅Al_{1.55-0.65}Sb_{1.45-2.35}.

The existence of four ternary compounds was established at 600 °C. Their crystal structures belong to ternary structure types that are ordering derivatives of the binary structure types TiAl₃ (UCuAl₂), UAs₂ (Zr₂CuSb₃), and W₅Si₃ (Nb₅SiSn₂). A tendency for ordering of Al and Sb was observed.

Crystallographic data for the ternary compounds of the system Zr–Al–Sb

Compound	Structure type	Pearson symbol	Space group	Unit-cell parameters, Å	
				<i>a</i>	<i>c</i>
ZrAl _{2.78} Sb _{0.22}	UCuAl ₂	<i>tI8</i>	<i>I4/mmm</i>	3.96555(11)	9.0221(3)
Zr ₂ AlSb ₃	Zr ₂ CuSb ₃	<i>tP6</i>	<i>P-4m2</i>	3.91644(6)	8.72525(13)
Zr ₅ Al _{2.55} Sb _{0.45}	Nb ₅ SiSn ₂	<i>tI32</i>	<i>I4/mcm</i>	11.0740(4)	5.4407(2)
Zr ₅ Al _{1.0-0.4} × ×Sb _{2.0-2.6}	Nb ₅ SiSn ₂	<i>tI32</i>	<i>I4/mcm</i>	11.0892(4)- 11.1121(3)	5.5339(2)- 5.5671(3)

**NEW RESULTS ON THE PHASE STABILITY AND COMPETING CRYSTAL
STRUCTURES IN THE FORMATION OF THE INTERMETALLIC COMPOUND
 $\text{Cu}_5(\text{As}_{1-y}\text{Sb}_y)_2$**

Marianne Mödlinger¹, Alessia Provino^{1,2}, Pavlo Solokha¹, Serena De Negri¹,
and Pietro Manfrinetti^{1,2}

¹ *Department of Chemistry, University of Genova, 16146 Genova, Italy*

² *Institute SPIN-CNR, 16152 Genova, Italy*

marianne.moedlinger@gmail.com

An experimental investigation of the ternary system Cu–As–Sb, for which no literature data were available, was undertaken. During this study, the new intermetallic phase $\text{Cu}_5(\text{As}_{1-y}\text{Sb}_y)_2$ was identified. Like the known parent binary Cu_5As_2 , the new ternary compound was found to be sub-stoichiometric in Cu, with the composition $\text{Cu}_{5-x}(\text{As}_{1-y}\text{Sb}_y)_2$. Solid solubility was found within the compositional ranges 68.9-71.5 at.% for Cu, 23.2-28.6 at.% for As, and 1.9-5.1 at.% for Sb. However, there appears to exist no continuous solid solubility between Cu_5As_2 and the new phase, as the ternary phase seems to form for Sb contents higher than about 2 at.%. Like the binary compound, $\text{Cu}_{5-x}(\text{As,Sb})_2$ crystallizes in a structure of the orthorhombic Mg_5Ga_2 structure type (*oI28*, *Ibam*, No. 72). The lattice parameters were found within the ranges $a = 5.968\text{-}5.977(1)$ Å, $b = 11.55\text{-}11.565(3)$ Å, $c = 5.530\text{-}5.573(3)$ Å. Similarly to the parent binary compound, $\text{Cu}_{5-x}(\text{As,Sb})_2$ is a high-temperature phase. It forms peritectically at 635-650 °C and, upon lowering the temperature, it starts to decompose at about 360-380 °C and at about 310 °C it is fully decomposed into hexagonal Cu_{3-x}As (Cu_3P -type, *hP24*, *P6_3cm*, No. 185) and (As,Sb) (As-type, *hR6*, *R-3m*, No. 166). Its formation (and therefore its thermodynamic stability) is in strong competition with the formation of the two other, very close solid-solution compounds $\text{Cu}_{3-x}(\text{As}_{1-y}\text{Sb}_y)$ (Cu_3P -type; *hP24*, *P6_3cm*, No. 185) and $\text{Cu}_{3-x}(\text{As}_z\text{Sb}_{1-z})$ (Cu_9TeSb_2 -type; *cP32*, *Pm-3m* No. 223). No evidence of the existence of high-temperature (HT) and low-temperature (LT) polymorphic phases was found.

EXPERIMENTAL AND DFT STUDY OF THE Er–Cu–Sb TERNARY SYSTEM

L. Romaka¹, V. Romaka², Yu. Stadnyk¹, and A. Horyn¹

¹ Department of Inorganic Chemistry, Ivan Franko National University of Lviv,
Kyryla i Mefodiya St. 6, 79005 Lviv, Ukraine

² Technische Universität Dresden (TUD), Bergstrasse 66, 01069 Dresden, Germany
lyubov.romaka@lnu.edu.ua

The RE–Cu–Sb systems attract attention due to the formation of RE₃Cu₃Sb₄ (RE = La, Ce, Gd, Er) antimonides of the Y₃Au₃Sb₄ structure type, whose electrical transport properties make them interesting as potential thermoelectric materials [1]. However, the phase equilibria with neighbouring phases for most of them are still unknown, which prevents the further development of synthesis strategies and tuning of their thermoelectric properties.

The phase relations in the Er–Cu–Sb ternary system were studied using powder X-ray diffraction, scanning electron microscopy, and energy-dispersive X-ray spectroscopy. All samples were prepared by the conventional arc-melting technique with 3-5 wt.% excess of Sb, depending on the composition. The alloys were annealed at 870 K for 720 h in evacuated quartz ampoules, followed by quenching in cold water. The isothermal section at 870 K of the Er–Cu–Sb ternary system was constructed over the whole concentration range. The system is characterized by the formation of three known ternary compounds: Er₃Cu_{22.28}Sb_{8.72} (Dy₃Cu_{20+x}Sb_{11-x}-type, space group *F*-43*m*, *a* = 1.65705(6) nm), Er₃Cu₃Sb₄ (Y₃Au₃Sb₄-type, space group *I*-43*d*, *a* = 0.94797(4) nm), ErCuSb₂ (HfCuSi₂-type, space group *P*4/*nmm*, *a* = 0.4238(2), *c* = 0.9773(5) nm), and a new ternary phase ErCu_{3.03}Sb₂ (TmCu_{2.93}Sb₂-type, space group *Pnmm*, *a* = 0.70025(7), *b* = 0.78798(8), *c* = 0.42658(4) nm). The crystal structure of ErCu_{3.03}Sb₂ was refined from powder X-ray diffraction data (STOE Stadi P, Cu *K*α₁ radiation) and showed partial occupancy of one 4g position for Cu atoms, which corresponds to the formula ErCu_{3.03}Sb₂. The binary phases of the Er–Sb system show partial solubility of Cu. In particular, the solubility of Cu in ErSb (NaCl-type) reaches ~9 at.% (*a* = 0.6112(4)-0.6123(2) nm), while the Er₅Sb₃ binary (Yb₅Sb₃-type) dissolves up to ~5 at.% Cu along the Er isoconcentrate (*a* = 1.1698(3)-1.1689(3), *b* = 0.9128(3)-0.9119(3), *c* = 0.8022(1)-0.8008(2) nm). The electrical transport properties of the ErCu_{3.03}Sb₂, Er₃Cu_{22.28}Sb_{8.72}, and ErCuSb₂ compounds were studied in the temperature range 78-400 K and showed metallic conductivity. Density functional theory (DFT) calculations were used to evaluate the chemical bonding, thermodynamic, elastic, and electrical properties of the ternary phases.

The work was carried out within the framework of the Ministry of Education of Ukraine (grant No. 0124U000989). V.R. is grateful for support from the SFB1143 project of the German Research Society (DFG). The authors gratefully acknowledge the computing time made available to them on the high-performance computer at the NHR Center of TU Dresden (p_quantummat project).

[1] K. Fess, W. Kaefer, Ch. Turner, K. Friemelt, Ch. Kioc, E. Bucher, *J. Appl. Phys.* 83 (1998) 2568-2573.

PHASE EQUILIBRIA IN THE Tl–Pb–Te SYSTEM

M. Sabov^{1,2}, M. Filep², A. Pogodin¹, T. Malakhovska¹, V. Sabov¹, and M. Piasecki³

¹ *Department of Inorganic Chemistry, Uzhhorod National University,
Pidhirna St. 46, 88000 Uzhhorod, Ukraine*

² *Department of Biology and Chemistry, Ferenc Rákóczi II Transcarpathian Hungarian
University, Kossuth Square 6, 90202 Berehove, Ukraine*

³ *Faculty of Science and Technology, Jan Długosz University,
al. Armii Krajowej 13/15, 42-200 Częstochowa, Poland
marian.sabov@uzhnu.edu.ua*

Thallium tellurides and ternary phases formed in the thallium–lead–tellurium system are typical narrow-bandgap semiconductors. The narrow gap with low thermal conductivity, especially phonon conductivity, is the reason for their perspectives as thermoelectric materials. On the other hand, these materials have been reported to possess Dirac-like surface states, placing them in the category of topological materials.

The interaction in the ternary system Tl–Pb–Te has been studied in many works. However, the data are contradictory. The existence of the ternary compound Tl₄PbTe₃ has been reported by many authors. According to some of them it forms by a peritectic reaction in the isopleth section Tl₅Te₃–PbTe or quasi-binary section Tl₂Te–PbTe. Others report that Tl₄PbTe₃ melts congruently, whereas some authors claim that it forms in the Tl₂Te–PbTe quasi-binary, and moreover, that a continuous solid solution forms in the Tl₂Te–Tl₄PbTe₃ subsystem, while others state that this subsystem is not quasi-binary.

For this reason, a physico-chemical investigation of the interactions in the Tl–Pb–Te system was carried out. It includes establishing the quasi-binary and partially quasi-binary systems, and determination of the phase equilibria in the isothermal section at 523 K.

It was established that five sections based on Tl₄PbTe₃ (Pb–Tl₄PbTe₃, Tl–Tl₄PbTe₃, PbTe–Tl₄PbTe₃, Tl₂Te–Tl₄PbTe₃, and Tl₅Te₃–Tl₄PbTe₃) are quasi-binary and three sections, based on peritectic binary thallium tellurides, are partially quasi-binary in the subsolidus region (PbTe–TlTe, Pb–Tl₂Te₃, and TlTe–Tl₄PbTe₃). Particularly interesting are the Tl₂Te–Tl₄PbTe₃, and Tl₅Te₃–Tl₄PbTe₃ systems.

The Tl₅Te₃–Tl₄PbTe₃ system shows a simple eutectic phase diagram. The eutectic point has the coordinates ~4 mol.% Tl₄PbTe₃, 713 K. Despite the fact that the phases are isostructural, there is an immiscibility region (~12 mol.%) in the solid state on the binary side. The solubility in Tl₅Te₃ is very small, while the solid solutions range formed by Tl₄PbTe₃ reaches nearly 85 mol.%. The phase diagram of the Tl₂Te–Tl₄PbTe₃ system, similarly to the previous system, is characterized by a small homogeneity range of the binary telluride and a wide range of solid solutions (more than 80 mol.%) based on the ternary compound. The Tl₂Te–Tl₄PbTe₃ system is characterized by an invariant peritectic point with coordinates 2 mol.% Tl₄PbTe₃, 721 K. The formation of solid solutions is also indicated by a linear change of the lattice parameters in both systems.

Phase diagrams were also established for the other quasi-binary systems, three isopleth sections (PbTe–TlTe, Pb–Tl₂Te₃ and TlTe–Tl₄PbTe₃) and the isothermal section at 523 K of the Tl–Pb–Te system. Among the quasibinaries, the phase diagram of Pb–Tl₄PbTe₃ and PbTe–Tl₄PbTe₃ are of the eutectic type whereas that of Tl–Tl₄PbTe₃ is peritectic.

THE FORMATION OF INTERMETALLIC COMPOUNDS ON THE BOUNDARY OF METALLIC MICROPARTICLES AND Ga-BASED MELTS

S. Mudry, Yu. Kulyk, N. Popilovskyi, O. Kovalskyi, K. Starushenko, N. Sembratovych,
and I. Shtablavyi

*Department of Metal Physics, Ivan Franko National University of Lviv,
Kyryla i Mefodiya St. 8, 79005 Lviv, Ukraine
ihor.shtablavyi@lnu.edu.ua*

The growing interest in low-melting-point liquid metals is motivated by several factors, the most important being the development of stretchable and flexible electronics. In many application fields, stretchable conductive materials represent an important and fundamental component and remain the focus of intense research. Liquid metals possess suitable properties for stretchable conductors, such as high electrical conductivity, extreme stretchability, patternability, and mechanical compliance, which stem from their inherent liquid nature.

Despite the extensive research conducted so far, the advantages of liquid metals are still largely limited by the presence of a substrate. Another problem is related to the requirement to obtain a liquid-metal thin film, which is typically formed on the surface of a substrate. Due to the high surface tension of liquid metals, it is very difficult to obtain stable liquid-metal thin films.

In this work, we present the results of studying the behaviour of a Ga–In–Sn ternary eutectic melt on a polymer surface used as a substrate. In order to enhance the interaction between the polymer and the melt, small nickel particles were introduced into the polymer surface by simple mechanical pressing. In this procedure, we also analysed our earlier results on the structure of liquid Ni–Ga, Ni–Sn, and Ni–In alloys. Literature data on the enthalpy of mixing for these binary systems were also taken into account. Such an analysis allowed us to assume that the tendency for interaction between the constituents of the eutectic melt and nickel should reduce the surface tension of the melt.

The results of X-ray diffraction measurements show that the short-range order structure is not significantly different from that of the bulk eutectic melt. Slight differences between the structural parameters of the thin film and the bulk melt are mainly caused by cluster size rather than changes in interatomic distances or the number of neighbouring atoms. Thus, the formation of intermetallic particles makes it possible to reduce the surface tension without significant changes in the structural parameters, which is important for maintaining the key properties responsible for practical applications.

This work was supported by the National Research Foundation of Ukraine, project No. 2025.07/0286.

THE TERNARY SYSTEMS La–{Si,Ge}–Bi AT 600 °C

R. Vynnyk, Ya. Tokaychuk, and R. Gladyshevskii

Department of Inorganic Chemistry, Ivan Franko National University of Lviv,

Kyryla i Mefodiya St. 6, 79005 Lviv, Ukraine

roman.vynnyk@lnu.edu.ua

The isothermal sections of the phase diagrams of the ternary systems La–Si–Bi and La–Ge–Bi at 600 °C were constructed in the whole concentration range by means of X-ray diffraction and X-ray spectroscopy of 19 and 22 ternary alloys, respectively. The samples were synthesized by arc-melting high-purity metals (La \geq 99.85 mass%; Si \geq 99.999 mass%; Ge \geq 99.999 mass%; Bi \geq 99.98 mass%) under argon, using a water-cooled copper hearth, a tungsten electrode and Ti sponges as a getter. The alloys were annealed at 600 °C for 1 month under vacuum and quenched into cold water. Phase analysis and structure refinements were performed on X-ray powder diffraction data collected at room temperature on diffractometers DRON-2.0M (Fe $K\alpha$ radiation) and STOE Stadi P (Cu $K\alpha_1$ radiation). The profile and structural parameters were refined by the Rietveld method using the FullProf Suite program package. The compositions of the phases were determined by energy-dispersive X-ray spectroscopy, performed on a scanning electron microscope TESCAN VEGA3 LMU, equipped with an energy-dispersive X-ray analyzer Oxford Instruments Aztec ONE with a detector X-Max^N20.

The existence of 19 compounds was confirmed at 600 °C in the boundary binary systems La–Si, La–Ge, and La–Bi: La₅Si₃ (structure type Cr₅B₃), La₃Si₂ (U₃Si₂), La₅Si₄ (Zr₅Si₄), LaSi (FeB), LaSi_{1.88} (GdSi_{1.4}), LaSi₂ (α -ThSi₂), La₃Ge (Ti₃P), La₅Ge₃ (Mn₅Si₃), La₄Ge₃ (Th₃P₄), La₅Ge₄ (Sm₅Ge₄), LaGe (FeB), La₃Ge₅ (Y₃Ge₅), La₄Ge₇ (Nd₄Ge₇), LaGe₂ (α -ThSi₂), La₂Bi (La₂Sb), La₅Bi₃ (Mn₅Si₃), La₄Bi₃ (Th₃P₄), LaBi (NaCl), and LaBi₂ with not established structure. The binary compounds do not dissolve significant amounts of the third component. The existence at 600 °C of two ternary compounds, La₅SiBi₂ and La₅Ge_{1.2}Bi_{1.8} with Y₂HfS₅-(anti)type structures (Pearson symbol *oP32*, space group *Pnma*) [1], was confirmed and a ternary compound, La₂Ge_{3.03}Bi_{0.81}, was synthesized [2].

The crystal structure of the ternary compound La₂Ge_{3.03}Bi_{0.81} was determined by X-ray powder diffraction (structure type Pr₂Ge_{3.26}Bi_{0.62}, *oS36*, *Cmcm*, *a* = 4.2289, *b* = 31.915, *c* = 4.4379 Å). The structure is characterized by partial disorder of Bi and Ge atoms, which form a statistical mixture on one site, and by positional disorder of Ge atoms, modeled by split positions. The structure type Pr₂Ge_{3.26}Bi_{0.62} belongs to a homologous series of linear intergrowth structures built by the intergrowth of AlB₂-type (triple layers of trigonal prisms) and CaF₂-type (double layers of “half octahedra”) slabs in the sequence (3AlB₂|2CaF₂)₂.

The isothermal section of the phase diagram of the ternary system La–Si–Bi at 600 °C contains 15 single-phase, 28 two-phase, and 14 three-phase fields. The corresponding section of the La–Ge–Bi system contains 17 single-phase, 35 two-phase, and 18 three-phase fields. In the system La–Si–Bi, the binary compound LaBi and the ternary compound La₅SiBi₂ form the highest numbers of equilibria (8). In the system La–Ge–Bi the highest number of equilibria (8) is formed by the ternary compound La₅Ge_{1.2}Bi_{1.8}.

[1] S.D. Barry, A.V. Tkachuk, H. Bie, P.E.R. Blanchard, A. Mar, *J. Solid State Chem.* 184 (2011) 21-29.

[2] Ya. Tokaychuk, R. Vynnyk, R. Dankevych, R. Gladyshevskii, *Chem. Met. Alloys* 13 (2020) 55-60.

STABILITY AND MAGNETIC PROPERTIES OF $Zr_2Fe_{12}P_7$ -TYPE INTERMETALLICS: EXPERIMENTAL OPTIMIZATION AND MACHINE LEARNING PREDICTION

C. Joubert, F. Gascoin, and S. Le Tonquesse

*Laboratoire de Cristallographie et Sciences des Matériaux, Université de Caen Normandie, ENSICAEN, CNRS, Normandie Univ, CRISMAT UMR6508, F-14000 CAEN, France
chloe.joubert@ensicaen.fr*

Intermetallic compounds continue to attract strong interest due to their rich structural chemistry and their potential for functional applications, for instance, in magnetism and energy-related technologies. Among them, $Zr_2Fe_{12}P_7$ -type phases represent a promising class of materials combining complex crystal structures with tunable magnetic properties.

Magnetocaloric materials offer an environmentally friendly alternative to conventional vapor-compression refrigeration systems, which rely on harmful refrigerants and noisy, wear-prone mechanical components. Magnetocaloric refrigeration, which is more robust and free of polluting fluids, is nonetheless limited by the poor mechanical durability of giant magnetocaloric materials showing first-order magnetic transitions [1-3]. This highlights the need to develop new and more robust compounds.

A large family of intermetallic compounds crystallizes in the $Zr_2Fe_{12}P_7$ -type structure, which shows magnetocaloric potential due to its high content of magnetic elements and chemical flexibility [4]. In this study, we investigate the synthesis, structural stability, and magnetic behaviour of $Zr_2Fe_{12}P$ -type intermetallic compounds. Experimental efforts focus on optimizing synthesis conditions to stabilize the targeted phase and reduce the amount of secondary phases, followed by structural characterization and magnetic measurements using SQUID magnetometry. The influence of compositional variations on phase stability and magnetic response is systematically analysed.

To complement the experimental investigation, machine learning tools are employed to accelerate the identification of new magnetocaloric phases within this family. A dataset of compositions built from the literature is used to train classification models (tree-based models, SVM, *etc.*) based on simple atomic descriptors. The objective is to predict phase stability and accelerate the discovery of new high-performance compounds. In parallel, experimental syntheses are carried out to optimize the formation of these phases and validate the model predictions.

- [1] Ch. Hueppe *et al.*, *Energy Policy* 155 (2021) 112275.
- [2] A. Kitanovski, *Adv. Energy Mater.* 10(10) (2020) 1903741.
- [3] N.A. Zarkevich *et al.*, *Crystals* 10 (2020) 815.
- [4] E. Ganglberger, *Monatsh. Chem.* 99 (1968) 557-565.

MAGNETIC, THERMAL, AND TRANSPORT PROPERTIES OF THE LAVES PHASE COMPOUND $\text{Sc}_{0.4}\text{Ti}_{0.6}\text{Fe}_2$

V. Anière¹, T.J. Bednarchuk², and K. Synoradzki¹

¹*Institute of Molecular Physics, Polish Academy of Sciences, Poznań, Poland*

²*Institute of Low Temperature and Structure Research,
Polish Academy of Sciences, Wrocław, Poland
aniere@ifmpan.poznan.pl*

While Fe-based intermetallic binary Laves phases $A\text{Fe}_2$ (with A an early 3d or 4d transition metal, or rare-earth) have been extensively characterized [1,2], many compositions of pseudo-binary $A_{1-x}B_x\text{Fe}_2$ rare-earth-free Laves phases remain to be studied. Owing to the wide range of magnetic and mechanical properties they may span and the important sensitivity of these properties to chemical composition, these compounds represent an interesting base for exploring novel applications, such as in solid-state cooling and Zero- or Negative-Thermal-Expansion materials (ZTE/NTE) [3-6]. The presented work reports on the magnetic, thermal, and transport properties of polycrystalline $\text{Sc}_{0.4}\text{Ti}_{0.6}\text{Fe}_2$. This compound crystallizes in the C14 MgZn_2 -type hexagonal structure (space group $P6_3/mmc$). Magnetometry measurements in the temperature range 2-380 K in fields up to 9 T show a complex magnetic behaviour, which is connected to unconventional magnetovolume effects [6]. The observed magneto-structural transitions are further characterized *via* Differential Scanning Calorimetry (DSC) measurements between 200 and 500 K, and the resistance and magneto-resistance of the compound are measured from room temperature down to 2 K.

Funded by the National Science Centre, Poland, under the OPUS call in the Weave programme 2023/51/I/ST11/02562.

- [1] K.A. Gschneidner Jr., V.K. Pecharsky, *Z. Kristallogr. – Cryst. Mater.* 221 (2006) 375-381.
- [2] J.J.M. Franse, R.J. Radwański, In: *Handbook of Magnetic Materials*, Chapter 5, Elsevier, 1993, pp. 307-501.
- [3] F. Stein, A. Leineweber, *J. Mater. Sci.* 56 (2021) 5321-5427.
- [4] Y. Nakamura, *J. Magn. Magn. Mater.* 31-34 (1983) 829-834.
- [5] L. Sun, H. Yibole, O. Tegus, F. Guillou, *Crystals* 10 (2020) 410.
- [6] Y. Song, Q. Sun, M. Xu, J. Zhang, Y. Hao, Y. Qiao, S. Zhang, Q. Huang, X. Xing, J. Chen, *Mater. Horiz.* 7 (2020) 275-281.

FEATURES OF THE CRYSTAL STRUCTURE AND PHYSICAL PROPERTIES OF THE INTERMETALLIC SEMICONDUCTOR SOLID SOLUTION $Zr_{1-x}Nb_xNiSn$: FROM MODELLING TO EXPERIMENTAL RESEARCH

A. Horyn¹, V.A. Romaka², Yu. Stadnyk¹, L. Romaka¹, V.V. Romaka³, and A. Zelinskiy¹

¹ *Department of Inorganic Chemistry, Ivan Franko National University of Lviv, Kyryla i Mefodiya St. 6, 79005 Lviv, Ukraine*

² *National University "Lvivska Politehnika", S. Bandera St. 12, 79013 Lviv, Ukraine*

³ *Technische Universität Dresden (TUD), Bergstrasse 66, 01069 Dresden, Germany
andriy.horyn@lnu.edu.ua*

Half-Heusler phases with the structure type MgAgAs are intensively studied as efficient thermoelectric materials. Doping them with additives optimizes their thermoelectric properties, particularly by enhancing the figure of merit, Z . Experimental and DFT studies of the semiconductive $Zr_{1-x}Nb_xNiSn$ solid solution are presented in this work.

$Zr_{1-x}Nb_xNiSn$ solid-solution alloys were synthesized by arc-melting and homogenized at 1073 K. According to the X-ray diffraction patterns, the samples with a Nb content of $x = 0-0.05$ belong to the structure type MgAgAs. The nearly linear decrease in the parameter $a(x)$ for $0 < x \leq 0.02$ is consistent with the simulation. At Nb concentrations $0.02 < x \leq 0.05$, the rate of change of the parameter $a(x)$ decreases, which may be associated both with the replacement of larger Zr atoms and Ni atoms present in position $4a$ by Nb atoms, and with the occupation of tetrahedral voids in the structure by Nb atoms. To determine the position of the Fermi level ε_F in relation to the continuous energy bands, the band-gap width ε_g , and the electrokinetic characteristics of the $Zr_{1-x}Nb_xNiSn$ solid solution, $x = 0-0.125$, the density of states (DOS) distribution was calculated. According to DOS, at the lowest concentration of Nb atoms, the Fermi level ε_F shifts from the band gap ε_g deep into the conduction band ε_C , indicating metallic conductivity. Modelling and experimental measurements of the temperature dependencies of the resistivity $\rho(T)$ and the thermopower coefficient $\alpha(T)$ for $Zr_{1-x}Nb_xNiSn$ showed a similar pattern. The resistivity $\rho(T,x)$ for all concentrations x increases with increasing temperature, indicating a dielectric-metal transition predicted by calculations (Anderson transition); the Fermi level ε_F is in the conduction band. Modelling and experimental data of the thermopower coefficient $\alpha(T,x)$, which has negative values at all temperatures, confirm that the Fermi level ε_F is in the conduction band. The reduction in the activation energy $\varepsilon_1^\alpha(x)$, calculated from the dependencies $\alpha(1/T,x)$, indicates a decrease in the compensation of the n-type semiconductor, which is possible when defects of donor nature and the corresponding energy states are generated in the crystal structure. It can occur under the condition of simultaneous partial substitution of Zr atoms by Nb atoms and occupation of tetrahedral voids by Nb atoms, which corresponds to structural changes. The magnetic susceptibility $\chi(x)$ of the $Zr_{1-x}Nb_xNiSn$ solid solution ($x = 0.01-0.05$) increases with increasing x , which is the result of an increase in the density of states at the Fermi level $DOS(\varepsilon_F)(x)$.

In conclusion, modelling and experimental studies of the characteristics of the semiconductor solid solution $Zr_{1-x}Nb_xNiSn$ indicate that, at all concentrations of Nb atoms in the n-type semiconductor, only defects of donor nature and their corresponding energy states are generated. This corresponds to the conditions for obtaining a thermoelectric material $Zr_{1-x}Nb_xNiSn$ with maximum values of the thermoelectric figure of merit Z .

The work was carried out within the framework of the Ministry of Education and Science of Ukraine (grants No. 0124U000989 and No. 0124U001146).

ION MIGRATION PATHWAYS IN TUNGSTATE- AND MOLYBDATE-CRYSTALS WITH SCHEELITE- OR WOLFRAMITE-TYPE STRUCTURES

V. Shevchuk and I. Kaiun

*Department of Sensory and Semiconductor Electronics,
Ivan Franko National University of Lviv, Dragomanova St. 50, 79005 Lviv, Ukraine
ihor.kaiun.hmh@lnu.edu.ua*

In this work, computer calculations and stereo-atomic crystal structure analyses were applied to AMO_4 compounds ($A = \text{Ba, Ca, Cd, Pb, Sr, Zn, Eu}$; $M = \text{W, Mo}$) and solid solutions based on them. Previous results of our investigations on ion migration pathways are reported in [1,2].

Possible migration 3D-paths and migration channels for W or Mo ions in scheelite- and wolframite-type structures of AMO_4 were considered at the nano-size level. The program package TOPOS was used for calculations of the ion migration in real crystals. Four factors (structure, partial cationic substitution, temperature, and technological conditions of the crystal growth technique) influence the possible ion migration paths until the conditions for the formation of a continuous network are ascertained.

In most cases, unlinked migration channels of the W ions were observed in the AWO_4 compounds. But in some cases, based on structural studies on X-ray diffraction data, continuous 3D-networks of W ion migration paths may be considered even at RT for undoped crystals. The probability of ion migration (the case of W ions) increased with increasing temperature.

The usefulness of the proposed approach as a tool for the investigation of structural point defects will be shown.

[1] V.N. Shevchuk, I.V. Kayun, *Chem. Met. Alloys* 9 (2016) 124-128.

[2] V. Shevchuk, I. Kayun, *Electron. Inf. Technol.* 19 (2022) 3-25.

DETAILED STUDIES OF THE SUPERCONDUCTING PROPERTIES OF $\text{Y}_3\text{Pt}_4\text{Ge}_6$

Jakub Nachowski, Sudip Malick, Duygu Yazici, and Tomasz Klimczuk
*Faculty of Applied Physics and Mathematics, Gdansk University of Technology,
Narutowicza 11/12, 80-233 Gdansk, Poland
s194210@student.pg.edu.pl, tomasz.klimczuk@pg.edu.pl*

We present a thorough analysis of the superconducting properties of $\text{Y}_3\text{Pt}_4\text{Ge}_6$. A very high-purity polycrystalline sample of $\text{Y}_3\text{Pt}_4\text{Ge}_6$ has been synthesized by arc melting and solid-state reaction. Powder X-ray diffraction (pXRD) confirms that $\text{Y}_3\text{Pt}_4\text{Ge}_6$ forms in a monoclinic crystal structure with the space group $P2_1/m$ (No. 11). The lattice parameters obtained from pXRD refinement using the LeBail method are $a = 8.7001(3)$ Å, $b = 4.3101(1)$ Å, $c = 13.187(1)$ Å, $\beta = 99.5(1)^\circ$. Energy-dispersive X-ray spectroscopy revealed the expected chemical composition of this compound. Systematic magnetic, thermodynamic, and electrical resistivity measurements in the ^3He option using the Physical Property Measurement System (Quantum Design) reveal a superconducting transition temperature $T_C = 2.5$ K, consistent with the previous report [1]. The measurements show that $\text{Y}_3\text{Pt}_4\text{Ge}_6$ is a type-II superconductor with lower and upper critical fields 240 Oe and 2.82 kOe, respectively. The observed specific-heat jump, $\Delta C_p/\gamma T_C = 1.55$, is consistent with that of a weak-coupling BCS superconductor with an isotropic superconducting gap. The obtained energy gap from the heat capacity data is 0.34 meV. The estimated coherence length $\xi(0)_{\text{GL}}$, penetration depth $\lambda(0)_{\text{GL}}$, and Ginzburg–Landau (GL) parameter $\kappa(0)$ are 341 Å, 841 Å, and 2.46, respectively.

This work was supported by the PLATINUM Grant Programme of Gdańsk University of Technology, grant No. DEC-2/2/2023/IDUB/I.1B/Pt.

[1] N. Kase, T. Muranaka, J. Akimitsu, *J. Phys. Soc. Jpn.* 77(5) (2008) 054714.

LOCAL Fe ENVIRONMENT AND MAGNETIC INTERACTIONS IN HIGH-ENTROPY DOUBLE PEROVSKITES $\text{Sr}_2(\text{Fe,Co,Mn,Ti})\text{MoO}_6$

A. Nowak¹, M. Nowakowska², K. Berent³, J. Dąbrowa², M. Reissner⁴, and J. Cieślak¹

¹ Faculty of Physics and Applied Computer Science, AGH University, Krakow, Poland

² Faculty of Materials Science and Ceramics, AGH University, Krakow, Poland

³ Academic Centre for Materials and Nanotechnology, AGH University, Krakow, Poland

⁴ Institute of Solid State Physics, TU Wien, Austria

annaslawek@agh.edu.pl

The application of the high-entropy concept has provided a new approach to the design of functional materials characterized by complex chemical compositions and interesting physical properties. One of the main difficulties in studying such systems is their high chemical complexity, which hinders the identification of local atomic environments and the determination of their influence on macroscopic properties. In particular, the role of local transition metal environments and their influence on exchange interactions remain largely unexplored. Furthermore, in multicomponent oxide systems, conventional structural methods are often insufficient, requiring the use of techniques sensitive to the local environment.

The local environments of Fe ions and the magnetic properties of a series of multicomponent double perovskites $\text{Sr}_2(\text{Fe,Co,Mn,Ti})\text{MoO}_6$ were investigated using Mössbauer spectroscopy at room temperature and VSM measurements of the magnetization profiles $M(T)$ and $M(H)$. The Mössbauer spectra indicate the presence of Fe^{3+} in a high-spin state. For samples including Fe, Co or Mn, it was necessary to use two quadrupole splitting distributions, which indicates the presence of two types of local Fe environments with similar geometry but different electron densities. The smaller contribution of the component with a lower isomer shift is associated with the presence of Mo in the immediate vicinity of Fe. In the sample containing Ti, a single doublet is observed, indicating a more homogeneous Fe environment. Magnetization measurements revealed the absence of long-range magnetic order and the dominance of short-range interactions. The $M(H)$ curves do not show saturation in high fields, and a trace of hysteresis is observed only for the Fe–Mo sample. The results indicate that the magnetic properties of the studied systems are mainly determined by the competition of exchange interactions, rather than by changes in the local Fe environments.

Research supported by the Polish National Science Centre (NCN) under project No. UMO-2022/45/B/ST8/.

[1] A. Sarkar, R. Kruk, H. Hahn, *Dalton Trans.* 50 (2021) 1973-1982.

[2] C.M. Rost, E. Sachet, T. Borman, A. Moballeght, E. Dickey, D. Hau, J.L. Jones, S. Curtarolo, J.P. Maria, *Nat. Commun.* 6(1) (2015) 8485.

SERIES OF MODULATED $(\text{Ca},R)_{0.83}\text{CuO}_2$ COMPOSITES

L. Akselrud, O. Zaremba, V. Lesnianska, and R. Gladyshevskii
*Department of Inorganic Chemistry, Ivan Franko National University of Lviv,
 Kyryla i Mefodiya St. 6, 79005 Lviv, Ukraine
 lev.akselrud@lnu.edu.ua*

The investigation on $A-R-Cu-O$ systems, which rapidly developed following the discovery of high-temperature superconductivity in the 1980s, remains highly relevant today due to the ongoing search for new functional materials. Despite decades of study, many aspects of their phase diagrams, crystal chemistry, and structure-property relationships are still not fully revealed, leaving space for new insights. Continued investigation of $A-R-Cu-O$ compounds contributes not only to fundamental solid-state chemistry but also to the development of advanced materials for energy, electronics, and quantum technologies. This work is mainly devoted to a series of modulated composites $(\text{Ca},R)_{0.83}\text{CuO}_2$.

Polycrystalline samples of $\text{Ca}_{0.53}R_{0.3}\text{CuO}_2$, where R is a heavy lanthanide, were prepared *via* a solid-state reaction method using high-purity carbonates and oxides. The reagents were thoroughly ground and heated in a corundum crucible at 1000 °C for 24 h in air. The products were reground, pressed into pellets, and subjected to sintering under the same conditions. The grinding-pressing-annealing cycle was repeated, followed by an additional one-week annealing step to improve homogeneity. X-ray diffraction data were collected on a Rigaku SmartLab diffractometer (Cu $K\alpha$ radiation), and the crystal structure was refined using the WinCSD software package.

The crystal structure of the quasi-one-dimensional cuprates $(\text{Ca},R)_{0.83}\text{CuO}_2$ was analyzed within the superspace formalism. It can be described as comprising two interpenetrating subsystems: CuO_2 chains and an (Ca,R) atomic sublattice. The copper atoms exhibit square-planar coordination by oxygen atoms, whereas the (Ca,R) atoms are located at the centers of distorted O_6 octahedra. Due to positional modulation of the (Ca,R) and O atoms, the local oxygen coordination around the (Ca,R) sites effectively becomes tetrahedral. The Cu–O bond lengths range from 1.8 to 2.2 Å. Structure parameters were refined by the Rietveld method within the superspace group $P2_1/m11(0pq)0s$. The resulting lattice parameters are summarized in the table.

Refined lattice parameters of the modulated composites $(\text{Ca},R)_{0.83}\text{CuO}_2$

R	a , Å	b , Å	c , Å	α , °	Components of the modulation vector p, q
Tb	6.25355(4)	5.47803(4)	2.83097(4)	104.82(8)	0.98411(3), 0.82041(2)
Dy	6.2304(3)	5.4761(2)	2.8331(1)	104.82(8)	0.98060(3), 0.82271(3)
Ho	6.21370(3)	5.47040(4)	2.83366(3)	104.81(7)	0.97518(3), 0.82416(1)
Er	6.19926(4)	5.46533(4)	2.83425(3)	104.81(8)	0.97058(3), 0.82625(1)
Tm	6.18673(4)	5.46219(4)	2.83363(3)	104.86(8)	0.96581(3), 0.82778(1)
Yb	6.17175(4)	5.45850(5)	2.83441(4)	104.88(9)	0.96067(3), 0.82909(1)
Lu	6.16605(5)	5.45453(6)	2.83758(4)	104.87(9)	0.95483(3), 0.83242(1)

EXPANDING SODIUM PHOSPHIDOMETALATE CHEMISTRY: CRYSTAL CHEMISTRY OF Na₈TiP₄ and Na₁₀Ti₂P₆

Samuel Merk^{1,2}, Hanna Antoniuk¹, Viktor Hlukhyy¹, and Thomas F. Fässler¹

¹ *Chair of Inorganic Chemistry with Focus on Novel Materials, Technical University of Munich, Lichtenbergstraße 4, 85748 Garching, Germany*

² *TUMInt Energy Research GmbH, Lichtenbergstraße 4, 85748 Garching, Germany*
hanna.antoniuk@tum.de

Phosphide-based ionic conductors have recently attracted considerable attention as promising solid electrolyte materials for all-solid-state batteries (ASSBs). In particular, lithium phosphidotrirelates, phosphidotetrelates, and transition-metal phosphides have revealed remarkable ionic conductivities, highlighting the importance of understanding structure-property relationships in phosphide frameworks [1]. Due to the high natural abundance of sodium, Na-based ASSBs are currently a major focus of research. Therefore, we investigate if related compounds exist and report here the synthesis and structural characterization of the new sodium transition-metal phosphides Na₈TiP₄ and Na₁₀Ti₂P₆, which extend sodium phosphidometalate chemistry into the group 4 domain.

Na₈TiP₄ was synthesized by mechanochemical treatment of the elements followed by annealing at 873 K, while Na₁₀Ti₂P₆ was obtained analogously with subsequent annealing at 973 K. Single crystals suitable for X-ray diffraction were also prepared by direct high-temperature reactions from stoichiometric elemental mixtures. Na₈TiP₄ crystallizes in the cubic space group $Fd\bar{3}m$ (No. 227) and is isotypic to Na₈GeP₄ and LT-Na₈SnP₄, adopting the Na₈SnSb₄ structure type [2-3] and comprises isolated [TiP₄]⁸⁻ tetrahedra. Na₁₀Ti₂P₆, by contrast, crystallizes in the monoclinic space group $P2_1/n$ (No. 14), is isostructural to $A_{10}Tt_2Pn_6$ ($A = \text{Li, Na, K}$; $Tt = \text{Si, Ge, Sn}$; $Pn = \text{P, As}$) phases, and contains edge-sharing [Ti₂P₆]¹⁰⁻ double tetrahedra.

Both structures can be derived from close-packed anion arrangements, but they differ significantly in their tetrahedral and octahedral void occupation and thus in their sodium substructures. Full occupation of all crystallographic Na sites was confirmed by single-crystal and powder refinements and supported by DFT calculations. Raman spectra further distinguish both compounds by characteristic Ti–P stretching and framework deformation modes. The discovery of Na₈TiP₄ and Na₁₀Ti₂P₆ broadens the structural chemistry of sodium phosphidometalates and establishes new motifs for assessing sodium-ion transport in phosphide frameworks.

- [1] a) B. Eisenmann, M. Somer, *Z. Naturforsch. B* 40 (1985) 886-890; b) T.M.F. Restle, S. Strangmüller, V. Baran, A. Senyshyn, H. Kirchhain, W. Klein, S. Merk, D. Müller, T. Kutsch, L. van Wüllen, T.F. Fässler, *Adv. Funct. Mater.* 32 (2022) 2112377; c) S. Merk, S. Kollmannsberger, S. Zeitz, V. Baran, A. Senyshyn, T.F. Fässler, *Inorg. Chem.* 64 (2025) 16902-16911; d) D. Müller, T. Kutsch, S. Zeitz, V. Hlukhyy, G. Raudaschl-Sieber, W. Klein, T.F. Fässler, *Chem. Eur. J.* 32 (2026) e03124.
- [2] M. Botta, S. Zeitz, T.F. Fässler, *Z. Anorg. Allg. Chem.* 649 (2023) e202300166.
- [3] M. Botta, S. Merk, R.J. Spranger, A. Senyshyn, V. Baran, V. Dyadkin, L. van Wüllen, T.F. Fässler, *Angew. Chem. Int. Ed.* 64 (2025) e202419381.
- [4] B. Eisenmann, J. Klein, *Z. Naturforsch. B* 43 (1988) 69.

{Dy,Er}-Zn-Ga SYSTEMS CONTAINING UP TO 33 AT.% RE

I. Arseniuk, Yu. Drach, and B. Stelmakhovych

Department of Analytical Chemistry, Ivan Franko National University of Lviv,

Kyryla i Mefodiya St. 6, 79005 Lviv, Ukraine

ivankaarseniuk21@gmail.com

The ternary {Dy,Er}-Zn-Ga systems have previously been investigated; however, most studies focused on the existence of ternary compounds belonging to particular structure types [1-3]. In the present work, phase diagrams of the {Dy,Er}-Zn-Ga systems in the zinc-rich region were constructed using X-ray diffraction.

The samples were synthesized by sintering powders of rare-earth elements (RE), zinc, and a previously synthesized REGa₃ alloy. Homogenization annealing was performed in quartz ampoules that had been evacuated and filled with argon, at a temperature of 400 °C for at least 600 h; the samples were quenched in cold water without breaking the ampoules. Phase analysis of the synthesized samples was performed using powder diffractograms obtained using DRON-2.0 (Fe K α radiation), and DRON-3M (Cu K α radiation) diffractometers. Arrays of experimental intensities, obtained using a STOE Stadi P diffractometer with a modified Guinier alignment scheme, Cu K α radiation and a concave Ge(111) monochromator, were used to refine the crystal structure of polycrystalline samples. All calculations were performed using the WinCSD structural analysis software package [4].

Phase analysis of ternary samples revealed that gallium is only slightly soluble in the binary phases REZn₁₂ (ThMn₁₂-type structure) and RE₂Zn₁₇ (Th₂Zn₁₇-type structure), which dissolve up to 10 at.% of gallium, and a negligible solubility of zinc (up to 5 at.%) in the REGa₃ (AuCu₃-type structure) compounds. Based on the results of our studies, we have confirmed the formation of ternary compounds with the structure types BaHg₁₁ (space group *Pm-3m*) and La₃Al₁₁ (space group *Immm*), which exhibit significant regions of homogeneity. The composition of the latter compound is described by the formula Er₃Zn_{4.0-4.7}Ga_{7.0-6.3} ($a = 0.4209(4)$ - $0.4184(2)$, $b = 1.229(2)$ - $1.2305(4)$, $c = 0.9659(8)$ - $0.9860(4)$ nm).

- [1] Yu. Verbovytsky, N. Leal, A.P. Gonçalves, *Intermetallics*. 19(7) (2011) 1080-1084.
- [2] A. Iandelli, *J. Less-Common Met.* 169 (1991) 187-196.
- [3] I. Haiduk, M. Chykhriy, B. Stelmakhovych, *Visn. Lviv. Univ., Ser. Khim.* 52 (2011) 100-106.
- [4] L. Akselrud, Yu. Grin, *J Appl. Crystallogr.* 147 (2014) 803-805.

NEW QUATERNARY COMPOUNDS
 $R_2\text{Ni}(\text{Ni}_{1-x}\text{Ge}_x)\text{Al}_4\text{Ge}_6$ ($R = \text{Ce, La, Nd, Sm, Gd, Tb, Dy}$)

R. Datsko, N. Muts, Ya. Tokaychuk, and R. Gladyshevskii
Department of Inorganic Chemistry, Ivan Franko National University of Lviv,
Kyryla i Mefodiya St. 6, 79005 Lviv, Ukraine
roman.datsko@lnu.edu.ua

During the investigations of the phase equilibria in the Pr–Ni–Al–Ge system at 600 °C, the formation of a quaternary compound, $\text{Pr}_2\text{NiAl}_4(\text{Ni}_{0.062}\text{Al}_{0.938})(\text{Al}_{0.194}\text{Ge}_{0.806})_4\text{Ge}_2$ (Pearson symbol $tP28$, space group $P4/nmm$, Wyckoff sequence j^2fc^3a , $a = 5.9039(1)$, $c = 15.0901(3)$ Å) was established [1]. The crystal structure of this compound is closely related to the structures of $\text{Sm}_2\text{Ni}(\text{Ni}_{0.27}\text{Si}_{0.73})\text{Al}_4\text{Si}_6$ [2] and $\text{Ce}_2\text{CoGa}_9\text{Ge}_2$ [3].

In order to search for isostructural compounds with other rare-earth metals, a series of alloys of the nominal compositions $R_{12}\text{Ni}_{11}\text{Al}_{40}\text{Ge}_{37}$ ($R = \text{La, Ce, Nd, Sm, Eu, Dy}$) and $R_{15}\text{Ni}_9\text{Al}_{41}\text{Ge}_{35}$ ($R = \text{La, Nd, Sm, Gd, Tb, Dy, Ho, Er, Tm}$) were synthesized from pure bulk metals by arc melting under argon atmosphere. The samples were annealed at 600 °C under vacuum for 87 days and subsequently quenched in cold water.

The crystal structures were determined by means of X-ray powder diffraction using data collected on diffractometers STOE Stadi P (Cu $K\alpha_1$ -radiation), PROTO AXRD Benchtop (Cu $K\alpha$ -radiation) and DRON-2.0M (Fe $K\alpha$ -radiation). The profile and structural parameters were refined by the Rietveld method using the FullProf Suite program package. Energy-dispersive X-ray spectroscopy was carried out on a scanning electron microscope TESCAN Vega3 LMU equipped with an energy-dispersive X-ray analyzer Oxford Instruments Aztec ONE with an X-Max^N20 detector.

The existence of seven new quaternary compounds was established in the R –Ni–Al–Ge systems with $R = \text{Ce, La, Nd, Sm, Gd, Tb, Dy}$. The coordinates of the atoms in the structure of $\text{Sm}_2\text{Ni}(\text{Ni}_{0.27}\text{Si}_{0.73})\text{Al}_4\text{Si}_6$ were taken as structural model for the refinement of the crystal structures of the new intermetallics. Refined unit-cell parameters for the $R_2\text{Ni}(\text{Ni}_{1-x}\text{Ge}_x)\text{Al}_4\text{Ge}_6$ compounds: $a = 5.9575(2)$, $c = 15.1889(5)$ Å for the compound with La; $a = 5.9206(2)$, $c = 15.0909(6)$ Å for the compound with Ce; $a = 5.888(1)$, $c = 15.094(3)$ Å for the compound with Nd; $a = 5.8394(1)$, $c = 15.0137(3)$ Å for the compound with Sm; $a = 5.788(1)$, $c = 14.897(4)$ Å, $V = 499.05(2)$ Å³ for the compound with Gd; $a = 5.7835(7)$, $c = 14.899(3)$ Å, for the compound with Tb; $a = 5.7402(2)$, $c = 15.0052(7)$ Å for the compound with Dy.

The crystal structure of the synthesized phases can be described as an arrangement of two layers. One layer consists of cubes formed by Al atoms, half of which are empty, the others being centred by nickel atoms. The second layer is built from the coordination polyhedra centred by a statistical mixture of Al and Ge atoms – mono-capped square antiprisms and empty square pyramids formed by Ge atoms.

- [1] V. Humenchuk, R. Datsko, N. Muts, Ya. Tokaychuk, R. Gladyshevskii, *Coll. Abstr. XV Int. Conf. Cryst. Chem. Intermet. Compd.*, Lviv, 2023, p. 88.
- [2] X.Z. Chen, S. Sportouch, B. Sieve, P.W. Brazis, C.R. Kannewurf, J.A. Cowen, R. Patschke, M.G. Kanatzidis, *Chem. Mater.* 10 (1998) 3202-3211.
- [3] M.A. Zhuravleva, M.G. Kanatzidis, *Inorg. Chem.* 47 (2008) 9471-9477.

NOVEL QUATERNARY $REPt_2Ga_3In$ ($RE = La-Nd$ AND Sm) COMPOUNDS

M. Horiacha^{1,2}, O. Pavlosiuk³, G. Nychporuk¹, V. Zaremba¹, and S. Wurmehl²

¹Department of Inorganic Chemistry, Ivan Franko National University of Lviv,
Kyryla i Mefodiya St. 6, 79005 Lviv, Ukraine

²Leibniz Institute for Solid State and Materials Research (IFW) Dresden,
Helmholtz Str. 20, 01069 Dresden, Germany

³Institute of Low Temperature and Structure Research, Polish Academy of Sciences,
50-422 Wrocław, Poland
myroslava.horyacha@lnu.edu.ua

The quaternary $REPt_2Ga_3In$ ($RE = Y, Gd-Yb$) compounds crystallize with an ordered orthorhombic $NdRh_2Sn_4$ -type structure [1]. Temperature-dependent magnetic susceptibility data of $GdPt_2Ga_3In$ show Curie-Weiss paramagnetism. We have synthesized and studied new quaternary compounds of this type with La, Ce, Pr, Nd, and Sm.

$REPt_2Ga_3In$ ($RE = La, Ce, Pr, Nd, \text{ and } Sm$) were synthesized by arc-melting high-purity starting materials under an argon atmosphere. Single crystals were grown by a special heat treatment of the arc-melted sample with an 1:2:3:1 composition in an alumina crucible in an evacuated quartz tube. X-ray powder diffraction data for the compounds revealed isotypism with the orthorhombic $NdRh_2Sn_4$ -type, space group $Pnma$, Pearson symbol $oP28$.

The crystal structure was refined from X-ray powder (STOE Stadi, Co $K\alpha$ radiation) and single-crystal diffraction data (SuperNova Rigaku Oxford Diffraction, Mo $K\alpha$ radiation (TU Dresden)) using the Jana2006 program [2]. Polycrystalline samples and single crystals were also analysed semi-quantitatively with a Zeiss-EVO MA 15 scanning electron microscope.

The single-crystal study revealed a small degree of Ga/In mixing resulting in the following compositions: $LaPt_2Ga_{2.90(1)}In_{1.10(1)}$, $CePt_2Ga_{3.07(1)}In_{0.93(1)}$, $PrPt_2Ga_{3.07(1)}In_{0.93(1)}$, $NdPt_2Ga_{3.2(1)}In_{0.8(1)}$, and $SmPt_2Ga_{3.3(1)}In_{0.7(1)}$. The lattice parameters and R -factors are listed in the table. All positions are fully occupied. The unit-cell parameters for the series decrease with increasing atomic number of the rare earth.

Refined lattice parameters and R -factors for the $REPt_2Ga_3In$ series

RE	a , nm	b , nm	c , nm	R_1	wR_2	F^2	variables
La	1.78650(5)	0.43867(1)	0.68003(2)	0.0193	0.0433	826	47
Ce	1.77013(7)	0.43541(2)	0.67589(3)	0.0277	0.0364	1078	47
Pr	1.77100(4)	0.43415(1)	0.67568(2)	0.0240	0.0239	1076	46
Nd	1.76086(6)	0.43240(1)	0.67268(2)	0.0228	0.0487	1047	45
Sm	1.75383(3)	0.43036(1)	0.67104(1)	0.0242	0.0489	1523	45

The temperature dependence of the magnetic susceptibility for the Ce, Pr, and Nd compounds shows Curie-Weiss paramagnetism. In contrast, $LaPt_2Ga_3In$ exhibits diamagnetism, while $SmPt_2Ga_3In$ orders antiferromagnetically below a Néel temperature (T_N) of 12.7 K and shows a second magnetic transition at 4.5 K.

[1] M. Horiacha, V. Zaremba, F. Stegemann, R. Pöttgen, *Monatsh. Chem.* 150 (2019) 1409-1415.

[2] V. Petříček, M. Dušek, L. Palatinus, *Z. Kristallogr.* 229 (2014) 345-352.

SPARK PLASMA SINTERING OF B₄C–CrB₂ CERAMIC COMPOSITES

A. Ivanushko and R. Gladyshevskii

*Department of Inorganic Chemistry, Ivan Franko National University of Lviv,
Kyryla i Mefodiya St. 6, 79005 Lviv, Ukraine
andriana.ivanushko@lnu.edu.ua*

B₄C–CrB₂ composites were prepared by spark plasma sintering from a powder mixture containing 72 wt.% B₄C and 28 wt.% CrB₂ [1]. The powders were homogenized in a planetary ball mill and sintered under a pressure of 70 MPa at 1800 °C and 1900 °C. The phase composition and crystal structure were investigated by X-ray powder diffraction conducting Rietveld refinements, and the microstructure was studied by scanning electron microscopy. The experimental conditions and crystallographic data for the components of the ceramic materials B₄C–CrB₂ are presented in the Table.

At 1800 °C, a two-phase composite with a relative density of 97.6 % and a hardness of 34.1 GPa was obtained. Under these conditions, CrB₂ acts as a strengthening additive, contributing to improve the mechanical properties compared to pure B₄C. Sintering at 1900 °C led to changes in the phase ratio of the composite due to the partial transformation of CrB₂ into a liquid phase, accompanied by the formation of pores in the ceramic, as confirmed by scanning electron microscopy. These effects led to a decrease in the relative density, however, the hardness increased to 37.4 GPa.

Experimental conditions and results of the refinements of the crystal structures
of the components of the B₄C–CrB₂ ceramics

B ₄ C–CrB ₂ ceramic synthesized at 1800 °C		
Composition	B _{13.12(2)} C _{1.77(1)}	CrB ₂
Structure type	B ₁₃ C ₂	AlB ₂
Pearson symbol	<i>hR51</i>	<i>hP3</i>
Space group	<i>R-3m</i>	<i>P6/mmm</i>
Cell parameters, Å	<i>a</i> = 5.59897(8), <i>c</i> = 12.0750(2)	<i>a</i> = 2.97477(3), <i>c</i> = 3.07389(4)
Cell volume <i>V</i> , Å ³	327.819(9)	23.557(1)
Formula units per cell <i>Z</i>	3	1
Density <i>D_x</i> , g·cm ⁻³	2.477	5.189
Mass fraction, %	82.2(10)	17.8(2)
<i>R_B</i> , %	6.35	2.92
Profile reliability factors	<i>R_p</i> = 4.58 %, <i>R_{wp}</i> = 6.05 %	
B ₄ C–CrB ₂ ceramic synthesized at 1900 °C		
Composition	B _{13.120(6)} C _{1.760(4)}	CrB ₂
Structure type	B ₁₃ C ₂	AlB ₂
Pearson symbol	<i>hR51</i>	<i>hP3</i>
Space group	<i>R-3m</i>	<i>P6/mmm</i>
Cell parameters, Å	<i>a</i> = 5.60019(5), <i>c</i> = 12.08126(15)	<i>a</i> = 2.98519(18), <i>c</i> = 3.0923(2)
Cell volume <i>V</i> , Å ³	328.132(6)	23.864(3)
Formula units per cell <i>Z</i>	3	1
Density <i>D_x</i> , g·cm ⁻³	2.474	5.123
Mass fraction, %	98.2(5)	1.8(1)
<i>R_B</i> , %	4.58	10.6
Profile reliability factors	<i>R_p</i> = 3.84 %, <i>R_{wp}</i> = 5.02 %	

[1] A. Ivanushko, R. Gladyshevskii, *Chem. Met. Alloys* 18(3/4) (2025) 44-48.

INVESTIGATION OF QUATERNARY ALLOYS FOR SPIN-GAPLESS PROPERTIES

K.K. Johari¹, M. Modak², D. Tang¹, A. Patra², C. Barreteau¹, C. Mazumdar², and E. Alleno¹

¹ *Univ Paris-Est Creteil, ICMPE-CNRS, UMR 7182, rue H. Dunant 2, 94320 Thiais, France*

² *Condensed Matter Physics Division, Saha Institute of Nuclear Physics, 1/AF Bidhannagar, Kolkata 700064, India*

kishorjohari@gmail.com, eric.alleno@cnrs.fr

In recent years, spin-gapless semiconductors (SGSCs) have attracted attention due to their unique electronic structure, allowing high spin polarizability and electronic mobility, which is of high interest for next-generation spintronic applications. Their band structure bridges the properties of semiconductors and semimetals; one spin-polarized sub-band with an open band gap (semiconductor), while another spin-polarized sub-band with a zero-band gap (semimetal). Theoretically, several Heusler alloys have been predicted to be SGSC, but experimentally very few could be prepared [1,2]. Therefore, we are carrying out a thorough study starting from theoretical prediction to experimental confirmation.

We implemented high-throughput first-principles calculations of the electronic structure to screen ~12000 compositions in the family of Heusler alloys including both ternary (211 stoichiometry) and quaternary (1111 stoichiometry) compositions containing not only 3d-metals but also 4d- and 5d-metals. Among them, around fifteen quaternary compositions such as TiVAlSn, FeVZrGa and so on, were selected for experiments. These samples were synthesized *via* arc melting and were initially characterized *via* X-ray diffraction (XRD) and electron probe microanalysis (EPMA). Following preliminary results, we discarded a few samples including PtFeHfSn, TiZrFeCo, TiSiCrAl, because of their multiphase character, poor crystallization, or present of ternary half-Heusler as major phase, *etc.* The rest of them were found to be nearly single-phase and were therefore annealed. The major phase of these samples was identified as a C14 Laves phase (MgZn₂ type). By correlating the EPMA and synchrotron XRD results, the composition was revised from 1111 stoichiometry to 3243, such as Fe₃Mn₂Nb₄Si₃ and Fe₃Mn₂Ta₄Si₃.

In future work, the electronic structure of these new compositions will be calculated by implementing first-principles techniques and they will then be measured experimentally.

This work was carried out under the project “Novel spin-gapless semiconducting Heusler alloys for spintronics” funded by Centre Franco-Indien pour la Promotion de la Recherche Avancée (CEFIPRA).

- [1] S. Ouardi, G.H. Fecher, C. Felser, J. Kübler, *Phys. Rev. Lett.* 110 (2013) 100401.
- [2] L. Bainsla, A. Mallick, M.M. Raja, A. Coelho, A. Nigam, D. Johnson, A. Alam, K. Suresh, *Phys. Rev. B* 92 (2015) 045201.

NEW TERNARY PHOSPHIDES IN THE RE–Pd–P SYSTEMS

O. Karychort¹, O. Zhak¹, and Yu. Prots²

¹ Department of Analytical Chemistry, Ivan Franko National University of Lviv,
Kyryla i Mefodiya St. 6, 79005 Lviv, Ukraine

² MPI Chemical Physics of Solids, Nöthnitzer Str. 40, 01187 Dresden, Germany
Oksana.Karychort@lnu.edu.ua

Ternary rare-earth palladium phosphides are of particular interest due to their thermal stability, chemical resistance, and potential catalytic activity. Ternary RE–M–P systems (RE = rare-earth element, M = transition metal) exhibit a wide variety of ternary compounds and structure types [1]. Although many of these systems adopt well-known structure types such as CeAl₂Ga₂, TiNiSi, Hf₂Co₄P₃, and Zr₂Fe₁₂P₇, they remain insufficiently explored and offer significant potential for the discovery of new compounds and structure types.

The samples for investigation were prepared by solid-state reaction of the pure elements, followed by annealing at 600–1000 °C depending on the composition. Phase identification and crystal structure determination were performed using X-ray powder and/or single-crystal diffraction.

Nine new ternary phosphides were synthesized; their crystal structures were refined and peculiarities discussed.

Crystallographic characteristics of newly synthesized ternary RE–Pd–P phosphides

Compound	Space group	Structure type	Lattice parameters, nm		
			<i>a</i>	<i>b</i>	<i>c</i>
ScPdP	<i>Pmna</i>	TiNiSi	0.65540(8)	0.38175(5)	0.75208(9)
Y ₅ Pd ₁₉ P ₁₂	<i>C2/m</i>	Th ₅ Fe ₁₉ P ₁₂	3.2416(3)	0.39311(3) $\beta = 98.205^\circ$	0.97266(9)
Eu _{2.7} Pd ₂₀ P ₆	<i>Fm-3m</i>	Cr ₂₃ C ₆	1.20714(4)	–	–
Dy ₃ Pd ₂₀ P ₆	<i>Fm-3m</i>	Cr ₂₃ C ₆	1.21213(1)	–	–
Gd ₂ Pd ₁₂ P ₇	<i>P6₃/m</i>	Ho ₂ Rh ₁₂ As ₇	0.6991(1)	–	0.39780(1)
Tb ₂ Pd ₁₂ P ₇	<i>P6₃/m</i>	Ho ₂ Rh ₁₂ As ₇	0.97114(4)	–	0.39598(2)
Tb ₂ Pd ₄ P ₃	<i>P-62m</i>	Hf ₂ Co ₄ P ₃	1.31123(5)	–	0.39715(2)
Dy _{2-x} Pd _{4+x} P ₃ (<i>x</i> = 0.22)	<i>P-62m</i>	Hf ₂ Co ₄ P ₃	1.31333(5)	–	0.40032(2)
Ho ₂ Pd ₄ P ₃	<i>P-62m</i>	Hf ₂ Co ₄ P ₃	1.31727(4)	–	0.40150(2)

The obtained results reveal relationships between composition, rare-earth element, and adopted structure type, and confirm that RE–Pd–P systems remain a rich field for discovering new compounds and structure–composition relationships.

Work supported by a grant from the Ministry of Education and Science of Ukraine (No. 0126U002163). O.K. and O.Z. acknowledge financial support from the Simons Foundation (SFI-PD-Ukraine-00014574). O.K. thanks MPI CPfS for access to equipment.

[1] P. Villars, K. Cenzual (Eds.), *Pearson's Crystal Data – Crystal Structure Database for Inorganic Compounds*, Release 2021/22, ASM International, Materials Park, Ohio, USA.

CRYSTAL STRUCTURE OF THE TERNARY COMPOUND $\text{Ho}_2\text{Al}_{1.5}\text{Si}_{1.5}$

N. Klymentiy, S. Pukas, and R. Gladyshevskii

Department of Inorganic Chemistry, Ivan Franko National University of Lviv,

Kyryla i Mefodiya St. 6, 79005 Lviv, Ukraine

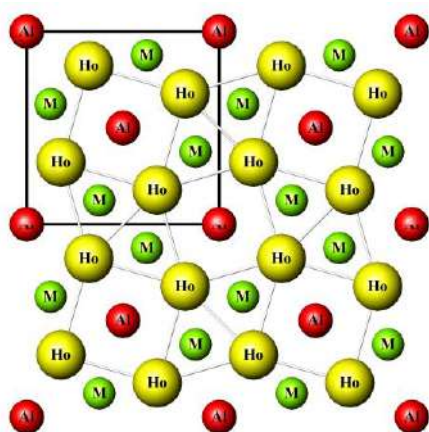
nastasia.klymentiy@lnu.edu.ua

The existence of the new ternary compound $\text{Ho}_2\text{Al}_{1.5}\text{Si}_{1.5}$ was observed at 600 °C by X-ray powder diffraction and energy-dispersive X-ray spectroscopy. It was established that the crystal structure of this holmium aluminosilicide belongs to the tetragonal type Mo_2FeB_2 [1]. The cell parameters determined by us fit well into the general behaviour of the cell parameters of isotypic compounds $R_2\text{Al}_{1.5}\text{Si}_{1.5}$, where $R = \text{Sc}, \text{Y}, \text{Dy}, \text{Ho}, \text{Er}, \text{and Yb}$ [2].

The refinement of the crystal structure of the new compound $\text{Ho}_2\text{Al}_{1.5}\text{Si}_{1.5}$ was carried out by the Rietveld method, based on the structure type model and taking into account literature data on isotypic compounds. The structure is characterized by a partially disordered arrangement of atoms; one of the three atom sites, namely the site in Wyckoff position 4g of space group $P4/mbm$, is occupied by a statistical mixture of Al and Si atoms (Table). The coordination environment of the Al atoms on the site occupied exclusively by Al atoms, is cuboctahedral (coordination number 12), while for the Al and Si atoms in the statistical mixture, a trigonal-prismatic environment with three additional atoms above the lateral faces of the prisms (coordination number 9) is observed.

Atom coordinates and isotropic displacement parameters in the structure of the compound $\text{Ho}_2\text{Al}_{1.5}\text{Si}_{1.5}$: structure type Mo_2FeB_2 , Pearson symbol $tP10$, space group $P4/mbm$, $a = 6.8554(3)$, $c = 4.2680(2)$ Å, $M = 0.25\text{Al} + 0.75\text{Si}$, $Z = 2$, $R_B = 0.0541$

Site	Wyckoff position	Atom coordinates			$B_{\text{iso}}, \text{Å}^2$
		x	y	z	
Ho	4h	0.1768(2)	0.6768(2)	½	1.19(4)
M	4g	0.6227(5)	0.1227(5)	0	1.40(1)
Al	2a	0	0	0	1.72(2)



Projection of the structure of the compound $\text{Ho}_2\text{Al}_{1.5}\text{Si}_{1.5}$ along the crystallographic direction [001]; the stacking of square and trigonal prisms is highlighted

The structure of the compound $\text{Ho}_2\text{Al}_{1.5}\text{Si}_{1.5}$ can be considered as a stacking of columns, running along the crystallographic direction [001], of square prisms of composition AlHo_8 , connected to each other by common square faces, and trigonal prisms of composition MHo_6 , connected to each other by triangular faces. Each square prism is in addition connected to four others by common edges, and each trigonal prism is connected to another trigonal prism and two square prisms by common rectangular prism faces.

- [1] W. Rieger, H. Nowotny, F. Benesovsky, *Monatsh. Chem.* 95 (1964) 1502-1503.
- [2] P. Villars, K. Cenzual (Eds.), *Pearson's Crystal Data – Crystal Structure Database for Inorganic Compounds*, Release 2023/24, ASM International, Materials Park, Ohio, USA.

CRYSTAL STRUCTURE OF THE TERNARY COMPOUND Sm_5AlSn_2

Yu. Kozak, N. Semuso, Ya. Tokaychuk, and R. Gladyshevskii

Department of Inorganic Chemistry, Ivan Franko National University of Lviv,

Kyryla i Mefodiya St. 6, 79005 Lviv, Ukraine

yurii.kozak.AKhMKh@lnu.edu.ua

The new ternary compound Sm_5AlSn_2 was found during a systematic investigation of the phase equilibria in the system $\text{Sm}-\text{Al}-\text{Sn}$ at 600 °C. Its crystal structure was determined by means of X-ray powder diffraction. An alloy of nominal composition $\text{Sm}_{62.5}\text{Al}_{12.5}\text{Sn}_{25}$ was synthesized from pure metals ($\text{Sm} \geq 99.9$ mass%; $\text{Al} \geq 99.99$ mass%; $\text{Sn} \geq 99.99$ mass%) by arc melting under argon, and annealed under vacuum at 600 °C for 1 month. An X-ray powder diffraction pattern was collected at room temperature on a powder diffractometer PROTO AXRD Benchtop (Cu $K\alpha$ -radiation). The profile and structural parameters were refined by the Rietveld method using the FullProf Suite program package. The composition of the ternary phase ($\text{Sm}_{5.00(3)}\text{Al}_{1.01(4)}\text{Sn}_{1.99(4)}$) was additionally determined by energy-dispersive X-ray spectroscopy, performed on a scanning electron microscope TESCAN VEGA3 LMU, equipped with an energy-dispersive X-ray analyzer Oxford Instruments Aztec ONE with a detector X-Max^N20. Phase analysis of the sample revealed the presence of a single phase – the new ternary compound Sm_5AlSn_2 .

The crystal structure of the ternary compound with refined composition $\text{Sm}_5\text{Al}_{1.00(3)}\text{Sn}_{2.00(3)}$ belongs to the structure type W_5Si_3 , Pearson symbol $tI32$, space group $I4/mcm$, $a = 12.2621(10)$, $c = 6.0876(6)$ Å, $R_B = 0.0713$. It is characterized by two sites ($16k$ and $4b$) occupied by Sm atoms and two sites ($8h$ and $4a$) by p -element atoms. The Al and Sn atoms are distributed over the two sites, forming statistical mixtures with different compositions. A tendency toward ordering of the p -element atoms is observed: site $8h$ is predominantly occupied by Sn atoms ($M1 = 0.099(11)\text{Al} + 0.901(11)\text{Sn}$), whereas site $4a$ is mainly occupied by Al atoms ($M2 = 0.797(13)\text{Al} + 0.203(13)\text{Sn}$). Complete ordering of these atoms in the positions $16k$ and $4b$ would lead to the formation of the structure type Nb_5SiSn_2 ($tI32$, $I4/mcm$), which is a ternary variant of the structure type W_5Si_3 .

Atom coordinates, site occupancies, and isotropic displacement parameters for $\text{Sm}_5\text{Al}_{1.00(3)}\text{Sn}_{2.00(3)}$, Pearson symbol $tI32$, space group $I4/mcm$, $a = 12.2621(10)$, $c = 6.0876(6)$ Å

Site	Wyckoff position	Atom coordinates			B_{iso} , Å ²	Occupancy
		x	y	z		
Sm1	$16k$	0.0810(3)	0.2161(3)	0	0.51(3)	1
Sm2	$4b$	0	$\frac{1}{2}$	$\frac{1}{4}$	0.57(3)	1
Al1	$8h$	0.1623(3)	0.1623(3)	0	0.85(5)	0.099(11)
Sn1						0.901(11)
Al2	$4a$	0	0	$\frac{1}{4}$	0.97(7)	0.797(13)
Sn2						0.203(13)

The structure of the compound Sm_5AlSn_2 is built up from infinite columns of M -centred square antiprisms $\underline{M}_2\text{Sm}_8$ and Sm-centred tetrahedra $\underline{\text{Sm}}M1_4$ along the crystallographic direction $[001]$.

STRUCTURAL INVESTIGATIONS ON SOLID SOLUTIONS $(A^{1-x}A^2_x)\text{Hg}_2$

D. Kraut and C. Hoch

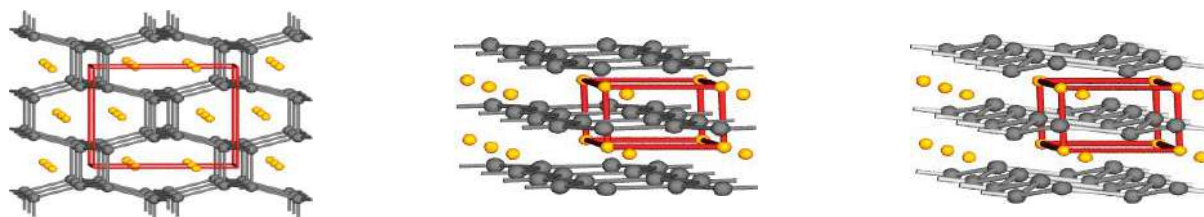
Department of Chemistry, LMU München,
Butenandtstr. 5-13 (D), 81377 München, Germany
Daniel.Kraut@cup.uni-muenchen.de

Amalgams of the composition $A\text{Hg}_2$ can adopt three different structure types: KHg_2 (*Imma*, for $A = \text{K, Rb, Cs, Sr, Ba}$), UHg_2 (*P6/mmm*, for $A = \text{Na, K, Ca, La, Ce, Sm, Eu, Dy-Er}$), or CeCd_2 (*P-3m1*, for $A = \text{Mg, Ca, La, Nd, Sm-Ho, Yb}$) [1-4]. Some compounds are dimorphic, with one structure type being a high-pressure variant, UHg_2 in the case of $A = \text{K}$, and CeCd_2 for $A = \text{Ca, La, Sm, Eu, Dy, Ho}$.

In order to test the stability ranges of these structure types as a function of atomic radii and valence electron concentration, series of solid solutions of the type $(A^{1-x}A^2_x)\text{Hg}_2$ were synthesized. Mixing the A position with atoms that share the same structure type in the binary amalgams resulted in no change in structure type. Mixing atoms that form binary amalgams of different structure types resulted in either KHg_2 , UHg_2 , or CeCd_2 -type structures, depending on the synthesis strategy. To test the influence of the valence electron concentration further, also substitution by In on the Hg positions in all three structure types was studied, as well as substitution by Zn to determine the effect the atomic radius has on the system. Thus, a multitude of new ternary amalgams in the $A\text{Hg}_2$ system were synthesized and structurally characterized.

Relative stabilities, phase formation, and phase transitions were studied by temperature-dependent X-ray powder diffraction (STOE Stadi P, Ag $K\alpha_1$ radiation) and thermoanalysis (TG-DTA/DSC Netzsch, STA 449 F5 Jupiter). Rietveld analysis was used to quantify the mixed occupations in the ternary amalgams.

Crystal structures of KHg_2 (left, projection along b), UHg_2 (middle, c pointing upwards), and CeCd_2 (right, c pointing upwards). A in orange, Hg/Cd in grey



This work was supported by DFG (Deutsche Forschungsgesellschaft) under research project number 545158079.

- [1] A. Iandelli, A. Palenzona, *J. Less Common Met.* 15 (1968) 273-284.
- [2] W. Harms, PhD thesis, University of Freiburg, 2008.
- [3] G. Bruzzone, *Rend. Lincei Sci. Fis. Nat.* 48 (1970) 235-241.
- [4] H.J. Deiseroth, A. Strunck, W. Bauhofer, *Z. Anorg. Allg. Chem.* 558 (1988) 128-136.

STRUCTURAL FEATURES AND PROPERTIES OF HOMO- AND HETERONUCLEAR SILVER(I) COORDINATION POLYMERS

O. Martsynko¹, Z. Vargová², O. Finik³, I. Seifullina¹, M. Rendošová², and G. Kuzderová²

¹ *Department of Inorganic Chemistry and Chemical Education, Odesa I.I. Mechnikov National University, Vsevoloda Zmiienka 2, 65082 Odesa, Ukraine*

² *Department of Inorganic Chemistry, P.J. Šafárik University, Moyzesova 11, 041 54 Košice, Slovak Republic*

³ *LLC "Bureau Veritas Commodities Ukraine", Udilny Lane 1, 65044 Odesa, Ukraine
martsinkoelena@gmail.com*

Solid silver(I) complexes with carboxylate and aminocarboxylate ligands are interesting in terms of structural diversity and application, as they exhibit antimicrobial, anti-inflammatory, and even antitumor properties. Since the structural organization of complexes is important in determining their physicochemical behaviour and biological activity, homo- and heterometallic coordination polymers of silver(I) are interesting for medical research.

In the polymeric structure $\{[\text{Ag}_2\text{Ge}(\text{HCit})_2(\text{H}_2\text{O})_2]\cdot 2\text{H}_2\text{O}\}_n$, an anion of citric acid HCit^{3-} acts as a tetradentate chelating and μ_4 -bridging ligand, coordinating to three Ag atoms and one Ge atom. The Ge atom is surrounded by six oxygen atoms from two ligands, forming a distorted octahedral polyhedron. Each Ag atom coordinates five oxygen atoms (four from different HCit^{3-} ligands and one from a water molecule) and adopts a distorted square-pyramidal geometry. Numerous hydrogen bonds link the individual units, forming a supramolecular 3D framework. This compound has antiviral activity against the human influenza viruses A/Hong Kong/1/68 (H3N2) and A/PR/8/34 (H1N1), as well as the avian influenza virus H5N3. This is promising for further investigation of this substance in animal models, with the aim of introducing it into medical practice.

Two silver(I) dipeptide complexes $[\text{Ag}(\text{GlyGly})]_n(\text{NO}_3)_n$ and $[\text{Ag}_2(\text{HGlyAsp})(\text{NO}_3)]_n$, were prepared and characterized by single-crystal diffraction. In the structure of $[\text{Ag}(\text{GlyGly})]_n(\text{NO}_3)_n$, the asymmetric unit consists of one molecule of HGlyGly , present as zwitterion, one silver(I) atom and one uncoordinated nitrate molecule. Silver(I) ions are arranged in a polymeric chain and connected by three HGlyGly molecules. The bond distance between two silver atoms Ag–Ag in the polymeric chain is 2.8930(8) Å. This bond distance is shorter than the van der Waals radii (3.44 Å), which indicates the presence of argentophilic interactions. Further, in the structure of the $[\text{Ag}_2(\text{HGlyAsp})(\text{NO}_3)]_n$ complex, the asymmetric unit consists of two silver(I) atoms, one HGlyAsp ligand, and one nitrate ligand, with the amino group in the aminoacidate ligand protonated. The central atom Ag1 exhibits a distorted tetrahedral geometry, while Ag2 has a trigonal geometry. The ligand acts as a multibridging ligand: the α -carboxylate group adopts a μ_2 - η^1 : η^1 coordination mode, and the β -carboxylate group adopts a μ_3 - η^1 : η^2 mode, resulting in the propagation of the structure in the *ac* plane. The Ag–O bond distances (where O is an oxygen atom from HGlyAsp^-) range from 2.181 to 2.459 Å. Within the two-dimensional network, argentophilic interactions are present, with Ag–Ag distances of 2.824 Å. In addition, the three-dimensional structure is supported by Ag–Ag interactions between individual networks, with an Ag–Ag distance of 3.196 Å. It has been shown that such types of complexes have great potential for the design of new antimicrobial, antibacterial, and anticancer agents.

This work was supported by the International Visegrad Fund (Grant No. 62510009) and Slovak grant agencies VEGA 1/0268/24, KEGA 007UPJŠ-4/2024.

CRYSTAL STRUCTURES OF THE QUATERNARY COMPOUNDS
La₂NiAl₄Ge_{4.245} and Pr₂NiAl₄Ge_{4.280}

N. Muts¹, R. Datsko¹, Ya. Tokaychuk¹, P. Solokha², S. De Negri², and R. Gladyshevskii¹

¹*Department of Inorganic Chemistry, Ivan Franko National University of Lviv,
Kyryla i Mefodiya St. 6, 79005 Lviv, Ukraine*

²*Department of Chemistry and Industrial Chemistry of University of Genoa,
via Dodecaneso 31, 16146 Genova, Italy
nataliya.muts@lmu.edu.ua*

The existence of two new quaternary compounds, La₂NiAl₄Ge_{4.245} and Pr₂NiAl₄Ge_{4.280}, was established during a systematic investigation of the phase equilibria in the system {La,Ce}–Ni–Al–Ge at 600 °C. Their crystal structures were determined by means of single-crystal and powder X-ray diffraction. The overall chemical compositions, as well as the compositions of the individual phases, were determined by energy-dispersive X-ray spectroscopy, performed on a scanning electron microscope Zeiss Evo 40, equipped with a Dispersive X-ray Spectroscopy system. Phase analysis of the samples was carried out using X-ray powder diffraction data collected at room temperature on a Rigaku SmartLab diffractometer (Cu K α -radiation).

A sample of nominal composition Pr₁₂Ni₁₁Al₄₀Ge₃₇ was prepared from the pure components by induction-melting, followed by slow cooling to room temperature. The arc-melted sample of nominal composition La₁₂Ni₁₁Al₄₀Ge₃₇ was remelted in an induction furnace, facilitating the growth of single crystals.

Good-quality single crystals were selected from mechanically crushed alloys using an optical microscope. The X-ray diffraction data were collected on a three-circle Bruker D8 QUEST diffractometer, equipped with a PHOTON III 14 detector, using graphite-monochromatized Mo K α radiation. APEX6 software was used to solve and refine the crystal structures.

The crystal structure of the quaternary compounds R₂NiAl₄Ge_{4+x} (Pearson symbol *tI48*, space group *I4/mmm*, Wyckoff sequence *mhge*³*d*, unit-cell parameters: *a* = 5.883(2), *c* = 26.203(5) Å for La₂NiAl₄Ge_{4.245(5)} and *a* = 5.838(2), *c* = 25.868(5) Å for Pr₂NiAl₄Ge_{4.280(4)}) is closely related to the structure type Ho₂CoGa₈ (*P4/mmm*, *tP11*, *ihgea*) [2]. The symmetry reduction path from the structure type Ho₂CoGa₈ to the new structure type La₂NiAl₄Ge_{4.245(5)} can be expressed as follows: *P4/mmm* (k2, **a-b**, **a+b**, **2c**; 1/2 1/2 1/2) → *I4/mmm*. A peculiar feature of the new crystal structure is the partial occupation by germanium atoms of one of the 4*e* positions: occ. = 0.245(5)Ge in La₂NiAl₄Ge_{4.245} and occ. = 0.280(4)Ge in Pr₂NiAl₄Ge_{4.280}.

[1] Y. Grin, Y.P. Yarmolyuk, E.I. Gladyshevskii, *Kristallografiya* 24 (1979) 242-246.

NEW TERNARY ALUMINIDE NdPd_{1.22}Al_{4.98}

Nazar Zaremba¹, Galyna Nychporuk², Waclaw Iwasieczko³, Mitja Krnel¹, Lev Akselrud²,
Eteri Svanidze¹, and Vasyl Zaremba²

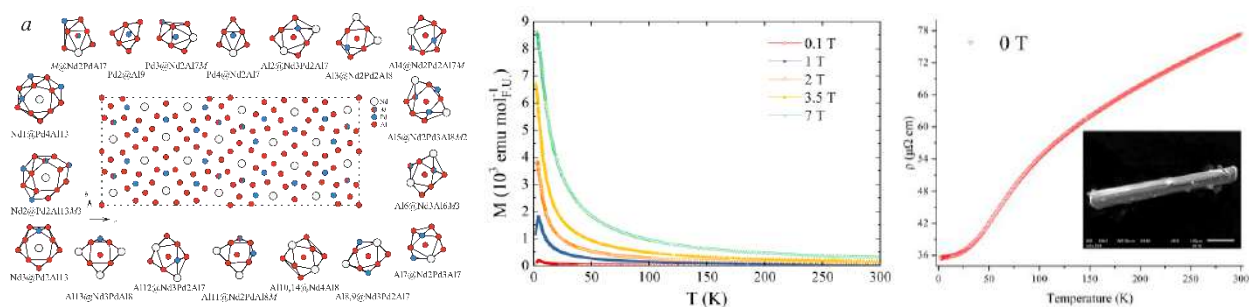
¹ Max Planck Institute for Chemical Physics of Solids, 01187 Dresden, Germany

² Department of Inorganic Chemistry, Ivan Franko National University of Lviv,
79005 Lviv, Ukraine

³ Institute of Low Temperature and Structure Research PAN, 50-422 Wroclaw, Poland
galynan@gmail.com

A sample with the starting composition Nd_{16.7}Pd_{16.7}Al_{66.6} was synthesized by the arc melting technique. Single crystals of the compound were grown using a Canfield-Svanidze Crucible Set [1] by applying a special heat treatment. The needle-shaped crystals were selected mechanically from the Al matrix and studied by single-crystal X-ray diffraction (Rigaku AFC7 diffractometer equipped with a Saturn 724+ CCD detector, Mo *K* α radiation). The WinGX suite of programs [2] and the WinCSD software package [3] were used for the structural refinement.

The new aluminide NdPd_{1.22}Al_{4.98} adopts an own structure type with the following parameters: space group *Cmcm*, $a = 4.2198(1)$, $b = 16.0736(7)$, $c = 38.5834(15)$ Å, $V = 2617.01(16)$ Å³, $R1 = 0.0452$, $wR2 = 0.0887$, 3855 reflections, 115 parameters.



Crystal structure (a), temperature-dependent magnetic susceptibility (b), and resistivity (c) of NdPd_{1.22}Al_{4.98}

The structure of the newly discovered compound can be described as composed of distorted pentagonal prisms around Nd, trigonal prisms around Pd, and distorted tetragonal prisms around Al, with centered side faces and edges (Fig. a).

The compound exhibits antiferromagnetic order below $T_N = 6$ K (Fig. b) and metallic-like electrical conductivity (Fig. c).

E.S. is grateful for the support of the Christiane Nüsslein-Volhard-Stiftung. E.S., N.Z., and M.K. acknowledge the support of the Boehringer Ingelheim Plus 3 Program. N.Z. is grateful for the support of the Alexander von Humboldt Foundation through the Philipp Schwartz Initiative.

[1] P.C. Canfield, E. Svanidze, Canfield-Svanidze Crucible Set, 2024.

[2] L.J. Farrugia, *J. Appl. Crystallogr.* 45 (2012) 849-854.

[3] L. Akselrud, Yu. Grin, *J. Appl. Crystallogr.* 47 (2014) 803-805.

CRYSTAL STRUCTURE OF THE TERNARY COMPOUND $\text{ZrSn}_{1.8}\text{Bi}_{0.2}$

I. Ohonovskiy, Ya. Tokaychuk, and R. Gladyshevskii

Department of Inorganic Chemistry, Ivan Franko National University of Lviv,

Kyryla i Mefodiya St. 6, 79005 Lviv, Ukraine

illia.ohonovskiy@lnu.edu.ua

A systematic investigation of the ternary system Zr–Sn–Bi at 600 °C indicated the formation of a new ternary compound $\text{ZrSn}_{1.8}\text{Bi}_{0.2}$. Its crystal structure was refined by the Rietveld method using X-ray powder diffraction data for an alloy with nominal composition $\text{Zr}_{33.3}\text{Sn}_{60.7}\text{Bi}_6$, collected at room temperature on a powder diffractometer PROTO AXRD Benchtop (Cu $K\alpha$ -radiation). The sample was synthesized from pure bulk metals (Zr \geq 99.95 mass%; Sn \geq 99.99 mass%; Bi \geq 99.98 mass%) by arc melting under argon and annealed under vacuum at 600 °C for 2 months. Phase analysis of the sample revealed the presence of three phases: the new ternary compound $\text{ZrSn}_{1.8}\text{Bi}_{0.2}$ (95.1(2) mass%), the binary compound ZrSn_2 (structure type TiSi_2 , Pearson symbol $oF24$, space group $Fddd$, 4.2(1) mass%), and Bi (As, $hR6$, $R-3m$, 0.7(1) wt.%). The profile and structural parameters were refined by the Rietveld method using the FullProf Suite program package. The composition of the ternary phase was verified by energy-dispersive X-ray spectral analysis, performed on a scanning electron microscope TESCAN VEGA3 LMU, equipped with an energy-dispersive X-ray analyzer Oxford Instruments Aztec ONE with a detector X-Max^N20.

The crystal structure of the ternary compound with refined composition $\text{ZrSn}_{1.796(4)}\text{Bi}_{0.204(4)}$ belongs to the hexagonal structure type CrSi_2 , Pearson symbol $hP9$, space group $P6_222$, $a = 5.5284(2)$, $c = 7.6667(3)$ Å, $R_B = 0.0364$. It is characterized by one site ($3c$) occupied by Zr atoms and one site ($6i$) by a statistical mixture of Sn and Bi atoms. The Zr atoms and the atoms of the statistical mixture are coordinated by 14-vertex rhombic dodecahedra of compositions $M_{10}\text{Zr}_4$ and Zr_5M_9 , respectively.

Atom coordinates, site occupancies, and isotropic displacement parameters for $\text{ZrSn}_{1.796(4)}\text{Bi}_{0.204(4)}$ (structure type CrSi_2 , Pearson symbol $hP9$, space group $P6_222$, $a = 5.5284(2)$, $c = 7.6667(3)$ Å)

Site	Wyckoff position	Atom coordinates			$B_{\text{iso}}, \text{Å}^2$	Occupancy
		x	y	z		
Zr	$3c$	$\frac{1}{2}$	0	0	0.82(5)	1
Sn	$6i$	0.1633(3)	0.3266(6)	0	0.70(2)	0.898(2)
Bi						0.102(2)

The crystal structure of the ternary compound $\text{ZrSn}_{1.8}\text{Bi}_{0.2}$ consists of close-packed ZrM_2 layers with a triangular mesh formed by Zr atoms. The structure type CrSi_2 is a stacking variant of the structure type TiSi_2 , to which the structure of the binary compound ZrSn_2 belongs. The ternary $\text{ZrSn}_{1.8}\text{Bi}_{0.2}$ and binary ZrSn_2 compounds form a two-phase equilibrium in the system Zr–Sn–Bi at 600 °C.

NEW TERNARY INTERMETALLICS IN THE U–Mn–Ge TERNARY SYSTEM

M. Pasturel¹, S. Lamy¹, P. Lemoine², B. Malaman², C. Prestipino³, and A. Vernière²

¹ Univ Rennes, CNRS, UMR6226 ISCR, 35042 Rennes, France

² Univ Lorraine, CNRS, IJL, 54000, Nancy, France

³ Univ Normandie Caen, CNRS, CRISMAT - UMR6508, 14050 Caen, France

mathieu.pasturel@univ-rennes.fr

Ternary uranium germanides are hot topics for solid-state scientists, not only for the wide range of stoichiometries and crystal structures they adopt [1,2], but mainly for the exotic physical properties they exhibit. Among them, the coexistence of superconductivity (SC) and ferromagnetic (FM) order in UGe₂ (ZrGa₂-type, *Cmmm*), UCoGe and URhGe (TiNiSi-type, *Pnma*), with complex magnetic phase diagrams, strongly contradicts the existing theories for the formation of Cooper pairs [3]. The uranium zig-zag chains, locally breaking the inversion symmetry in the FM ordered state, seem to play a crucial role in the formation of the SC state. Finding new compounds with such chains is necessary to support or invalidate this theory.

In this context, the U–Mn–Ge system remains largely unexplored, with only 3 ternary phases reported so far in the literature: UMn₂Ge₂ (CaAl₂Ga₂-type, *I4/mmm*), UMnGe (TiNiSi-type, *Pnma*), and U₂Mn₃Ge (Mg₂Cu₃Si-type, *P6₃/mmc*) [1,2].

Our preliminary investigation of the U–Mn–Ge system revealed the formation of at least 6 extra ternary phases. U₃Mn₄Ge₄ forms between the 1/1/1 and 1/2/2 phases. According to single-crystal XRD, it crystallizes in the Gd₃Cu₄Ge₄ structure-type with space group *Immm* and cell parameters $a = 4.127(1)$ Å, $b = 6.848(2)$ Å and $c = 13.788(3)$ Å. On the same line, a phase with composition UMn₆Ge₆ was identified by SEM-EDS analyses. Its powder XRD pattern is rather well indexed with the average monoclinic (*C2/m*) unit cell reported for UC₆Ge₆ [4], but the presence of modulation still needs to be checked on a single crystal. In the Mn-rich corner, UMn₄Ge₂ adopts the ZrFe₄Si₂ structure-type (*P4₂/mnm*) with $a \approx 7.50$ Å and $c \approx 3.95$ Å. Close to the U–Ge binary axis, U₄MnGe₈ forms with the Tb₄FeGe₈-type *P2₁/c* [5], an ordered distorted derivative of the CeNiSi₂-type. U₃₄Mn_{4-x}Ge₃₃ (U₃₄Fe_{3.32}Ge₃₃-type, *I4/mmm*) is obtained from the stabilization of the U₃₄Si_{34.5} structure by the transition element [6]. Finally, U₈Mn₃Ge₇ crystallizes in a new type with space group *Pnma*, and cell parameters $a = 17.654$ Å, $b = 5.708$ Å, $c = 14.243$ Å. There are 6 independent Wyckoff positions for U for a total of 72 atoms in the unit cell (Pearson symbol *oP72*).

The poster will present the U–Mn–Ge phase diagram, the crystal structures of the new phases, and some preliminary observations on the magnetic behaviour of these intermetallics.

- [1] P. Villars, K. Cenzual (Eds.), *Pearson's Crystal Data – Crystal Structure Database for Inorganic Compounds*, Release 2021/22, ASM International, Materials Park, Ohio, USA.
- [2] *Inorganic Crystal Structure Database*: D. Zagorac *et al.*, *J. Appl. Crystallogr.* 52 (2019), 918-925.
- [3] D. Aoki *et al.*, *J. Phys. Soc. Jpn.* 88 (2019) 022001 and references therein.
- [4] Z. Riedel *et al.*, arXiv.2511.05376, 2025.
- [5] P. Lemoine *et al.*, *Investigations on the influence of transition metals on the crystal structures and magnetic properties of CeNiSi₂-type derivative compounds*, this conference.
- [6] M.S. Henriques *et al.*, *J. Alloys Compd.* 606 (2014) 154-163.

CRYSTAL STRUCTURES OF THE TERNARY COMPOUNDS Gd₂AgGe₆ AND Gd₃Ag₄Ge₄

A. Parashchuk, N. Klymentiy, S. Pukas, and R. Gladyshevskii
Department of Inorganic Chemistry, Ivan Franko National University of Lviv,
Kyryla i Mefodiya St. 6, 79005 Lviv, Ukraine
svitlana.pukas@lnu.edu.ua

The existence of four ternary germanides, GdAg₂Ge₂, ~GdAgGe₃, Gd₃Ag₄Ge₄, and GdAgGe, has so far been reported in the system Gd–Ag–Ge system at 500 °C [1]. Two more compounds: Gd₂AgGe₆ and GdAg_{0.6}Ge_{1.4}, were reported at 600 °C [2]. Complete structure determinations have been performed for the two ternary compounds GdAgGe and GdAg₂Ge₂ [3,4]. The aim of the present work was to confirm the existence of the ternary compounds Gd₂AgGe₆ and Gd₃Ag₄Ge₄ at 600 °C and refine their crystal structures.

Alloys of nominal compositions Gd_{22.2}Ag_{11.1}Ge_{66.7} and Gd_{27.2}Ag_{36.4}Ge_{36.4} were synthesized by arc melting and annealed at 600 °C for 720 h. The overall composition of the sample and of the individual phases was investigated by means of energy-dispersive X-ray spectroscopy and the crystal structures of the phases were established by X-ray powder diffraction. The alloy Gd_{22.2}Ag_{11.1}Ge_{66.7} appeared to be multiphase. The main phase (75(1) mass%) was Gd₂AgGe₆ with a crystal structure belonging to the Ce₂CuGe₆-type (*oS18*, *Amm2*); the second phase (17(4) mass%) was GdAg₂Ge₂ (CeAl₂Ga₂, *tI10*, *I4/mmm*) and the third phase (8(1) mass%) was elementary Ge. The alloy Gd_{27.2}Ag_{36.4}Ge_{36.4} contained the phase Gd₃Ag₄Ge₄ and traces of GdAg₂Ge₂ and Gd₂AgGe₆ phases. The crystal structure of Gd₃Ag₄Ge₄ belongs to the Gd₃Cu₄Ge₄-type (*oI22*, *Immm*). A complete determination of the crystal structures of the compounds Gd₂AgGe₆ and Gd₃Ag₄Ge₄ was carried out.

Atom coordinates and isotropic displacement parameters for Gd₂AgGe₆ and Gd₃Ag₄Ge₄

Gd ₂ AgGe ₆ : <i>oS18</i> , <i>Amm2</i> , $a = 4.18971(4)$, $b = 4.05546(4)$, $c = 21.1487(2)$ Å, $R_B = 4.21$ %						Gd ₃ Ag ₄ Ge ₄ : <i>oI22</i> , <i>Immm</i> , $a = 4.34028(5)$, $b = 7.07186(8)$, $c = 14.4772(2)$ Å, $R_B = 3.97$ %					
Site	WP	<i>x</i>	<i>y</i>	<i>z</i>	B_{iso} , Å ²	Site	WP	<i>x</i>	<i>y</i>	<i>z</i>	B_{iso} , Å ²
Gd1	2 <i>b</i>	½	0	0.2064(1)	0.86(4)	Gd1	4 <i>j</i>	½	0	0.3727(1)	0.99(5)
Gd2	2 <i>b</i>	½	0	0.8678(1)	0.98(6)	Gd2	2 <i>a</i>	0	0	0	0.91(7)
Ag	2 <i>a</i>	0	0	0.4392(1)	1.19(7)	Ag	8 <i>l</i>	0	0.3045(2)	0.3315(1)	1.22(4)
Ge1	2 <i>b</i>	½	0	0.5045(2)	1.32(9)	Ge1	4 <i>i</i>	0	0	0.2153(2)	0.84(8)
Ge2	2 <i>b</i>	½	0	0.6075(2)		Ge2	4 <i>h</i>	0	0.1822(5)	½	1.08(8)
Ge3	2 <i>a</i>	0	0	-0.0081(2)							
Ge4	2 <i>a</i>	0	0	0.1086(3)							
Ge5	2 <i>a</i>	0	0	0.3195(3)							
Ge6	2 <i>a</i>	0	0	0.7360(2)							

- [1] O.V. Anisimova, E.I. Gladyshevskii, E.P. Marusyn, V.K. Pecharsky, *Coll. Abstr. VI Meet. Crystal Chem. Inorg. Coord. Compd.*, Lviv, Ukraine, 1992, p. 160.
- [2] O.V. Anisimova, E.P. Marusyn, V.K. Pecharsky, E.I. Gladyshevskii, *Coll. Abstr. 6 Int. Conf. Crystal Chem. Intermet. Compd.*, Lviv, Ukraine, 1995, p. 24.
- [3] B. Gibson, R. Pöttgen, R.K. Kremer, A. Simon, K.R.A. Ziebeck, *J. Alloys Compd.* 239 (1996) 34-40.
- [4] A. Parashchuk, N. Klymentiy, N. Semuso, S. Pukas, R. Gladyshevskii, *Coll. Abstr. IX Int. Scient. Conf. Stud. Young. Sci. Curr. Chem. Probl.*, Vinnytsia, Ukraine, 2026, p. 29.

NEW REPRESENTATIVES OF THE STRUCTURE TYPE $YNiAl_3$

N. Semuso, S. Pukas, P. Demchenko, and R. Gladyshevskii

Department of Inorganic Chemistry, Ivan Franko National University of Lviv,

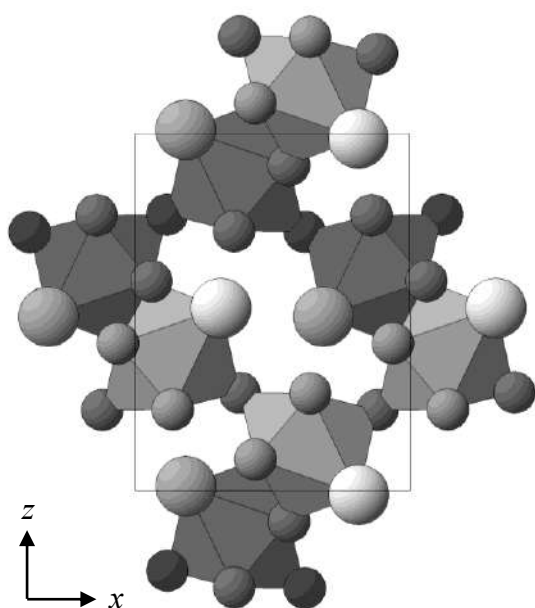
Kyryla i Mefodiya St. 6, 79005 Lviv, Ukraine

nataliya.semuso@lnu.edu.ua

The aim of the present work was to search for new representatives of the structure type $YNiAl_3$ ($oP20$, $Pnma$) [1] in $R-Ni-Al$ systems. According to Pearson's Crystal Data [2], this structure type has five representatives exclusively in $R-Ni-Al$ systems, where $R = Y, Sm, Gd, Tb,$ and Dy [3,4]. In this work, four new isotypic rare-earth nickel aluminides, $RNiAl_3$ ($R = Ho, Er, Tm,$ and Lu), were synthesized by arc melting, and their crystal structures were refined from X-ray powder diffraction data (diffractometer STOE Stadi P, $Cu K\alpha_1$ radiation).

Crystallographic parameters of the compounds $RNiAl_3$

Compound	$a, \text{\AA}$	$b, \text{\AA}$	$c, \text{\AA}$	$V, \text{\AA}^3$
HoNiAl ₃	8.1172(3)	4.0275(1)	10.5892(4)	346.2(1)
ErNiAl ₃	8.1018(2)	4.0217(1)	10.5674(3)	344.3(1)
TmNiAl ₃	8.0857(3)	4.0159(1)	10.5453(5)	342.4(1)
LuNiAl ₃	8.0729(2)	4.0097(1)	10.5235(4)	340.6(1)



Ni-centred tricapped trigonal prisms Y_2Al_7
in the structure type $YNiAl_3$

The orthorhombic structure type $YNiAl_3$ is built up of tricapped trigonal prisms of composition Y_2Al_7 (Y_2Al_4 prisms with three additional Al atoms capping the rectangular faces) centred by Ni atoms. Each polyhedron shares two vertices, two edges, and two triangular bases with other polyhedra.

Ni-centred trigonal prisms are also observed in the closely related structures of ternary aluminides with rare-earth metals and nickel that belong to the types $YNiAl_4$, $MgCuAl_2$, $LaNiAl$, $ZrNiAl$, and W_2CoB_2 . In these structures, characterized by the ratio $R:Ni = 1:1$, the composition of the trigonal prisms changes from R_2Al_4 to R_4Al_2 with decreasing Al content.

This work was carried out under the project "Search for new structure types" of the company Material Phases Data System (Vitznau, Switzerland).

[1] R.E. Gladyshevskii, E. Parthé, *Acta Crystallogr. C* 48 (1992) 229-232.

[2] P. Villars, K. Cenzual, *Pearson's Crystal Data – Crystal Structure Database for Inorganic Compounds*, Release 2023/24, ASM International, Materials Park, Ohio, USA.

[3] S. Delsante, R. Raggio, G. Borzone, *Intermetallics* 16 (2008) 1250-1257.

[4] S. Pukas, O. Matselko, R. Gladyshevskii, *Chem. Met. Alloys* 3 (2010) 35-41.

CRYSTAL STRUCTURE AND POLYMORPHISM OF YbGa_{6+x}

O. Sichevych¹, Yu. Prots¹, C. Curfs², Yu. Grin¹, and L. Akselrud^{1,3}

¹ *Max-Planck-Institut für Chemische Physik fester Stoffe, Nöthnitzer Straße 40,
01187 Dresden, Germany*

² *ESRF, B.P.220, 38043 Grenoble, France*

³ *Department of Inorganic Chemistry, Ivan Franko National University of Lviv,
Kyryla i Mefodiya St. 6, 79005 Lviv, Ukraine
akslev@gmail.com*

The gallium-richest compound in the system Yb–Ga was synthesized by the self-flux technique combined with high-temperature centrifugation-aided filtration. The powder X-ray diffraction experiment performed *in situ* (synchrotron, $\lambda = 0.354568 \text{ \AA}$ and XtaLAB Synergy-S, Dualflex diffractometer, Ag K, $\lambda = 0.56087 \text{ \AA}$) revealed a phase transition in YbGa_{6+x} at $25 \text{ }^\circ\text{C}$. The high-temperature modification possesses a primitive tetragonal structure of $\text{CeCu}_{0.6}\text{Ga}_6$ type with strong disorder in the Ga sublattice (space group $P4/mmm$, $a = 4.30823(3) \text{ \AA}$, $c = 7.66274(6) \text{ \AA}$, $V = 142.23(1) \text{ \AA}^3$ at $77 \text{ }^\circ\text{C}$).

Below room temperature, YbGa_{6+x} exhibits an orthorhombic lattice. Single-crystal diffraction experiment and powder X-ray diffraction on LT- YbGa_{6+x} revealed a 16-fold modulation superstructure (superspace group $P2mb(\frac{1}{2} 0 \gamma)000$, $a = 8.5784(2) \text{ \AA}$, $b = 34.4921(5) \text{ \AA}$, $c = 7.6412(1) \text{ \AA}$, $V = 2260.9(1) \text{ \AA}^3$, $\gamma = 0.25494(6)$ at $-77 \text{ }^\circ\text{C}$).

SYSTEMATIC STUDY OF PEROVSKITE PHASES ON THE CaMnO_3 – RMnO_3 CROSS-SECTIONS, WHERE R = RARE-EARTH METAL

K. Stepanovych, V. Lesnianska, O. Zarembo, and R. Gladyshevskii

Department of Inorganic Chemistry, Ivan Franko National University of Lviv,

Kyryla i Mefodiya St. 6, 79005 Lviv, Ukraine

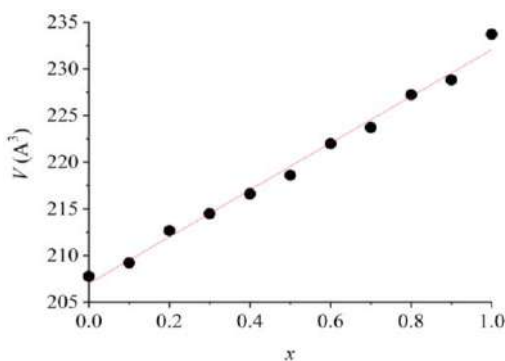
kateryna.stepanovych@lnu.edu.ua

Ceramic materials represent a promising field in modern science and technology. They possess numerous advantages, including high mechanical strength, thermal and chemical stability, low electrical and thermal conductivity, *etc.* Particular attention is paid to perovskite-type phases. Perovskites in A – R – T – O systems (A = alkaline-earth, R = rare-earth, T = $3d$ metal) are of special interest due to the mixed oxidation states of the transition metals. According to Pearson's Crystal Data [1], perovskite phases have been reported on the CaMnO_3 – RMnO_3 cross-sections for all rare-earth metals except promethium. We have previously demonstrated the existence of continuous solid-solution series with GdFeO_3 -type structure in the systems containing Pr and Nd, whereas in the case of Ho and Tm extended substitutional solid solutions based on the CaMnO_3 phase are formed. The aim of this work was to study the interaction of the components on the CaMnO_3 – RMnO_3 cross-sections, where R = Sm and Yb.

The samples were synthesized *via* a multistage solid-state synthesis route. Stoichiometric amounts of high-purity rare-earth metal oxides (Sm_2O_3 and Yb_2O_3), manganese(III) oxide (Mn_2O_3), and calcium carbonate (CaCO_3) were mixed and homogenized by grinding, followed by calcination at 1000 °C for 24 h to ensure complete decomposition of CaCO_3 . The obtained powders were reground, pressed into ~0.5 g pellets, and annealed at 1200 °C for 8 h to complete the reaction and promote the formation of the target phase. Powder X-ray diffraction was used for phase identification and crystal structure refinements.

As a result of the investigation of polycrystalline samples with compositions $\text{Ca}_{1-x}\text{Sm}_x\text{MnO}_3$, the existence of a continuous solid-solution series along the CaMnO_3 – SmMnO_3 cross-section within the CaO – Sm_2O_3 – Mn_2O_3 system was confirmed. This phase adopts an orthorhombic perovskite structure of the GdFeO_3 type (Pearson symbol $oP20$, space group $Pnma$). The unit cell volume of the $\text{Ca}_{1-x}\text{Sm}_x\text{MnO}_3$ phase increases with increasing samarium content (see Figure).

The phase diagram of the CaO – Yb_2O_3 – Mn_2O_3 system was constructed over the full compositional range. Under the conditions of the investigation, 8 single-phase, 14 two-phase, and 7 three-phase regions were identified, and the presence of a quaternary compound with the point composition $\text{Ca}_{0.5}\text{Yb}_{0.5}\text{MnO}_3$ was confirmed. This phase crystallizes in the orthorhombic perovskite structure type GdFeO_3 ($oP20$, $Pnma$, $a = 5.4730(3)$, $b = 7.4170(5)$, $c = 5.2685(3)$ Å, $R_B = 0.0774$).



[1] P. Villars, K. Cenzual (Eds.), *Pearson's Crystal Data – Crystal Structure Database for Inorganic Compounds*, Release 2023/24, ASM International, Materials Park, Ohio, USA.

SOLID SOLUTION WITH TII-TYPE STRUCTURE IN THE SYSTEM Tb–Zr–Al–Si

Kh. Yakymovych¹, N. Muts¹, Ya. Tokaychuk¹, P. Solokha², S. De Negri²,
and R. Gladyshevskii¹

¹ *Department of Inorganic Chemistry, Ivan Franko National University of Lviv,
Kyryla i Mefodiya St. 6, 79005 Lviv, Ukraine*

² *Department of Chemistry and Industrial Chemistry of University of Genoa,
via Dodecaneso 31, 16146 Genova, Italy
khrystyna.misko@lnu.edu.ua*

The existence of a phase with a TII-type structure (Pearson symbol *oS8*, space group *Cmcm*) in the Tb–Zr–Al–Si and Tb–Al–Si systems has been reported for the compositions (Tb_{0.03}Zr_{0.97})(Al_{0.22}Si_{0.78}), (Tb_{0.70}Zr_{0.30})(Al_{0.17}Si_{0.83}), and Tb(Al_{0.15}Si_{0.85}) [1]. To further study the interactions between the components in the systems Tb–Zr–Al–Si and Tb–Al–Si, new samples were prepared by arc-melting pure metals (Tb and Zr ≥ 99.9 mass%, Al and Si ≥ 99.999 mass%) under purified argon, and annealed under vacuum at 600 °C for 3 months.

New compositions for the phase with TII-type structure in the systems Tb–Zr–Al–Si and Tb–Al–Si were determined: (Tb_{0.43}Zr_{0.57})(Al_{0.40}Si_{0.60}), (Tb_{0.77}Zr_{0.23})(Al_{0.04}Si_{0.56}), (Tb_{0.81}Zr_{0.19})(Al_{0.23}Si_{0.77}), Tb(Al_{0.12}Si_{0.88}), and Tb(Al_{0.59}Si_{0.41}). The Tb atoms, or a statistical mixture of Tb and Zr atoms, occupy the positions of the I atoms, and the statistical mixture of Al and Si atoms the positions of the Tl atoms.

The crystal structure of the quaternary phase in the system Tb–Zr–Al–Si system was refined from X-ray single-crystal diffraction data (three-circle Bruker D8 QUEST diffractometer, equipped with a PHOTON III 14 detector, graphite monochromatized Mo *K*α-radiation), X-ray powder diffraction data (PROTO AXRD Benchtop diffractometer with Cu *K*α-radiation; Rigaku SmartLab diffractometer with Cu *K*α-radiation). The overall chemical compositions and compositions of individual phases were additionally determined by energy-dispersive X-ray spectroscopy, performed on a scanning electron microscope TESCAN Vega3 LMU equipped with an energy-dispersive X-ray analyzer Oxford Instruments Aztec ONE with an X-Max^N20 detector and Zeiss Evo 40 Scanning Electron Microscope equipped with a Dispersive X-ray Spectroscopy system.

Comparing the unit-cell parameters of the new compositions and the parameters of isostructural phases in the literature [1,2] for the binary compounds ZrAl and ZrSi, and the ternary phases ZrAl_xSi_{1-x} (*x* = 0-0.5) and Tb(Al_{0.15}Si_{0.85}), we assume the formation of an extended solid solution with a TII-type structure in the quaternary Tb–Zr–Al–Si system at 600 °C. The homogeneity region of this phase can range from the composition of the ternary compound Tb(Al, Si) and extend to a solid solution based on the binary compound ZrSi in the Zr–Al–Si system. The unit-cell parameters (space group *Cmcm*) within the four-component solid solution increase with increasing terbium content: *a* = 3.8941(2), *b* = 10.158(5), *c* = 3.749(2) Å for the composition (Tb_{0.43}Zr_{0.57})(Al_{0.40}Si_{0.60}) and *a* = 4.209(2), *b* = 10.491(5), *c* = 3.840(2) Å for the composition (Tb_{0.81}Zr_{0.19})(Al_{0.23}Si_{0.77}).

[1] N. Muts, R. Gladyshevskii, *Z. Anorg. Allg. Chem.* 632 (2006) 2345-2349.

[2] P. Villars, K. Cenzual (Eds.), *Pearson's Crystal Data – Crystal Structure Database for Inorganic Compounds*, Release 2023/24, ASM International, Materials Park, Ohio, USA.

CRYSTAL STRUCTURES OF THE NEW COMPOUNDS
 $R_2Pd_8Ge_3$ ($R = Pr, Nd, AND Sm$)

O. Zaremba¹, K. Stepanovych¹, Ya. Tokaychuk¹, P. Solokha², S. De Negri²,
and R. Gladyshevskii¹

¹ *Department of Inorganic Chemistry, Ivan Franko National University of Lviv,
Kyryla i Mefodiya St. 6, 79005 Lviv, Ukraine*

² *Department of Chemistry and Industrial Chemistry, Università degli Studi di Genova,
via Dodecaneso 31, I-16146 Genoa, Italy
oksana.zaremba@lnu.edu.ua*

The study of palladium-containing systems is of considerable interest due to the prospects for applications, particularly in the development of more efficient and cost-effective catalysts. Based on literature data regarding the existence of the perovskite-type intermetallic phase $SmPd_3Ge$ [1], the initial aim of the work was the synthesis and characterization of this compound, as perovskite-related phases are well-known for their wide range of physical properties and practical applications. However, during the examination of samples with compositions close to RPd_3Ge stoichiometry, the formation of new ternary compounds was revealed. The elucidation of their crystal structure represents the main objective of this report.

Alloys of nominal compositions $R_{15}Pd_{65}Ge_{20}$ were prepared by melting pure metals ($Pr, Nd, Sm \geq 99.8$ mass%, $Pd \geq 99.95$ mass%, $Ge \geq 99.9$ mass%) in an arc-furnace, followed by annealing at 600 °C for 1 month. High-quality crystals were selected after remelting the samples, placed inside tantalum containers, in an induction furnace. X-ray single-crystal data were collected on a Bruker D8 QUEST diffractometer equipped with a PhotonIIIC7 CPAD detector, using Mo $K\alpha$ radiation (graphite monochromator). APEX6 software was used to solve and refine the crystal structures.

As a result of our investigation, the existence of three ternary phases $R_2Pd_8Ge_3$ ($R = Pr, Nd, and Sm$) was established. These isostructural compounds represent a new structure type, possessing monoclinic symmetry with a primitive unit cell (Table).

Refined unit cell parameters of the new compounds $R_2Pd_8Ge_3$ ($R = Pr, Nd, and Sm$),
Pearson symbol $mP52$, space group $P2_1/m$ (11), $Z = 4$, Wyckoff sequence f^8e^{10}

R	Unit-cell parameters					$R1/wR2$
	$a, \text{Å}$	$b, \text{Å}$	$c, \text{Å}$	$\beta, ^\circ$	$V, \text{Å}^3$	
Pr	9.2230(3)	8.9361(3)	11.5675(4)	111.8440(10)	884.91(5)	0.0399/0.1058
Nd	9.2053(8)	8.9212(7)	11.5513(9)	111.816(3)	880.68(13)	0.0678/0.1019
Sm	9.174(7)	8.898(7)	11.513(9)	111.90(3)	872.0(12)	0.0486/0.0869

The unit cell of the $R_2Pd_8Ge_3$ structure contains 52 atoms, which occupy sites in two Wyckoff positions: $2e$ ($x \frac{1}{4} z$) and $4f$ ($x y z$). The atoms of the rare-earth metals are exclusively located at $2e$ positions, whereas the Pd and Ge atoms occupy both types of sites, *i.e.* general $4f$ and special $2e$.

[1] P. Villars, K. Cenzual (Eds.), *Pearson's Crystal Data – Crystal Structure Database for Inorganic Compounds*, Release 2023/24, ASM International, Materials Park, Ohio, USA.

SOLUBILITIES OF *d*-METALS IN THE Gd₂Cu₂In AND Gd₂Ni₂In COMPOUNDS

R. Zaremba¹, and Ya. Kalychak²

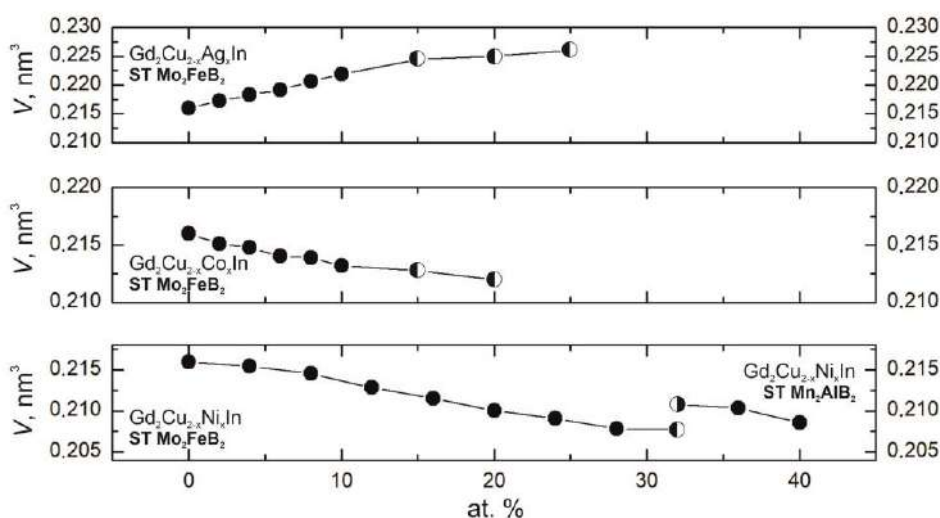
¹ Department of Inorganic Chemistry, Ivan Franko National University of Lviv,
Kyryla i Mefodiya St. 6, 79005 Lviv, Ukraine

² Department of Analytical Chemistry, Ivan Franko National University of Lviv,
Kyryla i Mefodiya St. 6, 79005 Lviv, Ukraine
roman.zaremba@lnu.edu.ua

Intermetallic compounds are a promising class of materials with tunable physical and chemical properties, particularly in systems containing rare-earth, *d*-, and *p*-elements. Such systems often exhibit enhanced magnetic, electrical, and thermal stability characteristics. Intermetallic-based hydrides are of particular interest due to their reversible hydrogen absorption and potential for high-density hydrogen storage without extreme conditions. These materials are also relevant for energy storage and functional applications. Compounds of the R_2M_2In type contain tetrahedral and octahedral voids suitable for hydrogen incorporation, enabling the formation of hydride phases. The aim of this work was to investigate the solubility of Ag, Co, and Ni in the Gd₂Cu₂In compound and of Cu in the Gd₂Ni₂In compound.

Samples were prepared from high-purity metals (Gd, Cu, Ag, Ni, Co, In) by arc melting in a purified argon atmosphere using a tungsten electrode on a water-cooled copper hearth. The alloys (1.5-2 g) were synthesized from accurately weighed components (± 0.001 g), and their compositions were verified by mass comparison, with deviations not exceeding 2 %. Homogenization was carried out by annealing in evacuated quartz ampoules at 870 K for 1440 h in muffle furnaces, followed by quenching in cold water. Phase and structure analyses were performed using X-ray diffraction.

The solubilities of silver, cobalt, and nickel at 870 K in the Gd₂Cu₂In compound ($a = 0.75272(8)$ nm, $c = 0.38120(6)$ nm), which crystallizes with a Mo₂FeB₂-type structure, were determined based on X-ray diffraction of 26 samples. The solubility of silver extends up to ~ 14 at.% ($a_{\max} = 0.7633(1)$ nm, $c_{\max} = 0.3854(1)$ nm); of cobalt ~ 12 at.% ($a_{\max} = 0.7484(1)$ nm, $c_{\max} = 0.3801(1)$ nm); and of nickel ~ 30 at.% ($a_{\max} = 0.7469(2)$ nm, $c_{\max} = 0.3724(2)$ nm). The Gd₂Ni₂In compound ($a = 0.3936(2)$ nm, $b = 1.4232(7)$ nm, $c = 0.3723(2)$ nm) with Mn₂AlB₂-type structure dissolves ~ 6 at.% of copper ($a_{\max} = 0.396(2)$ nm, $b_{\max} = 1.431(6)$ nm, $c_{\max} = 0.3719(9)$ nm).



Solubilities of *d*-metals in the Gd₂Cu₂In and Gd₂Ni₂In compounds

NEW REPRESENTATIVES OF THE Tb₃Ru_{0.97}In₃-TYPE STRUCTURE

Yu. Tyvanchuk¹, V. Babizhetskyy¹, A. Zelinskiy¹, V. Smetana², S. Baran³, and A. Szytuła³

¹ *Department of Inorganic Chemistry, Ivan Franko National University of Lviv,
Kyryla i Mefodiya St. 6, 79005 Lviv, Ukraine*

² *Department of Biological and Chemical Engineering and iNANO,
Aarhus University, 8000 Aarhus C, Denmark*

³ *Faculty of Physics, Astronomy and Applied Computer Science,
M. Smoluchowski Institute of Physics, Jagiellonian University,
Prof. Stanisława Łojasiewicza 11, PL-30-348 Kraków, Poland
anatoliy.zelinskiy@lnu.edu.ua*

Polycrystalline samples of nominal composition $RE_{46}T_{18}In_{36}$ ($RE = Tb, Ho, T = Rh, Ir$) were synthesized by arc melting of high-purity metals under an argon atmosphere in the course of our investigations of $RE-T-In$ systems ($RE =$ heavy rare-earth element). In addition to the Lu₅Ni₂In₄- and Nd₁₁Pd₄In₉-type compounds reported earlier [1,2], new intermetallic phases adopting the structure type Tb₃Ru_{0.97}In₃ [3] were identified.

The crystal structure of Tb₃RhIn₃ was investigated by X-ray powder diffraction of a Tb₄₆Rh₁₈In₃₆ sample. A PANalytical X'Pert PRO diffractometer (Cu $K\alpha$ radiation) and the FullProf program package were used for the data collection, phase analysis and Rietveld refinement. Tb₃RhIn₃ crystallizes in a Tb₃Ru_{0.97}In₃-type structure [3] (space group $Pbam$, Pearson symbol $oP28$) with lattice parameters $a = 11.344(2)$, $b = 16.290(3)$, $c = 3.6740(9)$ Å. The refinement converged to $R_F = 5.5\%$, $R_{Bragg} = 8.6\%$.

Intensity data from a single crystal extracted from the crushed Ho₄₆Ir₁₈In₃₆ sample were collected using a Bruker D8 Venture diffractometer with monochromated Mo $K\alpha$ radiation. The crystal structure was determined by direct methods using the SHELX-2018 program package. The compound adopts the Tb₃Ru_{0.97}In₃-type structure with lattice parameters: $a = 11.291(9)$, $b = 16.173(11)$, $c = 3.642(3)$ Å. The refined composition of the compound was Ho₃IrIn₃ or Ho_{42.9}Ir_{14.2}In_{42.9}, which agrees well with that established by EDX analysis. Based on 771 independent reflections [$I > 2\sigma(I)$], the crystal structure was refined to reliability factors $R1 = 5.3\%$ and $wR2 = 10.8\%$ with anisotropic displacement parameters refined for all atoms.

The Tb₃Ru_{0.97}In₃, Lu₅Ni₂In₄, and Nd₁₁Pd₄In₉ representatives have very similar compositions and belong to a large family of ternary rare-earth intermetallics composed of AlB₂- and CsCl-related slabs. Their structures consist of two layers alternating along the shortest axis, namely, a layer of the larger RE atoms and a layer of the smaller T/In atoms.

- [1] R. Zaremba, W. Hermes, M. Eul, R. Pöttgen, *Z. Naturforsch.* 63b (2008) 1447-1449.
- [2] Yu. Tyvanchuk, V. Babizhetskyy, S. Baran, A. Szytuła, V. Smetana, E.I. Jaffal, B. Selvaratnam, A.-V. Mudring, A.O. Oliynyk, *Chem. Mater.* 38 (2026) 2430-2444.
- [3] P. Villars, K. Cenzual, *Pearson's Crystal Data – Crystal Structure Database for Inorganic Compounds*, Release 2023/24, ASM International, Materials Park, Ohio, USA.

CRYSTAL STRUCTURE, PHYSICAL PROPERTIES, AND THEORETICAL ANALYSIS OF THE NEW COMPOUND $\text{Eu}_2\text{Pd}_3\text{Sn}_5$

I. Trabelsi^{1,4}, A. Martinelli², I. Čurlik³, G. Palla⁴, S. De Negri⁴, P. Solokha⁴, R. Freccero⁴, R. Ben Hassen¹, and M. Giovannini⁴

¹Lab. Materials and Environment for Sustainable Development, Univ Tunis El Manar, Tunisia

²SPIN-CNR, Corso F.M. Perrone 24, 16152 Genova, Italy

³Faculty of Humanities and Natural Sciences, University of Prešov, Prešov, Slovakia

⁴Department of Chemistry and Industrial Chemistry, University of Genova, Genova, Italy
imen.trabelsi@edu.unige.it, imen.trabelsi@etudiant-fst.utm.tn

The Eu–Pd–Sn ternary system has attracted considerable attention due to its rich variety of intermetallic compounds, each exhibiting unique physical properties [1]. Notably, $\text{Eu}_2\text{Pd}_3\text{Sn}_5$ crystallizes in the orthorhombic space group $Ibam$, with lattice parameters $a = 11.079(3)$ Å, $b = 12.900(4)$ Å, and $c = 6.4958(17)$ Å, and adopts the $oI40\text{-U}_2\text{Co}_3\text{Si}_5$ structure type. This compound features six distinct atomic sites: europium, palladium, and tin occupying $8j$, $(4b, 8j)$, and $(4a, 8g, 8j)$ positions, respectively.

$\text{Eu}_2\text{Pd}_3\text{Sn}_5$ revealed magnetic properties characterized by Curie-Weiss behaviour with an effective magnetic moment pointing to a divalent Eu^{2+} state [2], and a positive value of $\theta_p = 8.72$ K, indicating the presence of strong ferromagnetic interactions. Two distinct magnetic transitions were observed, an AFM at 13.8 K and an FM at about 5 K, as confirmed by specific heat measurements. This complex interplay between ferromagnetic and antiferromagnetic orders is influenced by the applied magnetic field. These experimental observations are supported by Density Functional Theory (DFT) calculations, in which a Hubbard U parameter [3] of 8 eV was introduced to properly treat the strongly correlated $4f$ -electrons [4]. The calculated magnetic moment, around 7 μB , is in fair agreement with the expected value for Eu^{2+} (7.94 μB) [2]. To further understand the electronic properties, band structure, density of states, and bonding analyses were performed using Quantum ESPRESSO and LOBSTER software [5,6]. The results indicate that the material is metallic, with finite states at the Fermi level. The valence band is mainly dominated by Pd- $4d$ states with a noticeable contribution from Sn- $5p$ orbitals, indicating Pd-Sn hybridization. At the same time, Eu $4f$ electrons remain localized below the Fermi level and do not contribute to conduction. A detailed analysis of the chemical bonds, using -pCOHP curves and ICOBI values, reveals that the bonding scenario is dominated by Sn–Sn covalent interactions (ICOBI=0.44), followed by Pd–Sn polar covalent bonds that have proven to be decisive in driving the crystallization into a specific type, as pointed out for other $R_2M_3X_5$ phases [7]. The Eu-Sn and Eu-Pd interactions are subsidiary, with significantly lower ICOBI, while the Eu-Eu and Pd-Pd interactions can be considered negligible. In conclusion, these results provide a clearer and comprehensive picture of the electronic structure and bonding mechanisms in $\text{Eu}_2\text{Pd}_3\text{Sn}_5$.

[1] W.K. Brown, M.A. Plata, M.E. Raines, J.Y. Chan, In: *Handbook on the Physics and Chemistry of Rare Earth Elements*, Vol. 64, 2023, pp. 1-92.

[2] C. Song *et al.*, *Rev. Mater. Res.* (2026) 100149.

[3] I.L. Locht *et al.*, *Phys. Rev. B* 94 (2016) 085137.

[4] A. Martinelli *et al.*, *J. Mater. Chem. C* 11 (2023) 7641-7653.

[5] S. Maintz *et al.*, *J. Comput. Chem.* 37 (2016) 1030-1035.

[6] P. Giannozzi *et al.*, *J. Phys.: Condens. Matter* 21 (2009) 395502.

[7] G. Palla *et al.*, *Inorg. Chem.* 64(42) (2025) 21067-21075.

INSIGHTS INTO THE ELECTRONIC STRUCTURE OF $\text{CeSi}_{2-x}\text{B}_x$ COMPOUNDS, A XANES AND DFT STUDY

Baptiste Vallet-Simond^{1,2}, Olivier Isnard², Volodymyr Babizhetskyy³, Jean-François Halet⁴, and Reinhard K. Kremer⁵

¹ European Synchrotron Radiation Facility, 71 avenue des Martyrs, 38043 Grenoble, France

² Université Grenoble Alpes, Institut Néel du CNRS, 38042 Grenoble, France

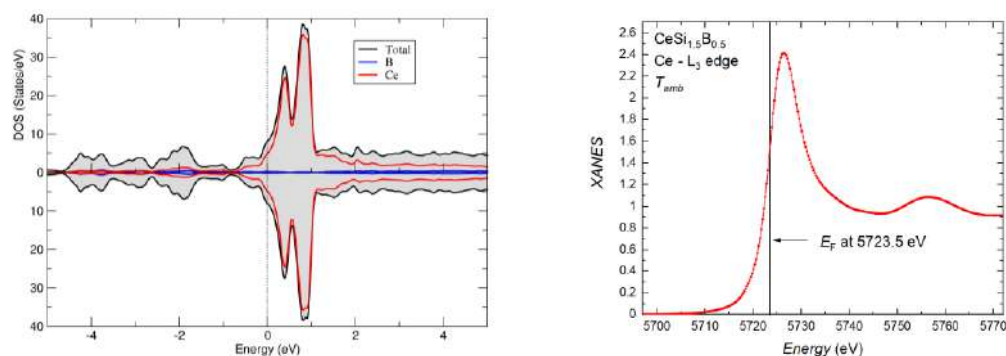
³ Department of Inorganic Chemistry, Ivan Franko National University of Lviv, Kyryla i Mefodiya St. 6, 79005 Lviv, Ukraine

⁴ Univ Rennes, CNRS, École Nationale Supérieure de Chimie de Rennes, Institut des Sciences Chimiques de Rennes (ISCR) – UMR 6226, 35000 Rennes, France

⁵ Max-Planck-Institut für Festkörperforschung, Heisenbergstrasse 1, Postfach 800665, D-70569, Stuttgart, Germany
baptiste.vallet-simond@esrf.fr

The compounds $\text{CeSi}_{2-x}\text{B}_x$ ($x = 0, 0.1, 0.2, 0.4,$ and 0.5) exhibit varying physical properties depending on their composition. For example, long-range ferromagnetic ordering of cerium atoms, driven by Ruderman-Kittel-Kasuya-Yosida (RKKY) interactions, has been observed at temperatures ranging from approximately 12 K to 1 K for compositions where x varies from 0.40 to 0.18. Within this range, Kondo behaviour (with Kondo temperatures T_K between 2 K and 22 K) is observed, resulting in the absence of magnetic ordering [1].

To explore how the presence of boron affects the structural and physical properties of these compounds, we conducted a comprehensive study of the electronic structure of $\text{CeSi}_{2-x}\text{B}_x$ compounds using both experimental and theoretical methods. X-ray Absorption Near Edge Structure (XANES) measurements at the Ce L_3 edge on $\text{CeSi}_{1.5}\text{B}_{0.5}$ revealed that Ce is in a 3+ state ($4f^1$ configuration). The results are discussed in the light of density functional theory calculations. The electronic state of Ce was also investigated in $\text{CeSi}_{2-x}\text{B}_x$ compounds adopting different structure types: $\alpha\text{-ThSi}_2$, $\alpha\text{-GdSi}_2$, and AlB_2 [2].



Total and atom-projected spin-polarized PBE0+SO electronic DOS of $\text{CeSi}_{1.5}\text{B}_{0.5}$ with an AlB_2 -derived ($P6/mmm$) structure type (left). XANES measured at the Ce L_3 edge for $\text{CeSi}_{1.5}\text{B}_{0.5}$ (right).

[1] V. Babizhetskyy, R.K. Kremer, R. Jardin, R. Gautier, B. Fontaine, J.-F. Halet, *Solid State Sci.* 146 (2023) 107378.

[2] B. Vallet-Simond, O. Isnard, V. Babizhetskyy, J-F Halet, R.K. Kremer, to be published.

NEW MgH₂-BASED COMPOSITES FOR EFFICIENT HYDROGEN GENERATION BY HYDROLYSIS

Vasyl Berezovets, Oleksandr Kononiuk, Ihor Zavaliy, and Yuriy Kosarchyn
*Karpenko Physico-Mechanical Institute of the National Academy of Sciences of Ukraine,
Naukova St. 5, 79060 Lviv, Ukraine
berezovets@ipm.lviv.ua*

Hydrogen-containing materials are one of the important sources of hydrogen supply for FC devices. Nano-sized Mg-based materials, usually obtained by mechanochemical milling, are promising hydrogen storage materials because of their high capacity (7.6 wt.% for pure MgH₂). But practical use of Mg and its alloys in H-storage systems is limited by the slow kinetics of hydrogenation-dehydrogenation and the necessity of high temperatures (>300 °C). Many studies have been devoted to the enhancement of these parameters, including the preparation of Mg by reactive ball milling in H₂ medium (RBM) and modification by different catalytic additives [1-3].

Oxygen-stabilized η -phases based on transition metals represent an important class of intermetallic suboxide compounds with Ti₂Ni-type structure, effective hydrogenation and catalytic properties. In this work, η -phases were used as catalysts for the synthesis and performance enhancement of magnesium hydride composites intended for hydrogen storage and on-demand hydrogen generation. MgH₂- η -phase (based on Zr, V, Ti, Fe) composites were prepared by high-energy reactive ball milling in a hydrogen atmosphere (2 MPa H₂, Fritsch Pulverisette-6). X-ray diffraction with Rietveld refinement showed complete transformation of Mg into a mixture of α - and γ -MgH₂, while the η -phase absorbed hydrogen, forming a hydride without decomposition of its crystal structure. The presence of the suboxide additive significantly accelerated the mechanochemical hydrogenation: the rate constant increased by 3-4 times compared to pure Mg and the hydrogen desorption kinetics were also markedly improved.

The selected composites demonstrated excellent hydrogen generation in hydrolysis reactions with a conversion > 90 %. Water solutions with chlorides (MgCl₂, FeCl₃, and NaCl) confirmed the positive influence on the kinetics of the hydrolysis reactions. The results highlight the promising role of oxygen-stabilized η -phases of transition metals as multifunctional additives that combine structural stability upon hydrogenation with superior catalytic activity in both reversible hydrogen storage and irreversible hydrogen generation processes.

- [1] I. Zavaliy, V. Berezovets, R. Denys *et al.*, *J. Energy Storage* 65 (2023) 107245.
- [2] V.V. Berezovets, R.V. Denys, I.Yu. Zavaliy, Y.V. Kosarchyn, *Int. J. Hydrogen. Energy* 47 (2022) 7289.
- [3] O.P. Kononiuk, I.Yu. Zavaliy, V.V. Berezovets *et al.*, *Mater. Sci.* 59 (2023) 313-319.

TRANSPORT PROPERTIES OF NANOSTRUCTURED $\text{Cu}_6\text{Te}_{3-x}\text{S}_{1+x}$ CHALCOGENIDES FOR THERMOELECTRIC COOLING

Adrianna Lis, Oleksandr Cherniushok, Krzysztof T. Wojciechowski, and Taras Parashchuk
*Thermoelectric Research Laboratory, Department of Inorganic Chemistry,
Faculty of Materials Science and Ceramics, AGH University of Krakow,
Mickiewicza Ave. 30, 30-059 Krakow, Poland
adlis@agh.edu.pl*

The growing demand for environmentally friendly thermoelectric materials has intensified the search for efficient and low-cost alternatives to conventional Bi_2Te_3 -based compounds. Among the emerging candidates, copper-based chalcogenides attract considerable attention due to their low thermal conductivity, good electrical transport properties, and reduced environmental impact. In particular, the $\text{Cu}_6\text{Te}_{3-x}\text{S}_{1+x}$ ($0 < x \leq 1$) system represents a promising class of materials with reduced tellurium content and improved structural stability.

In our previous work, $\text{Cu}_6\text{Te}_{3-x}\text{S}_{1+x}$ compounds were synthesized by a conventional solid-state method to establish their thermoelectric performance. Partial substitution of S for Te stabilized the γ -phase and suppressed the superionic phase transitions characteristic of Cu-based chalcogenides, resulting in improved transport properties and a thermoelectric figure of merit ZT approaching 1.1 at 500 K [1].

In the present study, a solvothermal synthesis method using 1-(2-aminoethyl)piperazine as a solvent was developed to obtain nanostructured $\text{Cu}_6\text{Te}_{3-x}\text{S}_{1+x}$ powders directly from elemental precursors under atmospheric pressure. Samples consolidated by PECS (Pulsed Electric Current Sintering) from nanopowders exhibited reduced thermal conductivity while maintaining comparable electrical transport properties, indicating enhanced phonon scattering due to nanostructuring.

The combination of low thermal conductivity, improved phase stability, and tunable transport properties makes nanostructured $\text{Cu}_6\text{Te}_{3-x}\text{S}_{1+x}$ chalcogenides promising materials for thermoelectric cooling applications.

The research was funded by the Foundation for Polish Science (FNP) under the First-Team programme, project no. FENG.02.02-IP.05-0012/25, "EcoCool: Eco-Friendly Semiconductor Cooling Solution with Dual-Use Applications", co-financed by the European Union under the European Funds for a Modern Economy Programme (FENG 2021-2027).

[1] O. Cherniushok, T. Parashchuk, G.J. Snyder, K.T. Wojciechowski, *Adv. Mater.* 37 (2025) 2420556.

ELECTRONIC STRUCTURE AND ELECTROCHEMICAL LITHIATION OF Ho₅In₃

I. Tarasiuk¹, V. Kordan¹, N. Pavlyuk¹, G. Dmytriv¹, and V. Pavlyuk^{1,2}

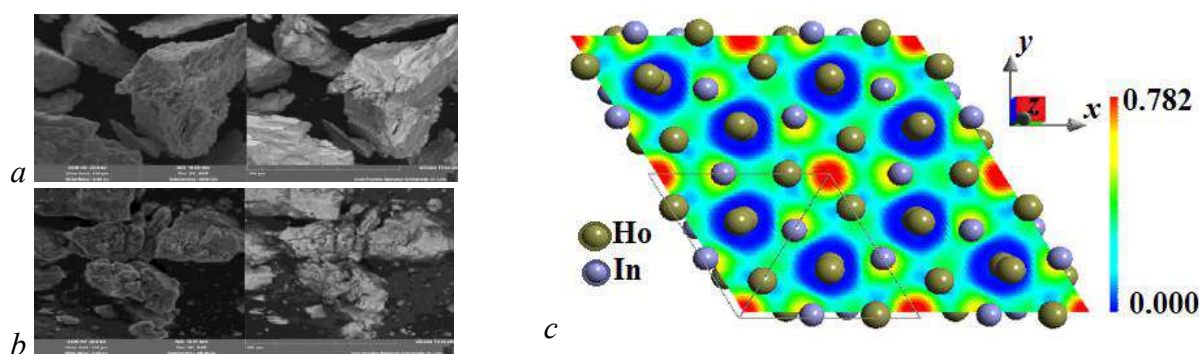
¹ Department of Inorganic Chemistry, Ivan Franko National University of Lviv,
Kyryla i Mefodiya St. 6, 79005 Lviv, Ukraine

² Institute of Chemistry, Jan Długosz University,
al. Armii Krajowej 13/15, 42-200 Czestochowa, Poland
ivan.tarasiuk@lnu.edu.ua

Intermetallic compounds are promising materials for use as electrodes in batteries. What is favourable for the intercalation/deintercalation of charge carriers is a layered crystal structure and lattice defects or large voids. This work presents the results of an investigation of Ho₅In₃ with such a type of structure and the effect of tin addition on the electrochemical properties.

Polycrystalline alloys with composition Ho_{62.5}In_{37.5} and Ho_{62.5}In_{18.75}Sn_{18.75} were synthesized by arc-melting with further annealing at 673 K. Electrochemical lithiation was carried out in the galvanostatic mode using a two-electrode Swagelok-type cell. The synthesized powder samples were tested as negative electrode materials during a discharge process. The alloys Ho_{62.5}In_{37.5} and Ho_{62.5}In_{18.75}Sn_{18.75} contained a phase with Mn₅Si₃-type structure (space group *P*6₃/*mcm*, Pearson symbol *hP*16) stable at room temperature [1]. The cell parameters before and after lithiation were: for Ho₅In₃ *a* = 8.981(6), *c* = 6.528(3) Å and *a* = 8.998(7), *c* = 6.535(8) Å respectively; for Ho₅In_{1.5}Sn_{1.5} *a* = 8.931(2), *c* = 6.502(3) Å and *a* = 8.943(4), *c* = 6.514(4) Å.

During the first stage of the electrochemical lithiation, Li-atoms occupy Wyckoff position *2b* with the formation of a Hf₃CuSn₃-type superstructure. At the second stage of the lithiation, lithium partially substitutes for Sn and In with the formation of by-products. The surface morphology before and after the electrochemical lithiation was studied with a scanning electron microscope Tescan Vega3 LMU (see Fig. *a* and *b*). The electronic structure of Ho₅In₃ was calculated using the linear muffin-tin orbital method (TB-LMTO-ASA). The electron localization function inside the empty octahedron [□Ho₆] of the Ho₅In₃ compound reaches 0.782, which confirms the high possibility of Li⁺-insertion (Fig. *c*).



SEM-images of Ho_{62.5}In_{37.5} before (*a*) and after (*b*) lithiation,
electron localization function of Ho₅In₃ (*c*)

This work was carried out under the project of the Ministry of Science and Education of Ukraine No. 0126U002473.

[1] M. Pustovoychenko, M. Manyako, V. Pavlyuk, B. Marciniak, Ya. Kalychak, *Chem. Met. Alloys* 1 (2008) 317-322.

ELECTROCHEMICAL LITHIATION OF THE Nd₂MnCoO₆ PEROVSKITE

M.-S. Teplinska, O. Zaremba, P. Demchenko, V. Kordan, and R. Gladyshevskii
*Department of Inorganic Chemistry, Ivan Franko National University of Lviv,
Kyryla i Mefodiya St. 6, 79005 Lviv, Ukraine
mariiasuzanna.teplinska@lnu.edu.ua*

The exploration of perovskites is one of the prominent trends in modern applied chemistry and materials science. Our attention was drawn to the Nd–Mn–Co–O system, where the existence of a conventional perovskite with an orthorhombic structure and a double perovskite with monoclinic symmetry has been reported [1]. The former is described by the formula ABO_3 , where the B site is occupied by a mixture of Mn and Co cations. The larger A cations are coordinated by eight oxygen atoms forming a tetragonal antiprism $[AO_8]$, whereas the smaller B cations are located at the centres of octahedra $[BO_6]$. The double perovskite is represented by the formula $A_2BB'O_6$, where A are the larger cations, while B and B' are two different smaller cations occupying alternating octahedral sites. The aim of this work was to synthesize the perovskite in the Nd–Mn–Co–O system and investigate its electrochemical properties.

A sample of nominal composition Nd₂MnCoO₆ was obtained by a two-stage solid-state synthesis under air at 1000 and 1200 °C. The starting materials (Nd₂O₃, Mn₂O₃, and CoCO₃) were manually mixed and ground to achieve homogeneity. The first stage of heating at 1000 °C was carried out for 24 h to decompose the carbonate. At the second stage, the mixture was ground, pelleted, and sintered at 1200 °C for 8 h. The crystal structure, morphology, qualitative and quantitative composition of the ceramic samples before and after lithiation were studied by X-ray diffraction (STOE Stadi P, Cu $K\alpha_1$) and SEM/EDX (Tescan Vega 3 LMU, Oxford Instruments Aztec ONE, X-Max^{N20}) analyses.

The orthorhombic perovskite crystallizing in the GdFeO₃-type structure was formed in the Nd–Mn–Co–O system under the conditions of our experiment ($a = 5.52790(16)$ Å, $b = 7.6784(2)$ Å, $c = 5.41525(15)$ Å, $V = 229.852(11)$ Å³, $R_1 = 0.0527$, $R_p = 0.0385$, $R_{wp} = 0.0522$, $R_{exp} = 0.0329$, $\chi^2 = 2.52$). It was tested as cathode material for lithium-ion batteries (2-electrode Swagelok-cell type in the galvanostatic mode), where commercial lithium served as the anode. An 1M solution of Li[PF₆] salt in a mixture of aprotic solvents (dimethyl carbonate and ethylene carbonate in the ratio 1:1) was used as electrolyte. As a result of the electrochemical lithiation the Nd₂MnCoO₆: x Li phase ($x = 0.150$) was formed. The basic crystal structure remained unchanged ($a = 5.5316(2)$ Å, $b = 7.6796(3)$ Å, $c = 5.41572(20)$ Å, $V = 230.063(15)$ Å³, $R_1 = 0.0649$, $R_p = 0.0279$, $R_{wp} = 0.0394$, $R_{exp} = 0.0308$, $\chi^2 = 1.64$). The increase in cell volume is only 0.09 %, which may indicate initial formation of a solid solution of inclusion type, followed by substitution during the lithiation process. The maximum amount of intercalated Li was 0.150 per formula unit. The chemical composition from EDX-analysis confirmed the perovskite stoichiometry. Scanning electron microscopy revealed the formation of Li-containing granules of irregular shape with a size of 0.4–2.2 µm.

[1] P. Villars, K. Cenzual (Eds.), *Pearson's Crystal Data – Crystal Structure Database for Inorganic Compounds*, Release 2023/24, ASM International, Materials Park, Ohio, USA.

SYNTHESIS, PHASE ANALYSIS AND ELECTROCHEMICAL HYDROGENATION OF Y- AND La-DOPED Tb₂Li_{0.2}Mg_{0.2}Ni_{6.6} ALLOYS

V. Voloshyn¹, V. Kordan¹, I. Tarasiuk¹, V. Nytko¹, O. Zelinska¹, and V. Pavlyuk^{1,2}

¹ *Department of Inorganic Chemistry, Ivan Franko National University of Lviv, Kyryla i Mefodiya St. 6, 79005 Lviv, Ukraine*

² *Institute of Chemistry, Jan Długosz University, al. Armii Krajowej 13/15, 42-200 Częstochowa, Poland
viktorii.voloshyn.hmh@lnu.edu.ua*

Intermetallic compounds based on rare-earth and transition metals are widely used for hydrogen storage applications due to their ability to absorb large amounts of hydrogen. This property stems from the presence of tetrahedral and octahedral voids in the crystal structures of these materials, which readily accommodate hydrogen atoms. The combination of substantial specific capacity and excellent cyclic stability makes these alloys promising anode materials for nickel-metal hydride batteries. The synthesis of new alloys with diverse elemental compositions is crucial for discovering materials with enhanced electrochemical properties compared to well-known systems.

Multicomponent alloys with the compositions Y_{0.25}Tb_{1.75}Li_{0.2}Mg_{0.2}Ni_{6.6}, La_{0.25}Tb_{1.75}Li_{0.2}Mg_{0.2}Ni_{6.6}, and Y_{0.25}La_{0.25}Tb_{1.5}Li_{0.2}Mg_{0.2}Ni_{6.6} were synthesized by arc-melting of pellets under a purified argon atmosphere. Metals of high purity (above 99.8 wt.%) were used for the synthesis; lithium and magnesium were added with a 5 wt.% excess to prevent mass loss. X-ray diffraction data were collected using a PROTO AXRD Benchtop diffractometer (Cu K α -radiation). The elemental composition of the samples was checked by X-ray fluorescence analysis (ElvaX Pro spectrometer), scanning electron microscopy, and energy-dispersive X-ray spectroscopy (EDX) (Tescan Vega3 LMU electron microscope with the Oxford Instruments Aztec ONE system and X-Max^N20 detector equipped with SE- and BSE-detector). The synthesized alloys were used as the negative electrode, while the positive electrode consisted of Ni(OH)₂ powder mixed with graphite to enhance the conductivity. Cyclic voltammetry and electrochemical impedance spectroscopy were carried out using a 3-electrode cell and a potentiostat VersaSTAT.

Phase analysis of the initial alloys showed the formation of solid solutions on the basis of α R₂Ni₇ (structure type Ce₂Ni₇, space group *P*6₃/*mmc*) and β R₂Ni₇ (Gd₂Co₇, *R*-3*m*), RNi₅ (CaCu₅, *P*6/*mmm*), and trace amounts of Ni (Cu, *Fm*-3*m*). The cell parameters of the main phase (Ce₂Ni₇) correlated well with the atomic radius of the rare-earth element: $a = 4.9277(3)$ Å, $c = 24.197(4)$ Å, $V = 508.85(8)$ Å³ for the Y-containing phase, and $a = 4.9796(3)$ Å, $c = 24.128(2)$ Å, $V = 518.16(6)$ Å³ for the La-containing phase. We observed a complex substitution mechanism (as determined by EDX analysis): Tb atoms were partially replaced by Y/La, while Li and Mg simultaneously substituted for Ni and R atoms.

The specific discharge capacity of the studied electrodes ranged from 207 to 235 mAh/g. Electrochemical impedance spectroscopy confirmed the electrochemical hydrogenation of three phases (the Nyquist Plot showed three semicircles and a good Warburg diffusion parameter). CVA and potentiodynamic curves showed that the studied alloys are stable in an alkaline electrolyte over a wide potential range.

This work was carried out under the Ministry of Science and Education of Ukraine grants No. 0124U001013 and No. 0126U002473.

SYNTHESIS, STRUCTURE, ELECTROCHEMICAL AND CATALYTIC PROPERTIES OF $\text{YMgNi}_{4-x}\text{Co}_x$ ($0 \leq x \leq 4$) ALLOYS AND THEIR HYDRIDES

Yuriy Verbovytskyi¹, Danylo Fatieiev², Ihor Bychko², Vasyl Berezovets¹,
Ihor Zavaliiy¹, Peter Strizhak², and Valérie Paul-Boncour³

¹ *Karpenko Physico-Mechanical Institute, NAS of Ukraine, 79060 Lviv, Ukraine*

² *L.V. Pisarzhevskii Institute of Physical Chemistry, NAS of Ukraine, 03028 Kyiv, Ukraine*

³ *Univ Paris Est Créteil, CNRS, ICMPE, UMR 7182, 94320 Thiais, France*
ihor.zavaliiy@gmail.com

Alloys of the R -Mg-Ni system (R = rare-earth metals) have long remained the object of attention as high-performance hydrogen-sorption materials. Due to their ability for rapid and reversible hydrogen absorption, they have found application in the production of anode materials for nickel-metal hydride (Ni-MH) batteries. One of the most effective approaches to optimizing the functional properties of such alloys is conceptual alloying. Modification of the composition by partial substitution of R or nickel by other elements allows fine-tuning the material characteristics, specifically: corrosion resistance, thermodynamic stability, electrochemical capacity, *etc.* [1].

Apart from the traditional application for solid-state hydrogen storage, hydrides of metals and intermetallic compounds have a significant potential as heterogeneous catalysts in chemical synthesis processes [2,3]. Their ability to act as active sites for the reduction of carbon oxides, particularly carbon dioxide, to valuable hydrocarbons or methane attracts special attention. The use of hydrides allows for the involvement of an atomic hydrogen flux directly from the crystal lattice, which significantly lowers the energy barriers of the reactions compared to traditional methods. Thus, the combination of hydrogen storage functions and catalytic use of CO/CO_2 opens new possibilities for creating closed energy cycles.

This work is dedicated to the synthesis and a comprehensive analysis of a series of alloys with the composition $\text{YMgNi}_{4-x}\text{Co}_x$ ($0 \leq x \leq 4$). Individual alloys of this system were first studied in [4]. The pressure-composition-temperature dependencies of the $\text{YMgCo}_4\text{-H}_2$, $\text{YMgNi}_4\text{-H}_2$, and $\text{YMgCo}_2\text{Ni}_2\text{-H}_2$ systems were investigated, and the thermodynamic parameters of saturated hydride formation were calculated. The hydrides $\text{YMgNi}_2\text{Co}_2\text{H}_{4.9}$ and $\text{YMgCo}_4\text{H}_{6.8}$ retain the cubic structure of the parent compounds with unit-cell volume expansions of 23 and 14.4 %, respectively. The focus of our presentation is on the ability of $\text{YMgNi}_{4-x}\text{Co}_x$ materials to operate as a secondary energy source and the effectiveness of these alloys in carbon oxide (CO and CO_2) reduction reactions, which is critically important for gas emission purification technologies and fuel synthesis.

The research was carried out within the framework of the NATO project SPS G6247 "New Green Energy Solution".

- [1] W. Jiang, Y. Chen, M. Hu *et al.*, *J. Alloys Compd.* 887 (2021) 161381.
- [2] S. Kato, A. Borgschulte, D. Ferri *et al.*, *Phys. Chem. Chem. Phys.* 14 (2012) 5518-5526.
- [3] S. Kato, S. Matam, P. Kerger *et al.*, *Angew. Chem. Int. Ed.* 55 (2016) 6028-6032.
- [4] V.V. Shtender, R.V. Denys, V. Paul-Boncour *et al.*, *J. Alloys Compd.* 603 (2014) 7-13.

MAGNETIC PROPERTIES OF COMPLEX TERNARY RARE-EARTH INTERMETALLICS IN THE LIGHT OF MACRO- AND MICRO-MEASUREMENTS

Andrzej Szytuła

Institute of Physics, Jagiellonian University, Prof. S. Lojasiewicza 11,

PL-30348 Kraków, Poland

szytula@if.uj.edu.pl

Lately, investigations on magnetic properties have been focusing on ternary R - T -In compounds, where R = rare-earth and T = transition element, with the composition 5:2:4 and 11:9:4 and orthorhombic crystal structures in which the rare-earth atoms occupy three and five different Wyckoff sites, respectively. The structures are composed of CsCl- (R In) and AlB_2 - (RT_2) type slabs in the ratio 4:1 and 9:2, respectively. Magnetic measurements indicate magnetic ordering at similar critical temperatures for both groups of compounds. Below these, additional magnetic transitions were detected at low temperatures. With the purpose to explain the complex magnetic properties, neutron diffraction measurements were performed. In $R_5T_2In_4$ (space group $Pbam$), the $R1$ site is located in Wyckoff position $2a$ with coordination number (C.N.) 12, $R2$ and $R3$ occupy $4g$ sites with C.N. 16 and 14, respectively. For $R_{11}T_4In_9$ (space group $Cmmm$), the R atoms occupy five non-equivalent sites with different local symmetry, namely m for $R1$ ($2p$ site), $m2m$ for $R2$ and $R3$ ($4i$ sites), $2mm$ for $R4$ ($4g$ site), and mmm for $R5$ ($2a$ site). The R atoms have different coordination numbers, $R1$: 14, $R2$: 13, $R3$: 16, $R4$: 16, and $R5$: 12. The formation and stability of the magnetic structures are the result of the competition between two dominant interactions: the indirect exchange interaction of the RKKY type and the interaction with the crystalline electric field. The competition of these is seen on the dependence of the critical temperatures of magnetic ordering on the de Gennes function. For these systems, the values for the compounds with $R = Tb$ and Dy are higher than those resulting from the above relation.

The neutron diffraction data indicate that the R magnetic moments at different sites order at different temperatures. In the $R_5T_2In_4$ compounds, the magnetic moments on $R1$ in $2a$ with C.N. equal 12 and $R3$ in $4g$ with C.N. equal 14 order first, while $R2$ in $4g$ with C.N. 16 orders at low temperatures. In the $R_{11}T_4In_9$ compounds, the magnetic moments on the $R2$ and $R5$ sites order first. Ordering of the moments on the other R sites is observed at low temperatures.

The data indicate that the observed magnetic structure results from the competition of complex interactions between magnetic moments in intra- and inter-sublattices that have ferro- and antiferro-character.

INDEX OF AUTHORS

Agarwal A.	67	Broz P.	14
Agnarelli L.	53	Bulanova M.	68
Agraval P.	68	Bullmann A.	85
Akselrud L.	56, 76, 83, 117, 130, 135	Burkhardt U.	51
Alam R.	44	Bursik J.	14
Alleno E.	41, 123	Bursikova V.	14
Anière V.	112	Buturlim V.	15, 86
Antoniuk H.	118	Bychko I.	148
Armbrüster M.	26	Cabala A.	28
Arseniuk I.	119	Campbell I.	35
Artini C.	25	Caputo R.	37
Babizhetskyy V.	140, 142	Cardoso-Gil R.	51, 84
Baczmański A.	46	Cario L.	45
Bai X.	44	Casas-Cabanans M.	24
Baran S.	140	Čermák P.	73
Baranets S.	44	Černá S.	15, 72
Barišić N.	65	Chajewski G.	31
Barreteau C.	123	Chauvel E.	17
Bastien G.	11	Chełkowska G.	70
Bauer E.	27	Cherniushok O.	16, 76, 82, 83, 84, 144
Bednarchuk T.J.	70, 112	Chudinovych O.	103
Ben Hassen R.	13, 141	Cieślak J.	46, 58, 116
Bendová A.	86	Colman R.H.	11, 77
Berent K.	46, 58, 116	Colombara D.	36
Berezovets V.	143, 148	Corrêa C.A.	11, 77
Berlie A.	77	Costamagna P.	25
Berthebaud D.	45	Crivello J.-C.	45
Bhardwaj R.	41	Curfs C.	135
Biniskos N.	73	Čurlík I.	13, 141
Blanton T.	37	Custers J.	86
Bławat J.	79	Da Cruz Q.	10
Bobet J.-L.	32, 63, 74	Dąbrowa J.	58, 116
Bobev S.	3	Darmonuk O.	98
Boča M.	94	Das P.	57, 87
Borchert Z.	78	Datsko R.	120, 129
Boucher Y.U.	65	De Negri S.	5, 47, 49, 96, 106, 129, 137, 138, 141
Bouquet V.	41	Demchenko P.	134, 146
Bourdarot F.	73	Deniard P.	45
Bourgès C.	45		
Braun T.	48		

Devanaboina S.V.V.U.K.	72	Giovannini M.	13 , 141
Dey T.	57	Girzhon V.	99
Dhami N.	65	Gladyshevskii R.	9 , 12, 51, 56, 76, 81, 83, 100, 105, 110, 117, 120, 122, 125, 126, 129, 131, 133, 134, 136, 137, 138, 146
Dias M.S.	73		
Diop L.V.B.	52, 62		
Dmytriv D.	88		
Dmytriv G.	61, 92, 145		
Dobroň P.	23		
Donyk H.	82	Goraus J.	54
Dorcet V.	41	Goreschnik E.	88
Dörflinger P.	99	Górnicka K.	7
Doucet E.	89	Grin Yu.	38 , 51, 56, 76, 83, 84, 135
Dovgaliuk I.	94		
Drach Yu.	119	Gubicza J.	23
Drozdenko D.	23	Gudac B.	65
Du Y.	29	Guizouarn T.	96
Eichenberger L.	17	Guo K.	29
El Rhazfouri M.N.	63	Gvozdetskyi V.	18
Elgalal S.	31	Haidamak T.	28, 77
Faithfull-Evans E.	50	Hájek F.	43
Falkowski M.	70	Halet J.-F.	142
Farkas A.	23	Harris S.	17
Farkas G.	23	Hauback B.C.	61
Fartushna I.	68	Hauspurg A.	28
Fässler T.F.	40 , 118	Havela L.	15 , 81
Fatieiev D.	148	Hébert S.	53
Feldl S.	22	Henriques M.	43
Fernandes B.	50	Herak M.	65
Filep M.	108	Hernandez O.	45
Finik O.	90 , 100, 128	Hirskyi Yu.	91
Flachbart K.	74	Hlukhyy V.	48 , 118
Freccero R.	36 , 75, 96, 141	Hoch C.	22 , 127
Gabáni S.	74	Hodroj A.	41
Gamża M.B.	50	Honda F.	15
Garbarino G.	75	Horiacha M.	121
Garces G.	23	Horyn A.	107, 113
Garmroudi F.	27	Hreb V.	91
Gascoin F.	111	Huot J.	32, 74
Gaudin E.	63	Inoue S.-I.	23
Gegenwart P.	11	Isnard O.	52, 142
Giester G.	14	Ivanushko A.	122

Iwasieczko W.	130	Kumar S.	11
Joanny L.	41	Kuzderová G.	128
Jobic S.	45	Lamura G.	49
Johari K.K.	123	Lamy S.	132
Joubert C.	111	Łapiński M.	59
Kaczkowski J.	70	Le Roy G.	33
Kaczorowski D.	15, 31 , 67, 97	Le Tonquesse S.	20 , 111
Kaiun I.	114	Lemoine P.	17 , 132
Kalychak Ya.	139	Lesnianska V.	117, 136
Kancko A.	11, 77	Li X.	29
Karychort O.	124	Lis A.	144
Kaštil J.	43	Lukashchuk I.	83
Katrusiak A.	34	Lužnik M.	33
Kawamura Y.	23	Maignan A.	53
Klicpera M.	43	Malakhovska T.	108
Klimczuk T.	7, 59, 78, 79, 85, 93, 101, 115	Malaman B.	62
Klymentiy N.	51, 125 , 133	Malaman B.	132
Knura R.	16	Malick S.	79 , 101, 115
Kolomiets O.	15	Manfrinetti P.	47 , 49, 106
Koloskova O.	15	Mangeolle L.	33
Kononiuk O.	143	Manuel P.	50
Konyk M.	104	Mar A.	18 , 57, 87, 102
Kordan V.	61, 92 , 98, 100, 145, 146, 147	Marciszko M.	46
Korichev S.	103	Martinelli A.	13, 49, 141
Korotoshyn B.	56 , 76	Martsynko O.	90, 100, 128
Kosarchyn Yu.	143	Maryshevych D.	105
Kovacevic J.	27	Mašková-Černa S.	81
Kovalskiy O.	66, 109	Massardo S.	25
Kowalczyk A.	70	Máthis K.	23
Kozak Yu.	126	Matselko O.	94
Kraut D.	22, 127	Mazumdar C.	123
Kremer R.K.	142	McLeod C.	87
Kretkovskiy O.	92	Meena P.K.	7, 59
Krnel M.	130	Merk S.	118
Królak S.	93	Michor H.	14
Kubinec O.	14	Milashius V.	92
Kuderowicz G.	69	Miliyanchuk K.	15, 81
Kulyk Yu.	60, 66, 109	Modak M.	123
Kumar A.	61	Mödlinger M.	106
		Mori T.	19 , 27, 45, 71
		Moussa M.	32, 74

Mudring A.-V.	47	Plevachuk Yu.	60, 66
Mudry S.	60, 66, 99, 109	Podloucky R.	14
Mumbaraddi D.	57	Pogodin A.	108
Muts N.	56, 76, 120, 129 , 137	Pöhls J.-H.	6, 89
Nachowski J.	115	Pokhvata O.	44
Netriová Z.	94	Popčević P.	65
Novak M.	65	Popilovskyi N.	60, 66, 109
Nowak A.	46, 116	Porée V.	96
Nowakowska M.	58, 116	Pospíšil J.	28, 52, 86
Nusser L.	22	Pransu G.	65
Nychyoporuk G.	121, 130	Prestipino C.	41, 132
Nykyruy Y.	60	Presto S.	25
Nytka V.	147	Pristáš G.	74
Ohonovskyi I.	131	Prokleška J.	28, 77
Oliynyk A.	21	Prokofiev A.	33, 99
Ollivier S.	41	Proschek P.	77
Onufriienko O.	74	Prots Yu.	53, 124, 135
Otteny M.	10	Provino A.	47, 49 , 106
Palla G.	36, 75 , 141	Pryga K.	76 , 83
Pani M.	25 , 47	Puente-Orench I.	50
Parashchuk A.	133	Pukas S.	51, 125, 133 , 134
Parashchuk T.	16, 76, 82, 83, 84 , 144	Rakhmatullin A.	94
Parmar D.	45	Raymond S.	73
Parzer M.	27	Reissner M.	58, 116
Paschen S.	33	Rendošová M.	128
Pasturel M.	17, 41 , 96, 132	Repetto G.	96
Patra A.	123	Reynaud M.	24
Patrashko A.	51	Riani P.	75
Paul-Boncour V.	148	Riedl H.	99
Pavlosiuk O.	64 , 67, 121	Rogal Ł.	34
Pavlyuk N.	61, 92, 145	Rogalev A.	15, 52
Pavlyuk O.	95	Rogl G.	14, 55
Pavlyuk V.	39 , 61, 92, 98, 145, 147	Rogl P.	14 , 55
Pawula F.	45	Röhr C.	10
Pechinka D.	90	Romaka L.	104, 107 , 113
Pelloquin D.	53	Romaka V.A.	113
Pereira Gonçalves A.	30	Romaka V.V.	55, 80 , 104, 107, 113
Piasecki M.	108	Romanova T.	31, 97
		Sabov M.	108
		Sabov V.	108

Saidov N.	81	Snyder J.G.	84
Sakai H.	77	Sologhub O.	27
Sakthivel S.	20	Solokha P.	5, 47, 49, 96, 106, 129, 137, 138, 141
Salamakha L.	27		
Šálka M.	72	Spennati E.	75
Samanta S.	71	Stadnik V.	91
Saracibar A.	24	Stadnyk Yu.	104, 107, 113
Sarr I.	62	Starushenko K.	109
Sartori S.	61	Staško D.	43
Sas W.	65	Stelmakhovych B.	119
Saurel D.	24	Stepanovych K.	136 , 138
Schmidt M.	53	Strizhak P.	148
Schweitzer T.	17	Suard E.	50
Sechovský V.	28	Svanidze E.	130
Sehmsdorf F.	10	Sviták D.	73
Seifullina I.	128	Świątek H.	79
Selvaratnam B.	18	Synoradzki K.	112
Sembratovych N.	109	Szum M.	58
Semuso N.	126, 134	Szytuła A.	140, 149
Sereni J.G.	13	Tahiyah R.	83
Serkiz R.	66	Tang D.	123
Serrano-Sevillano J.	24	Tarasiuk I.	92, 145 , 147
Shatruk M.	35	Taupin M.	33
Shevchuk V.	114	Tencé S.	4
Shpyrka Z.	98	Teplinska M.-S.	146
Shtablavyi I.	60, 66 , 99, 109	Thipe B.	44
Shved O.	99	Thomé A.	18
Sibille R.	17	Tobola J.	84
Sichevych O.	135	Tokaychuk Ya.	12 , 56, 76, 83, 105, 110, 120, 126, 129, 131, 137, 138
Sidis Y.	17		
Sikora M.	58	Tokunaga Y.	77
Silva B.H.	61	Tonet F.	36
Šimko F.	94	Trabelsi I.	13, 141
Singleton J.	79	Treu T.	11
Sjåstad A.O.	61	Tsujii N.	71
Slyvka Yu.	88	Tsymbaliuk K.	100
Smetana V.	47, 140	Turchanin M.	68
Smitiukh O.	82	Tyvanchuk Yu.	140
Smolyakov O.	99	Uhlarz M.	77
Śniadecki Z.	70		
Snurnikova O.	100		

Vališka M.	28	Zevalkink A.	83
Vallet-Simond B.	52, 142	Zhak O.	124
Vargová Z.	128	Zhao J.	29
Vasylechko L.	91	Zherlitsyn S.	28
Verbovytskyy Yu.	148	Zhydachevskyy Ya.	91
Vernière A.	62, 132	Zorych J.	74
Viviani M.	25		
Vlášková K.	43		
Voloshyn V.	147		
Vynnyk R.	110		
Wagner F.R.	8		
Walenczak B.	101		
Wang X.	35		
Wang Y.-X.	35		
Weiss K.	14		
Wendorff M.	10		
Wiendlocha B.	69, 76, 83, 84		
Wilhelm F.	15, 52		
Wilmanski A.	16		
Winiarski M.J.	59, 64, 78, 79, 93		
Wisniewski P.	67		
Wojciechowski K.T.	16, 76, 82, 83, 84, 144		
Wu Q.	102		
Wurmehl S.	121		
Xu T.	22		
Yakymovych Kh.	137		
Yan X.	33, 55		
Yang K.	29		
Yazici D.	93, 115		
Young D.	44		
Yubuta K.	55		
Zamula M.	103		
Zaremba N.	130		
Zaremba O.	117, 136, 138, 146		
Zaremba R.	139		
Zaremba V.	121, 130		
Zavaliy I.	143, 148		
Zehetbauer M.	55		
Zelinska O.	61, 147		
Zelinskiy A.	113, 140		

Підп. до друку 22.05.2026. Формат 30×42. Папір офсет.
Друк. арк. 19,5

Видавець та виготовлювач: Львівський національний університет імені Івана Франка,
вул. Університетська, 1, м. Львів 79007